Neuro-immune interactions in age-related macular degeneration: implications for future therapeutics

by

Rabah Dabouz

Department of Pharmacology & Therapeutics

McGill University

Montreal, Quebec, Canada

January 2024

A thesis submitted to McGill University in partial fulfillment of the requirements of the degree of

Doctorate of Philosophy

Table of Contents

List of Tables ix
List of Figures ix
List of Abbreviations ix
Abstract xv
Acknowledgements xix
Contribution to original knowledge xix
Author contributions xx
CHAPTER 1 - INTRODUCTION 1
1. Introduction 1
CHAPTER 2 – LITERATURE REVIEW 3
2.1 Age-related macular degeneration 3
2.1.1 Retinal degeneration: historical perspective 3
2.1.2 Epidemiology and risk factors 5
2.1.3 Classification 7
2.1.4 Pathophysiology 10
2.1.4.1 Aging-related changes in the retina 10
2.1.4.2 Oxidative stress 11
2.1.4.3 RPE dysfunction 13
2.1.4.3.1 Mitochondrial dysfunction 13
2.1.4.3.2 Defects in autophagy 15
2.1.4.3.3 RPE senescence 15
2.1.4.3.4 RPE cell death 16
2.1.4.4 Choroidal involution 18
2.1.4.5 Choroidal neovascularization 19
2.1.4.6 Inflammation 22
2.1.5 Treatment and limitations 22
2.1.5.1 Anti-VEGF therapy for wet AMD 22
2.1.5.2 Drugs targeting advanced dry AMD 24
2.1.6 Animal models for AMD 25

2.2 Inflammation 25
2.2.1 Overview of inflammation and homeostasis 25
2.2.2 Immune privilege in the retina 28
2.2.3 Chronic inflammation in AMD 29
2.3 Mononuclear phagocytes in AMD 31
2.3.1 Mononuclear phagocytes 31
2.3.2 Mononuclear phagocytes in the posterior segment of the eye 33
2.3.3 The role of mononuclear phagocytes in AMD 34
2.4 Interleukin-1 36
2.4.1 Overview of interleukin-1 36
2.4.2 Biosynthesis of IL-1β 37
2.4.2.1 NLRP3 inflammasome 39
2.4.3 Interleukin-1 receptors and signaling pathways 40
2.4.4 Anti-IL-1 therapeutics 42
2.4.4.1 Allosteric modulation 43
2.4.5 IL-1 in AMD 44
2.5 Mast cells 44
2.5.1 The significance of mast cells in the immune system 44
2.5.1.1 Origin of mast cells 45
2.5.1.2 Mast cell subtypes, heterogeneity, and plasticity 46
2.5.1.3 Activation of mast cells 46
2.5.2 Mast cell tryptase 48
2.5.2.1 Tryptase biosynthesis 48
2.5.2.2 Tryptase structure 49
2.5.2.3 Tryptase substrates and biological roles 50
2.5.3 Mast cells in AMD 51
2.6 Cell death 51
2.6.1 Regulated cell death 51
2.6.1.1 Apoptosis 52
2.6.1.1.1 Extrinsic pathway 53
2.6.1.1.2 Intrinsic pathway 55

2.6.1.2 Necroptosis 57
2.6.2 Cell death in retinal degeneration 60
2.7 Thesis rationale and objectives 61
CHAPTER 3 - An allosteric interleukin-1 receptor modulator mitigates inflammation and photoreceptor toxicity in a model of retinal degeneration 62
Abstract 64
Introduction 65
Materials and Methods 67
Animals 67
IL-1 receptor antagonists 68
Blue light exposure model 68
Retinal section preparation 68
Measurement of photoreceptor layer thickness 69
Retinal flat mount preparation 69
Quantification of activated MPs in the subretinal space 70
Single-cell RNA sequencing analysis 70
Terminal deoxynucleotidyl transferase dUTP nick end labeling assay 71
Isolation of bone marrow–derived monocytes 71
BMDM and retinal explant incubation 72
Quantitative RT-PCR 72
Western blotting 72
Enzyme-linked immunosorbent assay 73
Electroretinogram 73
Statistical analysis 74
Results 74
Blue light induces subretinal macrophage infiltration, which is suppressed by IL-1R antagonism 74
Single-cell RNA-seq analysis of Il1b and Il1r1 expression in the retina 75
Suppression of subretinal inflammation preserves photoreceptor integrity 75
Rytvela protects against macrophage-induced photoreceptor cell death in an ex vivo model 76

Discussion 76
Conclusion 80
References 81
Funding 90
Contributions 90
CHAPTER 4 – Mast cell activation contributes to subretinal inflammation and photoreceptor loss in an oxidative stress model of AMD 105
Abstract 106
Introduction 106
Materials and Methods 107
Animals 107
Drug and NaIO3 treatment 107
RPE/choroid flat mount preparation 107
Volume and sphericity analysis of MPs 108
Isolation of primary RPE cells 108
Isolation of peritoneal mast cells 109
Isolation of bone marrow-derived mast cells and adoptive transfer to mast-cell deficient mice 110
Terminal deoxynucleotidyl transferase dUTP nick end labeling (TUNEL) assay 110
Electroretinogram (ERG) 111
Statistical analysis 111
Results 111
Mast cells are activated in response to oxidative stress infliction in RPE 111
Mast cell stabilizer mitigates RPE degeneration in response to $NaIO_3$ 112
Mast cell activation contributes to intensification of subretinal inflammation in response to induced RPE injury 113
Mast cell activation elicits photoreceptor damage induced by $NaIO_3$ 113
Tryptase drives the mast cell-mediated inflammatory response 114
Discussion 114
References 117
Acknowledgments 122

Contributions 122
Conflict of interest statement 122
CHAPTER 5 - Mast cells promote experimental choroidal neovascularization in AMD 138
Abstract 139
Introduction 139
Materials and Methods 140
Animals 140
Laser-Induced CNV 141
Fundus fluorescein angiography 141
Immunohistochemistry 142
Isolation of peritoneal mast cells 142
Isolation of bone marrow-derived mast cells 143
Treatment of choroidal explants 143
Preparation of anti-CD31 antibody coated magnetic beads 144
Isolation and culture of choroidal endothelial cells 144
Scratch-wound assay 145
Tubule formation assay 145
RNA-seq sample preparation, sequencing, and analysis 145
Gene set enrichment analysis 146
GO pathway enrichment analysis 146
Collagen hybridizing peptide (CHP) binding 147
Statistical analysis 147
Results 147
Mast cells promote choroidal endothelial cell sprouting angiogenesis and migration 147
Mast cell deficiency (and stabilization) precludes choroidal neovascularization 148
Mast cell tryptase promote pathological angiogenesis in the choroid 148
Mast cells promote ECM remodelling 149
Discussion 150
References 152
Ethics declarations 156

Ethics approval 156
Availability of data and materials 156
Competing interests 156
Acknowledgement 156
Author contributions 156
Funding 157
CHAPTER 6 - Necroptosis blockade mitigates retinal toxicity in oxidative stress-induced retinal degeneration 168
Abstract 169
Introduction 170
Materials and Methods 171
Animals 171
Sodium iodate and drug treatment 171
Retinal section preparation 171
Measurement of photoreceptor layer thickness 172
RPE flat mount preparation 172
Quantification of mononuclear phagocytes (MPs) in the subretinal space 173
Analysis of volume and shape of MPs 173
Terminal deoxynucleotidyl transferase dUTP nick end labeling (TUNEL) assay 173
Western Blotting 174
Gene set enrichment analysis 174
Electroretinogram (ERG) 175
Statistics 175
Results 175
Necroptosis and apoptosis are engaged in retinal degeneration 175
MLKL deficiency alleviated photoreceptor loss and subretinal inflammation 176
Pharmacological targeting of necroptosis alleviated photoreceptor loss 177
RIPK3 kinase inhibition dampens subretinal inflammation 178
Discussion 178
References 180

Funding 184
Contributions 184
Conflict of interest statement 185
CHAPTER 7 – GENERAL DISCUSSION 196
7.1 Interplay between inflammation and cell death in neurodegeneration 196
7.2 Inflammation, IL-1, and AMD 196
7.3 Glia at the crossroads of neuroimmune interactions 198
7.4 Mast cells and choroidal inflammation 200
7.5 Deciphering the role of choroidal mast cells in AMD pathogenesis 200
7.6 Targeting mast cells in AMD 203
7.7 Complex pathways of photoreceptor cell death in: from apoptosis to necroptosis and beyond 204
7.8 Concluding remarks 206
References 208

List of Tables

Table I. Classification of AMD 9
Table II. Activators and mediators of mast cells 48

List of Figures

Figure 1. Senile macular disease by Haab. 5
Figure 2. OCT of AMD eyes 8
Figure 3. The process of sprouting angiogenesis. 21
Figure 4. NLRP3 inflammasome activation and IL-1β production. 40
Figure 5. IL-1R signalling pathway. 42
Figure 6. Extrinsic and intrinsic pathways of apoptosis. 56
Figure 7. Initiation and execution of necroptosis. 59

List of Abbreviations

4HB: 4-helical bundle
AAV: adeno-associated virus
AGEs: advanced glycation products
AIF: apoptosis-inducing factor
AIM2: absent in melanoma 2
AMD: age-related macular degeneration
Ang-2: angiopoietin 2
ANOVA: one-way analysis of variance
APAF1: apoptotic protease-activating factor 1
AREDS: Age-Related Eye Diseases Study
ARMS2: age-related maculopathy susceptibility protein 2
ATP: adenosine triphosphate, adenosine triphosphate
AUC: area under the curve
BAK: BCL-2 homologous antagonist/killer
BAX: BCL 2 associated x protein
BCL-2: B cell lymphoma 2
bFGF: basic fibroblast growth factor

BH3: BCL-2 homology 3

BLE: blue light exposure

BMDMCs: bone marrow-derived mast cells

BMDMs: bone marrow–derived monocytes

BOK: BCL-2 related ovarian killer

BRB: blood-retinal barrier

BSA: bovine serum albumin

CAD: caspase-activated deoxyribonuclease

CARD: caspase recruitment domain

CCL2: chemokine (C-C motif) ligand 2

CCR2: C-C chemokine receptor type 2

cFLIP: FLICE-like inhibitory protein

cGAS: cGMP-AMP synthase

CGRP: calcitonin gene-related peptide

CHP: collagen hybridizing peptide

cIAP: cellular inhibitor of apoptosis proteins

CLRs: c-type lectin receptors

CNS: central nervous system

CNV: choroidal neovascularization

CTMCs: connective-tissue mast cells

CTS: cathepsins

Cxcl10: C-X-C motif chemokine ligand 10

DAMPs: danger-associated molecular patterns

DCC: deleted in colorectal carcinoma

DD: death domain

DED: death effector domain

DEGs: differentially expressed genes

DISC: death-inducing signaling complex

DLL-4: delta-like ligand 4

DMSO: dimethyl sulfoxide

EBM-2: endothelial cell growth basal medium

ECM: extracellular matrix

EMR2: EGF-like module-containing mucin-like hormone receptor-like 2

eNOS: endothelial nitric oxide synthase

ERG: Electroretinogram

ERK: extracellular signal-regulated kinase

ESCRT: endosomal sorting complex required for transport

FACS: fluorescence-assisted cell sorting

FADD: Fas-associated death domain

FasL: Fas ligand

FBS: fetal bovine serum

FcεRI: Fcε receptor I

GCL: retinal ganglion cell layer

GFAP: glial fibrillary acidic protein

GO: gene ontology

GPCR: G protein-coupled receptor

GSEA: gene set enrichment analysis

GSL I: griffonia simplicifolia Lectin I

GWAS: genome-wide association studies

HIF1α: hypoxia-inducible factor 1 alpha

HMGB1: high mobility group box 1 protein

HTRA1: high-temperature requirement A serine peptidase 1

IFNARI: interferon-alpha/beta receptor subunit 1

IgE: immunoglobulin E

IL: interleukin

IL1R1: interleukin-1 receptor 1

IL-1Ra: IL-1 receptor antagonist

IL-1RAcP: interleukin 1 receptor accessory protein

ILC2: innate lymphoid type 2 cells

INL: inner nuclear layer

ip: intraperitoneally

iPSC: induced pluripotent stem cell

IRAKs: IL-1R-associated kinases

JNK: c-Jun N-terminal kinase

kDa: kilodaltons

LC3: microtubule-associated proteins 1A/1B light chain 3B

LPS: lipopolysaccharide

LRR: leucine-rich repeat domain

LUBAC: linear ubiquitin chain assembly complex

MAC: membrane attack complex

MAPK: mitogen-activated protein kinase

M-CSF: macrophage colony-stimulating factor

MDA5: melanoma differentiation-associated protein 5

MLKL: mixed lineage kinase domain-like protein

mMCP: mouse mast cell protease

MMCs: mucosal mast cells

MMPs: matrix metalloproteinases, metalloproteinases

mo MFs: monocyte-derived macrophages

MOMP: mitochondrial outer membrane permeabilization

MPs: mononuclear phagocytes

MRGPR: mas-related G protein-coupled receptor

mtDNA: mitochondrial DNA

mtHsp70: mitochondrial heat shock protein

MyD88: myeloid differentiation primary response 88

NINJ1: nerve injury-induced protein 1

NETs: neutrophil extracellular traps

NF-κB: nuclear factor kappa-light-chain-enhancer of activated B cells

NLRs: NOD-like receptors

nNOS: neuronal nitric oxide synthase

NO: nitric oxide

NOD: nucleotide-binding oligomerization domain

OCT: optical coherence tomography, optimal cutting temperature

ONL: outer nuclear layer

PAF: platelet activating factor

PAMPs: pathogen-associated molecular patterns

PAR: protease-activated receptor

PBS: phosphate-buffered saline

PDGF: platelet-derived growth factor

PEDF: pigment epithelial derived factor

PFA: paraformaldehyde

PlGF: placental growth factor

PMCs: peritoneal mast cells

PNA: peanut agglutinin

PRRs: pattern recognition receptors

PS: phosphatidylserine

Ptc: Patched

PUFAs: polyunsaturated fatty acids

pv MFs: perivascular macrophages

PYD: pyrin domain

RET: rearranged during transfection

RHIM: RIP homotypic interaction

RIG-I: retinoic acid-inducible gene I

RIP: receptor-interacting protein

RIPK3: receptor-interacting protein kinase 3

ROS: reactive oxygen species

RPE: retinal pigment epithelium

SASP: senescence-associated secretory phenotype

SCF: stem cell factor

scRNA-seq: single-cell RNA sequencing

SEM: standard error of the mean

SMAC: second mitochondria-derived activator of caspase

SNPs: single nucleotide polymorphisms

Sting: stimulator of interferon genes

tBID: truncated p15 BID

TGFβ: transforming growth factor β

TIR: toll/interleukin-1 receptor

TLRs: toll-like receptors

TNF receptor–associated factor: TRAF

TNFR: TNF receptor

TNFRS: TNFR superfamily

TNFα: tumor necrosis factor alpha

TPM: transcripts per million

TRADD: TNFR-associated death domain

TRAF6: TNF receptor-associated factor 6

TRAIL: TNF-related apoptosis-inducing ligand

TUNEL: terminal deoxynucleotidyl transferase dUTP nick end-labeling

UMAP: Uniform Manifold Approximation and Projection

UNC5H1-4: Unc-5 homologue 1–4

VEGF: vascular endothelial growth factor

VIP: vasoactive intestinal peptide

XIAP: X-linked inhibitor of apoptosis protein

ZBP1: Z-DNA-binding protein 1

Abstract

Aging is a universal process characterized by changes in various physiological functions, including cognitive decline and increased vulnerability to neurodegenerative disorders such as age-related macular degeneration (AMD). AMD is a major cause of vision loss in the elderly, characterized by progressive damage to the macula. AMD manifests in two main types: wet and dry. In the wet form, there is an abnormal and harmful proliferation of blood vessels that originate from the choroid and extend into the retina, leading to damage. The dry form is marked by the atrophy of retinal pigment epithelium (RPE) and photoreceptors. Immune system dysregulation and cell death are central processes in the pathogenesis of this complex disease. Understanding neuroimmune interactions within the retina is key to developing effective AMD interventions. Human- and animal-derived data demonstrate that mononuclear phagocytes (MPs) contribute significantly to AMD, with interleukin (IL) -1-generating MPs being abundant in AMD. Our study underscores the therapeutic potential of targeting IL-1 signaling, specifically pharmacological allosteric modulation using rytvela, which has shown efficacy in ameliorating inflammatory responses in retinal degeneration. We also present a novel perspective on the heterogeneity of MP populations, emphasizing that not all MPs are equal in their ability to produce IL-1, with a distinct subset, perivascular macrophages, being identified as key players. Within this complex landscape of immune involvement in AMD, it becomes apparent that the role of immune cells extends beyond MPs. Recently, border-associated immune cells have garnered increasing interest for their roles in the disease of the central nervous system (CNS). In this regard, mast cells, traditionally associated with allergic responses and known as frontline defenders of the immune system, have been implicated in the pathology of AMD. Their early activation within the choroid of AMD patients points to a role in the development and progression of the disease. We explored the role of mast cells in sodium iodate-induced retinal toxicity and in laser-induced choroidal neovascularization. In these settings, we demonstrate the activation of mast cells and the potential of mast cell stabilization and tryptase inhibition as novel therapeutic avenues to curb the progression of retinal degeneration, aiming to alleviate the inflammatory milieu, prevent choroidal neovascularization, and protect photoreceptor integrity. The inflammatory cascade implicated in retinal pathology culminates in photoreceptor cell

death, the terminal phase of AMD. This transition from inflammatory response to cellular degeneration results in irreversible visual impairment. We explored mechanisms of inflammation-driven photoreceptor death in retinal degeneration. We demonstrate the activation of necroptosis pathway in photoreceptors, marked by upregulation of mixed lineage kinase domain-like protein (MLKL). We show that MLKL deficiency and pharmacological blockade of necroptosis, particularly through receptor-interacting protein kinase 3 (RIPK3) kinase activity inhibition significantly alleviates photoreceptor loss and neuroinflammation. In summary, this thesis presents an integrated view of AMD, linking the roles of various immune cells with the mechanisms of cell death in the retina. Our study elucidates the complex interplay between immune responses and cell death mechanisms in AMD progression. By pinpointing specific molecular targets, such as IL-1 signaling, mast cell activity, and necroptosis pathways, we reveal promising therapeutic avenues.

Keywords: Age-Related Macular Degeneration, Inflammation, Mononuclear Phagocytes, Interleukin-1β, Mast cells, Choroidal Neovascularization, Cell Death, Necroptosis.

Resumé:

Le vieillissement est un processus universel caractérisé par des changements de diverses fonctions physiologiques, notamment un déclin cognitif et une vulnérabilité accrue aux troubles neurodégénératifs tels que la dégénérescence maculaire liée à l'âge (DMLA). La DMLA est une cause majeure de perte de vision chez les personnes âgées, caractérisée par des lésions progressives de la macula. La DMLA se manifeste sous deux types: humide et sèche. La forme humide est caractérisée par une croissance anormale et délétère de vaisseaux sanguins qui proviennent de la choroïde et s'étendent jusqu'à la rétine, entraînant des lésions. La forme sèche est marquée par l'atrophie de l'épithélium pigmentaire rétinien (EPR) et des photorécepteurs. La dérégulation du système immunitaire et la mort cellulaire sont des processus centraux dans la pathogenèse de cette maladie complexe. Comprendre les interactions neuro-immunes au sein de la rétine est essentiel au développement d'interventions efficaces contre la DMLA. Les données humaines et animales démontrent que les phagocytes mononucléés (PMs) contribuent de manière significative à la DMLA, avec les PMs générant de l'interleukine (IL) -1 étant abondantes dans la DMLA. Notre étude souligne le potentiel thérapeutique du ciblage de la signalisation de l'IL-1, en particulier de la modulation allostérique pharmacologique à l'aide du rytvela, qui s'est révélée efficace pour améliorer les réponses inflammatoires dans la dégénérescence rétinienne. Nous présentons également une nouvelle perspective sur l'hétérogénéité des populations de PMs, en soulignant que toutes les PMs ne sont pas égales dans leur capacité à produire de l'IL-1, un sous-ensemble distinct, les macrophages périvasculaires, étant identifié comme acteur clé. Dans ce paysage complexe d'implication immunitaire dans la DMLA, il devient évident que le rôle des cellules immunitaires s'étend au-delà des PMs. Récemment, les cellules immunitaires associées aux frontières ont suscité un intérêt croissant en raison de leur rôle dans les maladies du système nerveux central (SNC). À cet égard, les mastocytes, traditionnellement associés aux réponses allergiques et connus comme défenseurs de première ligne du système immunitaire, étaient impliqués dans la pathologie de la DMLA. Leur activation précoce dans la choroïde des patients atteints de DMLA suggère un rôle dans le développement et la progression de la maladie. Nous avons exploré le rôle des mastocytes dans la toxicité rétinienne induite par l'iodate de sodium et dans la

néovascularisation choroïdienne induite par le laser. Dans ces contextes, nous démontrons l'activation des mastocytes et le potentiel de la stabilisation des mastocytes et de l'inhibition de la tryptase en tant que nouvelles voies thérapeutiques pour freiner la progression de la dégénérescence rétinienne, visant à atténuer le milieu inflammatoire, à prévenir la néovascularisation choroïdienne et à protéger l'intégrité des photorécepteurs. La cascade inflammatoire impliquée dans la pathologie rétinienne aboutit à la mort des cellules photoréceptrices, phase terminale de la DMLA. Cette transition de la réponse inflammatoire à la dégénérescence cellulaire entraîne une déficience visuelle irréversible. Nous avons exploré les mécanismes de mort des photorécepteurs provoquée par l'inflammation dans la dégénérescence rétinienne. Nous démontrons l'activation de la voie de la nécroptose dans les photorécepteurs, marquée par une régulation positive de la protéine de type domaine kinase de lignée mixte (MLKL). Nous montrons que le déficit en MLKL et le blocage pharmacologique de la nécroptose, en particulier par l'inhibition de l'activité de la protéine kinase 3 interagissant avec les récepteurs (RIPK3), atténuent de manière significative la perte de photorécepteurs et la neuroinflammation. En résumé, cette thèse présente une vision intégrée de la DMLA, reliant les rôles de diverses cellules immunitaires aux mécanismes de mort cellulaire dans la rétine. Notre étude élucide l'interaction complexe entre les réponses immunitaires et les mécanismes de mort cellulaire dans la progression de la DMLA. En identifiant des cibles moléculaires spécifiques, telles que la signalisation de l'IL-1, l'activité des mastocytes et les voies de nécroptose, nous révélons des pistes thérapeutiques prometteuses.

Mots clés : Dégénérescence Maculaire Liée à l'Âge, Inflammation, Phagocytes Mononucléaires, Interleukine-1β, Mastocytes, Néovascularisation Choroïdienne, Mort Cellulaire, Nécroptose.

Acknowledgements

I would like to express my heartfelt gratitude to all those who have contributed to the completion of this thesis.

First and foremost, I am deeply indebted to my supervisor, Sylvain Chemtob for his unwavering support, continuous encouragement and for trusting in my vision. Throughout this journey, he provided me with the freedom to explore and follow my ideas, allowing me to truly own my research and academic development. I also want to extend my sincere thanks to my co-supervisor, Alfredo Ribeiro-da-Silva, for his diligent oversight and ensuring that I adhered to the necessary academic and research requirements. Their attention to detail and constructive feedback have been instrumental in maintaining the rigor and quality of this thesis.

I extend my thanks to my colleagues especially for their collaborative spirit and the discussions that enriched this work.

I am profoundly grateful to my family for your unwavering support, and encouragement throughout this journey.

I would like to acknowledge the financial support provided by the Fonds de recherche du Québec Santé, Vision Research Health Network, and Department of Pharmacology & Therapeutics of McGill University. which made this research possible.

Contribution to original knowledge

The results contained in this thesis present a comprehensive overview of the interplay between inflammation and cell death in the pathogenesis of retinal degeneration, highlighting novel mechanisms that drive photoreceptor loss in AMD. Original findings contribute to the knowledge base and introduce new targets for treating AMD. The findings presented in this thesis resulted in the following four manuscripts:

1. Dabouz R, Cheng CWH, Abram P, Omri S, Cagnone G, Sawmy KV, Joyal JS, Desjarlais M, Olson D, Weil GA, Lubell W, Rivera JC, Chemtob S. An allosteric interleukin-1 receptor modulator mitigates inflammation and photoreceptor toxicity in a model of retinal degeneration. Published in Journal of Neuroinflammation, 17(1):359, 2020.

2. Dabouz R, Abram P, Chemtob S. Mast cell activation contributes to subretinal inflammation and photoreceptor loss in an oxidative stress model of AMD (In preparation).
3. Dabouz R, Abram P, Rivera JC, Chemtob S. Mast cells promote angiogenesis in experimental choroidal neovascularization (In revision).
4. Dabouz R, Abram P, Gautam A, Omri S, Braverman N, Balachandran S, Chemtob S. Necroptosis blockade alleviates photoreceptor toxicity and dampens neuroinflammation in an experimental model of retinal injury (In preparation).

Author contributions

This dissertation adheres to the manuscript-based format following the guidelines from the Faculty of Graduate Studies and Research at McGill University. The following section outlines the specific contributions of the authors to each of the manuscripts incorporated into the dissertation:

Chapter 3: An allosteric interleukin-1 receptor modulator mitigates inflammation and photoreceptor toxicity in a model of retinal degeneration

Rabah Dabouz: lead investigator, study design, performed experiments, collected and analyzed data, manuscript writing.
Penelope Abram and Colin Cheng: Assisted in performing experiments.
Samy Omri, Michel Desjarlais, David Olson, William Lubell: logistic assistance.
Gael Cagnone, Khoushnouma V Sawmy, Jean-Sebastien Joyal: bioinformatic analysis
Jose Carlos Rivera: manuscript editing.
Sylvain Chemtob: principal investigator, grant acquisition, manuscript editing.

Chapter 4: Mast cell activation contributes to subretinal inflammation and photoreceptor loss in an oxidative stress model of AMD

Rabah Dabouz: lead investigator, study conceptualization and design, performed experiments, collected and analyzed data, manuscript writing.

Penelope Abram: experimental design, performed experiments, collected and analyzed data.
Sylvain Chemtob: principal investigator, grant acquisition.

Chapter 5: Mast cells promote angiogenesis in experimental choroidal neovascularization

Rabah Dabouz: lead investigator, study conceptualization and design, performed experiments, collected and analyzed data, manuscript writing.
Penelope Abram: Assisted in performing experiments.
Jose Carlos Rivera: manuscript editing.
Sylvain Chemtob: principal investigator, grant acquisition.

Chapter 6: Necroptosis blockade alleviates photoreceptor toxicity and dampens neuroinflammation in an experimental model of retinal injury

Rabah Dabouz: lead investigator, study conceptualization and design, carried out experiments, collected and analyzed data, manuscript writing.
Penelope Abram: carried out experiments, collected and analyzed data.
Avishekh Gautam: technical advice.
Samy Omri and Nancy Braverman: logistic support.
Siddharth Balachandran: scientific advice.
Sylvain Chemtob: principal investigator, grant acquisition.

CHAPTER 1 - INTRODUCTION

1. Introduction

Vision is more than just the perception of light; it serves as a vital element of perception, offering a distinctive perspective through which the world can be navigated and engaged. In tandem with other senses, reason, and introspection, vision represents an integral means by which a portion of the nature of existence is understood and knowledge is gained. With aging, however, this sensory channel undergoes transformation. The structures of the eye experience various alterations, such as the lens becoming less flexible, leading to difficulty focusing on close objects, a condition known as presbyopia. Additionally, the risk of developing age-related eye conditions like cataract, glaucoma, and macular degeneration increases (1). These changes can gradually impair visual acuity and perception, highlighting the delicate nature of vision with aging.

Among these, age-related macular degeneration (AMD) is a prominent issue. It stands as a major global health concern, primarily impacting the aging population. Its significance is rooted in its prevalence and in its capacity to drastically reduce the quality of life with profound psychological repercussions for affected individuals by impeding central vision (2, 3). AMD is a progressive eye condition that affects the macula, a small portion of the retina that is responsible for sharp, central vision. It is one of the primary causes of vision loss in older adults (4). Early AMD is characterized by the presence of drusen: lipid, carbohydrate, protein deposits within the Bruch's membrane (5). There are two primary manifestations of late AMD: the dry, also known as atrophic or geographic atrophy, and the wet (vasoproliferative) forms. The dry form is characterized by the loss of retinal pigment epithelium (RPE) and photoreceptors. It is the most common form, accounting for about 85-90% of AMD cases. Wet AMD, though less common, is more severe and is characterized by the growth of abnormal blood vessels under the retina, leading to the leakage of blood and fluid which can cause rapid and severe vision loss (6).

The complex etiology of AMD, while not entirely understood, intertwines with multiple factors. Beyond age, genetic determinants and environmental elements, such as smoking, diet, and obesity, play critical roles (7). These factors particularly amplify oxidative stress and chronic inflammation, both of which are recognized central pillars in

the progressive pathogenesis of AMD (8, 9). Laser photocoagulation, photodynamic therapy, and anti-angiogenic agents have shown promise in managing the symptoms of wet AMD. Yet, dry AMD remained a therapeutic challenge until the recent introduction of an anti-complement 3 drug. However, its impact, as evidenced in two phase 3 clinical trials, has been tempered by its lack of efficacy (10, 11). Given the global trend of an aging population, understanding and addressing AMD is of escalating importance.

This thesis aims to explore the interconnected biological processes of inflammation and cell death—both central to manifestations of AMD. Our goal is to shed light on the intricate mechanisms underpinning AMD and reveal potential therapeutic avenues. The initial exploration focuses on the potential of allosteric modulation of interleukin-1 receptor 1 (IL1R1) to alleviate the effects of dry AMD. Our findings highlight the efficacy of IL1R modulation in mitigating subretinal inflammation, gliosis and its protective effects on photoreceptors in a light model of dry AMD. Additionally, we trace the origin of IL-1β and its receptor to mononuclear phagocytes (MPs) in astroglial and vascular cells.

The study of inflammation in AMD was largely dominated by investigations into MPs. These cells were often the focal point of research, setting the precedent for understanding the inflammatory underpinnings of AMD. However, while MPs have provided invaluable insights, it is imperative to broaden our horizons and explore other cellular contributors to this complex pathology. Along these lines, the second manuscript explores a less-studied area by looking into the role of mast cells, which are usually linked to allergic reactions. We showcase their early activation in response to oxidative stress and establish their contribution to RPE injury, subretinal inflammation, and, consequently, photoreceptor death. The third paper reveals the impact of activated mast cells on wet AMD. We exhibit how these cells foster choroidal neovascularization (CNV) and contribute to extracellular matrix remodeling in a laser model of wet AMD. The fourth paper details the pathways leading to photoreceptor death in an oxidative stress model of AMD. Our work shows simultaneous activation of apoptosis and necroptosis, highlighting that a combined blockade of caspase and MLKL activation offers a potential therapeutic avenue for retinal protection.

CHAPTER 2 – LITERATURE REVIEW

2.1 Age-related macular degeneration

2.1.1 Retinal degeneration: historical perspective

The study of the eye and its diseases can trace its roots back to ancient civilizations. Descriptions of blindness and visual impairment pepper numerous ancient texts, such as the Ebers Papyrus from around 1500 BC (12). This ancient Egyptian text is among the oldest preserved medical documents and references eye diseases, treatments, and surgeries, though not explicitly retinal degeneration. A significant step in ocular understanding came during the medieval period. A prominent Andalusian scholar, Averroes (1126–1198 AD), was the first to propose that the retina possesses photoreceptor properties (13). Yet, a more comprehension of retinal function and its diseases would not emerge until the 19th century. Advancements in histological tools and the invention of the ophthalmoscope revealed the retina and its cellular structure in unprecedented detail. This century witnessed the first descriptions in medical literature of pigmentary irregularities and drusen in the retina.

The first descriptions in medical literature on pigmentary irregularities and drusen in the retina began in mid 19th century. In 1854, Carl Wedl reported the presence of colloid bodies in the choroid of the eye of elderly men. These colloid bodies were considered to be malformed or imperfectly developed cells because of the lack of nuclei and cell membranes (14). At that time, the Dutch ophthalmologist Franciscus Cornelis Donders, was one of the first to adopt the use of the newly invented ophthalmoscope. Donders began studying the eyes of living patients to better understand the differences he noticed between his observations with the ophthalmoscope and those from histological examination (15, 16). In 1855, Donders documented degenerative changes in the retina, RPE and choroid with loss of photoreceptors in the aged retinas. He noted the presence of yellowish-white bodies that he referred to as colloidal spheres ("Colloidkugeln"), likely originating from the RPE nuclei and which he found could displace the retina and were rarely absent in the eyes of individuals aged 70-80 years (15, 17). Importantly, Donders believed that these changes could have an impact on retinal function and contribute to visual disturbances. Donders also pointed out that the white spots, which he had seen in elderly people with amblyopia (reduced vision in the elderly) using the ophthalmoscope,

are more likely to correspond to colloidal species (17). In the following year, Heinrich Muller described spherical or “drusenoid” deposits found in clusters on the inner surface of the choriocapillaris. He named these deposits “drusen” because of their resemblance to geodes, with the term being derived from the German word for geode, which refers to a rock cavity lined by crystals. Drusen, as described by Muller, likely correspond to colloidal bodies or spheres observed by Wedl and Donders. Muller reported that drusen could be detached along with the Bruch’s membrane (referred to as glass lamella) from the choriocapillaris. He suggested that the origin of drusen was related to the thickening of Bruch’s membrane on the inner side of the choroid and behind pigment cells (18).

The first reports of AMD appeared in late 19th century. In 1875, Jonathan Hutchinson reported a choroid with numerous small yellowish-white deposits (drusen) and hemorrhage at the fovea. He suggested that the disease, termed central chorioretinal disease in senile persons, initially affected the choroid, with the retina being impacted secondarily (19). The same year, Pagenstecher and Genth originally described a neovascular lesion accompanied with choroidal inflammation, which is now recognized to be a feature of wet AMD (20). In 1876, Hubert Sattler also documented the presence of blood vessels between RPE and Bruch’s membrane (21). In 1884, Edward Nettleship noted the presence of a large area of atrophied choroid in both eyes of a 60-year-old woman, a case that he called central senile areolar choroidal atrophy (22). In 1885, Otto Haab described an ocular condition that he termed senile macular disease, which primarily involves pathological changes in the RPE and may propagate to the choroid under certain circumstances (Fig. 1) (23). The disease is typically bilateral and leads to serious visual disturbance. Interestingly, while Haab recognized that drusen are age-related changes, he dismissed their connection with the development of senile macular disease (24). It appears that descriptions provided by Nettleship and Haab align with characteristics of dry AMD.

It was only many decades later that Donald Gass postulated that drusen, atrophic lesions, and neovascular lesions are linked to the same degenerative disease process, although the relationship between their aetiologies has yet to be determined (25). Therefore, the term age-related macular degeneration now encompasses both the atrophic and the neovascular forms. To date, AMD persists as a main cause of visual

impairment worldwide and ongoing research endeavors to uncover new insights into the underlying mechanisms, refining therapies for this sight-threatening condition and enhancing early diagnosis.

A

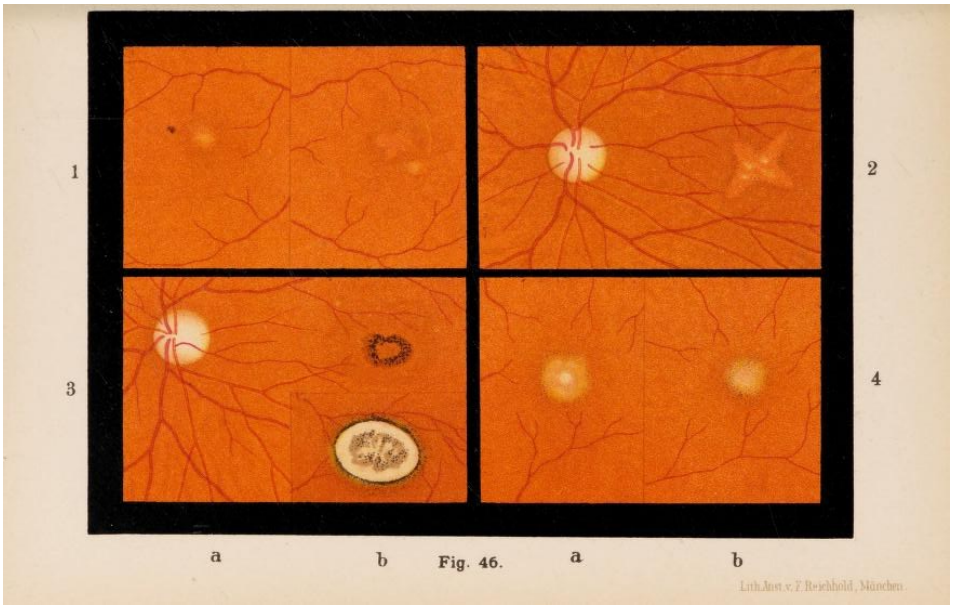

B

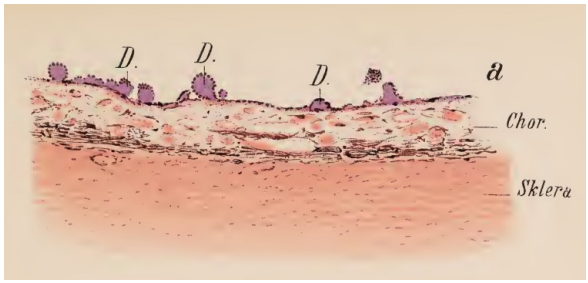

Figure 1. Senile macular disease by Haab.

(A) Senile macular disease as observed by Haab (23). (1a, b) Macula of both eyes of a 70-year-old-patient. (2a, b) No information provided (3a) The early stages of the disease three months after the onset of visual disturbance. (3b) The same region six months later. (4a, b) Two maculae of a 74-year-old patient. (B) Drusen of the vitreous layer (23).

2.1.2 Epidemiology and risk factors

AMD is a primary cause of visual impairment and blindness worldwide (4). The worldwide prevalence of AMD has been assessed through a comprehensive analysis

using systematic reviews and meta-analysis (26). In the age range of 45-85 years, the prevalence of early-stage AMD was found to be 8.01%, while the prevalence of late-stage AMD was estimated at 0.37% (26). The prevalence of AMD varies across different ethnic populations. For instance, AMD is more frequent in Caucasian than in black people (27). The prevalence of AMD in European individuals was 12.33% while Asian and African populations had a prevalence of 7.38% and 7.53%, respectively (26). Due to an increase in the global population, it is predicted that number of individuals with AMD will increase from 196 million in 2020 to 288 million in 2040 (26). Asia which accounts over half of the global population is expected to see an increase in the number of cases reaching 113 million cases by 2040, the highest globally. Europe will rank second due to its high prevalence making it another greatly affected continent (26).

AMD is a complex disease that is influenced by numerous risk factors. Aging, gender, racial background, diet, smoking, obesity, atherosclerosis, cardiovascular disease, have all been suggested to increase the risk of AMD (7, 28) but advanced age is the primary risk factor for AMD (29). Studies have shown an exponential increase with age in the prevalence of AMD, particularly late-stage AMD. Late-stage AMD affects approximately 1.4% of those aged 70, 5.6% of 80-year-olds, and 20% of 90-year-olds (29). Smoking is an important modifiable risk factor associated with an overall four-fold increase in incidence (30, 31). There is evidence indicating a connection between diet and AMD, particularly late-stage AMD. Notably, Mediterranean diets have aroused interest due to their association with a reduced risk of progressing to late-stage AMD (32, 33). Growing evidence supports a link between higher physical activity levels and a reduced incidence and progression of AMD, with high physical activity providing protection against the development of early AMD (34). The current evidence regarding the female sex as a risk factor for AMD is inconclusive (28).

Overwhelming evidence suggests that genetics play a role in the etiology of AMD, as supported by family aggregation studies and twin studies. The prevalence of AMD has been observed to be higher in first-degree relatives of AMD patients compared to relatives of controls (35). Twin studies revealed that a significant portion of AMD variation could be attributed to genetic factors, with heritability estimates ranging from 46% to 71% (36). Genome-wide association studies (GWAS) have pinpointed variants in the CFH gene at

1q31 locus (37, 38, 39) and age-related maculopathy susceptibility protein 2 (ARMS2)/ high-temperature requirement A serine peptidase 1 (HTRA1) genes at 10q26 locus (40, 41, 42), which are major contributors to the total heritability of late AMD, although distinguishing the causal variants has been challenging. A GWAS conducted by the International AMD Genomics Consortium identified 52 single nucleotide polymorphisms (SNPs) at 34 genetic loci to be significantly associated with AMD (43). These loci are related to distinct biological pathways such as inflammation, complement system, lipid transport, extracellular matrix remodeling, and angiogenesis (43). A more recent meta-analysis of GWAS, employing a multiple trait analysis approach, identified 69 SNPs at the genome wide significance (44). In summary, exploring epidemiology, risk factors, and genetic contribution to AMD provides insights into the mechanisms underlying its pathogenesis.

2.1.3 Classification

AMD is categorized using different classification systems, each providing different insights into the severity of the disease. Traditionally in a clinical setting, AMD has been classified as either dry or wet. For clinic-based studies and trials, the Age-Related Eye Diseases Study (AREDS) severity scale is a commonly used system. This scale assigns risk factors based on the presence of large drusen, pigment abnormalities, and medium drusen in both eyes. The AREDS simplified severity scale allocates a risk factor for each eye with large drusen, another for each eye with pigment abnormalities, and yet another if both eyes possess medium drusen but lack large ones (45). A more comprehensive classification is the Beckman classification, which is adopted both clinically and in research. Severity classification is based on the size of drusen, the presence or absence of pigmentary irregularities, and the existence of lesions linked to advanced-stage complications (Table I). This classification considers persons with no visible drusen or pigmentary abnormalities as persons with no signs of AMD. The presence of small drusen (< 63 μm) is a sign of normal aging rather than AMD (46). Early AMD is defined by the presence of medium-sized drusen (63–125 μm) without RPE abnormalities (hyperpigmentation or hypopigmentation) in the macular region. Intermediate AMD is characterized by extensive medium drusen (> 125 μm), the presence of pigmentary

abnormalities, or both. Late AMD is defined by the presence of signs indicating neovascular or atrophic AMD, or both (46). Neovascular AMD, also called wet AMD, is characterized by sub-RPE, subretinal, or intraretinal neovascularization. Atrophic AMD, also known as geographic atrophy or dry AMD, involves the loss of photoreceptors and RPE, presenting as a sharply defined pale area with exposed underlying choroidal blood vessels (47). It is essential to note that the Beckman classification is currently the most widely recognized and utilized system.

Despite these classifications being primarily relied on for clinical examinations or color fundus photography, advancements in imaging techniques, such as optical coherence tomography (OCT), have unveiled more detailed aspects of AMD. This progress has led to the development of new classification systems (Fig. 2) (6). The use of spectral-domain OCT has revealed earlier disease manifestations leading to the emergence of terms like "nascent geographic atrophy", which describes changes preceding drusen-associated atrophy. These changes, including the subsidence of the outer plexiform and inner nuclear layers or the formation of a hyporeflective, wedge-shaped band within the boundaries of the outer plexiform layer, could act as early surrogate endpoints in intervention trials for the initial stages of dry AMD (48).

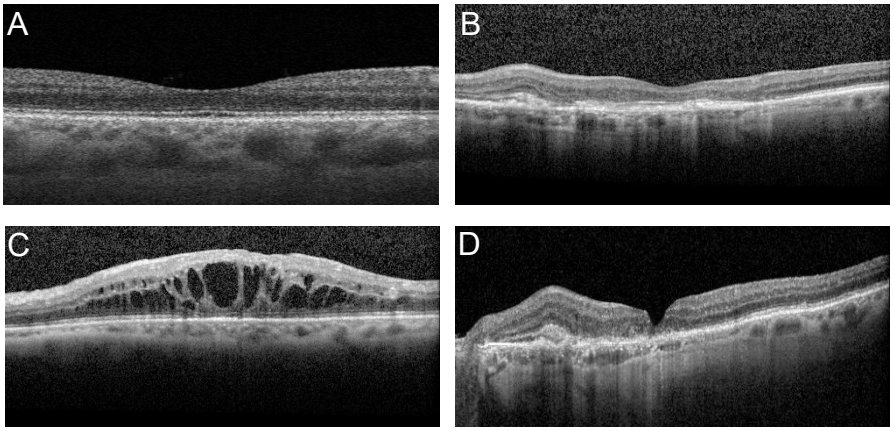

Figure 2. OCT of AMD eyes

Retinal OCT illustrating (A) normal retina, (B) drusen, (C) geographic atrophy, (D) wet AMD. Images kindly provided by Dr. Marisse Masis Solano.

Table I. Classification of AMD

AMD Classification	Description
No AMD	No visible drusen or pigmentary abnormalities in the macular region
Normal aging	Small drusen (< 63 μm) with no pigmentary abnormalities in the macular region
Early AMD	Presence of medium-sized drusen (63–125 μm) without RPE abnormalities in the macular region. Patients may show no symptoms or minor central vision distortion and difficulty reading in low-light conditions
Intermediate AMD	Extensive medium drusen (> 125 μm) or presence of pigmentary abnormalities in the macular region. May cause mild to moderate vision changes depending on the extent and location of abnormalities
Late AMD	Presence of signs indicating neovascular or atrophic AMD, or both: • Neovascular AMD: characterized by sub-RPE, subretinal, or intraretinal neovascularization. • Atrophic AMD: Involves the loss of photoreceptors and RPE, presenting as a sharply defined pale area. Exposes underlying choroidal blood vessels. Can lead to significant central vision loss

Neovascular lesions of AMD have been determined using fundus fluorescein angiography. The use of OCT scans has led to the identification of neovascular disease based on fluid presence. This prompted a change in nomenclature, proposing the histological localization of neovascularization. Type 1, 2, and 3 lesions were identified based on their location and features. Type 1 lesions represent neovascularization beneath the RPE, whereas type 2 neovascularization arises from the choroid and invades the subretinal space between the RPE and the neuroretina. Type 3 lesions are

characterized by intraretinal neovascularization that progresses to the subretinal space (defined as retinal angiomatous proliferation) (6).

2.1.4 Pathophysiology

AMD is a degenerative disease affecting the outer neural retina, RPE, Bruch's membrane, and the choroid. However, the locus of the primary insult and pathogenesis of AMD remain topics of debate. Key markers of the disease include both diffuse and focal thickening of Bruch's membrane, drusen formation, as well as the emergence of hypo- and hyper-pigmented regions within the RPE. This disease complexity suggests that its onset and progression likely result from a combination of processes. Genetic predisposition undoubtedly plays a part in the development of AMD. However, environmental factors such as smoking, diet, obesity, and atherogenesis also have a significant influence. At the molecular level, elements like inflammation, oxidative stress, RPE dysfunction, extracellular matrix (ECM) remodeling, and lipid mishandling are all believed to contribute critically to the progression of the disease. These underlying factors lead to anatomical and physiological alterations in the photoreceptors, RPE, Bruch's membrane, and the choriocapillaris, dictating the disease's trajectory (7).

2.1.4.1 Aging-related changes in the retina

Throughout a person's life, the macula experiences structural changes due to aging, which can lead to age-related visual impairments and decline (49). The RPE plays a crucial role in maintaining retinal homeostasis by transporting nutrients to photoreceptor cells, removing waste products, and performing additional functions. Aging-related changes in the RPE include melanin loss, drusen development, and microvilli atrophy (49). Lipofuscin granules accumulate in the RPE cells throughout life, eventually occupying up to 19% of cytoplasmic volume by 80 years of age (50). Lipofuscin accumulation is due to lysosomal malfunction and reduced capacity of photoreceptor outer segment degradation. This contributes to oxidative stress and impairs energy production and lysosomal enzyme activity in RPE cells (51).

Aging affects the Bruch's membrane, a structure that regulates metabolic exchange between the RPE and choriocapillaris, through increased thickness, reduced

permeability, and composition alteration (52, 53). The Bruch's membrane thickens due to the deposition of less soluble collagen fibers and accumulation of oxidized RPE metabolic waste products (54), including lipoproteins containing apolipoproteins B and E, cholesterol, and 7-ketocholesterol (55, 56, 57). The Bruch's membrane becomes more brittle primarily due to calcification (54), and accumulates advanced glycation end products (58). Enzyme activity involved in ECM processing decreases with age, resulting in ECM debris accumulation (49). Additionally, basal deposits and drusen, which are waste material accumulations, form between the RPE and Bruch's membrane (59). These changes disrupt efficient nutrient and waste exchange between the choriocapillaris and the RPE, creating a suboptimal outer retinal environment.

The choroid undergoes age-related changes, including reduced thickness and decline in choriocapillaris density (60, 61). Aging results in increased membrane attack complex deposition at the choriocapillaris level, which may contribute to their degeneration (62). These changes can have an impact on nutrient and oxygen supply to the outer retina.

Aging leads to significant photoreceptor loss, with rods degenerating before cones (63, 64, 65). This contributes to a decline in scotopic sensitivity and a prolonged dark adaptation time. It is not clear why rods in the central retina, which are adjacent to cones, are more susceptible to aging. The decline in cones may be attributed to their reliance on the release of rod-derived cone viability factor (66).

Collectively, age-related retinal changes can contribute to visual acuity decline and to predisposition to AMD development. Understanding these changes may offer insights for developing therapeutic strategies to counteract the detrimental effects of aging on the retina.

2.1.4.2 Oxidative stress

As one of the most metabolically active tissues in the human body (67), the retina is especially considerably vulnerable to oxidative stress, a key driver in the pathogenesis of AMD (8). Oxidative stress arises when an imbalance occurs between oxidants and antioxidants in favor of oxidants, disrupting redox signaling (68). In this regard, redox signaling and reactive oxygen species (ROS) play an important role in the regulation of a

variety of physiological processes. However, uncontrolled levels of ROS can cause oxidative damage to lipids, proteins, and nucleic acids which lead to cell dysfunction (69). The susceptibility of the retina to oxidative stress arises due to high oxygen consumption, extensive exposure to irradiation, the presence of a high proportion of polyunsaturated fatty acids in the photoreceptor outer segments, and an abundance of photosensitizers in the retina and RPE. Moreover, the process of phagocytosis of photoreceptor segments by the RPE generates ROS, further contributing to the oxidative burden (70). Nitric oxide and its by-products, along with other reactive nitrogen species, contribute to cellular signaling, inflammation, and the occurrence of nitrosative stress; a phenomenon that is hypothesized to be associated with AMD pathogenesis (71).

Given its elevated metabolic activity and high mitochondrial content, the RPE significantly contributes to ROS production. This phenomenon becomes more pronounced as age advances, exacerbating the generation of ROS in the RPE (72). The origin of ROS is mainly attributed to the mitochondrial electron transport chain, with additional contributions from other enzymes such as NADPH oxidase and xanthine oxidase (73). In addition, photoreceptors, which are abundant in polyunsaturated fatty acids (PUFAs), are highly prone to oxidative damage. The oxidation of PUFAs, aggravated by the aging process and weakened antioxidant defenses, plays a significant role in causing structural deterioration of cell membranes, ultimately leading to photoreceptor degeneration (74). The RPE engulfs and removes the oxidized membranes of outer segments, a process critical for mitigating oxidative stress in photoreceptors. However, these phagocytosed outer segments break down into by-products that form lipofuscin, within RPE cells. Lipofuscin, due to its molecular composition, exhibits photosensitivity and consequently heightens the vulnerability of the RPE to light-induced damage as age advances (75) and leads to complement activation (76). Moreover, RPE cells, being postmitotic, are at increased risk of accumulating mitochondrial DNA (mtDNA) damage. The phagocytosis of photoreceptor outer segments and ROS generation cause damage to mtDNA and other constituents of mitochondria resulting in mitochondrial dysfunction, RPE degeneration, and inflammatory responses (51). Modifiable factors such as cigarette smoking and high-fat diets are additional contributors to the cumulative burden of oxidative stress (77).

In AMD patients, the retina has been found to contain advanced glycation-end products, and lipid peroxidation products including malondialdehyde, 4-hydroxynonenal, and carboxyethylpyrrole, indicative of heightened oxidative stress (78). Upon their formation, lipid peroxidation end products initiate the activation of the nuclear factor kappa-light-chain-enhancer of activated B cells (NF-κB) signaling pathway. Subsequently, this activation triggers the release of diverse pro-inflammatory cytokines, thereby establishing a pro-inflammatory environment that may potentially contribute to the progression of AMD (79). Advanced glycation products (AGEs), which include chemically altered lipids, nucleic acids, and proteins, are found in higher levels in eyes with AMD. AGEs also induce the production of ROS, either directly or through interaction with their receptor, RAGE. Furthermore, AGEs can elevate the expression of vascular endothelial growth factor (VEGF) in RPE, which has the potential to trigger angiogenesis (80). In addition, RAGE plays a role in promoting inflammation through NF-κB signaling (9).

Although there is clear evidence linking oxidative stress to AMD, the causality remains uncertain, and it remains unknown when the levels of oxidative stress transition from serving physiological signaling roles to instigating pathologic damage. Furthermore, it is unclear to what extent exogenous and avoidable sources of oxidative stress can overload the defense mechanisms of RPE cells against oxidation (72).

2.1.4.3 RPE dysfunction

2.1.4.3.1 Mitochondrial dysfunction

The role of mitochondrial malfunction in RPE dysfunction is being recognized, particularly with regards to its impact on AMD (51). RPE cells, rich in mitochondria, experience high ROS levels which can damage the mitochondria and, in turn, disrupt various cellular functions (51). Microscopic observations revealed that with aging, there is a decline in both the quantity and size of mitochondria. Moreover, individuals with AMD exhibited more significant changes in mitochondria compared to controls of the same age (81). Notably, increased levels of mitochondrial DNA damage have been detected in the RPE of individuals affected by AMD; this damage was confined to the macular and peripheral RPE and did not extend to other regions of the retina (82).

Proteomic analysis on the RPE of human eyes afflicted with AMD showed alterations in mitochondrial proteins (83). Specifically, RPE cells in AMD patients exhibited reduced levels of α, β, and δ subunits of the adenosine triphosphate (ATP) synthase, which is crucial for energy production through oxidative phosphorylation (84). The impairment of ATP synthase has been linked to a variety of human diseases (85). Additionally, there was reduced expression of mitochondrial heat shock protein (mtHsp70) in the RPE cells of AMD patients (84). mtHsp70 acts as a molecular chaperone facilitating the import and folding of proteins within the mitochondria (86). It plays a critical role in the assembly of cytochrome C oxidase and ATP synthase (87, 88). In summary, the morphological and proteomic changes observed in the RPE cells of individuals with AMD could adversely affect mitochondrial functionality and energy production. This, in turn, has the potential to result in cellular dysfunction and contribute to the progression of AMD.

mtDNA damage in RPE can occur under stress conditions. For instance, experimentally induced phagocytosis, where cultured human RPE cells engulf photoreceptor outer segments, and blue light exposure, have been shown to induce mtDNA damage and a decline in mitochondrial function (89, 90). Interestingly, in Alu RNA-induced human RPE degeneration, there is an escape of mtDNA that triggers the cGMP-AMP synthase (cGAS)-stimulator of interferon genes (Sting) pathway and activates the innate immune system (91). Oxidative stress can also lead to damage in mtDNA, which is then translocated to the cytoplasm, where it activates an intracellular DNA receptor called Z-DNA-binding protein 1 (ZBP1) (92). Activation of ZBP1 by mtDNA results in the expression of proinflammatory markers in RPE cells. Furthermore, the extracellular vesicles released from the RPE cells were shown to contain mtDNA fragments. These extracellular vesicles can induce ZBP1 activation in microglia and promote a proinflammatory response (92). In conclusion, mtDNA damage in RPE cells under stress conditions has multiple implications, involving not only a decline in mitochondrial function but also activation of inflammatory pathways via innate immune sensors. This highlights the complexity of the interactions between mitochondrial dysfunction and inflammation in the context of RPE degeneration.

2.1.4.3.2 Defects in autophagy

The RPE is crucial for maintaining retinal function through mechanisms such as phagocytosis and autophagy. However, these functions can become impaired with aging and in conditions such as AMD (93, 94). Autophagy, a lysosome-mediated degradation process, allows the RPE to rejuvenate its components by recycling older mitochondria and other cellular waste. Nevertheless, with advancing age, this system can be impaired, leading to an accumulation of cellular debris, potential drusen formation, and RPE degeneration (94, 95). Interestingly, there is an elevated number of autophagosomes in the RPE of AMD patients, but despite this accumulation, the efficiency of autophagy decreases in AMD RPE cells. Specifically, when exposed to starvation conditions, AMD RPE cells demonstrated a failure to initiate autophagy, as seen by the lack of the increase in the microtubule-associated proteins 1A/1B light chain 3B (LC3)-II/LC3-I ratio, a key step in autophagy (94). Additionally, impaired autophagy can promote inflammasome activation, angiogenesis, and cell death contributing to AMD progression (96, 97). Therefore, these studies point toward a role of impaired autophagy in RPE as a contributory factor to the pathophysiology of AMD.

2.1.4.3.3 RPE senescence

Senescence, defined as an irreversible cell cycle arrest, is intertwined with a multitude of complex biological processes that include development, tissue repair, aging, and age-related disorders (98) It has been postulated that senescence contributes to the etiology of RPE degeneration, with both in vitro and in vivo studies providing evidence of RPE cells transitioning into a senescent state (99, 100). Additionally, the presence of senescent RPE cells was also observed in patients with diabetic retinopathy (101). Remarkably, cigarette smoking, an established risk factor for AMD, has been shown to induce premature senescence in the human RPE cell line, ARPE-19 (102). Furthermore, a correlation has been observed between advancing age in mice and an elevated expression of senescence markers such as $p16^{INK4a}$, p21, and β-galactosidase activity (103). A subsequent study introduced a doxorubicin-induced mouse model of RPE senescence, which displayed pathological features akin to those observed in the retina of patients with AMD. These included increases in subretinal aggregates, a thickening of

the Bruch's membrane, and a decline in visual function (104). Importantly, the targeted removal of senescent cells using a senolytic therapy resulted in the preservation of retinal function in this model. β-galactosidase-positive RPE cells were also noted in laser-induced CNV and Alu RNA-induced RPE degeneration, as well as in aged mice. Consistently, the implementation of a senolytic treatment in these models mitigated retinal complications (104).

One key feature of senescent cells is a characteristic known as senescence-associated secretory phenotype (SASP). In this phenotype, senescent cells secrete a range of substances, including inflammatory mediators, growth factors, and proteases (105). Specifically, senescent RPE cells were shown to secrete a variety of factors with diverse effects, such as VEGF and inflammatory cytokines (102). These secretions can potentially intensify neovascularization and inflammation, both of which are detrimental to the outer retina. Moreover, peripheral RPE cells have the ability to proliferate and replenish damaged or lost cells in the central retina through a compensatory repair mechanism (106). Yet, senescence in (peripheral) RPE cells, could potentially limit this reparative process thereby leading to a substantial reduction in the RPE cell population. While research on RPE senescence is still emerging, it is an area of growing interest and ongoing investigation.

2.1.4.3.4 RPE cell death

Research into the advanced stages of AMD has delved into the mechanisms underlying RPE cell death, which play a significant role in the development of geographic atrophy (107). These mechanisms are diverse, with cells succumbing to death in a multitude of ways. Terminal deoxynucleotidyl transferase dUTP nick end-labeling (TUNEL), a technique detecting DNA fragmentation in nuclei, has confirmed RPE cell death in postmortem eyes of patients with geographic atrophy (108). However, RPE loss seems to occur via multiple cell death forms.

Evidence of apoptosis in RPE cells comes from the detection of activated caspase-3 immunoreactivity in the RPE of human eyes with geographic atrophy (109). Apoptosis is defined as a programmed form of cell death that is generally not accompanied by a significant inflammatory response (110). A connection was observed between the

accumulation of Alu RNAs, repetitive elements in the human genome, and RPE cell toxicity (109). Further, when mouse RPE cells were treated with Alu RNA and IL-18, RPE degeneration ensued via caspase-8-mediated apoptosis (111). Amyloid-beta treatment of RPE activates apoptosis through the upregulation of caspase-3, and pyroptosis, through the NLRP3 inflammasome activation and proteolytic cleavage of full-length gasdermin D into N-terminal gasdermin D fragment (112). Pyroptosis, a form of lytic programmed cell death activated by inflammasomes, culminates in the loss of plasma membrane integrity (110). Notably, an interplay between apoptosis and pyroptosis was seen when lipofuscin-loaded ARPE-19 cells and primary human RPE cells were irradiated with blue light (113).

Necroptosis, a programmed form of necrosis mediated by receptor-interacting protein kinase (RIPK)3 and mixed lineage kinase domain-like (MLKL) (114) and which results in a strong inflammatory response, was also proposed as a possible mechanism for RPE death. When RPE cells are exposed to high concentrations of hydrogen peroxide, the resulting cell death bears the hallmark characteristics of necrosis (115, 116). Likewise, Hanus et al reported that oxidative stress induced by hydrogen peroxide or tert-butyl hydroperoxide led to RPE cell necrosis, with no detection of apoptosis or pyroptosis (117). It was further suggested that necroptotic cell death occurs in response to sodium iodate, as evidenced by morphological necrosis features, RIPK3 aggregation, high mobility group box 1 protein (HMGB1) release, and the protective effects of a RIPK1 inhibitor necrostatin (118). dsRNA analog poly (I:C) was also proposed to cause RPE necroptosis (119). Nevertheless, the limitation of these studies is that the activation of MLKL, a key component to validate the necroptosis pathway, was not explored (120).

Recently, ferroptosis, an iron-dependent regulated form of cell death (121), was also implicated in RPE cell death in response to hydrogen peroxide or tert-butyl hydroperoxide, along with necroptosis and apoptosis (122). This was determined by indicators such as glutathione depletion, lipid peroxidation, and increased levels of iron (Fe^{2+}), alongside the protective effect of ferrostatin-1 and deferoxamine, known inhibitors of ferroptosis. Similar results were observed in sodium iodate-induced RPE cell loss (123, 124).

In summary, the various ways RPE cells die contribute to the complexity of AMD progression. Whether it’s apoptosis, pyroptosis, necroptosis, ferroptosis, or other forms

of cell death, the loss of these cells is central to the development of geographic atrophy. This highlights the importance of ongoing research in this area.

2.1.4.4 Choroidal involution

The precise contribution of the choroid in the pathogenesis of AMD remains uncertain. The loss of the choriocapillaris could potentially occur either as a cause or as a consequence of the loss of photoreceptors and RPE. Based on histological examinations, a linear relationship between the loss of RPE and choriocapillaris in geographic atrophy was established. In regions of RPE atrophy, there was a drastic reduction in vascular area compared to regions with intact RPE in geographic atrophy eyes and control non-diseased eyes (125). A decrease in choriocapillaris vascular density and the presence of ghost capillaries were associated with drusen formation (126). Although complete loss of choriocapillaris was not seen even in areas with total RPE atrophy, the remaining capillaries were significantly constricted and exhibited a loss of fenestrations in their endothelium which may impair the exchange of nutrients and waste products (125). The pronounced constriction observed in the surviving capillaries may be linked to reduced levels of endothelial nitric oxide synthase (eNOS) and neuronal nitric oxide synthase (nNOS) in neurons and RPE of the choroid. These enzymes are essential for the generation of nitric oxide, a potent vasodilator agent (127).

Analysis of choriocapillaris ultrastructure and transport systems revealed that the number of fenestrations per millimeter of Bruch's membrane significantly decreased within the surviving choriocapillaris in the atrophic area of geographic atrophy. An increase in the caveolae area per choriocapillaris endothelial cell was also reported. These findings suggest a potential involvement of choriocapillaris transport in the pathogenesis of AMD (128). The presence of areas with RPE loss alongside normal-appearing choriocapillaris in geographic atrophy led to the hypothesis that RPE degenerates prior to choroidal thinning (125). This observation further aligns with the role of RPE-derived VEGF in the maintenance of the choriocapillaris (129).

In contrast, in wet AMD eyes, choriocapillaris dropout occurred without prior RPE atrophy near the CNV area, causing a significant reduction in vascular area when compared to the eyes of aged control individuals (125). It should be noted that treatment

of CNV with anti-VEGF leads to a reduction in sub-foveal total choroidal thickness. This indicates that anti-VEGF therapy has an impact not only on the neovascular membrane but also on the underlying choroid (130, 131). Laser Doppler flowmetry showed a progressive decline in choroidal blood flow with increasing risk of CNV, and eyes with CNV exhibited a significant reduction in choroidal volume and flow, suggesting hypoxia being a driver of neovascularization (132, 133). Collectively, these findings provide insights into the changes that occur in the choroid in AMD and suggest a complex interplay between the choroid and other retinal structures in the disease.

2.1.4.5 Choroidal neovascularization

Neovascularization refers to the formation of new blood vessels and occurs through two main mechanisms: sprouting angiogenesis and vasculogenesis. While angiogenesis involves new vessel formation from pre-existing vessels through endothelial cell proliferation, migration, and tubular structure formation, vasculogenesis is distinct as it involves the development of new vessels from endothelial progenitor cells (134).

The angiogenesis process initiates with the activation of quiescent endothelial cells within existing blood vessels, primarily triggered by signals such as VEGF that is produced in response to increased expression of hypoxia-inducible factor 1 alpha (HIF1α) (135). This activation stimulates the secretion of proteolytic enzymes, including matrix metalloproteinases (MMPs) and serine proteases, which degrade the basement membrane and the ECM, facilitating the migration of endothelial cells towards the angiogenic stimuli. The ECM, a complex network of proteins and carbohydrates, provides essential structural and biochemical support to cells and is composed mainly of laminins, collagen IV, and heparan sulfate proteoglycans (136, 137).

During the sprouting phase, endothelial cells differentiate into ‘tip’ and ‘stalk’ cells. A VEGF-A gradient plays a crucial role in this phase by creating a pioneering, highly motile tip cell that guides the nascent sprout. These tip cells, which exhibit minimal proliferation, extend filopodia and lamellipodia, directing the sprout toward the angiogenic stimulus. VEGF-A also stimulates the expression of delta-like ligand 4 (DLL-4) in these tip cells. DLL-4 then binds to Notch receptors on adjacent stalk cells, modulating their behavior by downregulating VEGFR-2 expression and thus preventing excessive angiogenesis. The

stalk cells, following the tip cells, proliferate and contribute to the elongation of the sprout and mediate lumen formation. This process involves complex cell rearrangements and the formation of intracellular vacuoles, essential for transforming a sprout of endothelial cells into a functional vessel. The final phase of angiogenesis involves the maturation and stabilization of the newly formed vessels. This is where pericytes, recruited by signals such as platelet-derived growth factor (PDGF), transforming growth factor β (TGFβ), and angiopoietin play a crucial role. Pericytes and smooth muscle cells provide structural support and stability to the new vessels (Fig. 3). Additionally, new basement membrane materials are deposited, further stabilizing the vessels. Once tissue vascularization is adequately restored, the levels of proangiogenic factors diminish, and endothelial cells revert to their quiescent state, characterized by their highly interconnected structure through junctional molecules (138, 139). Yet, angiogenesis can enter a regression phase under certain microenvironmental influences or due to the formation of non-functional neovessels, occurring through sprout retraction or apoptosis.

In the context of CNV, endothelial cells in the choroidal vasculature become activated in response to various stimuli, including hypoxia or inflammatory factors. Once activated, these endothelial cells proliferate and migrate through the Bruch's membrane (140). VEGF is a major driver of CNV. In AMD, elevated levels of VEGF are often observed, contributing to the pathological process of neovascularization (141). VEGF binds to its receptors (VEGFR1 and VEGFR2) on endothelial cells, initiating a cascade of intracellular signaling that promotes endothelial cell proliferation, migration, and survival. These actions facilitate the formation of new blood vessels (142). VEGF also increases vascular permeability, which leads to the leakage of fluid and proteins from these new vessels, contributing to retinal edema and further vision impairment.

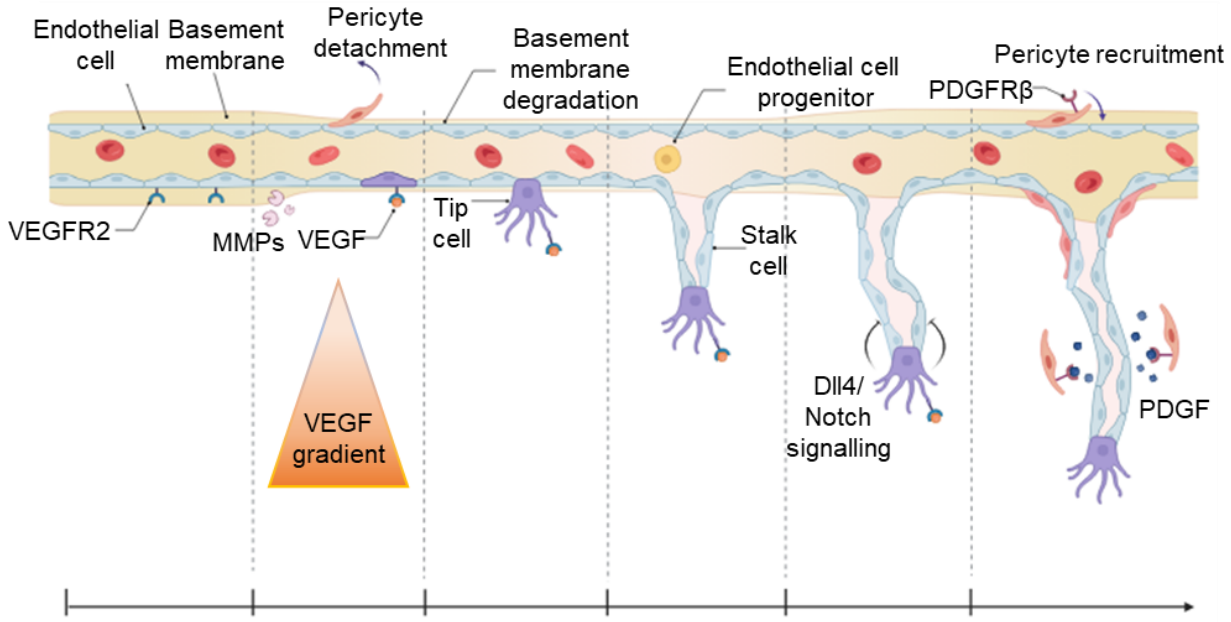

Figure 3. The process of sprouting angiogenesis.

Illustration of the sequential stages of angiogenesis, starting from the activation of endothelial cells, sprouting phase, lumen formation, and stabilization of the vessels. Figure generated by Biorender.

Initial animal studies identified the mobilization of bone marrow-derived cells, especially hematopoietic stem cells and endothelial progenitor cells, in the development of CNV (143, 144). These findings were corroborated by similar observations in human CNV (145). However, subsequent studies demonstrated a limited role for bone marrow-derived cells in endothelial differentiation during wound healing and angiogenesis (146, 147, 148). In contrast to the limited endothelial differentiation from bone marrow-derived cells, choroid tissue-resident progenitors, particularly side population cells, were shown to have proliferative capabilities and contribute to choroidal angiogenesis during laser-induced neovascularization. This suggests their involvement in the formation of endothelial cells within newly formed blood vessels (149).

2.1.4.6 Inflammation

The pathogenesis of AMD is intimately linked to Inflammation and the immune system. The interplay of several factors, including immune cells and the complement system, largely contributes to the chronic inflammatory aspect of the disease. The link between inflammation and AMD has been investigated in numerous studies, where a variety of inflammatory markers were found to be elevated in AMD patients. Some of these markers include C-reactive protein, complement factors, and certain cytokines (150). MPs, a group of cells that include microglia, macrophages, and monocytes in the retina play important roles in inflammation and AMD (151). These cells release pro-inflammatory cytokines and chemokines, which contribute to inflammation and cellular damage in the retina. In fact, infiltration of MPs into the subretinal space, which is physiologically devoid of immune cells, highlights their contribution to the inflammatory processes in AMD leading to degeneration of photoreceptors and CNV (151). The complement system, a component of the innate immune system, is widely accepted as a contributory factor in AMD pathogenesis. Complement proteins such as C3, C5, and CFH have been found in drusen, and their dysregulation can lead to complement activation, leading to subsequent inflammation (152). A detailed description of inflammation in AMD will be provided in later sections.

2.1.5 Treatment and limitations

Currently, there is significant interest and investment in finding effective treatments for AMD, with numerous drugs in various stages of development. The majority of these drugs are still in the early phases of discovery and pre-clinical testing, focusing primarily on addressing the vaso-proliferative form of AMD. Many of these drugs target VEGF, either alone or in combination with other agents that target angiogenic factors.

2.1.5.1 Anti-VEGF therapy for wet AMD

Current therapies for retinal vasculopathies are effective but present significant risks and drawbacks. Before anti-VEGF therapy, laser photocoagulation was effective for well-demarcated lesions but was only applicable to a small percentage of patients and can cause serious damage to the retina (153). Photodynamic therapy using a

photosensitizing dye (verteporfin) has shown significant reduction in vision loss for predominantly classic CNV, replacing photocoagulation as the standard treatment (153). The introduction of anti-VEGF agents for the treatment of neovascular AMD, the first of which appeared in 2004, marked a keystone breakthrough in medicine and ophthalmology (154). These agents primarily reduce vascular permeability and macular edema; however, they do not prevent CNV progression (155).

Bevacizumab (Avastin®, Genentech, Inc.), initially developed as a treatment for colorectal cancer, is a humanized monoclonal antibody specifically designed to target VEGF-A. It has been used off-label for the treatment of AMD (156, 157). Ranibizumab (Lucentis®, Genentech, Inc.) is a fully humanized monoclonal antibody fragment that binds to multiple isoforms of VEGF-A. It was first approved by the Food and Drug Administration (FDA) in 2006 for the treatment of neovascular AMD, making it a targeted treatment option for this condition (158, 159). Aflibercept, a 2012 FDA-approved drug for the treatment of AMD, is a soluble decoy receptor fusion protein. It merges the binding domains of human VEGF receptors 1 and 2, along with the human Fc portion of immunoglobulin G, enabling it to effectively bind to VEGF-A, VEGF-B, and placental growth factor (PlGF) (160, 161). Faricimab is a novel humanized bispecific monoclonal antibody which can independently bind and neutralize both angiopoietin 2 (Ang-2) and VEGF-A. It was designed for intravitreal injections to treat AMD and was approved by the FDA in 2022 (162).

Novel gene therapy approaches have emerged as innovative methods to genetically modify retinal cells and generate anti-VEGF proteins (163). Ongoing trials are currently evaluating the effectiveness of RGX-314 (REGENXBIO Inc.) and ADVM-022, and early results are demonstrating promising outcomes. RGX-314 employs adeno-associated virus (AAV)8 vectors to produce a monoclonal antibody fragment akin to ranibizumab, intended for subretinal or suprachoroidal routes of administration. On the other hand, ADVM-022 utilizes the AAV.7m8 capsid to generate an aflibercept-like protein, intended for intravitreal injections (163).

While anti-VEGF therapy has demonstrated success in improving vision, it has resulted in significant concerns. Some patients may develop geographic atrophy as a response to the treatment, contributing to apprehension towards its use (164, 165).

Another issue is the dependency on repeated dosing for vision stability, imposing burdens on finances and quality of life. Moreover, even with optimal anti-VEGF therapy, the risk of progression to fibrotic scars remains (166). Given these concerns, recent attention has shifted toward investigating non-VEGF mechanisms for blood vessel formation as alternatives to anti-VEGF therapies.

2.1.5.2 Drugs targeting advanced dry AMD

Drugs targeting advanced dry AMD can be classified into the following categories: neuroprotective, antioxidant, anti-inflammatory (mostly anti-complement and inflammasome inhibitors) visual cycle modulators, and stem cells (167). Notably, anti-complement therapies are heavily based on genetic studies but are administered to patients without requiring genetic testing. Of these, pegcetacoplan (APL-2 [Apellis]) is the first and only FDA-approved drug for geographic atrophy, having received recent approval in 2023. It functions as a complement C3 inhibitor, specifically a pegylated peptide that binds to C3 and prevents its cleavage (10). The OAKS study demonstrated a statistically significant but clinically mild reduction in the progression of geographic atrophy lesion with APL-2 treatment. The reduction ranged from 16% with monthly intravitreal injections to 22% with injections administered every other month. However, the DERBY study did not meet the primary endpoint for lesion growth reduction, achieving only a 12% reduction (10, 11). Avacincaptad (IVERIC Bio) is another FDA-approved C5 inhibitor for geographic atrophy, which has shown a reduction in the progression of geographic atrophic lesions. Avacincaptad pegol demonstrated a mean reduction of 27% over 12 months, which further increased to a mean reduction of 30% over 18 months (168, 169). It is worth mentioning that adverse events of neovascularization were noted in clinical trials for both pegcetacoplan and avacincaptad (11, 169).

Visual cycle modulators based on the structure of retinoic acid or inhibitors of RPE65, an enzyme essential in recycling all-trans-retinyl esters to 11-cis-retinol for phototransduction, have failed to meaningfully attenuate the progression of geographic atrophy over the past decade (170). Stem cells offer potential in treating degenerative conditions such as AMD, where there is a loss of RPE. However, there are still challenges

to overcome, including the risk of improper integration of cells resulting in abnormal synapse formation, retinal detachment, and most notably, inflammation (171, 172).

2.1.6 Animal models for AMD

The complex etiology of AMD has led to the creation of diverse animal models for its study. Although no single model fully replicates the complexity and progression of AMD, several approaches, including rodent and transgenic models, have been useful in mimicking critical aspects of the disease, which is essential for advancing pharmacological treatments (173, 174). However, it is important to note that rodents do not have a macula, limiting their ability to fully model AMD. Exposure to intense light, especially in the blue spectrum, can damage the RPE and photoreceptors, triggering subretinal inflammation leading to photoreceptor degeneration. This model has been useful in studying the dry form of AMD. The underlying mechanism is thought to involve oxidative stress, which is a known factor in AMD pathology (175). Sodium iodate can also be used to induce an advanced form of geographic atrophy. It is a chemical that specifically targets the RPE cells, causing their degeneration and leading to retinal atrophy reminiscent of geographic atrophy. When administered systemically or subretinally, it creates a pattern of RPE damage followed by photoreceptor degeneration (176). Although this model effectively replicates the RPE cell loss seen in late-stage AMD, it does not capture the early-stage drusen formation or the chronic progression typical of the disease. For neovascular AMD, the laser photocoagulation technique is employed. The procedure involves applying a series of laser burns to the Bruch's membrane, which results in an inflammatory response and subsequent neovascularization. This model has been used extensively to study the pathogenesis of CNV and to evaluate anti-angiogenic therapies, such as anti-VEGF treatments (177).

2.2 Inflammation

2.2.1 Overview of inflammation and homeostasis

In order to illustrate the relationship between inflammation and AMD, it is imperative to comprehend the fundamental aspects of inflammation and homeostasis. These two physiological processes are essential for the human body's ability to maintain

internal stability and respond to external challenges such as infections and injuries. Homeostasis refers to the complex network of feedback loops that help the body maintain a stable internal environment, ensuring optimal function. It involves the continuous monitoring and regulation of various physiological parameters, such as temperature, pH, ions, and nutrient levels. Additionally, at the cellular level, homeostasis encompasses the maintenance of cell integrity and regulation of ECM composition which is crucial for maintaining tissue structure and function (178).

When a disruption in homeostasis occurs, stress responses are triggered to restore homeostasis. Depending on the severity and nature of the challenge, this may escalate to inflammation, which is aimed at defending and ultimately restoring homeostasis (178). Inflammation is an adaptive response that becomes active when other homeostatic control mechanisms are insufficient. It usually occurs during severe disturbances in homeostasis like infections, tissue injuries, or the presence of foreign bodies. However, inflammation can also be triggered by milder tissue malfunctions, with the degree of tissue malfunction influencing the magnitude of the inflammatory response (179).

The initiation of acute inflammation, whether caused by tissue injury or infection, heavily relies on the innate immune system. Tissue-resident cells, including macrophages, mast cells, dendritic cells, fibroblasts, epithelial cells, and sensory neurons play a crucial role in monitoring the state of cells and tissues (178, 179, 180). These cells employ a diverse range of sensors including, but not limited, to pattern recognition receptors (PRRs) to identify specific patterns found on invading pathogens (known as pathogen-associated molecular patterns or PAMPs) and signals indicating damage or stress within the host (known as danger-associated molecular patterns or DAMPs). These receptors consist of both membrane-bound receptors that survey the extracellular environment and endosomal compartments (e.g., toll-like receptors [TLRs] and c-type lectin receptors [CLRs]), as well as cytoplasmic receptors that detect nucleic acids (e.g., DNA sensors like absent in melanoma 2 [AIM2], and RNA sensors such as retinoic acid-inducible gene I [RIG-I], and melanoma differentiation-associated protein 5 [MDA5]), along with the intracellular nucleotide-binding oligomerization domain (NOD)-like receptors (NLRs) (181). During stress or tissue malfunction, these tissue-resident

immune cells receive different signals via PRRs, which allow them to detect PAMPs and DAMPs. In response to these signals, the cells produce various mediators, such as cytokines, chemokines, proteolytic enzymes, lipid mediators, complement components, vasoactive amines, and vasoactive peptides (179, 180). They also act by recruiting other immune cells, such as monocytes and neutrophils, to the site of inflammation, thereby enhancing the immune defense against invading pathogens or tissue damage. Additionally, these molecules affect target tissue and induce local changes in tissue composition and function facilitating the necessary adaptations for resolving the disturbance and restoring homeostasis (182). Through their actions, these inflammatory mediators play a key role in coordinating the complex interplay between immune cells, promote tissue repair, and support the overall inflammatory response.

The production of these inflammatory mediators is tightly regulated and coordinated to ensure an effective immune response. Their purpose is to remove or sequester the source of the disturbance, allowing the host to adapt to the abnormal conditions and, ultimately, restore functionality and homeostasis to the tissue (179). In cases where abnormal conditions are transient, a successful acute inflammatory response occurs. This response involves the activation of anti-inflammatory mechanisms and the production of specialized pro-resolving mediators, which helps restore the system to its basal homeostatic set points.

In instances of mild or sustained tissue stress that do not escalate to full-scale inflammation, a distinct state known as 'parainflammation' emerges. Parainflammation represents a moderated and typically localized response, serving as a transitional phase between basal homeostasis and overt chronic inflammation. It aims to adapt to and mitigate stress, facilitating tissue recovery and balance restoration. Nonetheless, this state is crucially poised; inadequate regulation or prolonged activation of parainflammation can inadvertently progress to chronic inflammation. Chronic inflammation ensues when the inflammatory stimulus persists or when homeostatic restoration is incomplete, leading to altered physiological set points. This maladaptation promotes sustained inflammatory signaling, tissue dysfunction, and potentially the onset of chronic disease (179, 183).

2.2.2 Immune privilege in the retina

The retina is a delicate structure responsible for visual function which faces significant vulnerability to internal and external damage due to its intricate neuronal composition and limited capacity for repair. The retina has a specialized built-in tolerance mechanism called retinal immune privilege (184). Immune privilege, first discovered by Peter Medawar, refers to a property of certain tissues, including the eye and the brain, where foreign grafts placed in these tissues can survive for extended periods without eliciting an immune response. Various ocular compartments, such as the anterior chamber, vitreous cavity, and subretinal space, have been found to promote the survival of allogeneic grafts (185). Ocular immune privilege has evolved to balance pathogen clearance and prevention of immunopathogenic tissue collateral damage, which could impair visual function. The eye's unique features, such as its delicate visual axis and limited regenerative capacity, require immune protection against pathogens while avoiding intense, destructive inflammation to maintain retinal homeostasis (186, 187).

A major component of retinal immune privilege is the blood-retinal barrier (BRB), which maintains the integrity of the retinal vasculature and prevents the entry of immune cells into the retina, thereby establishing immune privilege in the retina (184). In addition, while the absence of lymphatic drainage is not fully confirmed, the presence of immunosuppressive signals further contribute to immune privilege by modulating immune cell activity (187). Specifically, the subretinal space, which lies between the RPE and the photoreceptor outer segments, is devoid of MPs in physiological conditions due to the influence of immunosuppressive signals derived from the RPE and inner neurons.

Immunomodulatory molecules, such as Fas ligand, TGF-β, somatostatin, thrombospondin and pigment epithelial derived factor (PEDF), are derived from the RPE and play crucial roles in suppressing the presence and promoting the clearance of immune cells in the subretinal space (188, 189, 190). Defects in the expression of Fas ligand or its receptor Fas result in impaired clearance of subretinal MPs (191). Additionally, factors from inner retinal neurons including CX3CL1, CD200, SIRP1α, CD22, and translocator protein, inhibit the activation of microglial cells, that are located in the inner retina in physiological conditions (151). CX3CL1, acting as the ligand for its receptor, CX3CR1, plays a critical role in mediating an inhibitory signal on microglial cells (192).

The absence of CX3CR1 leads to recruitment of MPs and impaired MP clearance in the subretinal space (193).

Given that AMD is an age-related disease, it is reasonable to consider that with aging, the balance between immune privilege and immune activation can become disrupted. Inflammaging, characterized by hyperactivation of the innate immune response (194), may potentially impact immune privilege mechanisms in the retina, influencing immune responses and increasing vulnerability to immune-mediated damage. Aging-related changes, such as a decline in the expression of key immune regulatory molecules like CD200 and CX3CL1, contribute to dysregulated microglial activation and subretinal inflammatory responses in the aging retina (184). Additionally, age-associated increases in the chemokine (C-C motif) ligand 2 (CCL2) results in the recruitment of circulating monocytes to the subretinal space (195). Further investigation is needed to fully understand the relationship between inflammaging and immune privilege in retinal disorders.

2.2.3 Chronic inflammation in AMD

There is an expanding body of evidence supporting the notion that inflammation plays a crucial role in the initiation and progression of AMD (9, 193, 196, 197). During the aging process, the retina experiences a continuous, mild oxidative stress, which triggers the activation of the retinal immune system and initiates a reparative para-inflammatory response. However, in the case of AMD, this regulatory para-inflammatory mechanism becomes dysregulated, resulting in persistent low-grade inflammation. This chronic inflammation damages the macula and compromises the integrity of the BRB, leading to the development of retinal lesions and a breach in retinal immune privilege (198). Various genetic variants identified as risk factors are related to immune and inflammatory pathways. Notably, genes related to the complement system, such as CFH, complement factor B, and chemokines such as CX3CR1, have a strong association with AMD (199). Additionally, other gene variants such as apolipoprotein E and HTRA1 have also shown to promote subretinal inflammation in animal models of AMD (191, 200, 201). These genetic variants can impact the regulation of the inflammatory response and contribute to the chronic inflammation observed in AMD.

Inflammation in AMD is mediated by a diverse range of cellular and molecular processes. The complement system, consisting of a cascade of proteins playing a crucial role in immune response and defense against pathogens (202), has been implicated in AMD. Different complement components, including C3, C5, and the membrane attack complex (MAC), have been found in drusen of AMD patients, and their levels are elevated in the serum of these patients (203). Complement activation is also found in animal models where it contributes to chronic inflammation and the recruitment of leukocytes in the retina. CFH binding to CD11b in MPs hinders the activation of CD47 by TSP-1, resulting in the inhibition of their elimination from the subretinal space. This mechanism contributes to the persistence of MPs and the establishment of chronic non-resolving inflammation (204). MAC formation and deposition of C3 were observed in neovascularization lesions following laser photocoagulation. Deletion of C3 or inhibition of MAC formation led to a reduction in the area of neovascularization (205). Complement fragments C3a and C5a act as chemoattractants, to recruit leukocyte and promote laser-induced CNV through recruitment of immune cells and stimulation of VEGF expression (206). Complement system activation was also observed in sodium iodate-induced retinal degeneration, where C3a and C5a contribute to the loss of photoreceptors through the recruitment of circulating MPs (207, 208, 209).

Immune cells play a pivotal role in the pathogenesis of AMD, actively contributing to the chronic inflammation and tissue damage observed in the disease. Histological studies revealed that MPs are the main immune cells in the subretinal space and photoreceptor layer of patients with AMD (193, 210, 211). Indeed, several studies have correlated MP accumulation in the subretinal space with photoreceptor loss and CNV (151). In early AMD patients, infiltrating neutrophils have been detected in the retina and sub-macular choroid, indicating their presence in AMD tissue sections (212). Additionally, elevated levels of neutrophil extracellular traps (NETs) have been observed in the serum of individuals with AMD, suggesting their involvement in the disease. Notably, amyloid β1-40, the main amyloid-beta component of AMD-associated drusen, has been identified as a potential inducer of NET formation (213). Hence, it is plausible that drusen could serve as sites for the formation of NETs within the retina. In the context of laser-induced CNV, early inflammatory responses involve the infiltration of neutrophils (214, 215). Depletion

of neutrophils has been found to reduce CNV responses and decreased expression of VEGF protein (215). Neutrophils were also shown to contribute to the disruption of RPE barrier integrity through the secretion of MMP9 (216).

The choroid serves as a site of inflammation associated with AMD. Emerging research has implicated mast cells, resident cells within the choroid, in the development of AMD (217). An elevated number of mast cells and their degranulation within the choroidal regions affected by early AMD, exudative AMD, and geographic atrophy have been observed. These mast cells are mainly found in deeper layers housing larger choroidal vessels (217). These findings highlight the potential role of mast cells in AMD pathogenesis. In addition, recent research has implicated choroidal gamma delta (γδ) T cells in animal models of AMD. in laser-induced CNV lesions, infiltrating γδ T cells were found to produce IL-17 (218). In the sodium iodate model of retinal degeneration, γδ T cells express genes encoding immunosuppressive cytokines, such as IL-4 and IL-10, with γδ T-cell deficiency resulting in profound retinal damage (219).

The contribution of adaptive immunity in AMD pathogenesis remains less clear and uncertain. Cytotoxic CD8+ T cells were found in the macular choroid of eyes with drusen, suggesting the importance of the local environment (220). Additionally, the presence of autoantibodies against retinal antigens has been detected in AMD patients, raising the hypothesis of an autoimmune component in AMD (221, 222, 223).

Understanding the role of chronic inflammation in AMD is vital, as it can lead to the development of novel therapeutic strategies aimed at modulating the inflammatory response to treat or prevent AMD.

2.3 Mononuclear phagocytes in AMD

2.3.1 Mononuclear phagocytes

MPs are a group of immune cells that play a crucial role in development, maintaining homeostasis, defending against pathogens, and modulating inflammatory responses. They are part of the innate immune system, which is the first line of defense against pathogens and foreign substances. The innate immune system is non-specific, meaning it reacts to a wide range of invaders, as opposed to the adaptive immune system, which specifically tailors responses to each invader. The MP system consists of a variety

of cells including monocytes, macrophages, microglia, dendritic cells, and their precursors (224). While monocytes can serve as precursors to macrophages and dendritic cells, it is important to note that not all macrophages and dendritic cells originate from monocytes (224). Monocytes are formed in the bone marrow and released into the bloodstream. While circulating in the blood, monocytes can migrate into tissues in response to various signals, such as chemokines and cytokines, and differentiate into macrophages or dendritic cells (225). During an inflammatory response, monocytes are among the first cells to migrate to the site of infection or injury, where they can contribute to inflammation through the production of cytokines and other mediators (225). Dendritic cells are specialized in antigen presentation to T cells. They capture, process, and present antigens to T cells, acting as a bridge between the innate and adaptive immune systems (226). Dendritic cells originate from bone marrow precursors and are found in peripheral tissues. Upon activation, they migrate to lymphoid organs where they are essential for initiating T cell responses (227). Macrophages are highly phagocytic cells found in tissues throughout the body. They engulf pathogens, cellular debris, and foreign substances. Macrophages are also involved in tissue repair and remodeling, and they play a role in regulating inflammation (228). Microglia are resident macrophages of the central nervous system (CNS). They originate from yolk sac progenitors during embryonic development (229) and are involved in immune surveillance within the CNS, synaptic pruning, and responding to injury (230). Perivascular macrophages are located adjacent to blood vessels, especially within the CNS. These macrophages were initially thought to originate from blood monocytes (231); however, recent studies have revealed that these macrophages have distinct developmental origins. They arise early during embryogenesis and are derived from the yolk sac, similar to parenchymal microglia. Notably, perivascular macrophages are maintained independently of circulating monocytes, persisting over extended periods without relying on replenishment from circulating myeloid cells (232, 233). These specialized macrophages fulfill important roles in regulating immune responses, phagocytosis, and maintaining the integrity of blood-tissue barriers (234). Perivascular macrophages are also involved in neuroinflammation and can contribute to disease progression within the CNS (235).

2.3.2 Mononuclear phagocytes in the posterior segment of the eye

MPs have an important role within the eye, where they maintain homeostasis, regulate the immune system, promote blood vessel growth, and respond to injuries and diseases. Since the eye is an immune-privileged site, MP function is carefully orchestrated to prevent excessive inflammation that could compromise the integrity of the retina. The posterior segment of the eye is populated by various types of MPs. Among them, retinal microglia are specialized resident macrophages located in the ganglion cell layer and in the inner and outer plexiform layers of the retina (236). Retinal microglia are integral to the developing and mature retina. They participate in developmental neuronal cell death through phagocytosis, contribute to synaptic pruning, neuroplasticity, neurogenesis, and organization of retinal angiogenesis (237). In the adult retina, microglia adopt a highly branched morphology and establish an organized territorial network. They incessantly scan the surface of retinal neurons, playing an indispensable role in debris clearance and in maintaining retinal homeostasis. In addition, microglia interact with Müller cells, instigating the release of neurotrophic factors that support photoreceptor survival and promote recovery from retinal injuries (238). While microglia are not acutely required for the maintenance of retinal architecture or survival of retinal neurons, they are essential for the maintenance of synaptic structure and synaptic transmission in the outer plexiform layer. In fact, microglial depletion resulted in the degeneration of photoreceptor synapses in the outer plexiform layer, leading to a progressive reduction in retinal light responses (239). Importantly, microglia play a significant role in retinal degenerative diseases, including AMD, glaucoma, and diabetic retinopathy. In pathological conditions, microglia transition into a state of pathological activation, releasing inflammatory mediators that contribute to tissue damage and disease progression (240).

Furthermore, the retina houses a population of perivascular macrophages. These macrophages reside in close proximity to the retinal blood vessels, specifically on the outer surface of the vascular endothelial basal lamina and are closely associated with pericytes (241). In a sodium iodate-induced retinal degeneration model, autofluorescent perivascular macrophages, in conjunction with microglia, were observed migrating from the inner retina to the photoreceptor layer and subretinal space (242). In the presence of blood-retinal barrier disruption, perivascular macrophages demonstrate the ability to

migrate toward the site of leakage (242). However, further studies are required to elucidate the specific functions of perivascular macrophages in retinal health and disease, potentially through targeted depletion of this population.

Resident macrophages are also found within the choroid. These choroidal macrophages form extensive networks and exhibit a dendriform or elongated fusiform morphology and are closely associated with the choroidal vasculature (243). Although the precise role of choroidal macrophages is not extensively studied, they are believed to possess antigen-presenting capabilities and play a role in maintaining the structure of choroidal blood vessels, as well as clearing debris and dead cells (244). In addition to choroidal macrophages, dendritic cells have been identified in the choroid (245, 246), and have been associated with severe uveitis (247). During autoimmune inflammation, dendritic cells can also be found in peripheral regions of the retina, with their detection being rare under normal conditions. These dendritic cells are believed to contribute to the activation of autoreactive T cells, potentially playing a role in the development of diseases such as experimental autoimmune uveoretinitis (247). The mechanisms underlying antigen presentation and interaction between dendritic cells and T cells in the retina remain incompletely understood. Further research is needed to elucidate the specific roles of dendritic cells in these ocular compartments and their impact on inflammatory processes and diseases. In pathological conditions such as retinal inflammation or degenerative diseases, it is vital to highlight that the integrity of the blood-retinal barrier may be compromised, allowing monocytes from the bloodstream to infiltrate the retina, where they can transform into macrophages and participate in the local inflammatory response (248).

2.3.3 The role of mononuclear phagocytes in AMD

MPs play an integral role in the pathophysiology of AMD and considerably contribute to the chronic inflammation detailed in the previous section (151). Pathological conditions such as AMD instigate an influx of MPs into the subretinal space and photoreceptor layer such as seen in patients with geographic atrophy and CNV (193, 210, 211). The number of MPs is also increased in the choroid of AMD patients (249). Additionally, these cells are also prominent in the subretinal space of mouse models with

accelerated age- and light- associated photoreceptor degeneration, sodium iodate-induced RPE loss, and laser-induced CNV (161, 163, 165, 182). This invasion is typically a response to photoreceptor or RPE stress where MPs serve as scavengers of cell debris and toxic by-products. Interestingly, the response efficiency of MPs to tissue injury is diminished in older mice compared to younger ones (250).

Importantly though, the nature of MP subpopulations present in the subretinal space have been challenging to identify due to the lack of specific markers. To overcome this limitation, fate mapping experiments have been conducted to shed light on the cellular composition of the subretinal space during light-induced and sodium iodate-induced retinal degeneration (251, 252). These experiments have revealed that microglia, rather than monocytes, are the predominant population in the subretinal space. Interestingly, recruited monocytes were found to occupy the inner retina instead. On the other hand, due to the expression of C-C chemokine receptor type 2 (CCR2) mainly on monocytes and not microglia, the presence of CCR2-positive cells in the subretinal space led to the conclusion that monocytes can also occupy the subretinal space in response to light challenge and in inherited retinal degeneration (195, 253). Moreover, depletion of circulating monocytes using systemic clodronate liposome reduced the accumulation of MPs in the subretinal space, supporting the presence of monocyte-derived MPs in the subretinal space (195). Of note, the depletion of circulating monocytes did not completely eliminate the presence of MPs in the subretinal space. This observation indicates that the remaining populations of MPs in the subretinal space are likely to be composed of microglia or resident macrophages. In summary, the presence of microglia/resident macrophages in the subretinal space is well-supported by existing evidence. However, the ability of circulating monocytes to invade and occupy the subretinal space is still a topic of ongoing debate and investigation.

In specific conditions, such as amyloid β-induced retinal degeneration, MP invasion can serve a protective role; the recruitment of MPs to the subretinal space limits photoreceptor loss and RPE degeneration, potentially by facilitating the clearance of amyloid β (254). This protective role is further demonstrated by the fact that MP depletion results in RPE structure disorganization in light-induced retinal degeneration (251), and photoreceptor loss in models of retinal detachment (255). However, MPs are a proverbial

double-edged sword, capable of both preserving and disrupting retinal integrity. In addition to their protective response, activated MPs can adopt a maladaptive (deleterious) response, contributing to the progression of retinal degeneration (248).

Depletion or inhibition of circulating monocyte recruitment, achieved through the deletion of the chemokine CCL2 or its receptor CCR2 (CCR2), as well as pharmacological inhibition of CCR2, has demonstrated a protective effect against photoreceptor degeneration in light-induced retinal degeneration (195, 256). Similarly, this approach has demonstrated efficacy in reducing the area of laser-induced CNV (257, 258, 259).

The role of MPs in AMD is mediated by a complex network of mediators, which play crucial roles in modulating the immune response and driving inflammatory processes. Several key cytokines, IL-1β, tumor necrosis factor alpha (TNFα), and IL-6, all of which have been implicated in AMD pathogenesis (151). Furthermore, MPs can phagocytose living damaged photoreceptors by phagoptosis via IL-1β-dependant mechanism (260, 261).

2.4 Interleukin-1

2.4.1 Overview of interleukin-1

Interleukins are a group of cytokines that play crucial roles in modulating the immune system and inflammatory responses (262). They serve as central signaling molecules within the immune system, acting as messengers to relay information not only among immune cells but also with other cell types. One of the most well-studied and significant interleukins is IL-1, originally referred to as human leukocytic pyrogen, and which was identified as a protein responsible for causing fever (263). It consists of two main proteins, IL-1α and IL-1β. Though IL-1α and IL-1β share minimal similarities in their genetic makeup, they were initially believed to have similar functions. Nonetheless, recent studies have revealed differences in their clinical responses to biological targeting, suggesting distinct biological properties between the two interleukins. These differences emerge from variations in their distribution, maturation processes, and release mechanisms (262).

IL-1α is constitutively expressed by epithelial cells, endothelial cells, and astrocytes. The IL-1α precursor is biologically active and acts as an "alarmin" to signal

tissue damage or necrosis. Upon cell damage or death, IL-1α is passively released into the extracellular environment, where it can rapidly trigger an inflammatory response. Additionally, IL-1α can be found on the cell surface, where it is referred to as membrane IL-1α which is also biologically active. Interestingly, apart from the secreted form, intracellular IL-1α is also active and exhibits certain functions where it acts as a transcription factor to control inflammation (264).

Unlike IL-1α, IL-1β is not constitutively expressed but rather induced in response to various stimuli. These stimuli include TLR activation by microbial pathogens, complement components, and other cytokines like TNFα and IL-1. This induction occurs as part of the immune response to infections and inflammatory processes. Moreover, the precursor form of IL-1β (pro-IL-1β) is inactive and requires proteolytic processing to become active. Active IL-1β is released from cells, particularly immune cells like macrophages, and plays a key role in initiating and amplifying inflammatory responses (265).

The IL-1 receptor antagonist (IL-1Ra) is another critical member of the IL-1 family that serves as a natural inhibitor of the IL-1 signaling pathway. IL-1Ra competes with IL-1α and IL-1β for binding to the IL-1 receptor but does not trigger downstream signaling pathways (266). Its primary role is to limit inflammation; thus, the relative levels of IL-1Ra and IL-1 within tissues determine the varying physiological or pathological consequences of IL-1. Some anti-inflammatory drugs work by mimicking the function of IL-1Ra, thereby suppressing the immune response and reducing inflammation (266).

Blocking IL-1 activity has shown therapeutic benefits in inflammatory diseases. IL-1 contributes to autoinflammatory disease, acute-onset ischemic diseases such as myocardial infarction and stroke, as well as chronic conditions like diabetes, gout, osteoarthritis, and rheumatoid arthritis (239).

2.4.2 Biosynthesis of IL-1β

The biosynthesis of IL-1β is initiated at the genetic level with the IL-1β gene, which is located on human chromosome 2. This gene is transcribed into mRNA in response to various signals such as microbial products, pro-inflammatory cytokines, and specific stress signals. The mRNA molecule is then translated into an inactive precursor,

pro-IL-1β, with a size of approximately 31 kilodaltons (kDa). Subsequently, a conversion process is necessary for the precursor to transform into the biologically active form of IL-1β, which is roughly 17 kDa (267). This conversion of the inactive pro-IL-1β into active IL-1β is facilitated by caspase-1. Caspase-1, in its initial state, exists as the inactive pro-caspase-1 and needs to undergo a conversion process to become active caspase-1 (268). This conversion is mediated by intracellular protein complexes referred to as inflammasomes. Canonical inflammasomes, which include NLRP1, NLRP3, NLRC4, NLRP6, and AIM2, can activate caspase-1. The NLRP3 inflammasome, in particular, has been extensively characterized (269). It is important to note that the production of mature IL-1β can also proceed independently of the inflammasome through alternative processing mechanisms. Various enzymes, including neutrophil-derived serine proteases (proteinase 3, elastase, cathepsin-G), metalloproteinases (meprin α and β), and other serine proteinases (chymase, chymotrypsin), are capable of cleaving the precursor pro-IL-1β, resulting in the generation of bioactive IL-1β moieties (270).

To exert their effects, mature IL-1β must be secreted, and various mechanisms of IL-1β secretion have been elucidated through experimental evidence. Unlike proteins that follow the endoplasmic reticulum-Golgi secretory pathway, IL-1β lacks a signal peptide. However, it can be secreted through different mechanisms. One such mechanism involves the release of IL-1β from vesicles that fuse with the plasma membrane. Additionally, IL-1β can be packaged in exosomes or shed through microvesicles from the plasma membrane. Another important mode of IL-1β secretion occurs during pyroptosis (271), whereby a gasdermin D-dependent mechanism has been identified (272). Gasdermin D, a substrate for caspase-1, can be cleaved to form the N-terminal fragment of gasdermin D, which subsequently forms pores in the plasma membrane, allowing the release of IL-1β (272). Having said that, it is worth noting that gasdermin D possesses the ability to form pores that enable the secretion of IL-1β without inducing pyroptosis or causing cell death. Specifically, the pores formed by gasdermin D allow for the controlled release of IL-1β while keeping cells alive (272). Interestingly, while pro IL-1β is negatively charged, mature IL-1β acquires a positive charge and interacts with the negatively charged phosphatidylinositol of the plasma membrane. This maturation process enables IL-1β to relocate to the plasma membrane, facilitating its slow secretion through

gasdermin D-independent mechanisms, as well as rapid secretion through gasdermin D-dependent mechanisms (273). Recently, cleavage of gasdermin E was also shown to promote the continuous release of IL-1β (274). Additionally, during necroptosis, MLKL-mediated membrane disruption was shown to be sufficient for the release of IL-1β independently of gasdermin D (275).

2.4.2.1 NLRP3 inflammasome

The role of inflammasomes in immune response regulation has been an important focus of recent research. A prominent member of this family, the NLRP3 inflammasome, is central to the activation of IL-1β (Fig. 4). The NLRP3 inflammasome is a multi-protein intracellular complex that consists of NLRP3, an adaptor protein ASC (apoptosis-associated speck-like protein containing a caspase recruitment domain [CARD]), and caspase-1 (276). The assembly of these proteins is initiated in response to a diverse array of stress signals or cellular damage. NLRP3 consists of a pyrin domain (PYD), a NACHT domain, and a leucine-rich repeat domain (LRR). ASC contains a PYD and a CARD, while caspase-1 consists of a CARD, a large catalytic domain (p20), and a small catalytic subunit domain (p10) (277). When activated, NLRP3 undergoes oligomerization by engaging in homotypic interactions mediated by NACHT domains. Subsequently, the PYD domain of NLRP3 becomes accessible for binding to the PYD domain of ASC. The CARD domain of ASC then recruits pro-caspase-1 through CARD-CARD interactions. As a consequence of the clustering of pro-caspase-1 on oligomerized NLRP3, caspase-1 is self-cleaved and activated, leading to the processing of various cytoplasmic targets including the pro-inflammatory cytokines IL-1β and IL-18 (277).

NLRP3 inflammasome activation involves two phases: priming and activation. The priming phase involves the upregulation of NLRP3 components initiated by TLR ligands or cytokines. During the activation phase, NLRP3 assembles and activates in response to activators, including bacterial, viral, and parasitic infections. NLRP3 senses DAMPs released during cellular, or tissue damage caused by infectious agents, such as ATP, crystals, amyloid-β fibrils, and hyaluronan (278). Despite progress in this field of research, the specific pathways of NLRP3 activation remain unclear. Multiple proposed mechanisms include potassium efflux, chloride efflux, lysosomal disruption, mitochondrial

dysfunction, and metabolic alterations, but a consensus model has yet to be established due to overlapping and contradictory pathways (277).

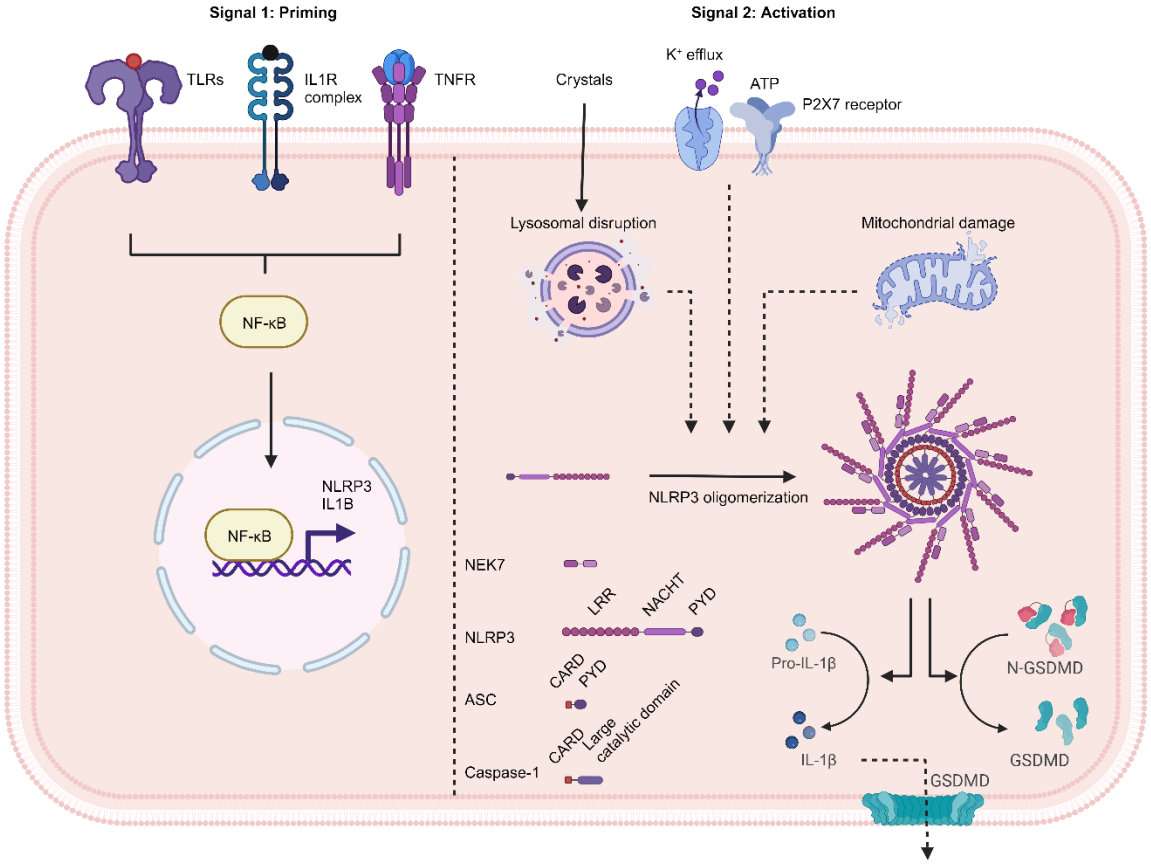

Figure 4. NLRP3 inflammasome activation and IL-1β production.

NLRP3 inflammasome activation involves two phases: priming and activation. The priming phase involves the upregulation of NLRP3 components initiated by TLR ligands or cytokines. During the activation phase, NLRP3 assembles and activates in response to activators, including bacterial, viral, and parasitic infections. NLRP3 senses DAMPs

2.4.3 Interleukin-1 receptors and signaling pathways

IL-1 exerts its effect by binding to IL-1R1, which has an extracellular portion responsible for binding IL-1 and a cytoplasmic portion known as the toll/interleukin-1 receptor (TIR) domain. The extracellular portion of IL-1R1 contains three immunoglobulin-like domains and facilitates high-affinity binding to IL-1, whereas the cytoplasmic portion serves as the signaling domain, transmitting IL-1-mediated signals (279). The binding of IL-1 triggers a conformational change in IL-1R1, leading to the recruitment of interleukin

1 receptor accessory protein (IL-1RAcP) and initiation of intracellular signaling pathways. IL-1R2 is another receptor in the IL-1 receptor family which lacks the TIR domain required for signalling. When IL-1 binds to IL-1R2, it induces conformational changes that recruit IL-1RAcP. However, without the TIR domain, IL-1R2 cannot initiate downstream signaling. As a result, IL-1R2 acts as a decoy receptor, inhibiting IL-1 from interacting with IL-1R1 and blocking the signaling cascade (279). Additionally, soluble forms of both IL-1R1 and IL-1R2 can be produced by alternative splicing or shedding from the cell surface, and these can also act as decoy receptors.

Upon IL-1 binding and dimerization of IL-1R1 and IL-1RAcP, the TIR domain of IL-1R1 recruits the adapter protein myeloid differentiation primary response 88 (MyD88), which in turn recruits a series of proteins, including IL-1R-associated kinases (IRAKs) and TNF receptor-associated factor 6 (TRAF6). This complex triggers a cascade of intracellular events, activating various downstream pathways, including NF-κB and mitogen-activated protein kinases (MAPKs) such as p38 and c-Jun N-terminal kinase (JNK) (Fig. 5) (280). Activation of these pathways leads to the transcription of a broad range of genes. It promotes the expression of adhesion molecules and chemokines, facilitating the recruitment of inflammatory cells to the site of inflammation. Additionally, it stimulates the production of enzymes like phospholipase A2, cyclo-oxygenase 2, and inducible nitric oxide synthase, which subsequently leads to the release of inflammatory mediators such as prostaglandin E2 and nitric oxide (NO), contributing to both local and systemic responses (281).

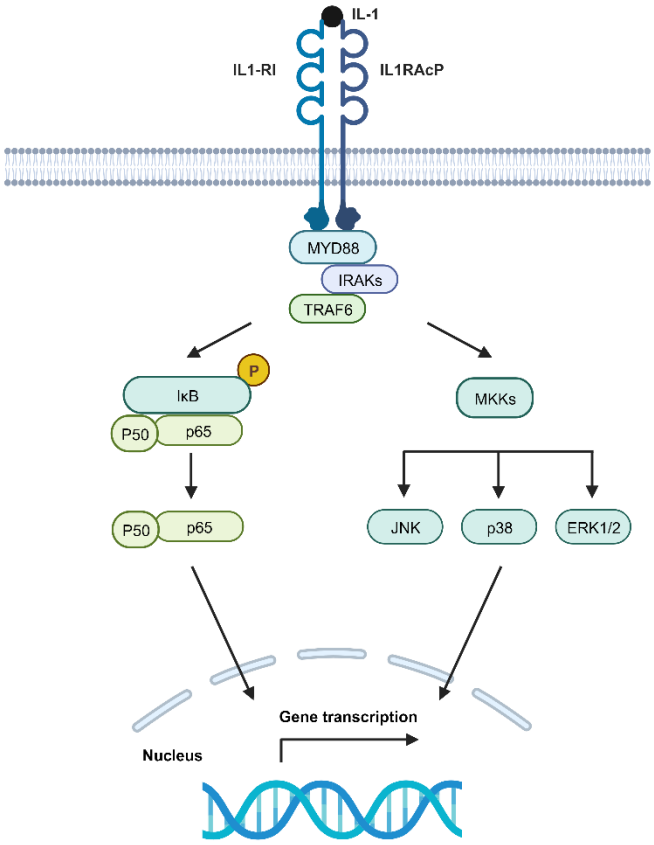

Figure 5. IL-1R signalling pathway.

Upon binding of Interleukin-1 (IL-1) and dimerization of the IL-1 receptor type 1 (IL-1R1) and interleukin-1 receptor accessory protein (IL-1RAcP), the adapter protein myeloid differentiation primary response 88 (MyD88) is recruited. MyD88, in turn, assembles a complex that includes interleukin-1 receptor-associated kinases (IRAKs) and TNF receptor-associated factor 6 (TRAF6). This complex initiates a cascade of intracellular events leading to the activation of various downstream pathways, including nuclear factor-kappa B (NF-κB), which consists of p65 and p50, and mitogen-activated protein kinases (MAPKs), such as p38, extracellular signal-regulated kinase (ERK), and c-Jun N-terminal kinase (JNK).

2.4.4 Anti-IL-1 therapeutics

Given the central role of IL-1 in numerous diseases, targeting this cytokine has emerged as a highly promising therapeutic approach for a range of inflammatory conditions. A number of effective strategies have been developed to modulate IL-1

activity. Anakinra, a recombinant form of human IL-1Ra, acts as a potent inhibitor of IL-1 signaling. Canakinumab, a monoclonal antibody developed by Novartis, specifically targets IL-1β, providing targeted neutralization of this pro-inflammatory cytokine. Rilonacept, developed by Regeneron, functions as a soluble IL-1 decoy receptor, effectively sequestering IL-1 and preventing its binding to cellular receptors (282).

2.4.4.1 Allosteric modulation

In drug discovery, the conventional approach was to screen for molecular leads that interact with the natural binding site of a receptor, known as the orthosteric binding site. Orthosteric ligands exhibit spatial overlap with the endogenous agonist, ensuring specificity in their activity. However, these orthosteric ligands can sometimes lead to unintended side effects because they either activate (agonists) or disrupt (antagonists) the signals triggered by receptor activation. To address these challenges, alternative approaches have been explored such as targeting allosteric sites on receptors. An allosteric modulator refers to a compound that binds to a structurally distinct allosteric site on the receptor. By binding to these sites, allosteric modulators can modulate receptor activity by inducing conformational changes, influencing the receptor's response to orthosteric ligands and altering their affinity or signaling properties (283, 284).

Ligands that bind to remote allosteric sites are generally associated with greater selectivity, as the sequences within these allosteric sites of receptor subtypes are often less conserved. In addition, allosteric modulators offer a therapeutic advantage over orthosteric medications due to their saturable effects and non-competitive binding to receptors. This finite modulation of signaling, known as the ceiling effect, reduces the risk of overdose (285). Moreover, allosteric modulators have the ability to induce bias in signaling pathways by altering the conformational states of receptors and modifying their interaction with other ligands and intracellular proteins. This bias can lead to preferential activation or inhibition of specific signaling pathways, providing a means to selectively target desired cellular responses (286).

Currently available IL-1 inhibitors, including anakinra, rilonacept, and canakinumab prevent IL-1β from binding to its orthosteric site on the IL-1R, thereby inhibiting all IL-1 signals. In contrast, gevokizumab, a monoclonal antibody, offers a distinct mechanism

with allosteric properties. By binding to IL-1β, gevokizumab reduces its binding and signaling through IL-1R1, while leaving IL-1β binding to IL-1R2 or soluble IL-1 receptors unaffected (287). Notably, all of the aforementioned compounds are large biologics, with molecular weights ranging from 17.5 to 251 kDa. In contrast, rytvela, derived from a loop sequence in IL-1RacP, is a small peptide that demonstrates specificity for IL-1R, good potency, and efficacy. It exhibits allosteric modulator properties (288), and pharmacological signal selectivity by inhibiting the JNK/p38 pathway while preserving NF-κB signaling (289). Notably, rytvela holds an advantage over anakinra, as anakinra has been associated with retinal toxicity at clinically relevant dosages (290), whereas rytvela has been demonstrated to be safe even when exposed to developing retinal tissue (291).

2.4.5 IL-1 in AMD

Observational and experimental studies reveal involvement of dominant components of innate-immune inflammation involving activation of the inflammasome and generation of IL-1 in AMD-associated neurodegeneration (292, 293, 294). The evidence from both human and animal studies supporting the participation of the inflammasome and IL-1 in AMD is compelling. For instance, animal models of AMD have shown an abundance of IL-1-generating MPs (295). Furthermore, the NLRP-3 component of the inflammasome and downstream mediators such as IL-1 and IL-18 are overexpressed in AMD (296). Aβ 1-40, a constituent of drusen, triggers NLRP3 activation and IL-1 generation (297). Importantly, elevated levels of IL-1 have been shown to exert cytotoxic effects on photoreceptors (298, 299). The modulation of CD36 in degenerative retinopathy is largely dependent on IL-1 (300).

2.5 Mast cells

2.5.1 The significance of mast cells in the immune system

Mast cells, crucial components of the immune system, play a significant role in the body's response to pathogens and diseases. These cells were first described by Paul Ehrlich in 1878 for their unique morphological characteristics and dye-staining properties (301). Mast cells are prevalent in vascularized tissue and in regions exposed to external

environments like the skin, airways, and gastrointestinal tract. This strategic positioning enables them to act as sentinels, responding as first defenders against pathogens, allergens, toxins, and other environmental substances (302). Although often associated with conditions like asthma, allergies, and anaphylaxis (303), the importance of mast cells extends beyond these illnesses. These cells play a fundamental role in the immune system, with their evolutionarily preserved ability to recognize pathogens and infection signs contributing to both innate and adaptive immune responses (304). Evidence suggests that mast cells influence a broad spectrum of diseases, including (but not limited to) mastocytosis, chronic pain, cancer, cardiovascular, and neurodegenerative diseases (305, 306, 307, 308). Recent reports have also shed light on a novel role of mast cells in mediating behavioral responses such as food aversion (309, 310).

2.5.1.1 Origin of mast cells

Despite expanding research, mast cell origins and their life-long contributions from progenitors remain unclear. Early in fetal development, they arise from the yolk sac and fetal liver, colonizing different organs at specific stages. Tissue-specific signals and environmental factors significantly affect their maintenance and regeneration. In adulthood, blood mast cell progenitors can contribute to tissue repopulation in adult mice. Under normal circumstances, mast cells in mouse connective tissue receive little supplementation from bone marrow, while mucosal sites may attract more bone marrow progenitors. However, the overall contribution of these progenitors to adult homeostasis is relatively low compared to other tissue-resident lineages. Notably, the hypothesis of self-maintenance of tissue-resident mast cells has garnered attention. During inflammation, however, there is a shift in mast cell populations as they are replenished through bone marrow progenitors. Circulating and resident mast cell progenitors are mobilized to the affected tissues (311). It is worth noting that mature mast cells are not found in the bloodstream, as they migrate and mature locally under the control of local signals.

2.5.1.2 Mast cell subtypes, heterogeneity, and plasticity

Mast cells are diverse, displaying various subtypes based on their granule contents, protease expression profiles, and responses to stimuli. In mice, these include connective-tissue mast cells (CTMCs) and mucosal mast cells (MMCs), each located and functioning differently based on their tissue environment. CTMCs are located in the skin, peritoneal cavity, and muscularis propria of the gastrointestinal tract, whereas MMCs are found in the gastrointestinal mucosa. These cell populations differ based on granule contents, mast cell protease expression, and their responses to activation stimuli (312). In humans, mast cells are identified based on the presence or absence of specific proteases in their granules. Some subsets contain both tryptase and chymase in their granules, while others only have tryptase, without detectable chymase (312). However, this classification oversimplifies reality and does not adequately capture mast cell heterogeneity and plasticity. In fact, mast cells exhibit considerable heterogeneity, with their functions influenced by different tissue environments. Their roles and responses can vary based on location, as seen in the diverse reactions of bladder and kidney mast cells during urinary tract infections. Mast cells display plasticity in their responses to inflammatory stimuli, shifting between type 1 and type 2 immune responses as needed, which can influence adaptive immune responses (313). Furthermore, it is noteworthy that these cells exhibit transcriptional plasticity, implying the presence of tissue-specific epigenetic mechanisms (314). Additionally, the concept of trained immunity posits that mast cells, given their enduring lifespan and activation potential, possess the capacity to adapt to recurrent stimuli (315).

2.5.1.3 Activation of mast cells

Mast cells are known for their dense granules, also referred to as secretory lysosomes, that occupy a significant part of their cytoplasm. These granules contain a variety of preformed compounds and can be visualized through staining techniques due to their characteristic metachromatic pattern. Upon activation, mast cell secretory granules fuse with one another and with the plasma membrane, leading to the rapid release of granule mediators through a process known as degranulation. As a result of this degranulation, various compounds are released, exerting their influence on a wide

range of physiological and pathological processes. However, it is important to note that mast cell activation does not always result in degranulation; certain stimuli may trigger the release of cytokines without visible degranulation (316). Another fascinating aspect is mast cell regranulation: after degranulation, mast cells synthesize and reassemble new granules, ensuring their reactivation potential to future stimuli (317). This process ensures that mast cells can be reactivated and respond to subsequent stimuli effectively and goes in line with the long-lived properties of these cells.

Mast cells can participate in various physiological and pathological processes. Immunoglobulin E (IgE) crosslinking to the high affinity Fcε receptor I (FcεRI) is a common mechanism for mast cell activation leading to immediate hypersensitivity reactions such as anaphylaxis and chronic allergic inflammation, especially in asthma (303). However, mast cell activation is not limited to IgE-mediated mechanisms. Interestingly, mast cells can also interact with the nervous system, responding to neuropeptides like substance P and calcitonin gene-related peptide (CGRP), indicating a role in neurogenic inflammation (318). Mast cells can also be activated by complement fragments such as C3a and C5a through C3aR and C5aR respectively (319, 320). This versatility extends to IgG receptors, TLRs, NLRs, RIG-I-like receptors, purinergic receptors, receptors for neurotransmitters, lipid mediators, and hormones (321). A newly identified human G protein-coupled receptor (GPCR), (MRGPR)X2 (or Mrgprb2 in mice), has gained interest due to its capacity to be activated by a wide range of ligands such as substance P and certain drugs implicated in pseudoallergic reactions (322, 323, 324). Finally, physical stimuli such as vibrations and temperature variations can induce mast cell activation (325, 326). This capacity of mast cells to adapt and respond to varied stimuli underlines their vital role in numerous biological processes.

Upon activation, mast cells release a spectrum of pre-stored or de novo formed mediators (Table II). These range from biogenic amines such as histamine and serotonin to an array of serine and other proteases, lysosomal enzymes, cytokines, chemokines, and growth factors. Additionally, mast cells release lipid mediators including leukotrienes, prostaglandins, and platelet activating factor (PAF) (327, 328, 329). Interestingly, under certain conditions, mast cells were shown to form tunneling nanotubes (membranous projections) (330, 331), release extracellular traps (332), and extracellular vesicles (333).

These mast cell mediators contribute to diverse physiological processes such as immune responses, allergic reactions, inflammation, wound healing, and tissue remodeling.

Table II. Activators and mediators of mast cells

Activators	Types of Mediators Released
• Immunoglobulin E (IgE) crosslinking to FcεRI • Neuropeptides (Substance P, CGRP) • Complement fragments (C3a, C5a) • IgG receptors, TLRs, NLRs, RIG-I-like receptors, purinergic receptors, receptors for neurotransmitters, lipid mediators, hormones • MRGPRX2 ligands Physical stimuli (vibrations, temperature variations)	• Histamine, serotonin • Tryptase, chymase, cathepsin G • β-glucuronidase, β-hexosaminidase, arylsulfatase • Cytokines: Interleukins, TNF • Chemokines • Lipid mediators: Leukotrienes, prostaglandins, platelet activating factor

2.5.2 Mast cell tryptase

2.5.2.1 Tryptase biosynthesis

In humans, the tryptase genes reside on chromosome 16p13.3, at approximately 1.2 megabases from the telomeric end. The genes situated on chromosome 16p13.3 give rise to multiple tryptase transcripts, tryptases α, β, γ, and δ. The proteases encoded by these transcripts assemble into tetramers and share a high sequence similarity. In mice, the corresponding genes are designated as mouse mast cell protease (mMCP)-6, mMCP-7, Prss31, and Prss34, and are situated on chromosome 17A3.3. This region spans a serine protease gene cluster of nearly 11.8 megabases, encoding 13 functional tryptic-like proteases (334). Among these, the most prevalent tryptases are α and β in humans, while mMCP6 and mMCP7 dominate in mouse mast cell granules (316).

Tryptase is initially synthesized as an inactive precursor protein requiring subsequent activation. It was shown that recombinant monomeric β protryptase

undergoes autolytic cleavage between Arg-3 and Val-2, resulting in monomer formation under acidic pH conditions in the presence of heparin or dextran sulfate. The dipeptidyl peptidase I subsequently removes two residues to facilitate the formation of an active tetramer under the same conditions (335, 336). In contrast, the α protryptase precursor harbors a mutation where Arg-3 is substituted by Gln-3, which inhibits autolytic processing, leaving it as an inactive precursor (335). α tryptase was observed to be the predominant form of tryptase in normal human serum and thus suggest that this form is constitutively released (337). Further investigations revealed that cathepsins (CTS) L and CTSB are essential for the processing of β protryptase into mature β tryptase in human mast cells (338).

2.5.2.2 Tryptase structure

The functional state of mast cell tryptase is an enzymatically active and stable tetramer. The stability and functionality of this complex are preserved by its association with the glycosaminoglycan, heparin. The dissociation from heparin and subsequent breakdown into individual monomers leads to the loss of enzymatic activity, thus highlighting the critical role of heparin in maintaining the activity of the tetrameric structure (339).

The crystalline structure of human β-tryptase comprises four near-identical monomers configured in a planar square arrangement. The four active centers of the tetramer converge toward a central pore, thereby restricting access to large molecular substrates and enzyme inhibitors (340). The stability of the complex is attributed to heparin chains binding to a positively charged region that spans two neighboring monomers (341). Consequently, this structural arrangement results in tryptase demonstrating resistance to biological protease inhibitors (342). The crystal structure of mature human α-tryptase also revealed a tetrameric structure which, intriguingly, does not rely on heparin binding for stability (343). While α-tryptase is generally considered to lack in vivo catalytic activity, it was found that it can form an active heterotetrameric complex with β-tryptase (344).

Interestingly, low molecular weight heparin was found to be capable of forming β-tryptase and mMCP-6 monomers that are catalytically active, rather than forming

tetramers (345, 346). Unlike tetramers, monomers can degrade fibronectin, a process that tetramers cannot achieve due the large size of fibronectin which impedes entry into the central pore of the tryptase tetramer. This points to distinct functional properties between monomers and tetramers. Additionally, unlike their tetramer counterparts, monomers are susceptible to protease inhibitors (345). Active β-tryptase monomers can also be generated from mature tetrameric β-tryptase in vitro under specific conditions (neutral pH and a temperature of 37°C) mirroring those occurring after tryptase release (347).

2.5.2.3 Tryptase substrates and biological roles

Tryptases possess trypsin-like activity, preferentially cleaving after lysine or arginine residues. The β-tryptase exhibits a preference for substrates with an arginine or lysine residue at the P1 position. It can also cleave after lysine/arginine at the P3 position and after proline at the P4 position. mMCP-6 displayed a preference for lysine over arginine in the P1 position and a slight inclination for proline in the P4 position, while mMCP-7 has preference to substrates with Arginine at the P1 position and serine or threonine at the P2 position (348).

Tryptase has been demonstrated to cleave a variety of substrates, including components of the ECM like fibronectin and collagen, pro-MMPs, peptides such as CGRP and vasoactive intestinal peptide (VIP), and lipoproteins (349). Additionally, tryptase can activate the protease-activated receptor (PAR) 2 by cleaving N-terminal of the receptor, a GPCR, leading to the exposure of a tethered ligand domain. The tethered ligand serves as an agonist for the cleaved receptor, triggering a cascade of intracellular signaling events (350). The EGF-like module-containing mucin-like hormone receptor-like 2 (EMR2) is another receptor that can be cleaved and activated by tryptase (344). Furthermore, tryptase can cleave IL-33, leading to the creation of the mature form of this cytokine (351). Intriguingly, tryptase has also been found to relocate from the granules to the nucleus, where it plays a role in epigenetic regulation within mast cells (352, 353).

Tryptases perform a wide range of biological functions, including activating other immune cells and initiating a cascade of inflammatory reactions against infections (354). They have a significant role in allergic reactions and asthma (355), and are implicated in

various inflammatory conditions such as arthritis, joint inflammation, multiple sclerosis, psoriasis, and atopic dermatitis (348). Beyond these immune-related roles, tryptase contributes to essential biological processes such as tissue remodeling, wound healing, angiogenesis, and fibrosis (349).

2.5.3 Mast cells in AMD

Mast cells have been observed in varying amounts in the uvea, displaying a specific distribution pattern in the choroid, ciliary body, and iris (356, 357, 358). In AMD, there is a marked increase in mast cell numbers and degranulation in the choroid, especially in regions showing choriocapillaris loss, which is evident in cases of geographic atrophy and exudative AMD (217). In eyes with geographic atrophy, tryptase is present near the choriocapillaris and Bruch's membrane, with tryptase diffused through the surrounding stroma (359). Interestingly, mast cell degranulation was linked to changes in the ECM in individuals genetically predisposed to AMD, even in the absence of clinical disease symptoms (360). Experiments using compound 48/80, known to induce mast cell degranulation, caused acute ocular inflammation, RPE degeneration, vascular dilation, increased choroidal vessel permeability, and retinal detachment. This process involved infiltration of polymorphonuclear and macrophage cells, along with elevated inflammatory factors (361). Continuous stimulation of choroidal mast cells resulted in RPE degeneration along with choroidal thinning (362). This highlights the distinct outcomes of acute and prolonged mast cell activation, with the former contributing to choroidal vasodilation and the latter contributing to choroidal thinning.

2.6 Cell death

2.6.1 Regulated cell death

Cells can die by different routes which are classified into two primary types: accidental cell death and regulated cell death. Accidental cell death is induced by severe external factors, such as extreme physical conditions (e.g., high temperatures, pressures), chemical exposure (e.g., strong detergents, pH changes), or mechanical stresses (e.g., shearing). This form of cell death occurs almost instantly and not amenable to any pharmacological or genetic interventions. On the other hand, regulated cell death

relies on genetically encoded molecular processes and can be influenced by pharmacological and genetic interventions that target key components of this intricate process (363).

Regulated cell death serves a crucial mechanism that engages when cells encounter perturbations of intracellular or extracellular homeostasis. Cells have evolved complex mechanisms to maintain homeostasis; however, when the stress levels overwhelm the capacity of these adaptive responses, cells undergo regulated cell death as a strategy to maintain the overall homeostasis of the organism (364). Of note, regulated cell death is not only a consequence of environmental changes but also plays a role in normal physiological processes such as embryonic development, tissue maintenance, and immune responses. When it occurs within these physiological contexts, regulated cell death is often referred to as programmed cell death (363, 365). The Nomenclature Committee on Cell Death recognizes and classifies various forms of regulated cell death, including apoptosis, necroptosis, pyroptosis, and ferroptosis, among others (366).

2.6.1.1 Apoptosis

First coined by John Kerr in 1972, the term 'apoptosis' comes from the Greek word 'apoptōsis,' which means 'falling off'. This concept described the morphological characteristics of cell death (367). Apoptosis is characterized by cell shrinkage, chromatin condensation (pyknosis), nuclear fragmentation, plasma membrane blebbing, and the formation of apoptotic bodies (368). These apoptotic bodies are small fragments of cells that contain cytoplasm and tightly packed organelles. They are enveloped by an intact plasma membrane, which prevents the leakage of proinflammatory intracellular contents. Phagocytes facilitate the clearance of apoptotic cells through a process known as efferocytosis, and when efferocytosis fails, cells undergo secondary necrosis (369, 370). The execution of apoptosis primarily occurs through two pathways: the extrinsic and the intrinsic pathways. Both use unique cell structures to initiate cell death and culminate in the activation of caspases that are integral to apoptosis (371). The name "caspase" is derived from its two catalytic properties, where "c" refers to a cysteine protease

mechanism, and "aspase" indicates its ability to cleave after aspartic acid residues (372). The extrinsic and intrinsic pathways are illustrated in Figure 6.

2.6.1.1.1 Extrinsic pathway

The extrinsic pathway commences with the binding of death ligands to specific death receptors located on the cell membrane. The death receptors are part of the TNF receptor (TNFR) superfamily (TNFRS). These include Fas (CD95), TNFR1, and the TNF-related apoptosis-inducing ligand (TRAIL) receptors known as TRAIL-R1 (DR4 or TNFRSF10A) and TRAIL-R2 (DR5 or TNFRSF10B). Only a single TRAIL receptor, mTRAIL-R, exists in mice (373, 374, 375). Other cell surface receptors known as dependence receptors can also trigger the extrinsic pathway of apoptosis. These include the nerve growth factor receptor p75NTR, RET (rearranged during transfection), neurotrophins receptors TrkA and TrkC, kremen-1, EPHA4, MET, ALK, netrin-1 receptors DCC (deleted in colorectal carcinoma) and UNC5H1-4 (Unc-5 homologue 1–4), neogenin, plexin D1, the insulin receptor and its related receptor IGF1R, some integrins, and the Sonic Hedgehog receptors Patched (Ptc) and CDON (376, 377).

Activation of the death receptors Fas by Fas ligand (FasL), and DR4 and DR5 by TRAIL, initiates oligomerization of these receptors into trimers; this occurs by interactions with each other through their intracellular death domains (DDs) (373, 378, 379). Subsequently, the adaptor protein Fas-associated death domain (FADD) is recruited. FADD recruitment drives the formation of the death-inducing signaling complex (DISC) which consists of FADD, FLICE-like inhibitory protein (cFLIP), and caspase-8. FADD, which contains both a DD and a death effector domain (DED), uses its DD to interact with the DDs of the death receptors. This interaction situates FADD in a position where its DED can engage in protein-protein interactions with other DED-containing proteins. One key interaction involves the recruitment of procaspase-8 by FADD. The DED of FADD interacts with the DED of procaspase-8, leading to the formation of procaspase-8 dimers. These procaspase-8 dimers then undergo conformational changes in their caspase domains, facilitating their auto-cleavage and activation (366, 380).

The interaction between TNF and preassembled TNFR1 leads to a conformation change in the cytoplasmic domain of the receptor, facilitating the recruitment of DD

containing-TNFR-associated death domain (TRADD) through DD (381). Consequently, TRADD further recruits RIPK1, E3 ubiquitin ligases TNF receptor–associated factor (TRAF) 2 or TRAF5, cellular inhibitor of apoptosis proteins (cIAP1 and cIAP2), and linear ubiquitin chain assembly complex (LUBAC), forming the complex I. RIPK1 ubiquitylation status acts as a molecular switch in maintaining the balance between cell survival and cell death. When RIPK1 is ubiquitylated by cIAPs and LUBAC, it promotes cell survival by facilitating the activation of NF-κB (382, 383). Alternatively, if RIPK1 remains deubiquitylated, it triggers apoptosis by initiating the formation of cytoplasmic signaling complexes known as complex IIa and complex IIb. In complex IIa, deubiquitylated RIPK1 combines with TRADD, FADD, pro-caspase-8, and the cFLIP in the cytosol. After the assembly of complex IIa, pro-caspase-8 undergoes self-cleavage and becomes activated, leading to the release of active caspase-8 into the cytosol. On the other hand, the assembly of complex IIb, which also induces apoptosis, occurs when RIPK1 is deubiquitylated but does not involve TRADD. RIPK1, in its non-ubiquitylated form, associates with RIPK3, pro-caspase-8, and cFLIP to create complex IIb, which subsequently triggers apoptosis in a similar fashion to the complex IIa pathway (384, 385).

The balance between survival and apoptosis is further regulated by the function of cFLIP which is expressed as long ($cFLIP_L$), short ($cFLIP_S$), and $cFLIP_R$ isoforms (386). While $cFLIP_S$ blocks procaspase-8 activation, the effects of $cFLIP_L$ are believed to be dose dependant (387). At low concentrations, $cFLIP_L$ facilitates the activation of procaspase-8, while at higher levels, $cFLIP_L$ leads to a concentration-dependent decrease in procaspase-8 activity (387).

For the execution phase of apoptosis, the activated caspase-8 cleaves and activates caspase-3/7, which in turn, cleave various cellular substrates leading to the characteristic morphological and biochemical features of apoptotic cell death (388). Caspase-3 activates the caspase-activated deoxyribonuclease (CAD) which is responsible for the fragmentation of nuclear DNA (389). Caspase-3 further facilitates the externalization of phosphatidylserine (PS) by inhibiting its internalization through the cleavage of phospholipid flippase (390, 391) and promoting its externalization by cleaving and activating phospholipid scramblase (392, 393). Additionally, caspase-3 cleaves

ROCK I, subsequently increasing the phosphorylation of the myosin light chain and causing membrane blebbing (394).

2.6.1.1.2 Intrinsic pathway

The intrinsic pathway of apoptosis is initiated by a variety of disturbances within the extracellular or intracellular microenvironment, which include DNA damage, ER stress, mitochondrial damage, excessive mitogenic stimulation, oncogene-induced cell death, and lack of proper stimuli such as growth factor withdrawal or nutrient deprivation (395). In reaction to such disturbances, a particular class of proteins known as B cell lymphoma 2 (BCL-2) homology 3 (BH3)-only proteins are either induced or post-translationally activated. Notable BH3-only proteins include Bim, Bid, Bad, Puma, Noxa, and Bik. Following induction or activation, BH3-only proteins provoke the activity of BCL-2-associated x protein (BAX) and BCL-2 homologous antagonist/killer (BAK). While BAX is primarily found in the cytoplasm and BAK in the mitochondria, they both possess the capability to shuttle between these locations; upon activation, there is a marked accumulation of BAX at the mitochondria (396, 397).

Once activated, BAX and BAK proteins undergo conformational changes, shifting from monomers to oligomers. This transition results in the perforation of the outer mitochondrial membrane, triggering mitochondrial outer membrane permeabilization (MOMP) (398). It is worth noting that there is also an alternative pathway that is not dependent on BAX/BAD. In this pathway, a BCL-2 protein similar to BAX and BAK, called BCL-2 related ovarian killer (BOK), can also trigger MOMP (399). To counteract this apoptotic process, anti-apoptotic BCL-2 proteins bind to BH3-only proteins and activated BAX or BAK, preventing MOMP. However, if MOMP occurs, various proteins escape from the mitochondrial intermembrane space, promoting caspase activation and initiating apoptosis (398). In the intrinsic pathway, a critical step is when cytochrome c, released from the mitochondrial intermembrane space to cytosol, binds to apoptotic protease-activating factor 1 (APAF1). This binding event leads to a conformational change and oligomerization of APAF1, ultimately forming a structure known as the apoptosome. The apoptosome then recruits, dimerizes, and activates the initiator caspase-9. Caspase-9 subsequently cleaves and activates executioner caspases, namely caspase-3 and

caspase-7, setting apoptosis in motion. Furthermore, the mitochondria also release second mitochondria-derived activator of caspase (SMAC, also known as DIABLO) and OMI (also known as HTRA2), which neutralize the caspase inhibitory function of X-linked inhibitor of apoptosis protein (XIAP) (400). Of note, there is a crosstalk between the extrinsic apoptotic pathway and the mitochondrial pathway through the cleavage of BID by caspase-8. This cleavage produces the truncated p15 BID (tBID), which strongly triggers MOMP (397).

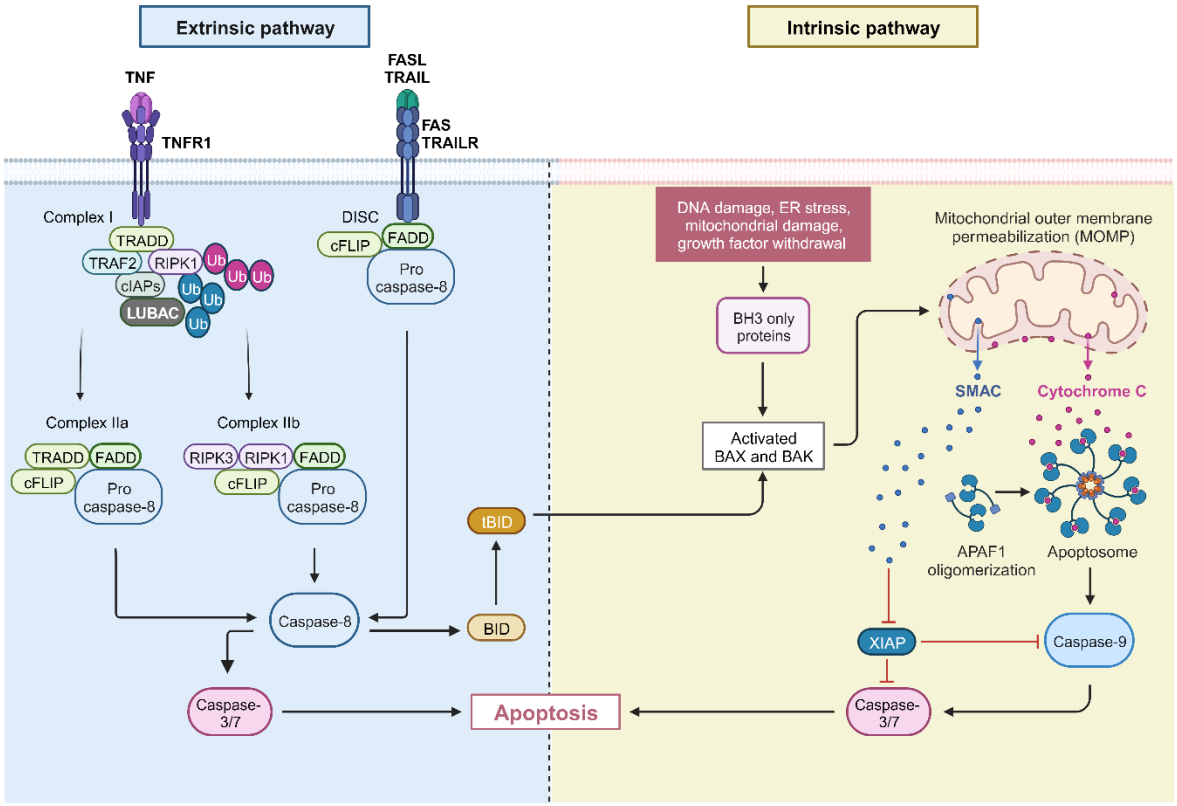

Figure 6. Extrinsic and intrinsic pathways of apoptosis.

The extrinsic pathway is initiated by TNF, FASL, and TRAIL. Upon ligation of TNF, TNFR1 recruits multiple proteins to form complex I. If RIPK1 is not ubiquitinylated or deubiquitylated, complex I is converted to complex IIa or complex IIb, resulting in the activation of caspase-8. Activation of FAS and TRAIL receptors leads to the formation of the DISC, subsequently activating caspase-8. Caspase-8 cleaves caspase-3/7 and BID. In the intrinsic pathway, BH3-only proteins are activated, which in turn activate BAX and BAK. BAX and BAK trigger mitochondrial outer membrane permeabilization (MOMP),

leading to the release of cytochrome C and the oligomerization of APAF1 to form the apoptosome. The apoptosome activates caspase-9, which in turn leads to the activation of caspase-3/7. Figure generated by Biorender.

2.6.1.2 Necroptosis

The term ‘necroptosis’ was introduced in 2005 to define one form of regulated necrotic cell death, which contradicts the previous belief that all necrotic cell death was accidental (401). This finding paved the path towards the concept of programmed necrosis. Necroptosis is a regulated type of cell death triggered by perturbations within the extracellular or intracellular microenvironment. A variety of receptors sense these disturbances, including death receptors (TNFR1, TRAILR, FAS), along with interferon-alpha/beta receptor subunit 1 (IFNARI), PRRs (TLR3, TLR4), and ZBP1 (114). In addition, osmotic stress (402) and heat stress (403) can also trigger necroptosis. The process of necroptosis is primarily driven by RIPK3 and its substrate, MLKL (404).

TNF-induced necroptosis, a well-explored pathway, diverges from the apoptotic pathway. As described in the apoptosis pathway, TNF stimulation results in the formation of either complex IIa or IIb. These complexes can trigger apoptosis but may also initiate necroptosis if caspase-8 is inhibited or deficient (405, 406, 407). Therefore, in the absence or inhibition of caspase-8, an active variant of the enzyme RIPK1 in complex II recruits and activates RIPK3. This leads to the creation of a structure known as the necrosome. The necrosome, akin to complex II in apoptosis, can have two forms, either containing TRADD, RIPK1, RIPK3, and FADD (complex IIa), or lacking TRADD (complex IIb) (407).

Both RIPK1 and RIPK3 possess receptor-interacting protein (RIP) homotypic interaction (RHIM) domains. Through these domains, RIPK1 interacts with RIPK3 (408, 409), leading to the formation of a hetero-oligomeric amyloid-like structure that allows the phosphorylation of RIPK3 (410, 411). Using super-resolution microscopy, necrosomes appear as either RIPK1 or RIPK3 homo-oligomers, or as RIPK1-RIPK3 mosaic oligomers. These entities possess distinct morphologies, ranging from round to rod-shaped configurations with helical structures (412). A pivotal aspect in this mechanism is RIPK1 autophosphorylation at serine 166, which has been pinpointed as crucial for activating the

RIPK1 kinase and thereby initiating the necroptosis process (412, 413). Furthermore, beyond the RHIM interaction, it is proposed that RIPK3 undergoes allosteric regulation through the dimerization of its kinase domain, subsequently leading to RIPK3 activation via cis-autophosphorylation (414).

Despite the critical role of RIPK1 in TNF-induced RIPK3 activation, it is important to note that RIPK3 can also be activated directly by TRIF and ZBP1, bypassing the need for RIPK1. TLR-triggered necroptosis involves the interaction of RHIM-containing TRIF and RIPK3 (415). Similarly, during viral infections or IFN stimulation, ZBP1, which also possesses the RHIM motif, initiates RIPK3-dependent MLKL activation and necroptosis by directly interacting with RIPK3 (416, 417, 418). Intriguingly, in a contrary manner, it has been observed that RIPK1 inhibits ZBP1-driven necroptosis through a kinase-independent mechanism facilitated by its RHIM interaction with ZBP1 (419). This interaction prevents ZBP1 from binding and activating RIPK3, which contrasts with its role in TNF-driven necroptosis, where RIPK1 induces RIPK3 activation (420).

RIPK3, upon phosphorylation, recruits and phosphorylates the pseudokinase MLKL at specific residues: threonine 357 and serine 358 in human MLKL or threonine 349, serine 345, and serine 347 in mouse MLKL (404, 421). Once phosphorylated, MLKL undergoes a structural rearrangement that exposes the 4-helical bundle (4HB) domain (422, 423, 424). The 4HB domain is essential for oligomerization MLKL, enabling the formation of multi-molecule MLKL complexes (425). These activated MLKL oligomers then move to the plasma membrane, forming pores that increase membrane permeability (120, 424, 426). This process is facilitated by the interaction between the positively charged patch on the 4HB domain and phosphatidylinositol phosphates present on the plasma membrane (425). MLKL activation has downstream effects on calcium dynamics; it governs calcium influx through the cation channel, TRPM7 (427). Additionally, it induces cellular membrane changes, such as the appearance of bubble-like protrusions on the surface and the external display of phosphatidylserine (428). The trafficking of MLKL from the cytosol to the cell periphery is mediated by Golgi-microtubule-actin-dependent mechanisms and occurs alongside tight junction proteins. Once at the plasma membrane, MLKL accumulates and forms high-activity regions termed 'hotspots'. If the concentration of MLKL at these hotspots surpasses a critical threshold, it damages the cell membrane,

resulting in cell death (Fig. 7) (429). In a similar vein, the nerve injury-induced protein 1 (NINJ1) has been recognized as a key player in causing plasma rupture during various forms of lytic cell death. Specifically, during necroptosis, NINJ1 is essential for the release of lactate dehydrogenase and HMGB1, among others, even when the cell succumbs to death (430). Although phosphorylated MLKL is a recognized necroptosis marker, its interaction with the endosomal sorting complex required for transport (ESCRT-III) can delay cell death if MLKL levels are kept under control. This allows some cells a chance to recover, thus avoiding necroptosis (428). However, this interaction can also promote the prolonged release of inflammatory signals, potentially impacting the overall immune response (428).

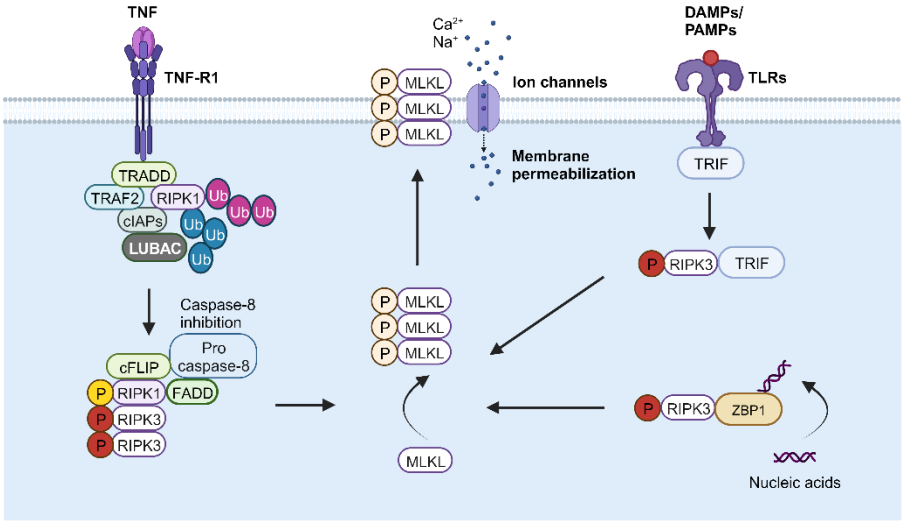

Figure 7. Initiation and execution of necroptosis.

Necroptosis can be triggered by death receptors (TNFR1), TLRs, and ZBP1. TNF leads to necroptosis when caspase-8 is inhibited and results the formation of RIPK1-RIPK3 complexes. Phosphorylated RIPK3 phosphorylates and activated MLKL. TLRs activate RIPK3 via a TRIF-dependant mechanism. ZBP1 can directly activate RIPK3. Phosphorylated MLKL undergoes oligomerization and is trafficked to the plasma membrane where it induces membrane rupture and regulation of ion influx. Figure generated by Biorender.

2.6.2 Cell death in retinal degeneration

Earlier in Section 2.1.4, various mechanisms behind RPE cell dysfunction were briefly explored, including different forms of cell death. The focus shifts towards a more comprehensive understanding of the broader landscape of retinal degeneration, with specific emphasis on photoreceptor cells. Photoreceptor cell death stands central to various ocular diseases such as AMD, retinitis pigmentosa, and diabetic retinopathy. This observation is supported by the identification of TUNEL-positive photoreceptors, a hallmark of cell death, in AMD patients (108). The consequences of photoreceptor cell death are severe, often leading to a dramatic loss of vision and, in some cases, complete blindness. Several mechanisms have been proposed to explain photoreceptor cell death. Multiple processes, such as apoptosis, necrosis, and autophagy have been identified as potential contributors (431). For instance, the apoptosis of photoreceptor cells following light exposure was suggested as a causative factor (432). Various studies using the retinal light injury model have sought to understand the role of caspases. Some findings indicate that the pan-caspase inhibitor Z-VAD might not consistently prevent photoreceptor loss after light exposure (433). Yet, under specific conditions concerning light intensity and inhibitor dosage, Z-VAD has shown protective effects (434). Another pathway of interest was the activation of calcium-activated calpains. However, experiments with calpain inhibitors in the rd mouse retina did not yield protective effect on photoreceptors (435). In the context of retinal detachment, a RIPK3-dependent mechanism seems to mediate cell death. While Z-VAD reduced apoptosis, it inadvertently increased necrotic photoreceptor death. Conversely, when combined with necrostatin-1, a RIPK1 inhibitor, this co-treatment effectively curbed necrotic photoreceptor death, suggesting a potential therapeutic avenue (436). These observations hint at the possible involvement of necroptosis and apoptosis in photoreceptor cell death, although conclusive evidence is still lacking. Furthermore, in the rd model of retinitis pigmentosa, both the mitochondrial protein AIF (apoptosis-inducing factor) and the ER-associated caspase-12 were noted to translocate to the nucleus of dying photoreceptors (437).

Additionally, a connection between phospho-MLKL oligomer formation, and lipofuscin accumulation has been observed. Specifically, formation of phospho-MLKL was observed in retinal cells of RPE and MPs, as well as in the neuroretina of $Abca4^{-/-}Rdh8^{-/-}$

animals (a model of lipofuscin buildup in RPE). Additionally, phospho-MLKL patches were detected in the RPE of patients with AMD (438). These findings further demonstrate the close interplay between necroptosis and neuroinflammation ocular conditions. In summary, while various mechanisms have been proposed, the exact roles of caspase- or RIPK3-dependent pathways in photoreceptor death remain debated, with no robust evidence confirming the dominance of one over the other.

2.7 Thesis rationale and objectives

AMD represents a major challenge in ophthalmology due to its multifaceted nature and progressive impact on vision. Current therapeutic options are limited, underscoring the need for novel approaches that target the underlying mechanisms of the disease. The disease is marked by various pathological processes, including high levels of IL-1β, mast cell activation, and cell death. Despite advancements in understanding of AMD, the precise interplay between these factors and their contribution to retinal degeneration remains unclear. Addressing these aspects can provide insights into novel therapeutic strategies.

The main hypothesis of this thesis is that: *the progression of AMD is driven by the synergistic effects of inflammatory cytokines IL-1β, mast cell activation, and cell death pathways, which collectively contribute to retinal degeneration. Targeting these mechanisms through specific pharmacological will provide novel therapeutic strategies to mitigate AMD progression*.

To address this hypothesis, the following specific aims were followed in preclinical models of AMD:

1. To evaluate the efficacy of IL-1R allosteric modulation in preserving retinal integrity.
2. To investigate the role of mast cells subretinal inflammation and photoreceptor loss.
3. To investigate the role of mast cells in CNV.
4. To explore the contribution of necroptosis to photoreceptor cell death.

CHAPTER 3 - An allosteric interleukin-1 receptor modulator mitigates inflammation and photoreceptor toxicity in a model of retinal degeneration

Authors: Rabah Dabouz[1,2,3], Colin W. H. Cheng[1,2,3], Pénélope Abram[2], Samy Omri[2], Gael Cagnone[3], Khushnouma Virah Sawmy[3], Jean-Sébastien Joyal[3], Michel Desjarlais[2], David Olson[4], Alexander G. Weil[5], William Lubell[6], José Carlos Rivera[2,3] and Sylvain Chemtob[1,2,3*]

1. Department of Pharmacology and Therapeutics, McGill University, Montreal, QC, Canada
   Rabah Dabouz, Colin W. H. Cheng & Sylvain Chemtob
2. Departments of Pediatrics, Ophthalmology, and Pharmacology, Hôpital Maisonneuve-Rosemont Research Center, 5415 Boul L'Assomption, Montreal, QC, H1T 2 M4, Canada
   Rabah Dabouz, Colin W. H. Cheng, Pénélope Abram, Samy Omri, Michel Desjarlais, José Carlos Rivera & Sylvain Chemtob
3. Hôpital Sainte Justine Research Centre, Montreal, QC, Canada
   Rabah Dabouz, Colin W. H. Cheng, Gael Cagnone, Khushnouma Virah Sawmy, Jean-Sébastien Joyal, José Carlos Rivera & Sylvain Chemtob
4. Department of Obstetrics & Gynecology, University of Alberta, Edmonton, AB, Canada
   David Olson
5. Department of Neurosurgery, Hôpital Sainte Justine, Montreal, QC, Canada
   Alexander G. Weil
6. Department of Chemistry, University of Montreal, Montreal, QC, Canada
   William Lubell

Preface: Observational and experimental studies have consistently illuminated the pivotal role of innate immune inflammation in AMD, particularly highlighting the inflammasome's activation and IL-1 generation as central elements in the neurodegenerative aspects of AMD. The evidence supporting the involvement of inflammasome and IL-1 in AMD is robust and multidimensional, spanning human and

animal studies. For instance, the prevalence of IL-1-generating MPs in AMD, the overexpression of the NLRP-3 inflammasome component and its downstream mediators IL-1 and IL-18, and the inflammasome's activation by complement and β-amyloid in senescent contexts all underline a critical inflammatory pathway at play. Moreover, the detrimental impact of IL-1 on photoreceptors and RPE, alongside the protective association of IL-1RI-inactivating polymorphisms and the therapeutic potential of IL-1R antagonism, further corroborate the significance of this pathway in AMD pathophysiology. Against this backdrop of compelling evidence, our study aims to investigate the potential of allosteric IL-1R modulation to mitigate retinal degeneration. By focusing on a light-induced model of retinal degeneration that encapsulates subretinal inflammation and photoreceptor demise, we aspire to elucidate a novel therapeutic avenue that could ameliorate the inflammatory underpinnings of AMD.

Abstract

Background

Inflammation and particularly interleukin-1β (IL-1β), a pro-inflammatory cytokine highly secreted by activated immune cells during early AMD pathological events, contribute significantly to retinal neurodegeneration. Here, we identify specific cell types that generate IL-1β and harbor the IL-1 receptor (IL-1R) and pharmacologically validate IL-1β's contribution to neuro-retinal degeneration using the IL-1R allosteric modulator composed of the amino acid sequence rytvela (as well as the orthosteric antagonist, Kineret) in a model of blue light–induced retinal degeneration.

Methods

Mice were exposed to blue light for 6 h and sacrificed 3 days later. Mice were intraperitoneally injected with rytvela, Kineret, or vehicle twice daily for 3 days. The inflammatory markers F4/80, NLRP3, caspase-1, and IL-1β were assessed in the retinas. Single-cell RNA sequencing was used to determine the cell-specific expression patterns of retinal Il1b and Il1r1. Macrophage-induced photoreceptor death was assessed ex vivo using retinal explants co-cultured with LPS-activated bone marrow–derived macrophages. Photoreceptor cell death was evaluated by the TUNEL assay. Retinal function was assessed by flash electroretinography.

Results

Blue light markedly increased the mononuclear phagocyte recruitment and levels of inflammatory markers associated with photoreceptor death. Co-localization of NLRP3, caspase-1, and IL-1β with F4/80+ mononuclear phagocytes was clearly detected in the subretinal space, suggesting that these inflammatory cells are the main source of IL-1β. Single-cell RNA sequencing confirmed the immune-specific expression of Il1b and notably perivascular macrophages in light-challenged mice, while Il1r1 expression was found primarily in astrocytes, bipolar, and vascular cells. Retinal explants co-cultured with LPS/ATP-activated bone marrow–derived macrophages displayed a high number of TUNEL-positive photoreceptors, which was abrogated by rytvela treatment. IL-1R antagonism significantly mitigated the inflammatory response triggered in vivo by blue

light exposure, and rytvela was superior to Kineret in preserving photoreceptor density and retinal function.

Conclusion

These findings substantiate the importance of IL-1β in neuro-retinal degeneration and revealed specific sources of Il1b from perivascular MPs, with its receptor Ilr1 being separately expressed on surrounding neuro-vascular and astroglial cells. They also validate the efficacy of rytvela-induced IL-1R modulation in suppressing detrimental inflammatory responses and preserving photoreceptor density and function in these conditions, reinforcing the rationale for clinical translation.

Introduction

Photoreceptor cell death is a hallmark of many retinal degenerative disorders including age-related macular degeneration (AMD) [1,2,3,4], the leading cause of vision loss in the aging populations of developed countries [5]. Two types of AMD are clinically recognized: wet AMD, distinguished by CNV, and dry AMD, characterized by the degeneration of the retinal pigmented epithelium (RPE) and photoreceptors. Wet AMD is generally treated with anti-vascular endothelial growth factor therapies [6], while no therapy is currently available for dry AMD.

Substantial evidence points to inflammation as a key player in photoreceptor cell loss in retinal degenerative disorders including dry AMD [4, 7,8,9,10,11,12,13]. Accumulation of mononuclear phagocytes (MPs), a family of cells which includes monocytes, macrophages, and microglia, has been associated with photoreceptor damage in retinal degeneration [12, 14,15,16,17,18]. Under normal physiological conditions, the subretinal space and photoreceptor layer are devoid of MPs. Conversely, in pathological conditions, MPs are activated, invade the outer and subretinal space, and secrete pro-inflammatory cytokines, including tumor necrosis factor-α, interleukin (IL)-6, and, importantly, IL-1β, which is considered to play a major role in retinal degeneration [11, 19].

High levels of IL-1β are detected in the eyes of AMD patients [20] and the same applies to models of macular degeneration wherein IL-1β is generated by

microglia/macrophages [21,22,23]. The NOD-like receptor family pyrin domain-containing 3 (NLRP3) inflammasome is the major mediator of IL-1β production in the retina [24, 25] and is required to activate caspase-1 which catalyzes the processing of pro-IL-1β into active IL-1β [26, 27]. IL-1, in turn, primes the assembly of NLRP3 and further augments inflammatory cytokine production via positive feedback [28]. Previous studies have shown that some components of drusen and the C1q complement protein can activate the NLRP3 inflammasome in macrophages [25] and promote the secretion of IL-1β [29]; the same applies with lipofuscin when it accumulates with age [30]. Once activated, the IL-1β signal amplifies inflammation in rodent eyes by inducing expression of Chemokine (C-C motif) ligand 2 (Ccl2), Chemokine (C-X-C motif) ligand 1 (Cxcl1), and C-X-C motif chemokine ligand 10 (Cxcl10), which recruit leukocytes [21]. Concordantly, transcriptomic analysis of human retinas afflicted with AMD reveals upregulation of the same chemokines [31].

However, opposing observations on the role of IL-1β in retinal degeneration have been reported. For instance, pronounced sub-retinal inflammation and photoreceptor degeneration are observed in pigmented Cx3cr1-null mice subjected to light exposure; under these conditions, IL-1 receptor antagonist (IL-1Ra) is protective against photoreceptor cytotoxicity [32]. Similar conclusions have been drawn regarding the role of IL-1β in photo-oxidative damage to photoreceptors in rats [21]. Concordantly, IL-1β can induce apoptosis of retinal endothelium [33], neuronal precursor cells [34], and photoreceptors, but the precise mechanism of photoreceptor death in retinal degeneration remains unclear [22, 23, 32, 35]. On the other hand, LaVail [36] demonstrated protective effects of IL-1β on photoreceptors, while others failed to observe preservation of photoreceptors by IL-1Ra in light-exposed rodents [37]. Hence, collectively, the role of IL-1β in photoreceptor degeneration is unclear and suggests possible opposing effects of IL-1β based on concentrations which can depend on cell types and presumed locations relative to targeted photoreceptors, as well as by genetic determinants including those that apply to the diverse signaling of the IL-1 receptor (IL-1R) resulting in neurodegeneration. Correspondingly, the specific identity of cells producing IL-1β and harboring the IL-1 receptor has not been clearly defined.

IL-1β can bind to two types of receptors, IL-1 receptor I (IL-1RI) and IL-1 receptor II (IL-1RII). The binding of IL-1 to IL-1R1 induces a conformational change that allows the binding of the IL-1 receptor accessory protein (IL-1RacP) to IL-1R1, which then triggers the inflammatory cascade [38]. IL-1RII acts as a decoy receptor as it binds IL-1 but does not transduce IL-1 signaling [39]. There are a limited number of anti-inflammatory therapies that target IL-1 signaling; this includes anakinra (commercially known as Kineret), a recombinant form of IL-1Ra that binds competitively to IL-1R and non-selectively blocks downstream signaling [40]. We had previously developed a novel all-D peptide allosteric modulator with the amino acid sequence rytvela, which is an intramolecular peptide derived from the sequence of IL-1RacP [41]. Intramolecular peptides function on the basis of disrupting protein-protein interactions [42], such as the interaction between IL-1R and IL-1RacP in the case of rytvela (remote from the IL-1β binding site), and may confer benefits such as functional selectivity, which is associated with improved efficacy and reduced side effects [43].

In the present study, we pharmacologically validate the role of IL-1β in a light-induced model of subretinal inflammatory photoreceptor degeneration [12, 18]. We hereby clarify using single-cell RNA sequencing–specific sources of IL-1β from perivascular MPs, and IL-1RI expression primarily on astroglia and vascular cells. We also show that rytvela (as well as the molecularly and pharmacologically distinct Kineret) inhibits inflammation and preserves photoreceptor density and function to a greater extent than Kineret in this model.

Materials and Methods

Animals

All animal experiments were approved by the Maisonneuve Rosemont Hospital Animal Care Committee and were performed in accordance with the Association for Research in Vision and Ophthalmology Statement for the Use of Animals in Ophthalmic and Visual Research. Male CD-1 mice (Charles River Laboratories, Kingston, NY) of 12–16 weeks of age were used in this study. We favored using these outbred mice since inbred mice may not reflect genetic diversity as observed in the human population. In addition, genetic background does not appear to contribute significantly to the variation

observed in measurements of phenotype [44]. Moreover, CD-1 mice are less susceptible to spontaneous lesions affecting the eye, which makes them a good model for pharmacological and long-term safety studies for ocular phenotypes [45]. CD-1 mice were housed with a 12-h light/dark cycle (100–200 lux) with water and normal diet food available ad libitum.

IL-1 receptor antagonists

Kineret (Sobi, Biovitrum Stockholm, Sweden) was supplied as a 150 mg/mL solution and diluted to the required concentrations for all experiments with phosphate-buffered saline (PBS). Rytvela (Elim Biopharmaceuticals, Hayward, CA) was supplied as a lyophilized powder, dissolved in PBS, and diluted to the concentrations required for the experiments described below.

Blue light exposure model

Mice were dark-adapted overnight, then pupils were dilated using topical atropine (Alcon) prior to light exposure. Mice were exposed to blue light from a light-emitting diode (wavelength 450 nm, Apluschoice) at a light intensity of 6,000 lux for 6 h and then returned to regular conditions under a standard 12-h light/dark cycle until sacrifice on day 3 post-illumination. Mice were intraperitoneally injected with IL-1 receptor antagonists Kineret (4 mg/kg/12 h) or rytvela (1.5 mg/kg/12 h), or with phosphate-buffered saline (PBS) twice a day starting on the day of illumination until day 3. These doses were determined from our previous study [33]. Subsequently, the mice were euthanized on day 3 by cervical dislocation under isoflurane anesthesia, and eyes collected.

Retinal section preparation

Eyes were enucleated and fixed in 4% paraformaldehyde (PFA) for 1 h at room temperature and then rinsed twice with PBS. The cornea and lens were gently removed from the eye. Posterior eyecups were kept in 30% sucrose overnight and then frozen in optimal cutting temperature (OCT) medium. Sections of the entire retina along the optic nerve were cut into 10-µm sagittal sections. Retinal sections were treated at room temperature for 1 h with a blocking solution consisting of 10% fetal bovine serum, 0.1%

Triton X-100, and 0.05% Tween-20 in PBS. Retinal sections were then incubated overnight with primary antibodies, 1:200 fluorescein-labeled peanut agglutinin (PNA) (FL-1071) or 1:100 Griffonia simplicifolia Lectin I (GSL I) isolectin B4, Fluorescein (FL-1201) at 4 °C. The antibodies used were 1:100 NLRP3 (Abcam, ab91413), 1:100 IL-1β (Abcam, ab9722), 1:100 caspase-1 (BioVision, 3019), glial fibrillary acidic protein (GFAP) (Dako, Z0334), and IL1R1 (Santa Cruz, sc-393998). The retinal sections were then washed thrice with PBS and incubated with a secondary antibody solution consisting of 1% bovine serum albumin (BSA), 0.1% Triton X-100, 0.05% Tween-20, 1:500 Alexa Fluor donkey 594 anti-rat (A21209, Invitrogen), and 1:500 Alexa Fluor 488 goat anti-rabbit (A11070, Invitrogen) for 2 h at room temperature. Retinal sections were washed thrice with PBS and then flat-mounted onto glass slides with coverslips and Fluoro-Gel mounting medium (Electron Microscopy Sciences, Hatfield, PA). Sections were imaged using a laser scanning confocal microscope (Olympus IX81 with Fluoview FV1000 Scanhead) with the Fluoview Software at 30X magnification. The integrated density of GFAP was determined using ImageJ (National Institutes of Health, Bethesda, MD, USA). The integrated density is the area above the threshold for the mean density minus the background.

Measurement of photoreceptor layer thickness

Fourteen measurements per central retinal section (with optic nerve) were performed at defined distances from the optic nerve. Analysis of outer nuclear layer thickness was performed using ImageJ. The area under the curve was integrated using Prism version 7.0A (GraphPad software).

The length of the photoreceptor cone segments was measured using ImageJ, with 4 to 6 measurements made per central retinal section.

Retinal flat mount preparation

Eyes were enucleated and fixed in 4% PFA for 1 h and then rinsed twice with PBS. The neuroretina was carefully separated from the RPE/choroid/sclera complex and processed for immunostaining. Retinas were treated at room temperature for 1 h with a blocking solution consisting of 1% BSA, 1% normal goat serum, 0.1% Triton X-100, and 0.05% Tween-20 in PBS. The retinas were then labeled overnight at 4 °C with gentle

shaking using the following primary antibodies: 1:400 anti-F4/80 (ab6640, Abcam) and 1:500 anti-IL-1β (ab9722, Abcam). The retinas were then washed thrice with PBS and incubated with a secondary antibody solution consisting of 1% BSA, 0.1% Triton X-100, 0.05% Tween-20, 1:500 Alexa Fluor donkey 594 anti-rat (A21209, Invitrogen), and 1:500 Alexa Fluor 488 goat anti-rabbit (A11070, Invitrogen) for 2 h at room temperature. Retinas were washed thrice with PBS and then flat-mounted onto glass slides with coverslips and Fluoro-Gel mounting medium (Electron Microscopy Sciences, Hatfield, PA). For MP quantification, images were captured and stitched together using the MosaiX feature of Axiovision 4.

Quantification of activated MPs in the subretinal space

F4/80-stained cells were counted on flat mounts with photoreceptor segments facing the objective. Cell numbers were expressed as the mean number of F4/80+ cells per mm2.

Single-cell RNA sequencing analysis

The Mus musculus wild-type retina single-cell RNA sequencing datasets were obtained using the accession numbers GSM3854512, GSM3854514, GSM3854516, and GSM3854518 and analyzed using the Seurat R package [46]. Cells having a unique feature count between 100 and 4000, a total molecule number of less than 10000, and a mitochondrial RNA percentage of less than 25 were included. A global scaling normalization method, LogNormalize, was employed. This function normalizes the feature expression measurements for each cell by the total expression, multiplies this by a scale factor (10,000 by default), and log-transforms the result. After normalization, the scale expression (z-scores for each gene) was calculated for downstream dimensional reduction. After integration using the Seurat alignment procedures, the integrated matrix was then used for downstream analysis and visualization. Principal component analysis was run on the scaled integrated data and the results of dimensionality reduction were visualized with Uniform Manifold Approximation and Projection (UMAP). The clusters obtained were annotated using the markers provided by Heng et al. [47]. The expression of the genes Il1r1 and Il1b were illustrated using dot plots.

The Mus musculus immune single-cell RNA sequencing datasets were obtained using the accession number GSE126783 and analyzed using the Seurat R package [46]. Light-damaged and control Cx3cr1YFP+ cells were filtered based on unique feature counts and mitochondrial counts. Cells having a unique feature count of less than 4000 and a mitochondrial RNA percentage of less than 10 were kept. The 2 Seurat Objects were then merged. An integration was performed on this object following the Integration and Label Transfer Vignette (SATIJA LAB). The integrated matrix was then used for downstream analysis and visualization. Principal component analysis was run on the scaled integrated data and the results were visualized with UMAP. The clusters obtained were annotated using the markers provided by O'Koren et al. [48]. All the microglia sub-clusters were regrouped together, and 3 different cell types were annotated: microglia, perivascular macrophages (pv MFs), and monocyte-derived macrophages (mo MFs). The expression of the genes Il1r1 and Il1b were illustrated using dot plots.

Terminal deoxynucleotidyl transferase dUTP nick end labeling assay

TUNEL staining was performed according to the manufacturer's protocol (In Situ Cell Death Detection Kit; Roche Diagnostics). Briefly, retinal flat mount or retinal sections were fixed in 4% PFA for 30 min and washed in PBS. Flat mounts or sections were then incubated for 90 min at 37 °C with the reaction mixture and the reaction was stopped by washing with PBS. Nuclei were stained with 4′, 6-diamidino-2-phenylindole (DAPI, Sigma, St. Louis, MO, USA). Images were captured with a laser scanning confocal microscope (Olympus IX81 with Fluoview FV1000 Scanhead) with the Fluoview Software at 30X magnification.

Isolation of bone marrow–derived monocytes

Bone marrow–derived monocytes (BMDMs) were harvested from 12- to 16-week-old CD-1 mice sacrificed by cervical dislocation. Total mononuclear cells were flushed from femurs and tibiae with PBS. to subsequently isolate the BMDM population. Briefly, the suspension was centrifuged at 1500 rpm for 10 min. The supernatant was discarded, and the pellet was resuspended in Dulbecco's Modified Eagle Medium (DMEM) supplemented with 10% FBS (085-150, Wisent Bioproducts), 1% penicillin and

streptomycin, and 0.125 µg/mL macrophage colony-stimulating factor (M-CSF) (576406; Biolegend). The suspension of BMDMs was filtered using sterile cell strainers (40 µm; 352340; Corning) and seeded in 24-well plates. The culture medium was renewed every 2 days for 1 week.

BMDM and retinal explant incubation

BMDMs were treated or not with 50 ng/mL lipopolysaccharide (LPS) (Escherichia coli 10004557; Thermos Fisher) for 24 h and then 1 mM of adenosine triphosphate (ATP; R0441; Thermo Fisher Scientific) was added for 30 min. BMDMs were washed twice with DMEM supplemented with 0.2% BSA (800-095-EG; Wisent). BMDMs were cultured for 24 h and the supernatant served as conditioned media. Mouse retinas were prepared and placed on either 100,000 adherent BMDMs for 18 h at 37 °C in DMEM with 0.2% BSA or in BMDM-derived conditioned media in the absence or presence of rytvela (1 µM), Kineret (1.5 mg/mL), or an anti-IL-1β antibody (150 ng/mL, Abcam 9722). Doses of rytvela and Kineret were determined based on our previous study [49]. After 18 h, the explants were evaluated by TUNEL assay.

Quantitative RT-PCR

Total RNA was extracted from mice retinas using the RNeasy mini kit (Qiagen) according to the manufacturer's protocol and was reverse transcribed using iScript™ Reverse Transcription Supermix (Bio-Rad) according to the manufacturer’s guidelines to generate cDNA. qPCR reactions were performed using 25 ng of sample cDNA, 2 µM of specific primers for the selected mRNAs (Table 1), and Universal SYBR Green Master Mix (BioRad). Relative expression (RQ = 2−ΔΔCT) was calculated using a detection system (ABI Prism 7500, Applied Biosystems, Foster City, CA, USA) and normalized to β-actin (Actb) and 18S.

Western blotting

Proteins were extracted from mice retinas by sonication in lysis buffer RIPA buffer (pH = 8) containing 50 mM Tris-HCl, 150 mM NaCl, 5 mM EDTA, 1% Triton 100×, 0.5% sodium deoxycholate, 0.1% SDS, and a cocktail of protease and phosphatase inhibitors

(MiniComplete, PhosphoStop, and PMSF, Roche, Bâle, Switzerland). Protein concentrations were determined using the Bicinchoninic Acid Protein Assay Kit (Pierce, Rockford, IL, USA). Thirty micrograms of protein per sample were electrophoresed on 15% sodium dodecyl sulfate-polyacrylamide gels using an electrophoresis system (Mini-Protean Tetra System, Bio-Rad, Hercules, CA, USA) and then transferred onto polyvinylidene difluoride membranes (Millipore, Billerica, MA, USA). Membranes were blocked with 5% skim milk in Tris-buffered saline containing 0.1% Tween-20 for 1 h at room temperature, and incubated with the following primary antibodies: 1:800 IL-1β (Abcam, ab9722), 1:500 caspase-1 (BioVision, 3019), and 1:1000 β-actin (Santa Cruz, sc47778) then incubated with 1:6000 horseradish peroxidase-conjugated secondary antibodies (Millipore, AP307P and Millipore, AP308P). Densitometric analysis of western blotting bands was quantified using the ImageJ software and normalized to β-actin.

Enzyme-linked immunosorbent assay

Conditioned media from BMDMs incubated with retinal explants were collected. The concentrations of IL-1β were measured using a commercial ELISA kit (R&D Systems, MLB00C) according to the manufacturer's instructions. Calibration curves were prepared using purified standards for IL-1β which were provided as part of the ELISA kit.

Electroretinogram

Electroretinograms (ERGs) were recorded using an Espion ERG Diagnosys apparatus equipped with a ColorDome Ganzfeld stimulator (Diagnosys LLC, Lowell, MA). Mice were initially dark-adapted overnight and anesthetized intraperitoneally with a mix of ketamine (100 mg/kg) and xylazine (20 mg/kg). Corneas were anesthetized with proxymetacaine hydrochloride (0.5% Alcaine; Alcon, Fort Worth, TX, USA) and pupils dilated with 0.5% atropine (Alcon, Fort Worth, TX, USA). Body temperature was maintained at 37.5 °C with a heating pad. ERGs were measured using corneal DTL Plus electrodes (Diagnosys LLC), a forehead reference electrode, and a ground electrode subcutaneously in the tail. To evaluate rod photoreceptor function (scotopic ERG), five-strobe flash stimuli were presented with flash intensities of 0.01 candela*second/meter2 (cds/m2), 0.1 cds/m2, 0.5 cds/m2,1.0 cds/m2, and 3.0 cds/m2. Six waveforms were

averaged per light intensity. All procedures were performed in a dark room under dim red-light illumination. The amplitude of the a-wave was measured from baseline to the primary negative peak, and b-wave was measured from the trough of the a-wave to the maximum of the fourth positive peak.

Statistical analysis

Values are presented as means ± standard error of the mean (SEM). Data were analyzed by independent t-tests or one-way analysis of variance (ANOVA) followed by post hoc Holm-Sidak tests for comparison of means. Statistical significance was set at $p < 0.05$. Statistical analysis was performed using Prism 7.0A (GraphPad Software).

Results

Blue light induces subretinal macrophage infiltration, which is suppressed by IL-1R antagonism

Blue light elicited substantial infiltration of MPs as evidenced by the presence of F4/80+ cells in the outer and subretina (Fig. 1a), consistent with reported observations [12, 18]. MPs are not seen in the subretinal space of unexposed (intact) retinas. Kineret, and to a slightly greater extent, rytvela mitigated this MP infiltration and maintained MP morphology in a ramified, quiescent state, rather than the activated ameboid state seen in vehicle-treated animals (Fig. 1a). Glial fibrillary acidic protein (GFAP), a marker of retinal gliosis [50, 51] which is upregulated upon MP activation [52] and used as an index of retinal degeneration, was dramatically increased throughout most of the entire retina (Fig. 1b); this effect was largely prevented by rytvela and Kineret. Concordantly, light-induced increases in pro-inflammatory Il1b, Il6, and Ccl2 mRNA levels were also significantly reduced by the IL-1R inhibitors rytvela and Kineret (Fig. 1c). Similar observations were made for inflammasome components and products, whereby increased blue light–induced NLRP3, caspase-1, and IL-1β at different stages of maturation (Fig. 2a) co-localized in F4/80+ MPs (Figs. 2b and 3). Of relevance, retinal flat-mount staining revealed that IL-1β largely co-localized with MPs (Fig. 2b), suggesting that infiltrating MPs are the major source of this pro-inflammatory cytokine.

Single-cell RNA-seq analysis of Il1b and Il1r1 expression in the retina

We analyzed the transcriptomic profiles of Il1b and its receptor Il1r1 in the mouse retina. Single-cell mRNA transcriptomic analysis using 10× Genomics revealed that immune cells are the main producers of Il1b in the retina and that Il1r1 is mostly expressed in vascular cells (pericyte and endothelial cells) as well as astrocytes and bipolar cells (Fig. 4a). More importantly, Ilr1 expression was not detected in photoreceptors and MPs (Fig. 4a). We next analyzed the proportions of different FACS-sorted live Cx3cr1 MPs in control and light-damaged retinas. Among the 3 different cell types identified (Fig. 4b), light-damaged retinas showed a higher proportion of mo MF cells compared with the non-illuminated retinas (Fig. 4b, c), while microglia and pv MF distributions remained relatively unaffected. However, we found that Il1b was only upregulated in pv MFs but not in mo MFs or microglial cells in light-challenged mice compared with control (Fig. 4d). Expression of IL-1R1 was confirmed by immunofluorescence, showing that it colocalizes with GFAP and IB4 lectin in astrocytes and blood vessels, respectively (Fig. 4e, f), but not in MPs (Suppl Fig. 1).

Suppression of subretinal inflammation preserves photoreceptor integrity

Next, we evaluated whether the suppression of subretinal inflammation using rytvela or Kineret was associated with preservation of photoreceptor integrity. Mice exposed to blue light experienced significant photoreceptor degeneration evidenced by a thinner outer nuclear layer (ONL; Fig. 5a), a loss of cone inner and outer segments (evaluated by peanut agglutinin [PNA] staining; Fig. 5b), high apoptotic rate in the ONL corroborated by augmented TUNEL positivity (Fig. 5c), and associated loss of the a-wave ERG amplitude generated from the photoreceptors (Fig. 6a). At an optimal flash intensity of 3.00 cds/m2, the a-wave amplitude of light-exposed animals decreased by half compared with the control group; as expected, b-wave amplitude was also lower in vehicle-treated animals since it is triggered in bipolar and Müller cells by the a-wave signal (Fig. 6b). Rytvela and Kineret prevented apoptosis (Fig. 5c, d) and preserved photoreceptor layer thickness, including its outer segments (Fig. 5a, b), and photoreceptor function, with rytvela apparently being more effective than Kineret (Figs. 5a, b; and 6).

Rytvela protects against macrophage-induced photoreceptor cell death in an ex vivo model

We next proceeded to clarify if inflammation triggered by inflammasome activators, notably LPS, causes photoreceptor cell death, and if inhibition of IL-1β would prevent the latter. To evaluate this mechanism, we induced a pro-inflammatory phenotype in isolated murine BMDMs stimulated with LPS/ATP (which also stimulates formation of mature IL-1β [53]; Fig. 7a). LPS/ATP-stimulated BMDMs were incubated facing the photoreceptor layer of neuroretinal explants in the presence or absence of the IL-1R antagonists rytvela (1 µM) or Kineret (1.5 mg/mL) (Fig. 7a). Photoreceptor apoptosis was quantified by measuring TUNEL-positive cells in retinal explants. Exposure of retinal explants to LPS/ATP-stimulated BMDMs caused pronounced apoptosis of photoreceptors as witnessed by high numbers of TUNEL-positive cells (Fig. 7b); rytvela and Kineret prevented LPS/ATP-induced photoreceptor cell death. The number of TUNEL-positive cells did not differ between retinal explants cultured in the absence of BMDMs and the presence of non-activated BMDMs. In order to determine whether IL-1R inhibition in the neuroretina has a protective effect on photoreceptors, we treated neuroretinas with conditioned medium from BMDMs stimulated or not with LPS/ATP. Conditioned media from LPS/ATP-stimulated BMDMs caused an increase in the number of TUNEL-positive cells that was prevented by treating the neuroretina with rytvela or Kineret; these treatments did not affect the levels of IL-1β (Fig. 7c, d). To further clarify that IL-1β from activated BMDMs is involved, we used an IL-1β-neutralizing antibody which abrogated cell death (Fig. 7c). Taken together, these in vivo and ex vivo observations highlight the role of IL-1β and show that modulation of IL-1R signaling using rytvela (or IL-1R antagonist Kineret) interferes with detrimental subretinal inflammation in models of retinal phototoxicity and preserves photoreceptor density and function.

Discussion

Neuroinflammation-induced photoreceptor cell death is a common feature of several ocular neurodegenerative disorders, including retinitis pigmentosa and AMD [54]. The recruitment and activation of MPs are key components in the progressive loss of

photoreceptors in these types of ocular disorders [55, 56]. Several studies have suggested that pro-inflammatory mediators released by these infiltrating immune cells in the subretinal space are the main contributors to neuronal damage [57,58,59]. In this context, the major proinflammatory cytokine IL-1β has been suggested to promote acute neuronal loss in experimental studies and has been implicated in chronic neurodegenerative disorders [60,61,62,63], including those of the eye [11]. IL-1β levels are found to be increased in the vitreous humor of patients with AMD [20] and have been reported to contribute to photoreceptor degeneration in different animal models [21, 23, 32]. Yet, experimentally, a cytotoxic role for IL-1β has been questioned by others [36, 37], inferring possible distinct mechanisms including those based on IL-1β concentration and/or genetic determinants including those applied to the diversity in IL-1RI-coupled signaling processes. Moreover, the identity (and presumed location) of cells generating IL-1β and harboring IL-1RI remains to be clarified in order to better elucidate the role that IL-1β plays in retinal degeneration.

The present study used a blue light–triggered model of inflammation-induced photoreceptor toxicity, which is commonly utilized [12] to experimentally recapitulate the phenotypic changes observed in neuro-retinal degenerative disorders [64, 65]. We observed infiltration/activation of MPs associated with increased pro-inflammatory cytokines, including IL-1β and photoreceptor cell death. Essentially, pv MFs were the main source of elevated Il1b expression, whereas the receptor Ilr1 was separately expressed on astroglia and vascular cells. The detrimental effects of light-induced inflammation were prevented by treatment with a negative modulator of IL-1R, to an extent superior to that observed with an orthosteric antagonist.

Under physiological conditions, the subretinal space hardly harbors any MPs due to immunosuppression mediated by inhibitory signals from neurons [66] and RPE cells [67]. However, MPs migrate to the subretinal space upon damage to the photoreceptors and/or RPE cells to scavenge cell debris in a process of efferocytosis which does not involve inflammatory responses [68]. With time upon exposure to light, exaggerated signals generated by trans-retinal Müller cells [55], RPE [69], and other MPs [56]. Activated MPs (revealed by their ameboid morphology, absence of cell processes, and inflammatory cytokine profile) can contribute to retinal gliosis wherein Müller cells further

release factors that amplify the inflammatory response [70]. In this sense, we showed augmented GFAP immunoreactivity in Müller glia associated with subretinal MP infiltration after blue light exposure. Although one of the roles of Müller cells is to protect tissues from damage, their over-activation can contribute to neurodegeneration and curtail regenerative processes [71]; concordantly, GFAP gene knockout prevents gliosis and protects photoreceptors [72]. Relevantly, the IL-1R modulator rytvela suppressed MP activation and recruitment, minimized gliosis, and exerted neuroprotection.

MPs are reported to elicit their pathogenic effects at least in part through IL-1β [32]. We detected infiltrating MPs as the main source of IL-1β associated with photoreceptor phototoxicity. In support of the fact that the NLRP3 inflammasome is a key regulator of IL-1β maturation via the activation of caspase-1 [73], we observed the colocalization of the inflammasome components NLRP3, caspase-1, and IL-1β in infiltrating subretinal MPs (F4/80+). Our findings reveal that IL-1R antagonism suppresses IL-1β production as well as neuroretinal phototoxicity in cells that separately express IL-1β and IL-1RI. Rytvela prevented elevations in IL-1β levels after blue-light exposure mostly by reducing the accumulation of IL-1β-producing MPs into the subretinal space. It was also shown to reduce activation of glial cells (gliosis), which is reported to upregulate IL-1β production via ATP release and activate the inflammasome in a P2X7-dependent mechanism [74]; cytotoxicity is also known to release ATP (and high mobility group box 1 [HMGB1]) to stimulate IL-1β release by macrophages. Rytvela (and Kineret) in turn suppresses IL-1RI-dependent (photoreceptor) apoptotic processes involving mechanisms such as TRIF [75], IL-8 [76], glutamate transport [77], and reactive oxygen/nitrogen species [78]. Hence, one can envisage that light exposure triggers a macrophage chemotactic and activating signal (such as through release of DAMPs and chemokines) [79] which would generate IL-1β in MPs; IL-1β would be amplified by IL-1R signaling which can sustain activation of infiltrating MPs while also triggering cell death [32]. Antagonism of IL-1R (with rytvela or Kineret) would arrest this cycle and protect photoreceptors.

Since an important feature in this study applies to the fundamental role of infiltrated MPs that produce IL-1β, which contributes to photoreceptor degeneration, we specifically designed an experiment to show that activated BMDMs (known to generate high levels of IL-1β) or their conditioned media can trigger photoreceptor death in retinal explants,

and is preventable by rytvela and Kineret, which act on IL-1RI-expressing neuroretina without reducing IL-1β concentrations in the BMDM conditioned media.

Using single-cell RNA-seq analysis, we validated that the long-lived pv MFs, which represent a small population of retinal MPs, were the main source of upregulated IL-1β. pv MFs can be defined by their location in contact or close association with the abluminal side of blood vessels [80]. Interestingly, these MPs can migrate from the perivascular space to the photoreceptor layer, participating in retinal degeneration [81].

Although subretinal MPs are implicated in photoreceptor toxicity via IL-1β secretion, one cannot rule out the involvement of other retinal cell types in modulating inflammation during retinal dystrophies. For instance, IL-1β secreted by infiltrating microglia/macrophages was shown to induce chemokine (Ccl2, Cxcl1, and Cxcl10) expression in Müller and RPE cells implicated in photo-oxidative retinal damage [21]. Conversely, IL-1β inhibition suppressed chemokine expression [21], consistent with our observations. In the mouse retina, we found that Il1r1 expression was essentially in astrocytes, pericytes, endothelial cells, and bipolar cells. The failure to detect this receptor in MPs and photoreceptors suggests that IL-1β-induced neurotoxicity occurs through other cell type–specific IL-1R1 signaling pathways. One plausible mechanism of this effect might be in part due to the action of IL-1β on astrocytes to trigger glial activation/gliosis. We showed that IL-1R antagonism attenuates retinal gliosis, which is known to cause photoreceptor death. In addition, the action of IL-1β on astrocytes can result in the breakdown of blood-retinal barrier to increase vascular permeability which allows recruitment of MPs to the site of inflammation [82, 83]. Similarly, IL-1β can directly act on pericytes and endothelial cells to disrupt the integrity of blood-retinal barrier [84,85,86,87] which in turn, favors vascular permeability. Along these lines, the higher proportion of the short-lived mo MFs in the illuminated retinas suggests a possible disruption of the blood-retinal barrier to allow the infiltration of circulating monocytes [56]. Taken together, phototoxicity releases mediators that attract and stimulate macrophages at the site of injury, which amplify neuroretinal damage via activation of IL-1R. Additional studies are needed to further elucidate the distinct roles of IL-1R in different cell types.

IL-1β plays a complex role which also appears to be concentration-dependent, such that physiologic (low) levels of IL-1β confer protection against photoreceptor

degeneration [36, 88]. Low levels of IL-1β enhance production of growth factors [89, 90] such as basic fibroblast growth factor (bFGF), which are relevant to vasculature and photoreceptor protection [21]. Conversely, pathologically elevated levels of IL-1β cause vascular decay [37, 91, 92]. Despite the evidence pointing toward an important function of IL-1 in photoreceptor death, a previous study has shown that Ilr1 and Casp1 deletion was not protective in a light-model of retinal degeneration [93]. However, these results with Ilr1 knockout animals must be interpreted with caution since compensatory changes may have been adopted during development. In contrast, a more recent study showed that Caspase-1/11 ablation has a protective role in retinal degeneration [94]. All in all, it is thus reasonable to propose that modulation of IL-1R would be a better alternative to (total) orthosteric antagonism of IL-1R, as the former would bias signaling and induce pharmacological selectivity, whereas the latter would inhibit all signals linked to IL-1R [95]. Along these lines, the allosteric modulator rytvela confers an advantage over orthosteric inhibitors of IL-1R by inhibiting the canonical JNK/p38/c-Jun/AP-1 pathway while preserving NF-κB, which is important for immune vigilance and photoreceptor survival [49, 96, 97]. Accordingly, rytvela protects the choroid and retina from inflammation without displaying adverse effects [33, 91, 98].

In summary, this study pharmacologically validates a major role for IL-1β in triggering neuro-retinal inflammatory responses and neural tissue damage in a model of light-exposed inflammation-triggered neurodegeneration. The development of pharmacologic allosteric IL-1R modulators represents a novel and promising therapeutic approach to tackle retinal degenerative diseases in which IL-1β is implicated. In this context, the advantages of the small peptide rytvela are its superior cytoprotective efficacy and small size compared with current anti-IL-1 therapeutics molecules conferring better distribution [49], ease of administration, low risk of immunogenicity [41], and maintenance of immune vigilance [97].

Conclusion

Our study implicates an important role of IL-1β signaling in subretinal inflammation and photoreceptor death. We report astroglial and vascular expression of Ilr1 and that Il1b is exclusively upregulated in pv MFs in response to light challenge. Additionally, the

IL-1R modulator rytvela confers neuroprotection in photoreceptors following photooxidative stress to the retina. IL-1 receptor modulation is a promising therapeutic avenue to suppress the inflammatory response and preserve photoreceptor integrity in ocular degenerative diseases. It is hoped that our findings will pave the way for future investigations and culminate in clinical trials involving ophthalmic patient populations.

Availability of data and materials

All datasets and analyses used in the current study are available from the corresponding author on reasonable request.

References

1. Xu H, Chen M, Forrester JV. Para-inflammation in the aging retina. Prog Retin Eye Res. 2009;28(5):348–68.

2. Pfeiffer RL, Marc RE, Jones BW. Persistent remodeling and neurodegeneration in late-stage retinal degeneration. Prog Retin Eye Res. 2020;74:100771.

3. Clerin E, Marussig M, Sahel JA, Leveillard T. Metabolic and redox signaling of the nucleoredoxin-like-1 gene for the treatment of genetic retinal diseases. Int J Mol Sci. 2020;21(5):1625.

4. Canto A, Olivar T, Romero FJ, Miranda M. Nitrosative stress in retinal pathologies: review. Antioxidants (Basel). 2019;8(11):543.

5. Wong WL, Su X, Li X, Cheung CM, Klein R, Cheng CY, et al. Global prevalence of age-related macular degeneration and disease burden projection for 2020 and 2040: a systematic review and meta-analysis. Lancet Glob Health. 2014;2(2):e106–16.

6. Coleman HR, Chan CC, Ferris FL 3rd, Chew EY. Age-related macular degeneration. Lancet. 2008;372(9652):1835–45.

7. Combadiere C, Feumi C, Raoul W, Keller N, Rodero M, Pezard A, et al. CX3CR1-dependent subretinal microglia cell accumulation is associated with cardinal features of age-related macular degeneration. J Clin Invest. 2007;117(10):2920–8.

8. Gupta N, Brown KE, Milam AH. Activated microglia in human retinitis pigmentosa, late-onset retinal degeneration, and age-related macular degeneration. Exp Eye Res. 2003;76(4):463–71.

9. Haines JL, Hauser MA, Schmidt S, Scott WK, Olson LM, Gallins P, et al. Complement factor H variant increases the risk of age-related macular degeneration. Science. 2005;308(5720):419–21.
10. Klein RJ, Zeiss C, Chew EY, Tsai JY, Sackler RS, Haynes C, et al. Complement factor H polymorphism in age-related macular degeneration. Science. 2005; 308(5720):385–9.
11. Wooff Y, Man SM, Aggio-Bruce R, Natoli R, Fernando N. IL-1 Family members mediate cell death, inflammation and angiogenesis in retinal degenerative diseases. Front Immunol. 2019;10:1618.
12. Mellal K, Omri S, Mulumba M, Tahiri H, Fortin C, Dorion MF, et al. Immunometabolic modulation of retinal inflammation by CD36 ligand. Sci Rep. 2019;9(1):12903.
13. Rozing MP, Durhuus JA, Krogh Nielsen M, Subhi Y, Kirkwood TB, Westendorp RG, et al. Age-related macular degeneration: a two-level model hypothesis. Prog Retin Eye Res. 2019;76:100825.
14. Damani MR, Zhao L, Fontainhas AM, Amaral J, Fariss RN, Wong WT. Age-related alterations in the dynamic behavior of microglia. Aging Cell. 2011; 10(2):263–76.
15. Cruz-Guilloty F, Saeed AM, Echegaray JJ, Duffort S, Ballmick A, Tan Y, et al. Infiltration of proinflammatory m1 macrophages into the outer retina precedes damage in a mouse model of age-related macular degeneration. Int J Inflamm. 2013;2013:503725.
16. Whitcup SM, Nussenblatt RB, Lightman SL, Hollander DA. Inflammation in retinal disease. Int J Inflamm. 2013;2013:724648.
17. Guillonneau X, Eandi CM, Paques M, Sahel JA, Sapieha P, Sennlaub F. On phagocytes and macular degeneration. Prog Retin Eye Res. 2017;61:98–128.
18. Lavalette S, Conart JB, Touhami S, Roubeix C, Houssier M, Augustin S, et al. CD36 deficiency inhibits retinal inflammation and retinal degeneration in Cx3cr1 knockout mice. Front Immunol. 2019;10:3032.
19. Block ML, Zecca L, Hong JS. Microglia-mediated neurotoxicity: uncovering the molecular mechanisms. Nat Rev Neurosci. 2007;8(1):57–69.
20. Zhao M, Bai Y, Xie W, Shi X, Li F, Yang F, et al. Interleukin-1beta level is increased in vitreous of patients with neovascular age-related macular degeneration (nAMD) and polypoidal choroidal vasculopathy (PCV). PLoS One. 2015;10(5):e0125150.

21. Natoli R, Fernando N, Madigan M, Chu-Tan JA, Valter K, Provis J, et al. Microglia-derived IL-1beta promotes chemokine expression by Muller cells and RPE in focal retinal degeneration. Mol Neurodegener. 2017; 12(1):31.
22. Kataoka K, Matsumoto H, Kaneko H, Notomi S, Takeuchi, Sweigard JH, et al. Macrophage- and RIP3-dependent inflammasome activation exacerbates retinal detachment-induced photoreceptor cell death. Cell Death Dis. 2015;6:e1731
23. Eandi CM, Charles Messance H, Augustin S, Dominguez E, Lavalette S, Forster V, et al. Subretinal mononuclear phagocytes induce cone segment loss via IL-1beta. Elife. 2016;5:e16490.
24. Tarallo V, Hirano Y, Gelfand Bradley D, Dridi S, Kerur N, Kim Y, et al. DICER1 loss and Alu RNA induce age-related macular degeneration via the NLRP3 inflammasome and MyD88. Cell. 2012;149(4):847–59.
25. Doyle SL, Campbell M, Ozaki E, Salomon RG, Mori A, Kenna PF, et al. NLRP3 has a protective role in age-related macular degeneration through the induction of IL-18 by drusen components. Nat Med. 2012;18(5):791–8.
26. Munoz-Planillo R, Kuffa P, Martinez-Colon G, Smith BL, Rajendiran TM, Nunez G. K(+) efflux is the common trigger of NLRP3 inflammasome activation by bacterial toxins and particulate matter. Immunity. 2013;38(6):1142–53.
27. Mariathasan S, Weiss DS, Newton K, McBride J, O'Rourke K, Roose-Girma M, et al. Cryopyrin activates the inflammasome in response to toxins and ATP. Nature. 2006;440(7081):228–32.
28. Gross O, Yazdi AS, Thomas CJ, Masin M, Heinz LX, Guarda G, et al. Inflammasome activators induce interleukin-1alpha secretion via distinct pathways with differential requirement for the protease function of caspase-1. Immunity. 2012;36(3):388–400.
29. Gao J, Cui JZ, To E, Cao S, Matsubara JA. Evidence for the activation of pyroptotic and apoptotic pathways in RPE cells associated with NLRP3 inflammasome in the rodent eye. J Neuroinflammation. 2018;15(1):15.
30. Brandstetter C, Patt J, Holz FG, Krohne TU. Inflammasome priming increases retinal pigment epithelial cell susceptibility to lipofuscin phototoxicity by changing the cell death mechanism from apoptosis to pyroptosis. J Photochem Photobiol B. 2016;161:177–83.

31. Newman AM, Gallo NB, Hancox LS, Miller NJ, Radeke CM, Maloney MA, et al. Systems-level analysis of age-related macular degeneration reveals global biomarkers and phenotype-specific functional networks. Genome Med. 2012;4(2):16.
32. Hu SJ, Calippe B, Lavalette S, Roubeix C, Montassar F, Housset M, et al. Upregulation of P2RX7 in Cx3cr1-Deficient mononuclear phagocytes leads to increased interleukin-1beta secretion and photoreceptor neurodegeneration. J Neurosci. 2015;35(18):6987–96.
33. Rivera JC, Sitaras N, Noueihed B, Hamel D, Madaan A, Zhou T, et al. Microglia and interleukin-1beta in ischemic retinopathy elicit microvascular degeneration through neuronal semaphorin-3A. Arterioscler Thromb Vasc Biol. 2013;33(8):1881–91.
34. Guadagno J, Swan P, Shaikh R, Cregan SP. Microglia-derived IL-1beta triggers p53-mediated cell cycle arrest and apoptosis in neural precursor cells. Cell Death Dis. 2015;6:e1779.
35. Zhao L, Zabel MK, Wang X, Ma W, Shah P, Fariss RN, et al. Microglial phagocytosis of living photoreceptors contributes to inherited retinal degeneration. EMBO Mol Med. 2015;7(9):1179–97.
36. LaVail MM, Unoki K, Yasumura D, Matthes MT, Yancopoulos GD, Steinberg RH. Multiple growth factors, cytokines, and neurotrophins rescue photoreceptors from the damaging effects of constant light. Proc Natl Acad Sci U S A. 1992;89(23):11249–53.
37. Lavalette S, Raoul W, Houssier M, Camelo S, Levy O, Calippe B, et al. Interleukin-1beta inhibition prevents choroidal neovascularization and does not exacerbate photoreceptor degeneration. Am J Pathol. 2011;178(5):2416–23.
38. Dinarello CA. Overview of the IL-1 family in innate inflammation and acquired immunity. Immunol Rev. 2018;281(1):8–27.
39. Colotta F, Re F, Muzio M, Bertini R, Polentarutti N, Sironi M, et al. Interleukin-1 type II receptor: a decoy target for IL-1 that is regulated by IL-4. Science. 1993;261(5120):472–5.
40. Braddock M, Quinn A, Canvin J. Therapeutic potential of targeting IL-1 and IL-18 in inflammation. Expert Opin Biol Ther. 2004;4(6):847–60.
41. Quiniou C, Sapieha P, Lahaie I, Hou X, Brault S, Beauchamp M, et al. Development of a novel noncompetitive antagonist of IL-1 receptor. J Immunol. 2008;180(10):6977–87.

42. McDonnell JM, Beavil AJ, Mackay GA, Jameson BA, Korngold R, Gould HJ, et al. Structure based design and characterization of peptides that inhibit IgE binding to its high-affinity receptor. Nat Struct Biol. 1996;3(5):419–26.
43. Smith JS, Lefkowitz RJ, Rajagopal S. Biased signalling: from simple switches to allosteric microprocessors. Nat Rev Drug Discov. 2018;17(4):243–60.
44. Tuttle AH, Philip VM, Chesler EJ, Mogil JS. Comparing phenotypic variation between inbred and outbred mice. Nat Methods. 2018;15(12):994–6.
45. Mukaratirwa S, Petterino C, Naylor SW, Bradley A. Incidences and range of spontaneous lesions in the eye of Crl:CD-1(ICR)BR mice used in toxicity studies. Toxicol Pathol. 2015;43(4):530–5.
46. Butler A, Hoffman P, Smibert P, Papalexi E, Satija R. Integrating single-cell transcriptomic data across different conditions, technologies, and species. Nat Biotechnol. 2018;36(5):411–20.
47. Heng JS, Hackett SF, Stein-O'Brien GL, Winer BL, Williams J, Goff LA, et al. Comprehensive analysis of a mouse model of spontaneous uveoretinitis using single-cell RNA sequencing. Proc Natl Acad Sci U S A. 2019; 116(52): 26734–44.
48. O'Koren EG, Yu C, Klingeborn M, AYW W, Prigge CL, Mathew R, et al. Microglial function is distinct in different anatomical locations during retinal homeostasis and degeneration. Immunity. 2019;50(3):723–37 e7.
49. Nadeau-Vallee M, Quiniou C, Palacios J, Hou X, Erfani A, Madaan A, et al.
Novel noncompetitive IL-1 receptor-biased ligand prevents infection- and inflammation-induced preterm birth. J Immunol. 2015;195(7):3402–15.
50. Lewis GP, Matsumoto B, Fisher SK. Changes in the organization and expression of cytoskeletal proteins during retinal degeneration induced by retinal detachment. Invest Ophthalmol Vis Sci. 1995;36(12):2404–16.
51. Luna G, Lewis GP, Banna CD, Skalli O, Fisher SK. Expression profiles of nestin and synemin in reactive astrocytes and Muller cells following retinal injury: a comparison with glial fibrillar acidic protein and vimentin. Mol Vis. 2010;16: 2511–23.
52. de Raad S, Szczesny PJ, Munz K, Reme CE. Light damage in the rat retina: glial fibrillary acidic protein accumulates in Muller cells in correlation with photoreceptor damage. Ophthalmic Res. 1996;28(2):99–107.

53. Stoffels M, Zaal R, Kok N, van der Meer JW, Dinarello CA, Simon A. ATP-induced IL-1beta specific secretion: true under stringent conditions. Front Immunol. 2015;6:54.
54. Heneka MT, Kummer MP, Latz E. Innate immune activation in neurodegenerative disease. Nat Rev Immunol. 2014;14(7):463–77.
55. Rutar M, Natoli R, Provis JM. Small interfering RNA-mediated suppression of Ccl2 in Muller cells attenuates microglial recruitment and photoreceptor eath following retinal degeneration. J Neuroinflammation. 2012;9:221.
56. Sennlaub F, Auvynet C, Calippe B, Lavalette S, Poupel L, Hu SJ, et al. CCR2(+) monocytes infiltrate atrophic lesions in age-related macular disease and mediate photoreceptor degeneration in experimental subretinal inflammation in Cx3cr1 deficient mice. EMBO Mol Med. 2013;5(11):1775–93.
57. Nassar K, Grisanti S, Elfar E, Luke J, Luke M, Grisanti S. Serum cytokines as biomarkers for age-related macular degeneration. Graefes Arch Clin Exp Ophthalmol. 2015;253(5):699–704.
58. Hu Z, Zhang Y, Wang J, Mao P, Lv X, Yuan S, et al. Knockout of Ccr2 alleviates photoreceptor cell death in rodent retina exposed to chronic blue
light. Cell Death Dis. 2016;7(11):e2468.
59. Heneka MT, Kummer MP, Stutz A, Delekate A, Schwartz S, VieiraSaecker A, et al. NLRP3 is activated in Alzheimer's disease and contributes to pathology in APP/PS1 mice. Nature. 2013;493(7434):
674–8.
60. Lucas SM, Rothwell NJ, Gibson RM. The role of inflammation in CNS injury and disease. Br J Pharmacol. 2006;147(Suppl 1):S232–40.
61. Koprich JB, Reske-Nielsen C, Mithal P, Isacson O. Neuroinflammation mediated by IL-1beta increases susceptibility of dopamine neurons to degeneration in an animal model of Parkinson's disease. J Neuroinflammation. 2008;5:8.
62. Italiani P, Puxeddu I, Napoletano S, Scala E, Melillo D, Manocchio S, et al. Circulating levels of IL-1 family cytokines and receptors in Alzheimer's disease: new markers of disease progression? J Neuroinflammation. 2018; 15(1):342.
63. Allan SM, Tyrrell PJ, Rothwell NJ. Interleukin-1 and neuronal injury. Nat Rev Immunol. 2005;5(8):629–40.

64. Grimm C, Reme CE. Light damage as a model of retinal degeneration. Methods Mol Biol. 2013;935:87–97.
65. Nakamura M, Kuse Y, Tsuruma K, Shimazawa M, Hara H. The involvement of the oxidative stress in murine blue LED light-induced retinal damage model. Biol Pharm Bull. 2017;40(8):1219–25.
66. Galea I, Bechmann I, Perry VH. What is immune privilege (not)? Trends Immunol. 2007;28(1):12–8.
67. Levy O, Calippe B, Lavalette S, Hu SJ, Raoul W, Dominguez E, et al. Apolipoprotein E promotes subretinal mononuclear phagocyte survival and
chronic inflammation in age-related macular degeneration. EMBO Mol Med. 2015;7(2):211–26.
68. Westman J, Grinstein S, Marques PE. Phagocytosis of necrotic debris at sites of injury and inflammation. Front Immunol. 2019;10:3030.
69. Chen H, Liu B, Lukas TJ, Neufeld AH. The aged retinal pigment epithelium/choroid: a potential substratum for the pathogenesis of age-related macular degeneration. PLoS One. 2008;3(6):e2339.
70. Dharmarajan S, Fisk DL, Sorenson CM, Sheibani N, Belecky-Adams TL. Microglia activation is essential for BMP7-mediated retinal reactive gliosis. J Neuroinflammation. 2017;14(1):76.
71. Bringmann A, Iandiev I, Pannicke T, Wurm A, Hollborn M, Wiedemann P, et al. Cellular signaling and factors involved in Muller cell gliosis: neuroprotective and detrimental effects. Prog Retin Eye Res. 2009;28(6):423–51.
72. Nakazawa T, Takeda M, Lewis GP, Cho KS, Jiao J, Wilhelmsson U, et al. Attenuated glial reactions and photoreceptor degeneration after retinal detachment in mice deficient in glial fibrillary acidic protein and vimentin. Invest Ophthalmol Vis Sci. 2007;48(6):2760–8.
73. Tschopp J, Schroder K. NLRP3 inflammasome activation: the convergence of multiple signalling pathways on ROS production? Nat Rev Immunol. 2010; 10(3):210–5.
74. Portillo JC, Lopez Corcino Y, Miao Y, Tang J, Sheibani N, Kern TS, et al. CD40 in retinal muller cells induces P2X7-dependent cytokine expression in

macrophages/microglia in diabetic mice and development of early experimental diabetic retinopathy. Diabetes. 2017;66(2):483–93.
75. Gentle IE, McHenry KT, Weber A, Metz A, Kretz O, Porter D, et al. TIR-domain-containing adapter-inducing interferon-beta (TRIF) forms filamentous structures, whose pro-apoptotic signalling is terminated by autophagy. FEBS J. 2017;284(13):1987–2003.
76. Wang JJ, Williams W, Wang B, Wei J, Lu X, Cheng JW, et al. Cytotoxic effect of interleukin-8 in retinal ganglion cells and its possible mechanisms. Int J Ophthalmol. 2018;11(8):1277–83.
77. Charles-Messance H, Blot G, Couturier A, Vignaud L, Touhami S, Beguier F, et al. IL-1beta induces rod degeneration through the disruption of retinal glutamate homeostasis. J Neuroinflammation. 2020;17(1):1.
78. Yasuhara R, Miyamoto Y, Akaike T, Akuta T, Nakamura M, Takami M, et al. Interleukin-1beta induces death in chondrocyte-like ATDC5 cells through mitochondrial dysfunction and energy depletion in a reactive nitrogen and oxygen species-dependent manner. Biochem J. 2005;389(Pt 2):315–23.
79. Garg AD, Nowis D, Golab J, Agostinis P. Photodynamic therapy: illuminating the road from cell death towards anti-tumour immunity. Apoptosis. 2010; 15(9):1050–71.
80. Lapenna A, De Palma M, Lewis CE. Perivascular macrophages in health and disease. Nat Rev Immunol. 2018;18(11):689–702.
81. Mendes-Jorge L, Ramos D, Luppo M, Llombart C, Alexandre-Pires G, Nacher V, et al. Scavenger function of resident autofluorescent perivascular macrophages and their contribution to the maintenance of the blood-retinal barrier. Invest Ophthalmol Vis Sci. 2009;50(12):5997–6005.
82. Argaw AT, Asp L, Zhang J, Navrazhina K, Pham T, Mariani JN, et al. Astrocyte-derived VEGF-A drives blood-brain barrier disruption in CNS inflammatory disease. J Clin Invest. 2012;122(7):2454–68.
83. Argaw AT, Zhang Y, Snyder BJ, Zhao ML, Kopp N, Lee SC, et al. IL-1beta regulates blood-brain barrier permeability via reactivation of the hypoxia-angiogenesis program. J Immunol. 2006;177(8):5574–84.
84. Luna JD, Chan CC, Derevjanik NL, Mahlow J, Chiu C, Peng B, et al. Bloodretinal barrier (BRB) breakdown in experimental autoimmune uveoretinitis: comparison with

vascular endothelial growth factor, tumor necrosis factor alpha, and interleukin-1beta-mediated breakdown. J Neurosci Res. 1997; 49(3):268–80.
85. Skaria T, Bachli E, Schoedon G. Wnt5A/Ryk signaling critically affects barrier function in human vascular endothelial cells. Cell Adhes Migr. 2017;11(1):24–38.
86. Daneman R, Zhou L, Kebede AA, Barres BA. Pericytes are required for blood-brain barrier integrity during embryogenesis. Nature. 2010;468(7323):562–6.
87. Persidsky Y, Hill J, Zhang M, Dykstra H, Winfield M, Reichenbach NL, et al. Dysfunction of brain pericytes in chronic neuroinflammation. J Cereb Blood Flow Metab. 2016;36(4):794–807.
88. Whiteley SJ, Klassen H, Coffey PJ, Young MJ. Photoreceptor rescue after low-dose intravitreal IL-1beta injection in the RCS rat. Exp Eye Res. 2001;73(4): 557–68.
89. Mantovani A, Bussolino F, Dejana E. Cytokine regulation of endothelial cell function. FASEB J. 1992;6(8):2591–9.
90. Carmi Y, Voronov E, Dotan S, Lahat N, Rahat MA, Fogel M, et al. The role of macrophage-derived IL-1 in induction and maintenance of angiogenesis. J Immunol. 2009;183(7):4705–14.
91. Beaudry-Richard A, Nadeau-Vallee M, Prairie E, Maurice N, Heckel E, Nezhady M, et al. Antenatal IL-1-dependent inflammation persists postnatally and causes retinal and sub-retinal vasculopathy in progeny. Sci Rep. 2018;8(1):11875.
92. Zhou TE, Rivera JC, Bhosle VK, Lahaie I, Shao Z, Tahiri H, et al. Choroidal involution is associated with a progressive degeneration of the outer retinal function in a model of retinopathy of prematurity: early role for IL-1beta. Am J Pathol. 2016;186(12):3100–16.
93. Samardzija M, Wenzel A, Thiersch M, Frigg R, Reme C, Grimm C. Caspase-1 ablation protects photoreceptors in a model of autosomal dominant retinitis pigmentosa. Invest Ophthalmol Vis Sci. 2006;47(12):5181–90.
94. Wooff Y, Fernando N, Wong JHC, Dietrich C, Aggio-Bruce R, Chu-Tan JA, et al. Caspase-1-dependent inflammasomes mediate photoreceptor cell death in photo-oxidative damage-induced retinal degeneration. Sci Rep. 2020;10(1):2263.
95. Kenakin T. Principles: receptor theory in pharmacology. Trends Pharmacol Sci. 2004;25(4):186–92.

96. Yang LP, Zhu XA, Tso MO. Role of NF-kappaB and MAPKs in light-induced photoreceptor apoptosis. Invest Ophthalmol Vis Sci. 2007;48(10):4766–76.
97. Sayah DN, Zhou TE, Omri S, Mazzaferri J, Quiniou C, Wirth M, et al. Novel anti-interleukin-1beta Therapy preserves retinal integrity: a longitudinal investigation using OCT imaging and automated retinal segmentation in small rodents. Front Pharmacol. 2020;11:296.
98. Geranurimi A, Cheng CWH, Quiniou C, Zhu T, Hou X, Rivera JC, et al. Probing Anti-inflammatory properties independent of NF-kappaB through conformational constraint of peptide-based interleukin-1 receptor biased ligands. Front Chem. 2019;7:23.

Funding

This study was funded by the Canadian Institutes of Health Research (CIHR) grant 950-231837 (SC). RD is supported by Fonds de Recherche du Québec-Santé (FRQS), The Antoine Turmel Foundation, and The Vision Health Research Network. SC holds a Canada Research Chair (Vision Science) and the Leopoldine Wolfe Chair in translational research in age-related macular degeneration.

Contributions

RD and SC designed the study. RD planned and directed experiments. RD carried out experiments, assisted by CWHC and PA. RD, GC, and KVS analyzed the data. RD wrote the manuscript. JCR and SC reviewed and edited the manuscript. SO provided scientific advice. JSJ, MD, DO, AGW, and WL provided technical guidance. All authors read and approved the final manuscript.

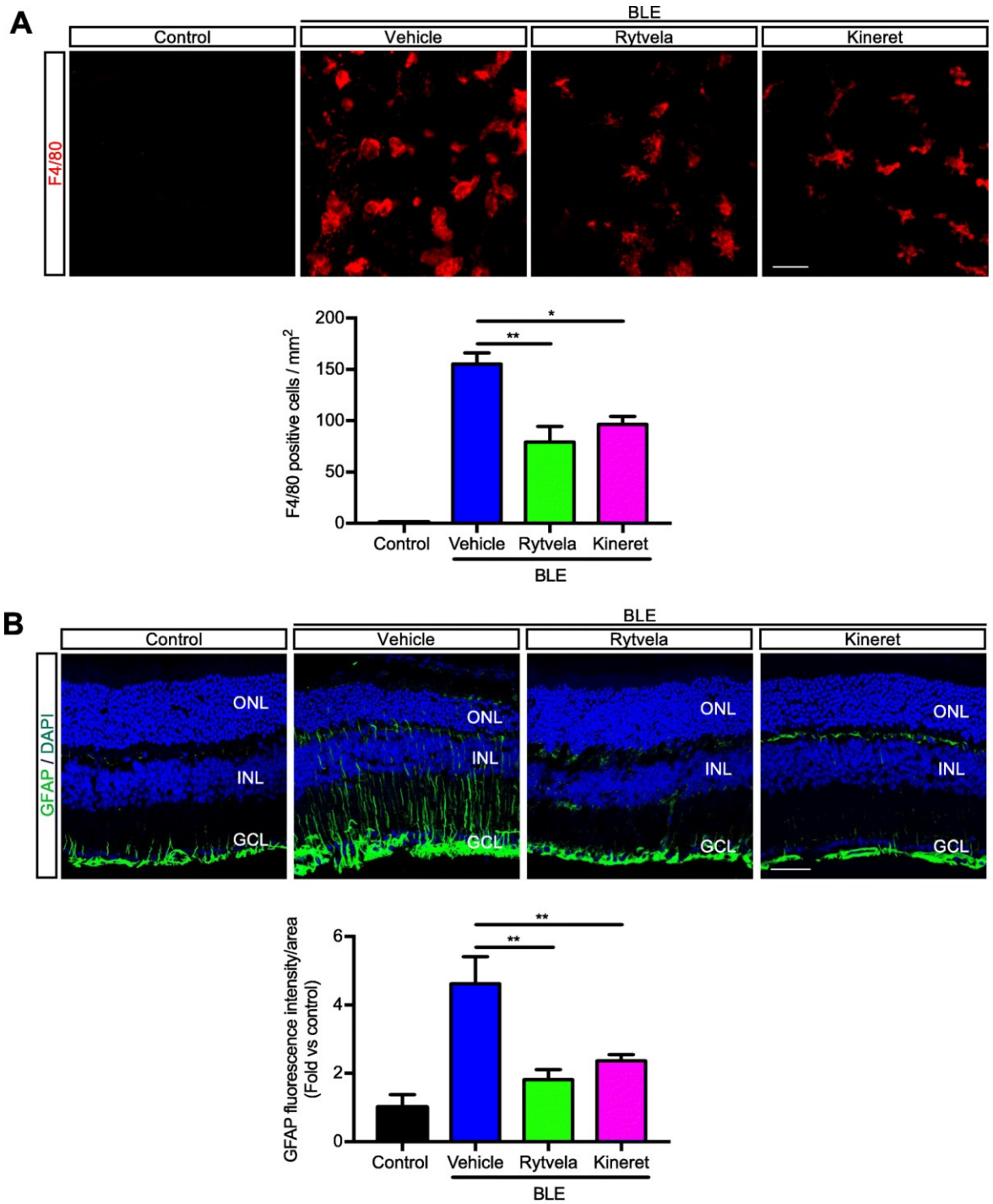
A
BLE
Control
Vehicle
Rytvela
Kineret
F4/80
F4/80 positive cells / mm2
200
150
100
50
0
*
**
Control
Vehicle
Rytvela
Kineret
BLE
B
BLE
Control
Vehicle
Rytvela
Kineret
GFAP / DAPI
ONL
INL
GCL
GFAP fluorescence intensity/area
(Fold vs control)
6
4
2
0
**
**
Control
Vehicle
Rytvela
Kineret
BLE
C
Fold change
6
4
2
0
**
***
**
**
*
**
Il1b
Il6
Ccl2
Control
BLE+vehicle
BLE+rytvela
BLE+Kineret

Figure 1. Subretinal macrophage infiltration and gliosis in blue light exposure to mice. **a** Representative images of retinal flat mounts showing infiltration of F4/80-labeled mononuclear phagocytes (red) of mice exposed or not to blue light exposure (BLE) and treated with vehicle, rytvela, or Kineret. Scale bar 50 μm. The graph represents compiled data on F4/80+ cell density in the subretina presented as a histogram. Data are expressed as mean ± SEM and analyzed by one-way ANOVA with Holm-Sidak correction for multiple comparisons; n = 4–8 per group. **p < 0.01 *p < 0.05. **b** Representative images of GFAP immunoreactivity (green) showing retinal gliosis in blue light-exposed animals treated with vehicle, and suppressed by rytvela and Kineret. Sections were co-stained with DAPI (blue) to show cell nuclei. Scale bar 50 μm. ONL: outer nuclear layer; INL: inner nuclear layer; GCL: retinal ganglion cell layer. The graph represents the quantitative analysis of GFAP immunofluorescence intensity compared with control light unexposed values set at mean of 1. Data are expressed as mean ± SEM and analyzed by one-way ANOVA with Holm-Sidak correction for multiple comparisons for n = 3–6 per group. **p < 0.01 (C) mRNA expression of Il1b, Il6, and Ccl2, standardized to control light unexposed values set at mean of 1. Data are expressed as mean ± SEM and analyzed by one-way ANOVA with Holm-Sidak correction for multiple comparisons for n = 3–6 per group. ***p < 0.001, **p < 0.01, *p < 0.05

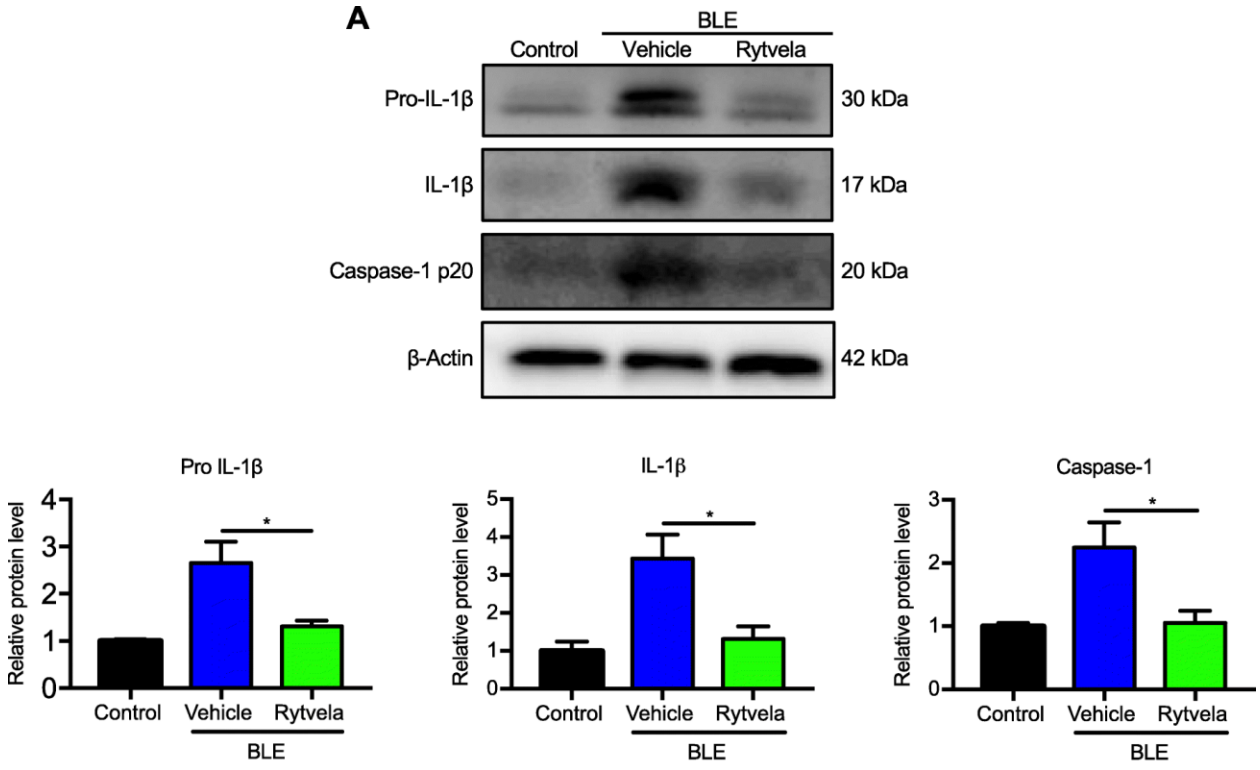
A
BLE
Control
Vehicle
Rytvela
Pro-IL-1β
IL-1β
Caspase-1 p20
β-Actin
30 kDa
17 kDa
20 kDa
42 kDa
Pro IL-1β
IL-1β
Caspase-1
Relative protein level
Control
Vehicle
Rytvela
BLE
*

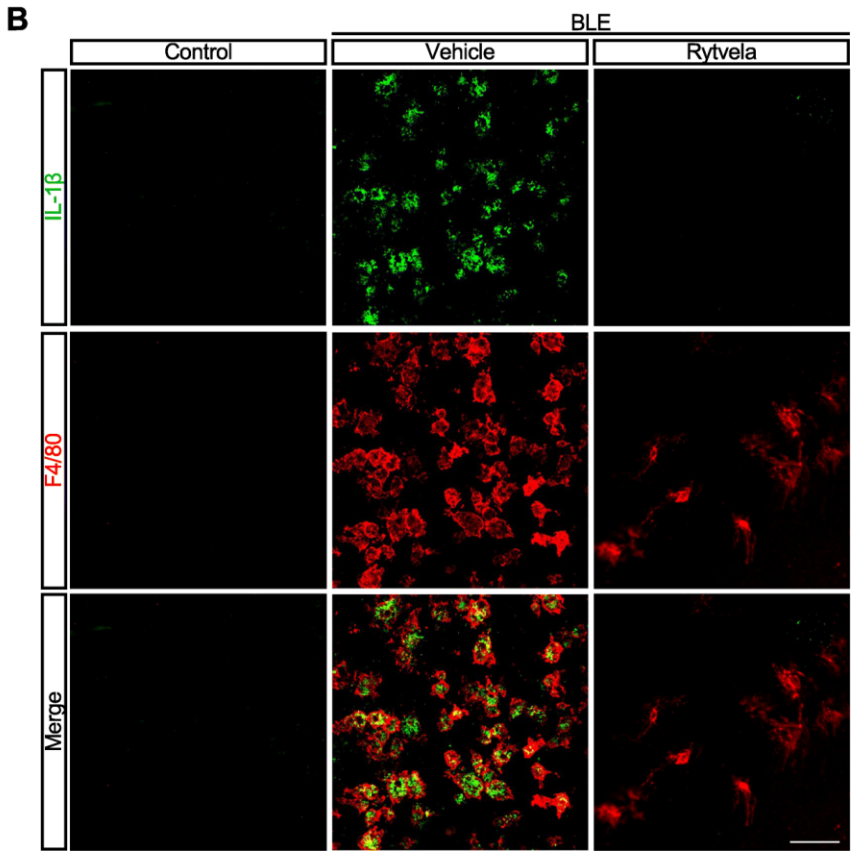
B
BLE
Control
Vehicle
Rytvela
IL-1β
F4/80
Merge

Figure 2. IL-1β production in blue-light-exposed mice. **a** Representative western blots (top panel) showing the expression of uncleaved pro-IL-1β, mature IL-1β, and cleaved caspase-1 p20 in retinal samples from blue light-exposed animals untreated (vehicle) or treated with rytvela and compared with non-illuminated animals (control). The bottom panel depicts compiled data in histogram format. Data are expressed as mean ± SEM and analyzed by independent t tests; n = 3–6 per group. **p < 0.01, *p < 0.05. **b** Representative images of retinal flat mounts showing co-localization of IL-1β (green) in mononuclear phagocytes F4/80+ cells (red) from blue light–exposed animals treated with vehicle or rytvela. Mice exposed to blue light and treated with rytvela displayed less IL-1β immunoreactivity; retinal samples from non-illuminated animals showed no positive reaction. n = 6 per group. Scale bar 50 μm

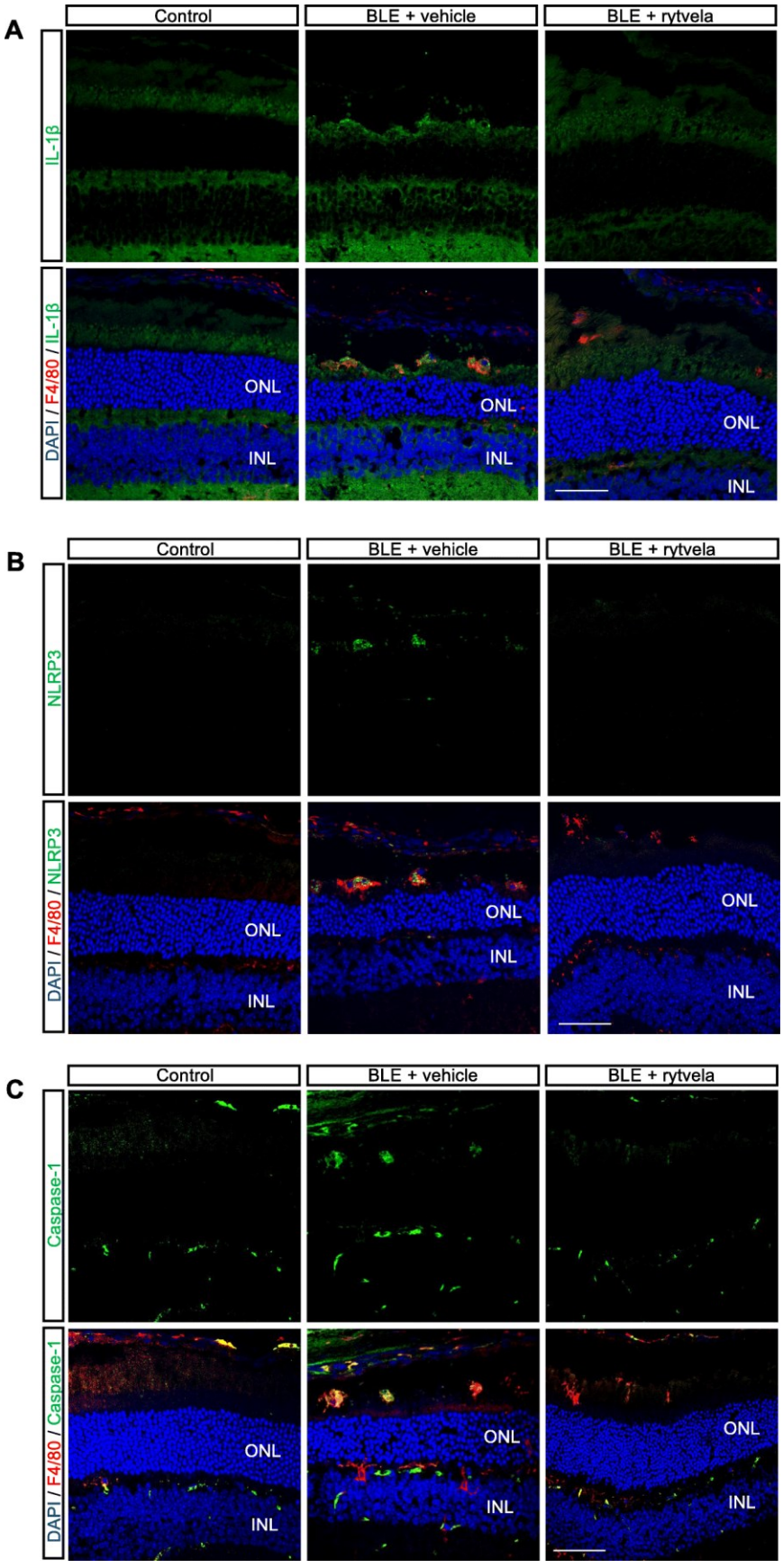
A
Control
BLE + vehicle
BLE + rytvela
IL-1β
DAPI / F4/80 / IL-1β
ONL
INL
B
NLRP3
DAPI / F4/80 / NLRP3
C
Caspase-1
DAPI / F4/80 / Caspase-1

Figure 3. Subretinal distribution of IL-1β, inflammasome (NRLP3), and caspase-1 after blue light exposure (BLE). Representative confocal images showing co-immunoreactivity of **a** IL-1β (green), **b** NLRP3 (green), and **c** caspase-1 (green) with MPs F4/80^{+} cells (red) in the subretinal space of animals non-exposed (Control) and exposed to blue light (BLE) treated or not with rytvela. Cell nuclei were counterstained with DAPI (blue). Rytvela reduced immunoreactivity of IL-1β, NLRP3, and caspase-1. *n* = 4–5 per group. Scale bar 50 μm. ONL: outer nuclear layer; INL: inner nuclear layer

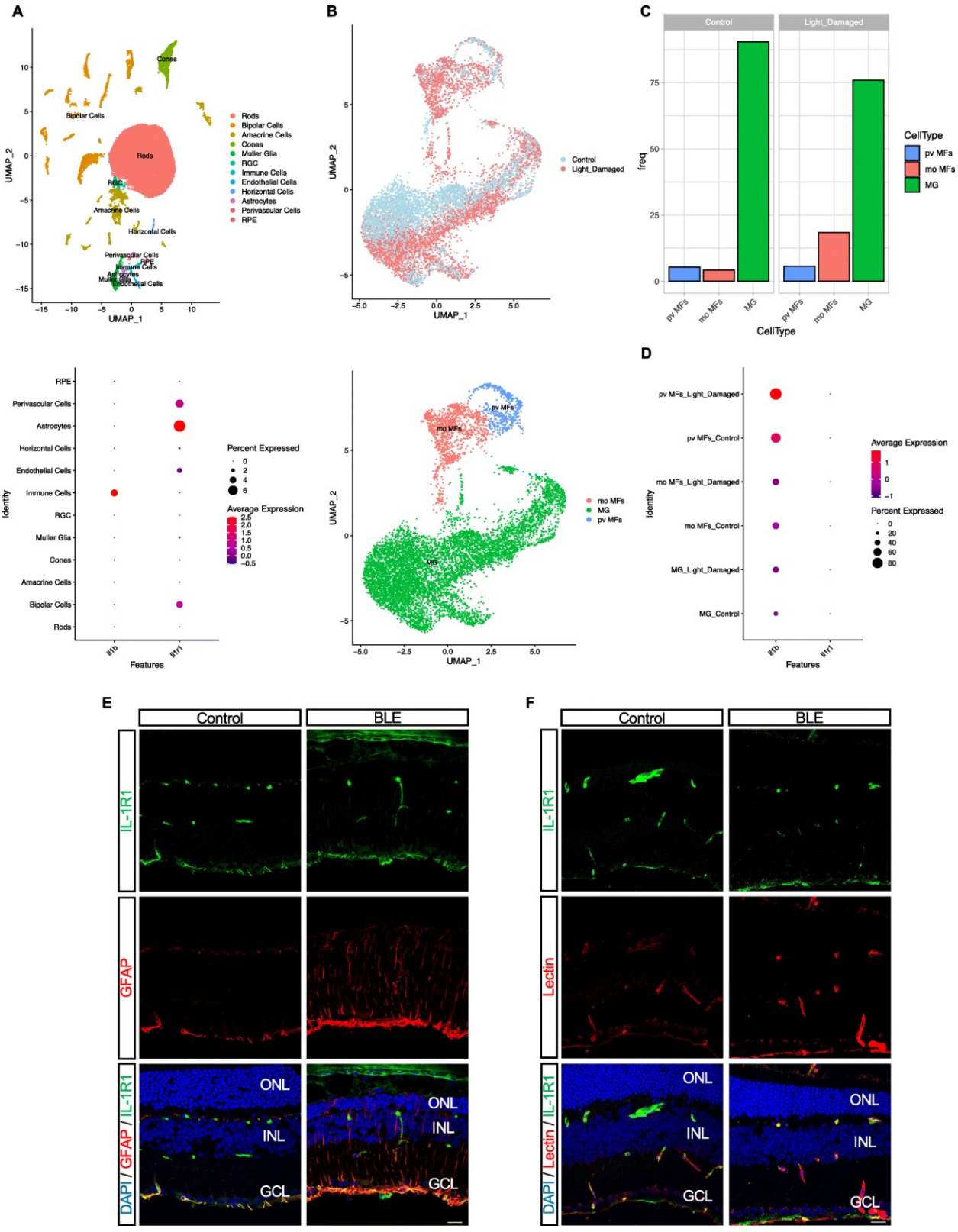
A
B
C
D
E
F
UMAP_1
UMAP_2
Rods
Cones
Bipolar Cells
Amacrine Cells
Muller Glia
RGC
Immune Cells
Endothelial Cells
Horizontal Cells
Astrocytes
Perivascular Cells
RPE
Control
Light_Damaged
freq
CellType
pv MFs
mo MFs
MG
Identity
Features
Percent Expressed
Average Expression
pv MFs_Light_Damaged
pv MFs_Control
mo MFs_Light_Damaged
mo MFs_Control
MG_Light_Damaged
MG_Control
Control
BLE
IL-1R1
GFAP
Lectin
DAPI / GFAP / IL-1R1
DAPI / Lectin / IL-1R1
ONL
INL
GCL

Figure 4. Expression of *Il1b* and *Il1r* genes across retinal cell clusters. **a** UMAP plot of droplet-based single-cell RNA sequencing (scRNA-seq) data obtained using 10× Genomics technology and representing retinal cell type from adult mouse retina (*n* = 4, 10–16 weeks). The plot shows a two-dimensional representation of global gene expression relationship among 33942 cells clustered into 12 retinal cell types (top panel). The expression levels of *Il1r1* and *Il1b* are represented as dot plots across all the 12 cell types; larger dots indicate broader expression within the cluster; deeper red denotes a higher expression level (bottom panel). **b** UMAP plot of droplet-based scRNA-seq data obtained using 10× Genomics technology showing different clusters (top panel). UMAP plot of droplet-based single-cell RNA sequencing (scRNA-seq) data obtained using 10× Genomics technology and representing retinal cell types from control and light-damaged (LD) adult mouse retina. scRNA-seq data were generated on fluorescence-assisted cell sorting (FACS)-sorted live Cx3cr1^{YFP+} cells from pooled neuroretinas of normal (*n* = 5) and LD (*n* = 8) mice. MG: microglia; pv MFs: perivascular macrophages; mo MFs: monocyte-derived macrophages. The plot shows a two-dimensional representation of global gene expression relationship among 10582 cells clustered into 3 retinal cell types (bottom panel). **c** Bar plot representation of Cx3cr1^{YFP+} cell proportions in different conditions. **d** The expression levels of *Il1r1* and *Il1b* are represented as dot plots across all the 3 immune cell types; larger dots indicate broader expression within the cluster; deeper red denotes a higher expression level. Representative confocal images showing co-immunoreactivity of IL-1R1 (green) with **e** GFAP^{+} cells (red) in the ganglion cell layer and **f** lectin (red). *n* = 4 per group. Scale bar 20 µm. ONL: outer nuclear layer; INL: inner nuclear layer; GCL: ganglion cell layer

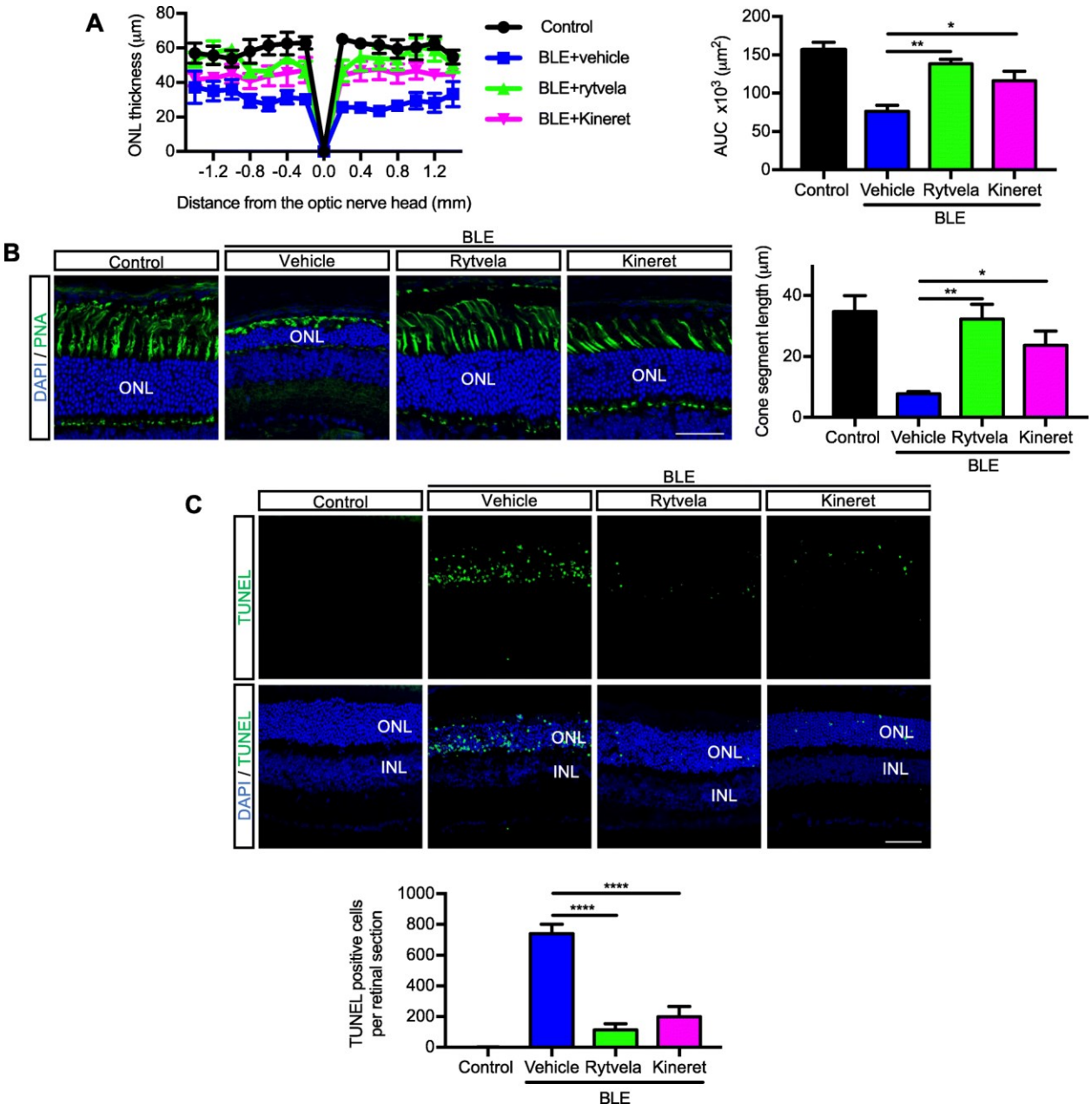

Figure 5. Prevention of photoreceptor cell death by the IL-1R modulator rytvela. **a** Spidergraph quantification of ONL thickness on DAPI-stained retinal sections from non-illuminated animals (control) and from blue light–exposed mice treated with vehicle, rytvela, or Kineret. Statistical analysis was performed using the area under the curve values (to assess photoreceptor density). Data are expressed as mean ± SEM and analyzed using one-way ANOVA with Holm-Sidak correction for multiple comparisons; n = 4–5. $^{**}p < 0.01$, $^{*}p < 0.05$. ONL: outer nuclear layer; AUC: area under the curve. **b** Representative images of photoreceptor cone outer and inner segments using

fluorescein-PNA (green)-stained retinas. Scale bar 50 µm. The graph illustrates the quantitative analysis of cone segment length. **c** Representative images of TUNEL (green)-stained retinas in control and blue light-exposed mice administrated with vehicle or rytvela. The graph illustrates the quantitative analysis of TUNEL-positive cells in the ONL. Scale bar 50 µm. Data are expressed as mean ± SEM and analyzed using one-way ANOVA with Holm-Sidak correction for multiple comparisons; $n = 6$ per group. ****$p < 0.0001$

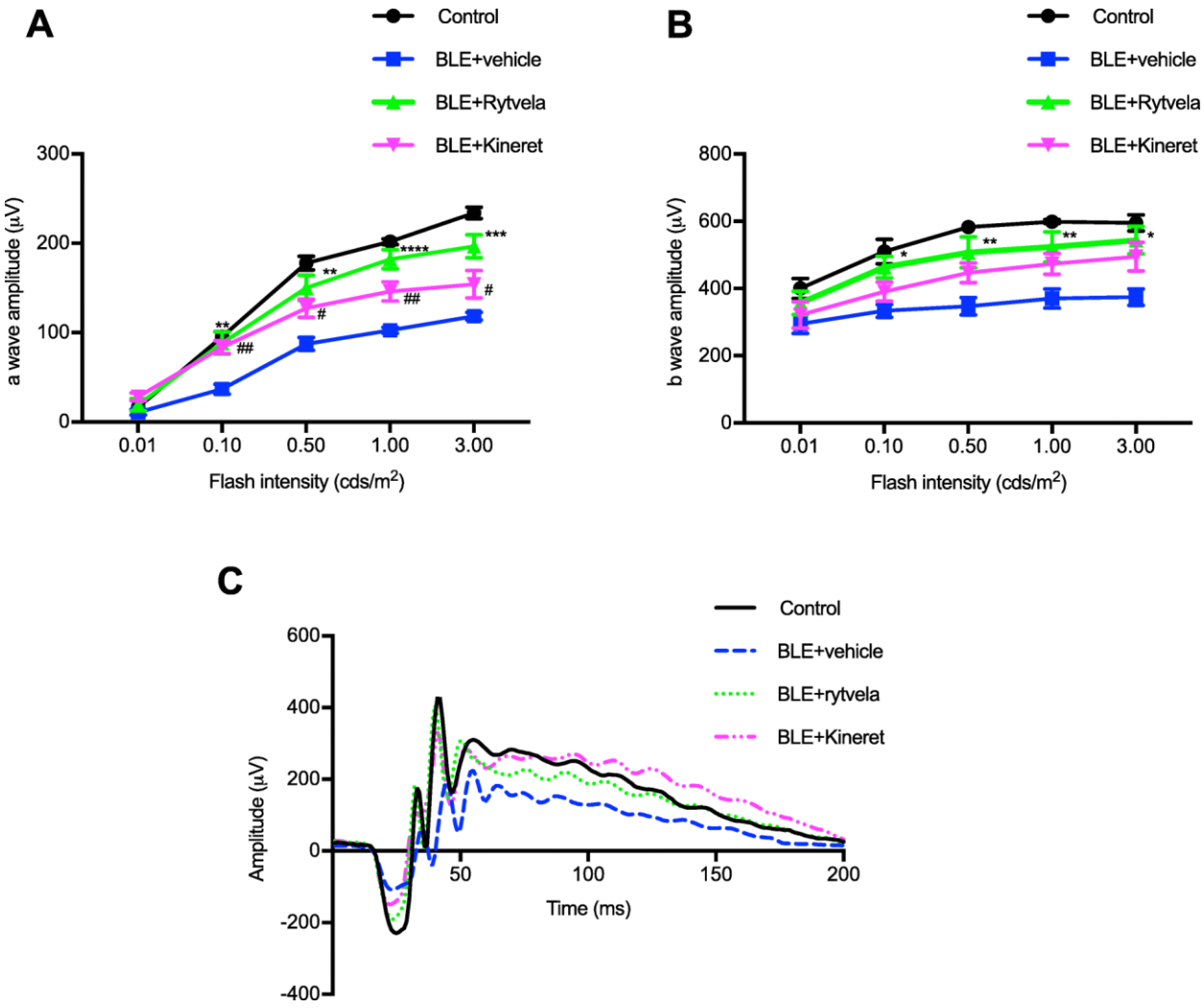

Figure 6. Preservation of photoreceptor function by the IL-1R modulator rytvela in light-exposed mice. Animals were exposed to blue light and treated as described in Fig. 1. Flash intensities of 0.01, 0.1, 0.5, 1, and 3 cds/m^2 were used in ERG analysis. Quantification of **a** a-wave amplitude and **b** b-wave amplitude of control, and blue light–exposed (BLE) mice treated or not with rytvela or Kineret. Data are expressed as mean ± SEM and analyzed using one-way ANOVA with Holm-Sidak corrections for multiple comparisons; n = 6–7 per group. ****p < 0.0001, ***p < 0.001, **p < 0.01 rytvela compared with vehicle. ##p < 0.01, #p < 0.05 Kineret compared with vehicle. **c** Representative waveforms of the electroretinogram recording at the flash intensity 3 cds/m^2 from non-illuminated animals (control) and from blue light–exposed mice treated with vehicle, rytvela, or Kineret

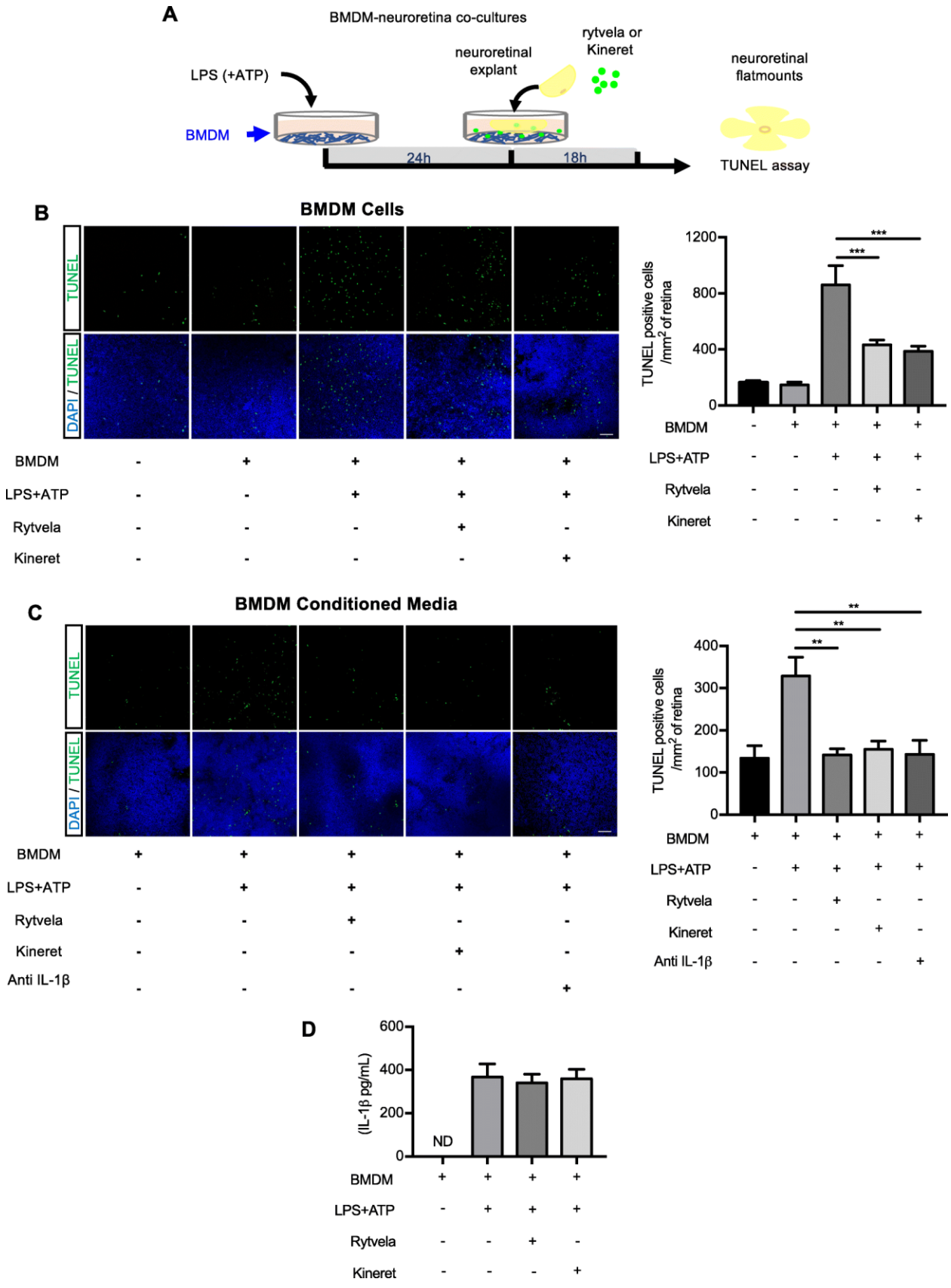
A
BMDM-neuroretina co-cultures
LPS (+ATP)
BMDM
neuroretinal explant
rytvela or Kineret
24h
18h
neuroretinal flatmounts
TUNEL assay
B
BMDM Cells
TUNEL
DAPI / TUNEL
TUNEL positive cells /mm2 of retina
1200
800
400
0
***
***
BMDM - + + + +
LPS+ATP - - + + +
Rytvela - - - + -
Kineret - - - - +
C
BMDM Conditioned Media
TUNEL
DAPI / TUNEL
TUNEL positive cells /mm2 of retina
400
300
200
100
0
**
**
**
BMDM + + + + +
LPS+ATP - + + + +
Rytvela - - + - -
Kineret - - - + -
Anti IL-1β - - - - +
D
(IL-1β pg/mL)
600
400
200
0
ND
BMDM + + + +
LPS+ATP - + + +
Rytvela - - + -
Kineret - - - +

Figure 7. Effects of IL-1R inhibition (using rytvela and Kineret) on BMDM-induced photoreceptor toxicity. **a** An illustration of the experimental design used to evaluate the effects of isolated murine bone marrow-derived MPs (BMDMs) stimulated with LPS/ATP (stimulant of IL-1β secretion). **b** TUNEL-stained retinal flat mounts cultured in contact with BMDMs for 18 h in the presence or absence of rytvela or Kineret. Scale bar 50 µm. The graph represents the quantification of TUNEL-positive nuclei in the ONL of retinal flat mounts. Data are expressed as mean ± SEM and analyzed by one-way ANOVA with Holm-Sidak correction for multiple comparisons; n = 5–6 per group. ***p < 0.001. **c** TUNEL-stained retinal flat mounts cultured with the conditioned medium of LPS/ATP-activated or not BMDMs in the presence or absence of rytvela, Kineret, or an anti-IL-1β antibody. Scale bar 50 µm. The graph represents the quantification of TUNEL-positive nuclei in the ONL of retinal flat mounts. Data are expressed as mean ± SEM and analyzed by one-way ANOVA with Holm-Sidak correction for multiple comparisons; n = 3–5 per group. **p < 0.01. **d** ELISA measurement of IL-1β in the conditioned medium derived from BMDMs treated or not with LPS + ATP. The conditioned medium was incubated with retinal explants for 18 h in the presence of vehicle, rytvela, or Kineret. n = 4–5 per group. ND: not detected

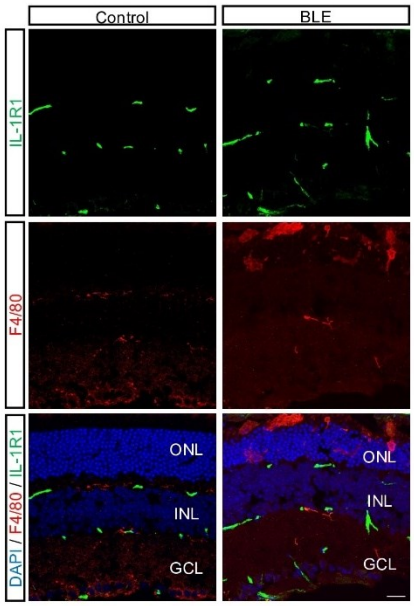

Supplementary Figure 1. The absence of colocalization of IL-1R1 with F4/80 in the neuroretina. Representative confocal images showing non-colocalization of IL-1R1 (green) with F4/80+ cells (red). *n* = 4 per group. Scale bar 20 µm. ONL: outer nuclear layer, INL: inner nuclear layer, GCL: ganglion cell layer.

CHAPTER 4 – Mast cell activation contributes to subretinal inflammation and photoreceptor loss in an oxidative stress model of AMD

Authors: Rabah Dabouz[1,2], Pénélope Abram[2,3], Sylvain Chemtob[1,2,3]

[1]Department of Pharmacology and Therapeutics, McGill University, Montréal, QC, Canada.

[2]Department of Ophthalmology, Hôpital Maisonneuve-Rosemont, Montréal, QC, Canada.

[3]Department of Pharmacology, Université de Montréal, Montréal, QC, Canada

Correspondence to Rabah Dabouz (rabah.dabouz@mail.mcgill.ca) or Sylvain Chemtob (sylvain.chemtob@umontreal.ca).

Preface

Chapter 3 explored the inflammatory events associated with the loss of photoreceptors, marked by the activation of proinflammatory mononuclear phagocytes and the upregulation of inflammatory cytokines. This phase corresponds to the peak of photoreceptor death, studied using a light-induced model that mimics subretinal inflammation and photoreceptor loss. However, this model does not encompass a critical event in the pathogenesis of AMD: the loss of RPE cells, which generally precedes photoreceptor death. In Chapter 4 we aim to explore the early inflammatory events that precede and potentially initiate the cascade leading to retinal degeneration, focusing on the loss of RPE cells. Using a sodium iodate model, this chapter aims to reproduce the sequential events of RPE cell loss, subsequent subretinal inflammation, and ultimately, photoreceptor death. Given the anatomical proximity and potential interactive role of RPE cells with choroidal mast cells, we hypothesize that damage to RPE cells activates mast cells, thereby triggering the inflammatory response observed in the later stages of the disease. This study extends our understanding of the inflammatory processes involved in retinal degeneration by addressing the early events that lead to the inflammatory cascade and photoreceptor death.

Abstract

Neuroinflammation is linked to the pathogenesis of neurodegenerative diseases, including those affecting the retina. Among the immune cells associated with neuroinflammation and the progression of neurodegenerative conditions, mast cells, typically known for their role in allergic reactions, have been implicated in age-related macular degeneration (AMD), a leading cause of vision loss. Despite this association, the specific role of mast cells in AMD pathogenesis remains poorly understood. This study aimed to elucidate the involvement of choroidal mast cells in retinal inflammation using a mouse model of retinal degeneration. Our findings reveal an early activation of mast cells during retinal degeneration, highlighting their potential contribution to disease progression. Significantly, we demonstrate that mast cell deficiency or pharmacological stabilization of mast cells can mitigate the inflammatory response, reduce photoreceptor cell death, and preserve retinal function. Furthermore, we identified mast cell-derived tryptase as a key mediator of inflammatory events. These results highlight the pivotal role of mast cells in the pathogenesis of retinal degeneration and suggest that targeting these cells holds promise as a therapeutic strategy for management of AMD.

Introduction

AMD is a primary cause of visual impairment and blindness worldwide (1). It is a complex disease that is influenced by numerous risk factors. Aging, gender, racial background, diet, smoking, obesity, cardiovascular disease, have all been suggested to increase the risk of AMD (2, 3). Late AMD is characterized by neovascular and/or atrophic AMD (4). Atrophic AMD, also known as geographic atrophy, involves the loss of photoreceptors and RPE, presenting as a sharply defined pale ocular fundoscopic area with exposed underlying choroidal blood vessels (5). While the exact pathogenesis of AMD remains unclear, there is an expanding body of evidence supporting the notion that neuroinflammation plays a crucial role in the initiation and progression of AMD (6, 7, 8, 9, 10). During aging, the retina experiences a continuous, mild oxidative stress, which triggers the activation of the retinal immune system and initiates a reparative para-inflammatory response. However, in the case of AMD, this regulatory para-inflammatory mechanism becomes dysregulated, resulting in persistent low-grade inflammation. This

ensuing chronic inflammation damages the macula and compromises the integrity of the blood-retinal barrier, leading to the development of retinal lesions as observed in AMD (11).

Mast cells are key tissue-resident players in allergic reactions and innate immunity (12). An increase in the number and degranulation of mast cells is observed in the choroid of patients with AMD (13). Induction of mast cell degranulation results in features of AMD including RPE degeneration followed by photoreceptor loss (14, 15). Yet, the contribution of mast cells in retinal degeneration upon response to oxidative stress is unclear and is the subject of this paper.

Materials and Methods

Animals

All animal protocols were approved by the Maisonneuve Rosemont Hospital Animal Care Committee and were performed in accordance with the Association for Research in Vision and Ophthalmology Statement for the Use of Animals in Ophthalmic and Visual Research. Adult C57BL/6J and $Kit^{W\text{-}sh/W\text{-}sh}$ mice (Jax) of age 10- to 12-week-old were used in the study. Animals were housed and maintained at local animal facilities under a 12-h light/dark cycle (100–200 lux) with water and normal diet food available ad libitum.

Drug and NaIO3 treatment

Ketotifen fumarate was injected intraperitoneally (i.p.) using a dose range of 5 or 25 mg/kg in physiological saline. APC 366 was diluted in 20% ethanol / water and injected i.p. at a dose of 5 mg/kg. Sodium iodate was diluted in PBS and injected i.p. at a dose of 30 mg/kg.

RPE/choroid flat mount preparation

Eyes were enucleated and fixed in 4% paraformaldehyde (PFA) for 1 h and then rinsed twice with phosphate-buffered saline (PBS). The neuroretina was carefully separated from the RPE/choroid/sclera complex and processed for immunostaining. The RPE/choroid complex was incubated at room temperature for 1 h with a blocking solution

consisting of 1% BSA, 1% normal goat serum, 0.1% Triton X-100 and 0.05% Tween-20 in PBS. The RPE/choroid complex was then labeled overnight at 4°C with gentle shaking using F-actin or the following primary antibody: 1:400 anti-IBA1 (019-19741, FUJIFILM Dako). The RPE/choroid complex was then washed thrice with PBS and incubated with a secondary antibody solution consisting of 1% BSA, 0.1% Triton X-100, 0.05% Tween-20, 1:500 Alexa Fluor donkey 594 anti-rat (A21209, Invitrogen) and 1:500 Alexa Fluor 647 goat anti-rabbit (A11072, Invitrogen) for 2 h at room temperature. The RPE/choroid complex was washed 3 times with PBS and then flat-mounted onto glass slides with coverslips and Fluoro-Gel mounting medium (Electron Microscopy Sciences, Hatfield, PA). For mononuclear phagocyte (MP) quantification, images were captured and stitched together using the MosaiX feature of Axiovision 4. IBA1–stained cells were counted on flat mounts with the RPE facing the objective.

Volume and sphericity analysis of MPs

The volume and sphericity analyses of MPs were performed on 4 randomly selected fields per mouse on flat mounts of the RPE/choroid complex with the RPE facing the objective. Images were captured at 40x magnification with z-stacks using a laser scanning confocal microscope (Olympus IX81 with Fluoview FV1000 scanning head) with Fluoview software. The images were opened in Imaris version 8.1 Surpass View software (Bitplane USA, Concord, MA, USA) and surfaces were created using background subtraction (0.5 μm). Voxel filtering was applied to eliminate nonspecific particles in the created surfaces. Cells touching or those with only part of the cell body visible were omitted. Finally, the volume and sphericity of each IBA1-positive cell were quantified using the Imaris software.

Isolation of primary RPE cells

RPE cells were isolated from the eyes of C57BL6 mice euthanized by cervical dislocation. Eyes were enucleated and rinsed with sterile PBS. Eyes were submerged in DMEM fortified with fungizone (25 μg/mL) and penicillin/streptomycin (P/S, 100 U/mL) and kept in the dark at room temperature overnight. On the subsequent day, excess scleral tissue around the globe is trimmed and the optic nerve is severed. For enzymatic

digestion, the eyes were bathed in DMEM supplemented with fungizone, P/S, trypsin (2 mg/ml), and collagenase 1 (2 mg/ml) for 30 minutes at 37°C. The enzyme action was terminated by transferring the eyes to DMEM enriched with 10% fetal bovine serum (FBS). The cornea and lens were then removed, and the sclera was gently separated from the retina. The RPE is detached from the sclera using fine forceps, ensuring choroidal vessels were also removed. The RPE tissue/cells were pipetted gently into a fresh 24-well plate with 1 mL DMEM (containing 10% FBS and 1% P/S) per eye. After being incubated for three days, the media was refreshed with DMEM supplemented with 10% FBS and 1% P/S.

Isolation of peritoneal mast cells

Using a 10 mL syringe with a 19-gauge needle, 3 mL of sterile 1X PBS and 2 mL of air were injected into the peritoneal cavity of the mouse. The mouse's abdomen was then massaged for 30 seconds to suspend the peritoneal cells in the 1X PBS. Peritoneal lavage was collected after laparotomy using the same syringe. The cells were washed twice by centrifugation at 1200 rpm at 4°C for 5 minutes in sterile 1X PBS, then suspended in Roswell Park Memorial Institute 1640 culture medium (RPMI 1640; Sigma-Aldrich #R8758) (supplemented with 2 mM L-glutamine, 0.07% β-mercaptoethanol, 10 mM HEPES, 10% FBS, 1% P/S, 10 ng/mL of IL-3, and 30 ng/mL of stem cell factor [SCF]), transferred to a T75 cell culture flask, and incubated at 37°C. On day 3 after isolation, non-adherent cells were discarded, and fresh culture medium was added to the adherent cells. On day 6, the culture medium was replaced with fresh culture medium. On day 9/10, the non-adherent cells were mature mast cells derived from the peritoneum and were ready for stimulation. The purity of the population was determined by flow cytometric analysis using CD117 (BD Biosciences) and FcεR-1α (BD Biosciences). Peritoneal mast cells (PMCs) were treated or not with compound 48/80 (Sigma) at 20 μM for 30 min. PMCs were washed twice with RPMI 1640 and the supernatant served as conditioned media.

Isolation of bone marrow-derived mast cells and adoptive transfer to mast-cell deficient mice

Bone marrow-derived mast cells (BMDMCs) were collected from 10 to 12-week-old C57BL/6 mice sacrificed by cervical dislocation. In brief, bone marrow cells from the femurs and tibias of the mice were flushed with RPMI 1640 culture medium. The culture medium was collected and then centrifuged at 1200 rpm for 5 minutes at room temperature. The supernatant was removed, and the pellet was resuspended in fresh culture medium, then centrifuged again at 1200 rpm for 5 minutes at room temperature. The supernatant was discarded, and the pellet was resuspended in RPMI 1640 culture medium containing 2 mM L-glutamine, 0.07% β-mercaptoethanol, and 10 mM HEPES, supplemented with 10% fetal calf serum (085-150, Wisent Bioproducts), 1% P/S, and 30 ng/mL recombinant mouse interleukin-3 (R&D Systems #403-ML). The BMDMC suspension was filtered using sterile cell strainers (40 μm; Corning #352340) and seeded into petri dishes. The cells were incubated in a standard incubator at 37°C in a humidified atmosphere containing 5% CO_2 (v/v). The culture medium was renewed every 3 days by removing the spent medium through low-speed centrifugation (1200 rpm, 5 minutes at room temperature). After 6 weeks of culture, complete differentiation of BMDMC was achieved, and the cells were collected and resuspended in basal RPMI 1640 culture medium at a concentration of 1×10^7/200 μL. Four-week-old $Kit^{W\text{-}sh/W\text{-}sh}$ mice received 200 μL of the BMDMC suspension intravenously. Experiments on these mice were conducted 6 weeks after the injection of BMDMC.

Terminal deoxynucleotidyl transferase dUTP nick end labeling (TUNEL) assay

TUNEL staining was performed according to the manufacturer's protocol (In Situ Cell Death Detection Kit; Roche Diagnostics). Briefly, retinal sections were fixed in 4% PFA for 30 min and washed in PBS. Sections were then incubated for 90 min at 37°C with the reaction mixture and the reaction was stopped by washing with PBS. Nuclei were stained with 4′, 6-diamidino-2-phenylindole (DAPI, Sigma, St. Louis, MO, USA). Images were captured with a laser scanning confocal microscope (Olympus IX81 with Fluoview FV1000 Scanhead) with the Fluoview Software at 30X magnification.

Electroretinogram (ERG)

ERGs were recorded using an Espion ERG Diagnosys apparatus equipped with a ColorDome Ganzfeld stimulator (Diagnosys LLC, Lowell, MA). Mice were initially dark-adapted overnight and anesthetized intraperitoneally with a mix of ketamine (100 mg/kg) and xylazine (20 mg/kg). Corneas were anesthetized with proxymetacaine hydrochloride (0.5% Alcaine; Alcon, Fort Worth, TX, USA) and pupils dilated with 0.5% atropine (Alcon, Fort Worth, TX, USA). Body temperature was maintained at 37.5°C with a heating pad. ERG was measured using corneal DTL Plus electrodes (Diagnosys LLC), a forehead reference electrode, and a ground electrode subcutaneously in the tail. To evaluate rod photoreceptor function (scotopic ERG), five-strobe flash stimuli were presented with flash intensities of 0.01 cds/m^2, 0.1 cds/m^2, 0.5 cds/m^2,1.0 cds/m^2, 3.0 cds/m^2, 5.0 cds/m^2, 10 cds/m^2, and 25 cds/m^2. All procedures were performed in a dark room under dim red-light illumination. The amplitude of the a-wave was measured from baseline to the primary negative peak and b-wave was measured from the trough of the a-wave to the maximum of the fourth positive peak.

Statistical analysis

Data are presented as mean ± standard error of the mean (SEM). Student's t-test was used to compare two different groups, a one-way analysis of variance (ANOVA) followed by post hoc Holm-Sidak tests for comparison of means or, when indicated, Kruskal-Wallis test followed by post hoc Dunn's test for comparison of means. A two-way ANOVA was conducted to analyze the effects of two independent variables. A $p < 0.05$ was considered statistically significant.

Results

Mast cells are activated in response to oxidative stress infliction in RPE

Mast cells have been observed in abundance in the choroid and sclera of humans and mice (16, 17) inferring a possible role in this environment. We examined whether oxidative stress in RPE can lead to choroidal mast cell activation. Oxidative stress-induced RPE injury was triggered by injection of sodium iodate ($NaIO_3$) (18). Avidin D labelling was used to visualize mast cells in the choroid (17, 19). Mast cell density in the

sub-RPE area was significantly increased following $NaIO_3$-induced RPE injury compared with that of control eyes (Fig. 1A, B). Additionally, examination of the structure of choroidal mast cells revealed a degranulation in response to $NaIO_3$ evidenced by (Avidin D+) granule extrusion from mast cells (Fig. 1C).

Mast cell stabilizer mitigates RPE degeneration in response to $NaIO_3$

RPE loss is a major characteristic of geographic atrophy. $NaIO_3$, believed to act by triggering oxidative stress, primarily targets RPE cells to degenerate (18). We explored the involvement of mast cells in RPE degeneration as observed upon $NaIO_3$ administration. Given that RPE loss is observed one day after exposure to $NaIO_3$ (20) along with concomitant activation of mast cells (Fig. 1B, C), we surmised that these resident immune cells could be implicated in RPE damage. As anticipated, $NaIO_3$ caused a significant disruption of RPE morphology, detected using F-actin staining (Fig. 2A). The mast cell stabilizer ketotifen fumarate mitigated these effects on RPE (Fig. 2A, B) by preserving the extent of $NaIO_3$-induced RPE damage (Fig. 2A, B); ketotifen fumarate did not display protection in mast cell depleted $Kit^{W\text{-}sh/W\text{-}sh}$ mice (Fig. 2A, B), indicating that the protective effect of ketotifen fumarate is mast cell-dependent. However surprisingly in $Kit^{W\text{-}sh/W\text{-}sh}$ mice, which lack functional mast cells, we did not observe RPE preservation (Fig. 2A, B), suggesting involvement of other mechanisms in $NaIO_3$-induced RPE damage. Yet, replenishment of mast cells with BMDMCs injected into $Kit^{W\text{-}sh/W\text{-}sh}$ mice significantly aggravated RPE damage (Fig. 2A, B), reinforcing the deleterious role of mast cells in this context. To directly assess the impact of mast cells on RPE integrity, we exposed primary RPE cells to conditioned media from peritoneal mast cells, treated or not with mast cell activator compound 48/80. Conditioned media from activated mast cells led to a reduced expression of tight junction protein ZO-1 (Fig. 2C) and an increase in TUNEL-positive cells (Fig. 2D, E), indicative of mast cell-derived mediator-induced cytotoxicity to RPE.

Mast cell activation contributes to intensification of subretinal inflammation in response to induced RPE injury

The retina is susceptible to neuroinflammatory conditions emphasizing the importance of understanding cellular contributions to such inflammation. In this regard, the role of mast cells in expansion of subretinal inflammation was assessed following $NaIO_3$ administration. Notably, mast cell activation preceded the recruitment and activation of IBA-1+ mononuclear phagocytes (MPs) (Fig. 1D, E). Mast cell-deficient $Kit^{W\text{-}sh/W\text{-}sh}$ mice (which lack mature mast cells due to an inversion mutation in the promoter region of the c-kit gene [(21) exhibited significantly fewer MPs (Fig. 3A, B). In addition, MPs in WT mice predominantly assumed a round shape, indicative of activation, whereas those in $Kit^{W\text{-}sh/W\text{-}sh}$ mice were more ramified, suggesting a lesser inflammatory phenotype (Fig. 3C-E). To ascertain observations made, we performed adoptive transfer of BMDMCs into $Kit^{W\text{-}sh/W\text{-}sh}$ mice in order to replenish mast cell population. Injection of mast cells in $Kit^{W\text{-}sh/W\text{-}sh}$ mice reinstated the increased number of rounded inflammatory MPs in the subretinal space of $NaIO_3$-treated mice (Fig. 3A-E).

Mast cell promotion of down-stream proinflammatory events was further studied pharmacologically using the mast cell stabilizer ketotifen fumarate. Mice were administered daily doses of ketotifen fumarate (at 5 or 25 mg/kg) or vehicle, starting two days prior to the $NaIO_3$ injection. Ketotifen fumarate treatment decreased subretinal accumulation of IBA-1+ MPs (Fig. 3F, G) which furthermore exhibited a more ramified morphology (Fig. 3H-J), supporting an upstream role of mast cells in amplifying retinal inflammation by involving MPs established to participate in outer and sub-retinal injury (22).

Mast cell activation elicits photoreceptor damage induced by $NaIO_3$

Infiltration of MPs into the subretinal space is usually detrimental (23), but may at times be protective to the retina (24). We examined if shifting the inflammatory state would impact on survival of photoreceptors (3 days) following administration of $NaIO_3$. $NaIO_3$ caused degeneration of photoreceptors (TUNEL-positive and thinning of outer nuclear layer) in wild-type mice, which was markedly diminished in mast cell-depleted $Kit^{W\text{-}sh/W\text{-}sh}$ mice (Fig. 4A-D). Replenishment of mast cells with BMDMCs into $Kit^{W\text{-}sh/W\text{-}sh}$ mice

reinstated photoreceptor death, underscoring the role of mast cells in inflammation-induced photoreceptor degeneration. Coherent effects were observed with mast cell stabilizer ketotifen fumarate (dose-dependently) (Fig. 4E-H). Concordant with photoreceptor density, mast cell depletion (using $Kit^{W\text{-}sh/W\text{-}sh}$ mice) and stabilization (using ketotifen fumarate) exerted a relative preservation of a-wave (photoreceptor generated) and b-wave (triggered by upstream a-wave signal) electroretinographic amplitudes (Fig. 5), reinforcing the central role of mast cells in this context.

Tryptase drives the mast cell-mediated inflammatory response

Mast cell tryptase is reported to be abundant in the choroid of patients with advanced stage geographic atrophy (25). We sought to elucidate the role of tryptase in response to RPE oxidative stress. To this end, we utilized the tryptase inhibitor APC 366 (administered daily) in the $NaIO_3$-induced oxidative stress mouse model. Three days after $NaIO_3$ injection, APC 366 was found to markedly reduce MP infiltration, enhance photoreceptor survival, and preserve retinal function (Fig. 6). However, APC 366 did not preserve RPE in mice treated with $NaIO_3$, suggesting that inhibition of tryptase is insufficient to prevent $NaIO_3$-induced RPE injury; concordantly, mast cell tryptase stimulant MCPT6 did not affect RPE tight junction ZO-1 expression or induce cell death (Supp Fig. 1); yet RPE migration was triggered by MCPT6 (Supp Fig. 1), which altogether rule out cytotoxic effects of tryptase on RPE at utilized concentrations.

Discussion

Oxidative stress has been identified as a key factor in AMD pathogenesis, primarily by contributing to the degeneration of the RPE and subsequent retinal damage (26). Our study focused on elucidating the role of mast cells in the retina subjected to oxidative stress challenge. For this purpose, we used the $NaIO_3$ model which induces oxidative damage selectively to the RPE, noting that the central and middle retinal regions experienced more pronounced damage (27). We observed a marked increase in mast cell density and their degranulation in response to $NaIO_3$-induced oxidative stress in RPE. Mast cells contribute to amplifying inflammation through involvement of MPs, which together in turn affect photoreceptor integrity and function, and imply a crosstalk between

choroidal mast cells and infiltrating phagocytes. The destruction of RPE layer, a critical component of the blood retinal barrier, by $NaIO_3$ seems to facilitate such interactions by allowing the diffusion of mast cell-derived mediators which can then interact with MPs. Relevantly, AMD involves the structural breakdown of the RPE that precedes photoreceptor degeneration (28, 29), potentially enabling such interactions. Notably, activated mast cells were found in proximity of geographic atrophy lesions (13). Interactions between the CNS and immune cells at the CNS borders are now identified as being critical for protecting the brain as well as in the pathogenesis of brain disorders (30, 31). More specifically, a role for mast cells was shown to interact with microglia in a model of Alzheimer's disease (32). These observations align with existing evidence regarding the interactions between choroidal immune cells and subretinal MPs upon $NaIO_3$-induced retinal toxicity (33).

We used the $Kit^{W\text{-}sh/W\text{-}sh}$ mouse strain which is depleted of mature mast cells. However, this mouse displays irregularities in the expression of Kit in other immune cell precursor populations. To circumvent potential confounding factors, we employed adoptive transfer experiments with *in vitro*-derived mast cells to specifically elucidate the role of mast cells (34). Reconstitution of mast cells reinforced their role in inducing subretinal inflammation and death of photoreceptors.

Mast cells were also targeted by pharmacologic stabilizers which prevent their degranulation. Treatment with the mast cell stabilizer ketotifen fumarate resulted in a preservation of RPE cells, alleviation of retinal inflammation and preservation of retinal function. Nonetheless, mast cells are not solely responsible for $NaIO_3$-induced RPE degeneration as it still occurred in the mast cell-deficient mice. Yet, ketotifen fumarate demonstrated a protective effect in wild type but not $Kit^{W\text{-}sh/W\text{-}sh}$ demonstrating a mast cell-dependant effect. Further, we also showed a direct toxicity of c48/80-activated mast cells on the disorganization and death of RPE cells evidenced by the loss of ZO-1 junctions and death of RPE cells. These findings suggest that targeting mast cells by mast cell stabilizers can prevent the progression of RPE loss as observed in geographic atrophy. Mast cell stabilizers inhibit mast cell degranulation and the release of mast cell mediators by stabilizing the cell membrane (35). While the exact mechanism of action remains

unclear, they have already been approved and are in use for conditions like asthma, rhinitis, and allergic conjunctivitis (36, 37).

Upon activation, mast cells release a variety of bioactive substances, contributing significantly to innate immune response (38). In this context, tryptase is predominantly secreted by mast cells. Our findings reveal that mast cells exert to a large extent their inflammatory effects via tryptase. The tryptase inhibitor, APC 366, suppressed retinal inflammation and aided in preserving photoreceptors. Tryptase is known to activate the protease-activated receptor 2 (PAR2), which in turn triggers a cascade of intracellular signaling events (39). Activation of PAR2, particularly on MPs, exacerbates neuroinflammation through production of inflammatory cytokines, resulting in neuronal death (40, 41, 42). These findings support the relevance of targeting tryptase in AMD.

Mast cells are prevalent throughout vascularized tissues and in areas exposed to the external environment (43). This strategic positioning enables them to serve as sentinel cells, initiating rapid responses to noxious agents such as pathogens, allergens, toxins, and other environmental substances (44). Their presence in such locations allows them to rapidly respond to tissue injury, potentially exacerbating local inflammation. Mast cells in the choroid can be activated by different means. Activation of choroidal mast cells by compound 48/80 resulted in the loss of RPE and the recruitment of phagocytes (15); activation by compound 48/80 is mediated through the Mas-related G protein-coupled receptor (MRGPR)X2/MrgprB2 receptor (45), which is also implicated in the response to substance P, a neuropeptide released by sensory nerves (46, 47). This suggests a potential pathway for neurogenic activation of mast cells in the choroid, consistent with innervation of the choroid by nerve fibers that could release substance P and calcitonin gene-related peptide (CGRP) (48, 49). Additionally, oxidative stress can elevate the levels of certain mediators derived from the RPE such as IL-33 (50), an alarmin that signals tissue damage, as well as complement fragments C3a and C5a (51, 52), all of which are powerful triggers for mast cell activation. Notably, elevated levels of complement deposition and membrane attack complex have been observed in the choroid of patients (53, 54), indicating a potential pathway for oxidative stress-induced mast cell activation in choroidal inflammation.

In summary, the findings of this study demonstrate that choroidal mast cells are activated in response to oxidative stress inflicted by sodium iodate in the RPE (Fig. 7). Mast cell deficiency or stabilization dampened neuroinflammation and alleviated retinal toxicity. Targeting mast cells can offer a novel interventional strategy for treating ocular diseases with advance RPE loss such as observed in geographic atrophy.

References

1. Blindness GBD, Vision Impairment C, Vision Loss Expert Group of the Global Burden of Disease S. Causes of blindness and vision impairment in 2020 and trends over 30 years, and prevalence of avoidable blindness in relation to VISION 2020: the Right to Sight: an analysis for the Global Burden of Disease Study. Lancet Glob Health. 2021;9(2):e144-e60.
2. Fleckenstein M, Keenan TDL, Guymer RH, Chakravarthy U, Schmitz-Valckenberg S, Klaver CC, et al. Age-related macular degeneration. Nat Rev Dis Primers. 2021;7(1):31.
3. Lambert NG, ElShelmani H, Singh MK, Mansergh FC, Wride MA, Padilla M, et al. Risk factors and biomarkers of age-related macular degeneration. Prog Retin Eye Res. 2016;54:64-102.
4. Ferris FL, 3rd, Wilkinson CP, Bird A, Chakravarthy U, Chew E, Csaky K, et al. Clinical classification of age-related macular degeneration. Ophthalmology. 2013;120(4):844-51.
5. Mitchell P, Liew G, Gopinath B, Wong TY. Age-related macular degeneration. Lancet. 2018;392(10153):1147-59.
6. Ambati J, Atkinson JP, Gelfand BD. Immunology of age-related macular degeneration. Nat Rev Immunol. 2013;13(6):438-51.
7. Combadiere C, Feumi C, Raoul W, Keller N, Rodero M, Pezard A, et al. CX3CR1-dependent subretinal microglia cell accumulation is associated with cardinal features of age-related macular degeneration. J Clin Invest. 2007;117(10):2920-8.
8. Kauppinen A, Paterno JJ, Blasiak J, Salminen A, Kaarniranta K. Inflammation and its role in age-related macular degeneration. Cell Mol Life Sci. 2016;73(9):1765-86.

9. Penfold PL, Killingsworth MC, Sarks SH. Senile macular degeneration: the involvement of immunocompetent cells. Graefes Arch Clin Exp Ophthalmol. 1985;223(2):69-76.
10. Rivera JC, Dabouz R, Noueihed B, Omri S, Tahiri H, Chemtob S. Ischemic Retinopathies: Oxidative Stress and Inflammation. Oxid Med Cell Longev. 2017;2017:3940241.
11. Chen M, Xu H. Parainflammation, chronic inflammation, and age-related macular degeneration. J Leukoc Biol. 2015;98(5):713-25.
12. Valent P, Akin C, Hartmann K, Nilsson G, Reiter A, Hermine O, et al. Mast cells as a unique hematopoietic lineage and cell system: From Paul Ehrlich's visions to precision medicine concepts. Theranostics. 2020;10(23):10743-68.
13. Bhutto IA, McLeod DS, Jing T, Sunness JS, Seddon JM, Lutty GA. Increased choroidal mast cells and their degranulation in age-related macular degeneration. Br J Ophthalmol. 2016;100(5):720-6.
14. Ogura S, Baldeosingh R, Bhutto IA, Kambhampati SP, Scott McLeod D, Edwards MM, et al. A role for mast cells in geographic atrophy. FASEB J. 2020;34(8):10117-31.
15. Bousquet E, Zhao M, Thillaye-Goldenberg B, Lorena V, Castaneda B, Naud MC, et al. Choroidal mast cells in retinal pathology: a potential target for intervention. Am J Pathol. 2015;185(8):2083-95.
16. McMenamin PG. The distribution of immune cells in the uveal tract of the normal eye. Eye (Lond). 1997;11 (Pt 2):183-93.
17. Zaitoun IS, Song YS, Zaitoun HB, Sorenson CM, Sheibani N. Assessment of Choroidal Vasculature and Innate Immune Cells in the Eyes of Albino and Pigmented Mice. Cells. 2022;11(20).
18. Bhutto IA, Ogura S, Baldeosingh R, McLeod DS, Lutty GA, Edwards MM. An Acute Injury Model for the Phenotypic Characteristics of Geographic Atrophy. Invest Ophthalmol Vis Sci. 2018;59(4):AMD143-AMD51.
19. Lehmann GL, Hanke-Gogokhia C, Hu Y, Bareja R, Salfati Z, Ginsberg M, et al. Single-cell profiling reveals an endothelium-mediated immunomodulatory pathway in the eye choroid. J Exp Med. 2020;217(6).

20. Hanus J, Anderson C, Sarraf D, Ma J, Wang S. Retinal pigment epithelial cell necroptosis in response to sodium iodate. Cell Death Discov. 2016;2:16054.
21. Nagle DL, Kozak CA, Mano H, Chapman VM, Bucan M. Physical mapping of the Tec and Gabrb1 loci reveals that the Wsh mutation on mouse chromosome 5 is associated with an inversion. Hum Mol Genet. 1995;4(11):2073-9.
22. Dabouz R, Cheng CWH, Abram P, Omri S, Cagnone G, Sawmy KV, et al. An allosteric interleukin-1 receptor modulator mitigates inflammation and photoreceptor toxicity in a model of retinal degeneration. J Neuroinflammation. 2020;17(1):359.
23. Sennlaub F, Auvynet C, Calippe B, Lavalette S, Poupel L, Hu SJ, et al. CCR2(+) monocytes infiltrate atrophic lesions in age-related macular disease and mediate photoreceptor degeneration in experimental subretinal inflammation in Cx3cr1 deficient mice. EMBO Mol Med. 2013;5(11):1775-93.
24. Yu C, Lad EM, Mathew R, Shiraki N, Littleton S, Chen Y, et al. Microglia at sites of atrophy restrict the progression of retinal degeneration via galectin-3 and Trem2. J Exp Med. 2024;221(3).
25. McLeod DS, Bhutto I, Edwards MM, Gedam M, Baldeosingh R, Lutty GA. Mast Cell-Derived Tryptase in Geographic Atrophy. Invest Ophthalmol Vis Sci. 2017;58(13):5887-96.
26. Datta S, Cano M, Ebrahimi K, Wang L, Handa JT. The impact of oxidative stress and inflammation on RPE degeneration in non-neovascular AMD. Prog Retin Eye Res. 2017;60:201-18.
27. Chowers G, Cohen M, Marks-Ohana D, Stika S, Eijzenberg A, Banin E, et al. Course of Sodium Iodate-Induced Retinal Degeneration in Albino and Pigmented Mice. Invest Ophthalmol Vis Sci. 2017;58(4):2239-49.
28. Vogt SD, Curcio CA, Wang L, Li CM, McGwin G, Jr., Medeiros NE, et al. Retinal pigment epithelial expression of complement regulator CD46 is altered early in the course of geographic atrophy. Exp Eye Res. 2011;93(4):413-23.
29. Ach T, Tolstik E, Messinger JD, Zarubina AV, Heintzmann R, Curcio CA. Lipofuscin redistribution and loss accompanied by cytoskeletal stress in retinal pigment epithelium of eyes with age-related macular degeneration. Invest Ophthalmol Vis Sci. 2015;56(5):3242-52.

30. Sankowski R, Suss P, Benkendorff A, Bottcher C, Fernandez-Zapata C, Chhatbar C, et al. Multiomic spatial landscape of innate immune cells at human central nervous system borders. Nat Med. 2024;30(1):186-98.
31. Rustenhoven J, Drieu A, Mamuladze T, de Lima KA, Dykstra T, Wall M, et al. Functional characterization of the dural sinuses as a neuroimmune interface. Cell. 2021;184(4):1000-16 e27.
32. Lin CJ, Herisson F, Le H, Jaafar N, Chetal K, Oram MK, et al. Mast cell deficiency improves cognition and enhances disease-associated microglia in 5XFAD mice. Cell Rep. 2023;42(9):113141.
33. Zhao Z, Liang Y, Liu Y, Xu P, Flamme-Wiese MJ, Sun D, et al. Choroidal gammadelta T cells in protection against retinal pigment epithelium and retinal injury. FASEB J. 2017;31(11):4903-16.
34. Grimbaldeston MA, Chen CC, Piliponsky AM, Tsai M, Tam SY, Galli SJ. Mast cell-deficient W-sash c-kit mutant Kit W-sh/W-sh mice as a model for investigating mast cell biology in vivo. Am J Pathol. 2005;167(3):835-48.
35. Zhang T, Finn DF, Barlow JW, Walsh JJ. Mast cell stabilisers. Eur J Pharmacol. 2016;778:158-68.
36. Grant SM, Goa KL, Fitton A, Sorkin EM. Ketotifen. A review of its pharmacodynamic and pharmacokinetic properties, and therapeutic use in asthma and allergic disorders. Drugs. 1990;40(3):412-48.
37. Sinniah A, Yazid S, Flower RJ. The Anti-allergic Cromones: Past, Present, and Future. Front Pharmacol. 2017;8:827.
38. Wernersson S, Pejler G. Mast cell secretory granules: armed for battle. Nat Rev Immunol. 2014;14(7):478-94.
39. Molino M, Barnathan ES, Numerof R, Clark J, Dreyer M, Cumashi A, et al. Interactions of mast cell tryptase with thrombin receptors and PAR-2. J Biol Chem. 1997;272(7):4043-9.
40. Park GH, Jeon SJ, Ko HM, Ryu JR, Lee JM, Kim HY, et al. Activation of microglial cells via protease-activated receptor 2 mediates neuronal cell death in cultured rat primary neuron. Nitric Oxide. 2010;22(1):18-29.

41. Ocak U, Eser Ocak P, Huang L, Xu W, Zuo Y, Li P, et al. Inhibition of mast cell tryptase attenuates neuroinflammation via PAR-2/p38/NFkappaB pathway following asphyxial cardiac arrest in rats. J Neuroinflammation. 2020;17(1):144.
42. Ossovskaya VS, Bunnett NW. Protease-activated receptors: contribution to physiology and disease. Physiol Rev. 2004;84(2):579-621.
43. Galli SJ, Kalesnikoff J, Grimbaldeston MA, Piliponsky AM, Williams CM, Tsai M. Mast cells as "tunable" effector and immunoregulatory cells: recent advances. Annu Rev Immunol. 2005;23:749-86.
44. Galli SJ, Nakae S, Tsai M. Mast cells in the development of adaptive immune responses. Nat Immunol. 2005;6(2):135-42.
45. McNeil BD, Pundir P, Meeker S, Han L, Undem BJ, Kulka M, et al. Identification of a mast-cell-specific receptor crucial for pseudo-allergic drug reactions. Nature. 2015;519(7542):237-41.
46. Lansu K, Karpiak J, Liu J, Huang XP, McCorvy JD, Kroeze WK, et al. In silico design of novel probes for the atypical opioid receptor MRGPRX2. Nat Chem Biol. 2017;13(5):529-36.
47. Green DP, Limjunyawong N, Gour N, Pundir P, Dong X. A Mast-Cell-Specific Receptor Mediates Neurogenic Inflammation and Pain. Neuron. 2019;101(3):412-20 e3.
48. Shih YF, Fitzgerald ME, Cuthbertson SL, Reiner A. Influence of ophthalmic nerve fibers on choroidal blood flow and myopic eye growth in chicks. Exp Eye Res. 1999;69(1):9-20.
49. de Hoz R, Ramirez AI, Salazar JJ, Rojas B, Ramirez JM, Trivino A. Substance P and calcitonin gene-related peptide intrinsic choroidal neurons in human choroidal whole-mounts. Histol Histopathol. 2008;23(10):1249-58.
50. Xi H, Katschke KJ, Jr., Li Y, Truong T, Lee WP, Diehl L, et al. IL-33 amplifies an innate immune response in the degenerating retina. J Exp Med. 2016;213(2):189-207.
51. Wang Y, Shen H, Pang L, Qiu B, Yuan Y, Guan X, et al. Qihuang Granule protects the retinal pigment epithelium from oxidative stress via regulation of the alternative complement pathway. BMC Complement Med Ther. 2023;23(1):55.
52. Trakkides TO, Schafer N, Reichenthaler M, Kuhn K, Brandwijk R, Toonen EJM, et al. Oxidative Stress Increases Endogenous Complement-Dependent Inflammatory and

Angiogenic Responses in Retinal Pigment Epithelial Cells Independently of Exogenous Complement Sources. Antioxidants (Basel). 2019;8(11).
53. Mullins RF, Dewald AD, Streb LM, Wang K, Kuehn MH, Stone EM. Elevated membrane attack complex in human choroid with high risk complement factor H genotypes. Exp Eye Res. 2011;93(4):565-7.
54. Nozaki M, Raisler BJ, Sakurai E, Sarma JV, Barnum SR, Lambris JD, et al. Drusen complement components C3a and C5a promote choroidal neovascularization. Proc Natl Acad Sci U S A. 2006;103(7):2328-33.

Acknowledgments

This study was funded by the Canadian Institutes of Health Research (CIHR). RD is supported by Fonds de Recherche du Québec-Santé (FRQS). PA is supported by CIHR, FRQS, The Vision Health Research Network, and FROUM.

Contributions

RD conceptualized and designed the study. RD and PA planned and carried out experiments and analyzed the data. RD wrote the manuscript. SC edited manuscript and was involved in grant acquisition.

Conflict of interest statement

The authors have no conflict with the subject matter or materials discussed in the manuscript.

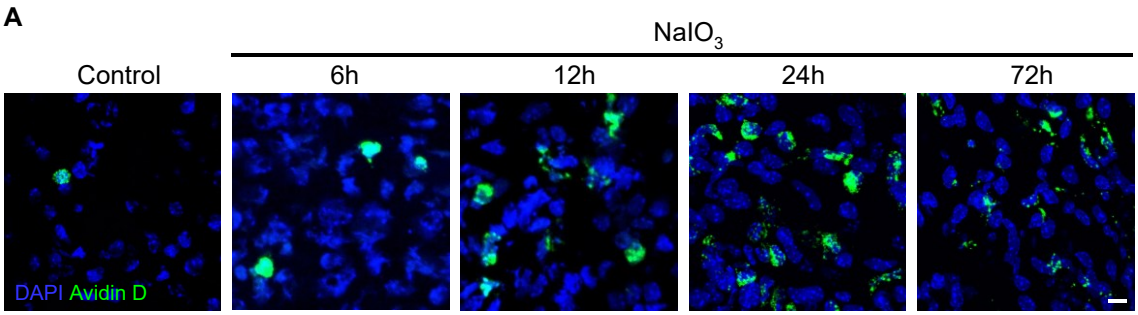
A
NaIO3
Control
6h
12h
24h
72h
DAPI Avidin D

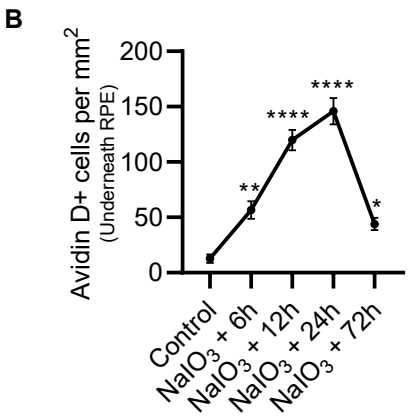
B
Avidin D+ cells per mm2
(Underneath RPE)
200
150
100
50
0
**
****
****
*
Control
NaIO3 + 6h
NaIO3 + 12h
NaIO3 + 24h
NaIO3 + 72h

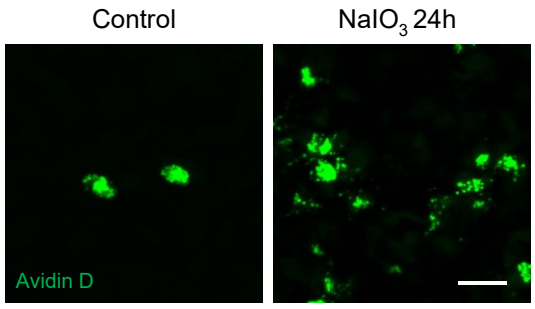
C
Control
NaIO3 24h
Avidin D

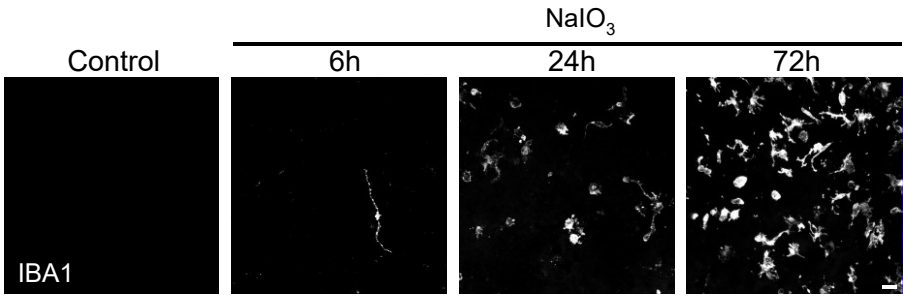
D
NaIO3
Control
6h
24h
72h
IBA1

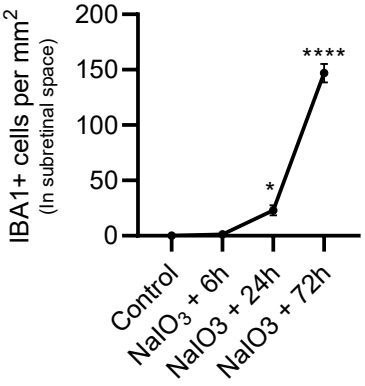
E
IBA1+ cells per mm2
(In subretinal space)
200
150
100
50
0
*
****
Control
NaIO3 + 6h
NaIO3 + 24h
NaIO3 + 72h

Figure 1. Mast cell activation in sodium iodate-induced retinal degeneration

Avidin D staining of mast cells following sodium iodate administration. (A) Representative images of choroidal flat mounts showing mast cell staining in mice injected with sodium iodate compared to controls. (B) Graph depicting the density of Avidin D-positive cells at various time points post-sodium iodate injection. Data are presented as mean ± SEM and statistical analysis was performed using one-way ANOVA with Holm-Sidak correction for multiple comparisons; n = 4. ****$p < 0.0001$, **$p < 0.01$, *$p < 0.05$ compared to control group. (C) Representative images of choroidal flat mounts illustrating mast cell degranulation after sodium iodate injection. Scale bar: 20 μm. (D) Representative images of RPE flat mounts depicting MP infiltration. Scale bar: 20 μm. (E) Quantification of IBA1+ cells following sodium iodate administration. Data are presented as mean ± SEM. Statistical analyses were performed using the Kruskal-Wallis test followed by post hoc Dunn's test for comparison of means; n = 4. **$p < 0.01$ compared to control group.

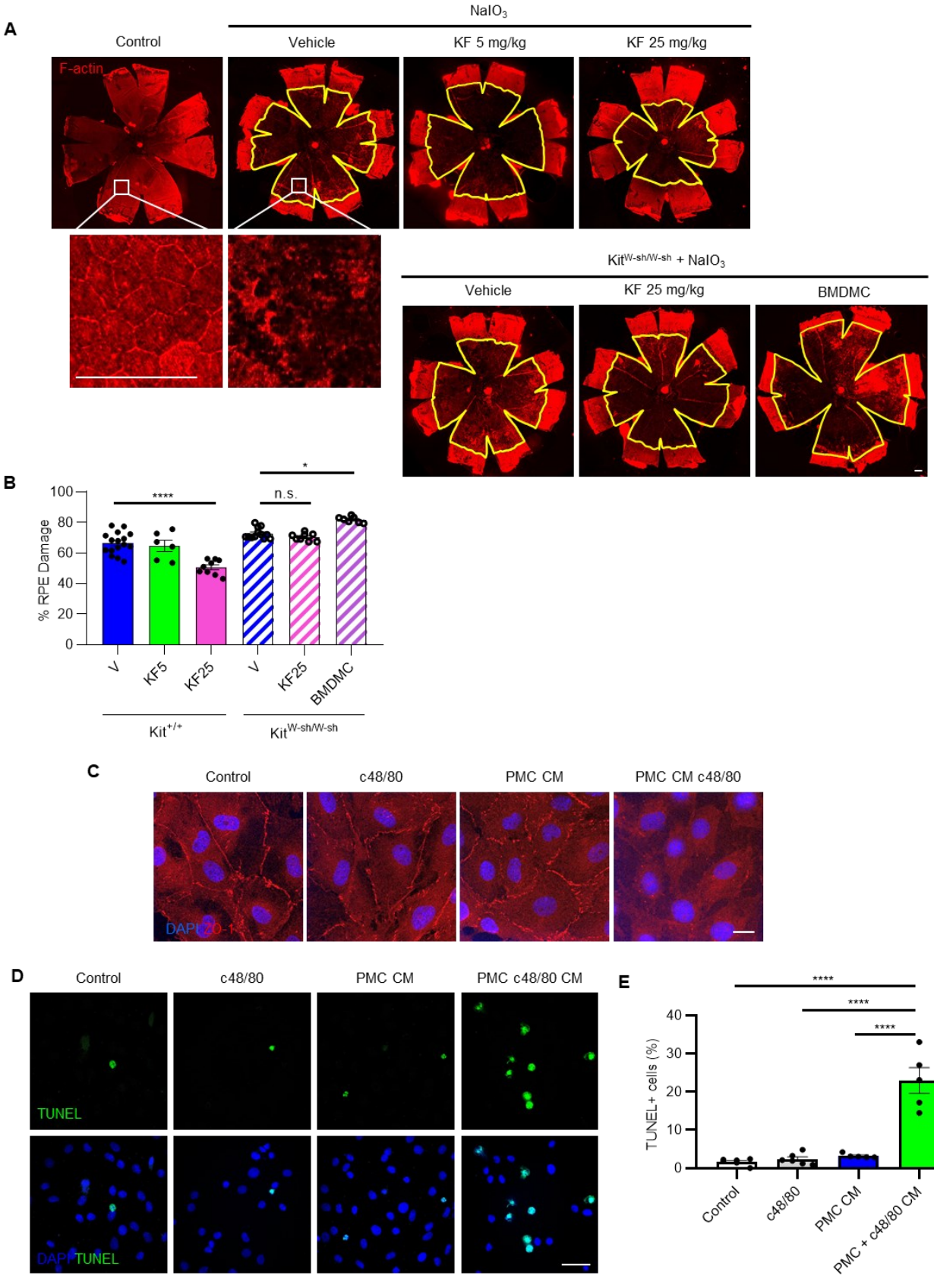
A
NaIO3
Control
Vehicle
KF 5 mg/kg
KF 25 mg/kg
F-actin
KitW-sh/W-sh + NaIO3
Vehicle
KF 25 mg/kg
BMDMC
B
% RPE Damage
****
n.s.
*
V
KF5
KF25
V
KF25
BMDMC
Kit+/+
KitW-sh/W-sh
C
Control
c48/80
PMC CM
PMC CM c48/80
DAPI ZO-1
D
Control
c48/80
PMC CM
PMC c48/80 CM
TUNEL
DAPI TUNEL
E
TUNEL+ cells (%)
****
****
****
Control
c48/80
PMC CM
PMC + c48/80 CM

Figure 2. Effects of mast cells on the integrity of RPE

(A) F-actin staining of flat-mounted eyecups to observe RPE damage. Mice were treated with sodium iodate. Scale bar: 200 μm. (B) Graph illustrating the damaged areas measured in eyecups and data were plotted as a percentage of total damaged RPE morphology. Data are expressed as mean ± SEM and analyzed using one-way ANOVA with Holm-Sidak corrections for multiple comparisons. n = 6-16. *$p < 0.05$, ****$p < 0.0001$. (C) Primary RPE cells treated with conditioned media from activated peritoneal mast cells and stained for ZO-1. Scale bar: 10 μm. (D) Primary RPE cells treated with conditioned media from activated peritoneal mast cells and stained. Scale bar: 50 μm. (E) Quantification of percentage of TUNEL+ cells. Data are expressed as mean ± SEM and analyzed using one-way ANOVA with Holm-Sidak corrections for multiple comparisons. n = 5-6 per group. ****$p < 0.0001$.

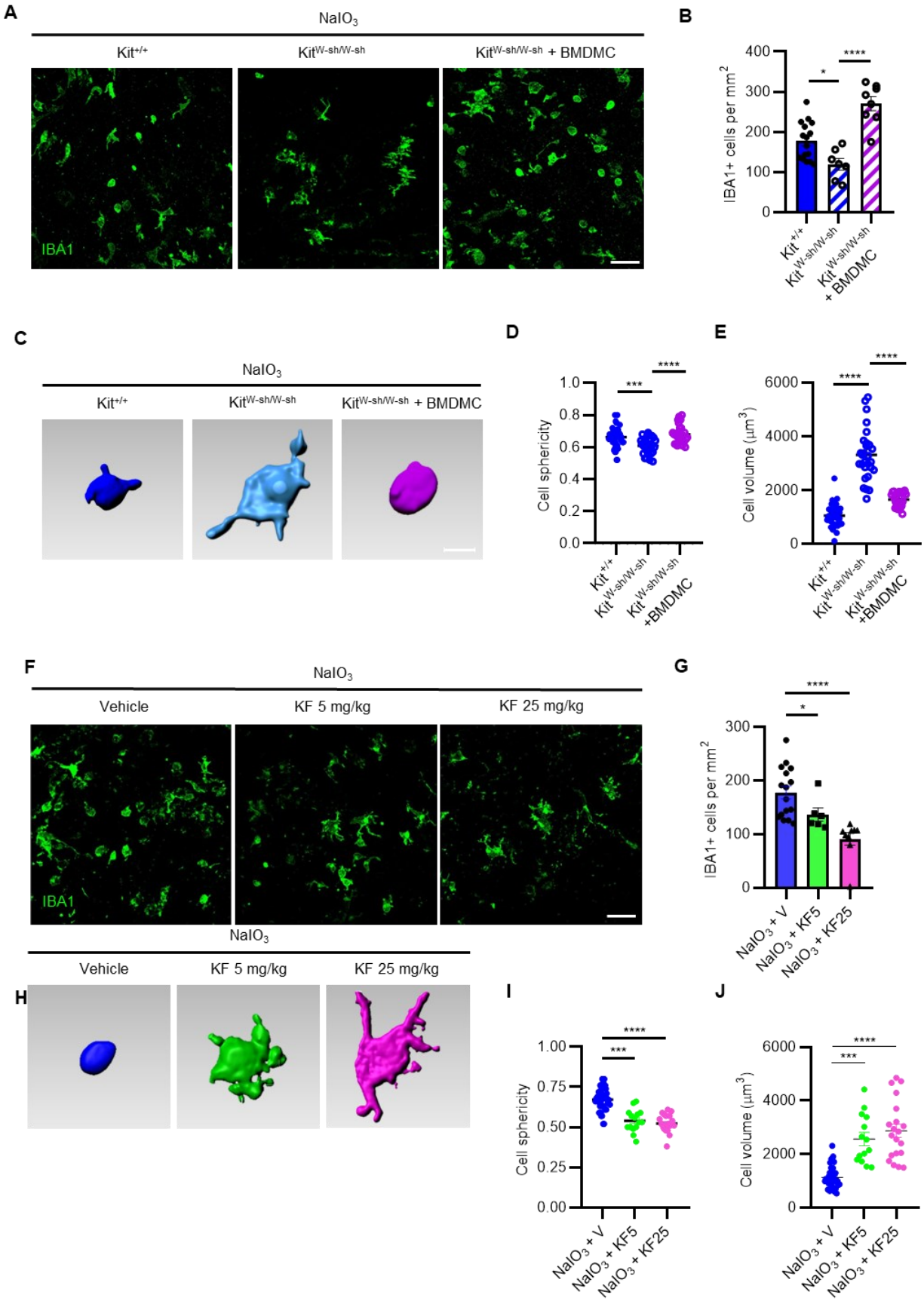
A
NaIO3
Kit+/+
KitW-sh/W-sh
KitW-sh/W-sh + BMDMC
IBA1
B
IBA1+ cells per mm2
Kit+/+
KitW-sh/W-sh
KitW-sh/W-sh + BMDMC
C
NaIO3
Kit+/+
KitW-sh/W-sh
KitW-sh/W-sh + BMDMC
D
Cell sphericity
Kit+/+
KitW-sh/W-sh
KitW-sh/W-sh +BMDMC
E
Cell volume (µm3)
Kit+/+
KitW-sh/W-sh
KitW-sh/W-sh +BMDMC
F
NaIO3
Vehicle
KF 5 mg/kg
KF 25 mg/kg
IBA1
G
IBA1+ cells per mm2
NaIO3 + V
NaIO3 + KF5
NaIO3 + KF25
H
NaIO3
Vehicle
KF 5 mg/kg
KF 25 mg/kg
I
Cell sphericity
NaIO3 + V
NaIO3 + KF5
NaIO3 + KF25
J
Cell volume (µm3)
NaIO3 + V
NaIO3 + KF5
NaIO3 + KF25

Figure 3. Effects of mast cell deficiency or stabilization on subretinal inflammation
(A) Representative images of RPE flat mounts showing infiltration of IBA1-labeled mononuclear phagocytes of wild type, $Kit^{W\text{-}sh/W\text{-}sh}$, and $Kit^{W\text{-}sh/W\text{-}sh}$ mice reconstituted with BMDMCs. Scale bar: 50 µm. (B) The graph represents compiled data on IBA1+ cell density in the RPE presented as a histogram. Data are expressed as mean ± SEM and analyzed using one-way ANOVA with Holm-Sidak correction for multiple comparisons; n = 7-16. ****p < 0.0001, *p < 0.05. (C) Reconstructed images of a representative IBA1+ cell. Scale bar: 10 µm. (D) Analysis of sphericity and volume of IBA1 cells. Data are expressed as mean ± SEM and analyzed using one-way ANOVA with Holm-Sidak correction for multiple comparisons; n = 27-47. ****p < 0.0001, ***p < 0.001. (E) Representative images of RPE flat mounts showing infiltration of IBA1-labeled cells of mice treated with ketotifen fumarate or vehicle. Scale bar: 50 µm. (F) Quantification of IBA1+ MPs in the subretinal space of mice treated with ketotifen fumarate or vehicle. Data are expressed as mean ± SEM and analyzed using one-way ANOVA with Holm-Sidak correction for multiple comparisons. n = 7-16. *p < 0.05, ****p < 0.0001. (G) Reconstructed images of a representative IBA1+ cell in the subretinal space of mice treated with ketotifen fumarate or vehicle. (H) Effects of ketotifen fumarate on the sphericity and size of IBA1+ MPs. Data are expressed as mean ± SEM and analyzed using one-way ANOVA with Holm-Sidak correction for multiple comparisons; n = 15-42. ***p < 0.001, ****p < 0.0001.

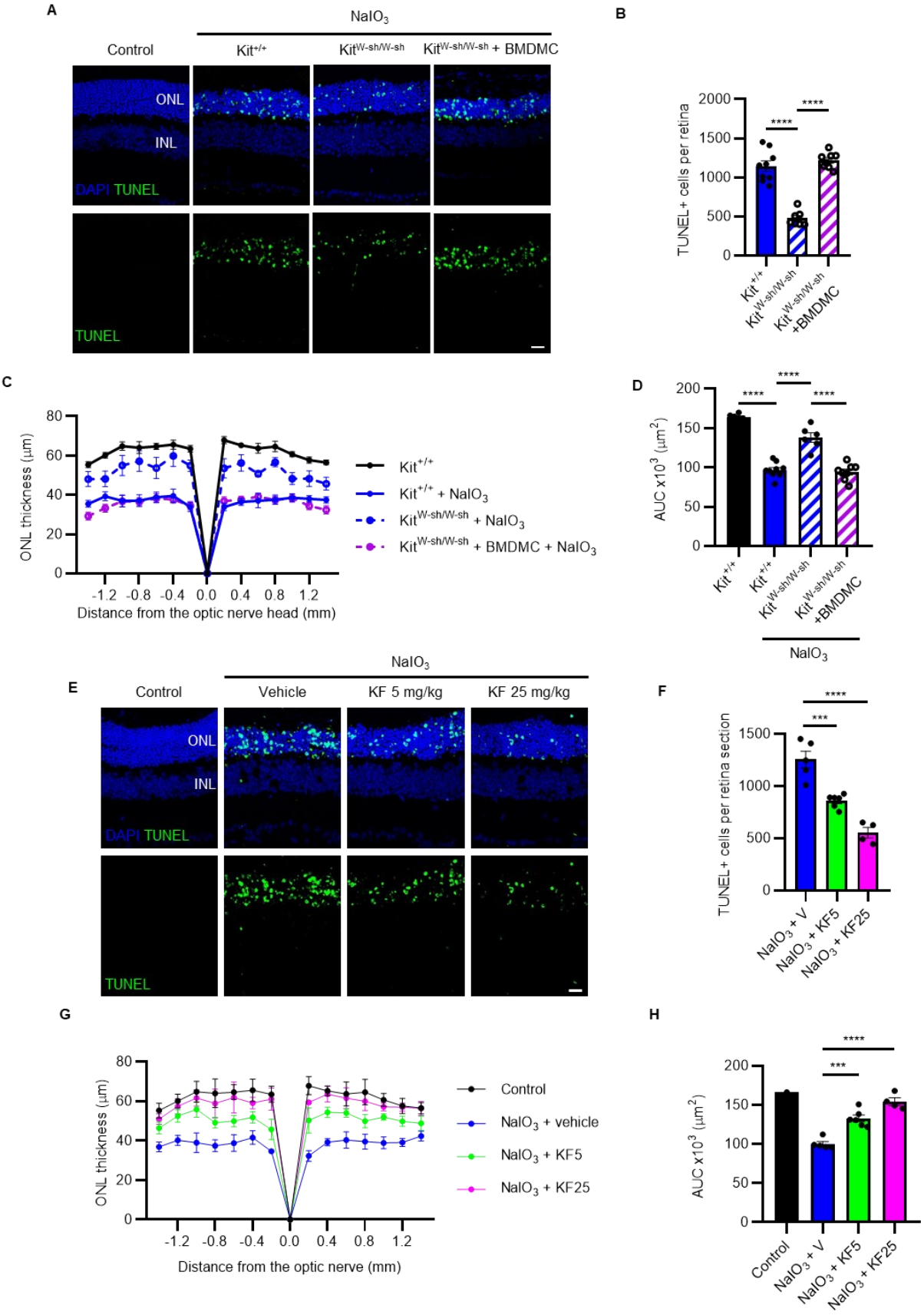
A
NaIO3
Control
Kit+/+
KitW-sh/W-sh
KitW-sh/W-sh + BMDMC
ONL
INL
DAPI TUNEL
TUNEL
B
TUNEL+ cells per retina
2000
1500
1000
500
0
****
****
Kit+/+
KitW-sh/W-sh
KitW-sh/W-sh +BMDMC
C
ONL thickness (µm)
80
60
40
20
0
-1.2 -0.8 -0.4 0.0 0.4 0.8 1.2
Distance from the optic nerve head (mm)
Kit+/+
Kit+/+ + NaIO3
KitW-sh/W-sh + NaIO3
KitW-sh/W-sh + BMDMC + NaIO3
D
AUC x10³ (µm²)
200
150
100
50
0
****
****
****
Kit+/+
Kit+/+
KitW-sh/W-sh
KitW-sh/W-sh +BMDMC
NaIO3
E
NaIO3
Control
Vehicle
KF 5 mg/kg
KF 25 mg/kg
ONL
INL
DAPI TUNEL
TUNEL
F
TUNEL+ cells per retina section
1500
1000
500
0
****
***
NaIO3 + V
NaIO3 + KF5
NaIO3 + KF25
G
ONL thickness (µm)
80
60
40
20
0
-1.2 -0.8 -0.4 0.0 0.4 0.8 1.2
Distance from the optic nerve (mm)
Control
NaIO3 + vehicle
NaIO3 + KF5
NaIO3 + KF25
H
AUC x10³ (µm²)
200
150
100
50
0
****
***
Control
NaIO3 + V
NaIO3 + KF5
NaIO3 + KF25

Figure 4. Mast cell inhibition on the survival of photoreceptors

(A) Images of TUNEL (green)-stained retinal cross-sections in control and sodium iodate-treated Kit+, $Kit^{W\text{-}sh/W\text{-}sh}$, and $Kit^{W\text{-}sh/W\text{-}sh}$ where bone marrow derived mast cells were restored. Scale bar: 20 µm. ONL: outer nuclear layer; INL: inner nuclear layer. (B) Graph illustrating the quantitative analysis of TUNEL-positive cells in photoreceptors. Data are expressed as mean ± SEM and analyzed using one-way ANOVA with Holm-Sidak correction for multiple comparisons; n = 7-9 per group. ****p < 0.0001. (C) Spider-graph quantification of ONL thickness on DAPI-stained retinal sections from control and from sodium iodate-treated mice. (D) Statistical analysis of the area under the curve (AUC) values to assess photoreceptor density. Data are expressed as mean ± SEM and analyzed using one-way ANOVA with Holm-Sidak correction for multiple comparisons; n = 6–9. ****p < 0.0001. (E) Photoreceptor cell death assessed by TUNEL on the retinal sections at 3 days following sodium iodate injection. Mice were treated with ketotifen fumarate or vehicle. Scale bar: 20 µm. (F) Graph illustrating the quantitative analysis of TUNEL-positive cells in photoreceptors. Data are expressed as mean ± SEM and analyzed using one-way ANOVA with Holm-Sidak correction for multiple comparisons; n = 4–6. ***p < 0.001, ****p < 0.0001. (G) Spider-graph quantification of ONL thickness on DAPI-stained retinal sections from control and from sodium iodate-treated mice. (H) Statistical analysis of the area under the curve values to assess photoreceptor density. Data are expressed as mean ± SEM and analyzed using one-way ANOVA with Holm-Sidak correction for multiple comparisons; n = 4-6. ***p < 0.001, ****p < 0.0001.

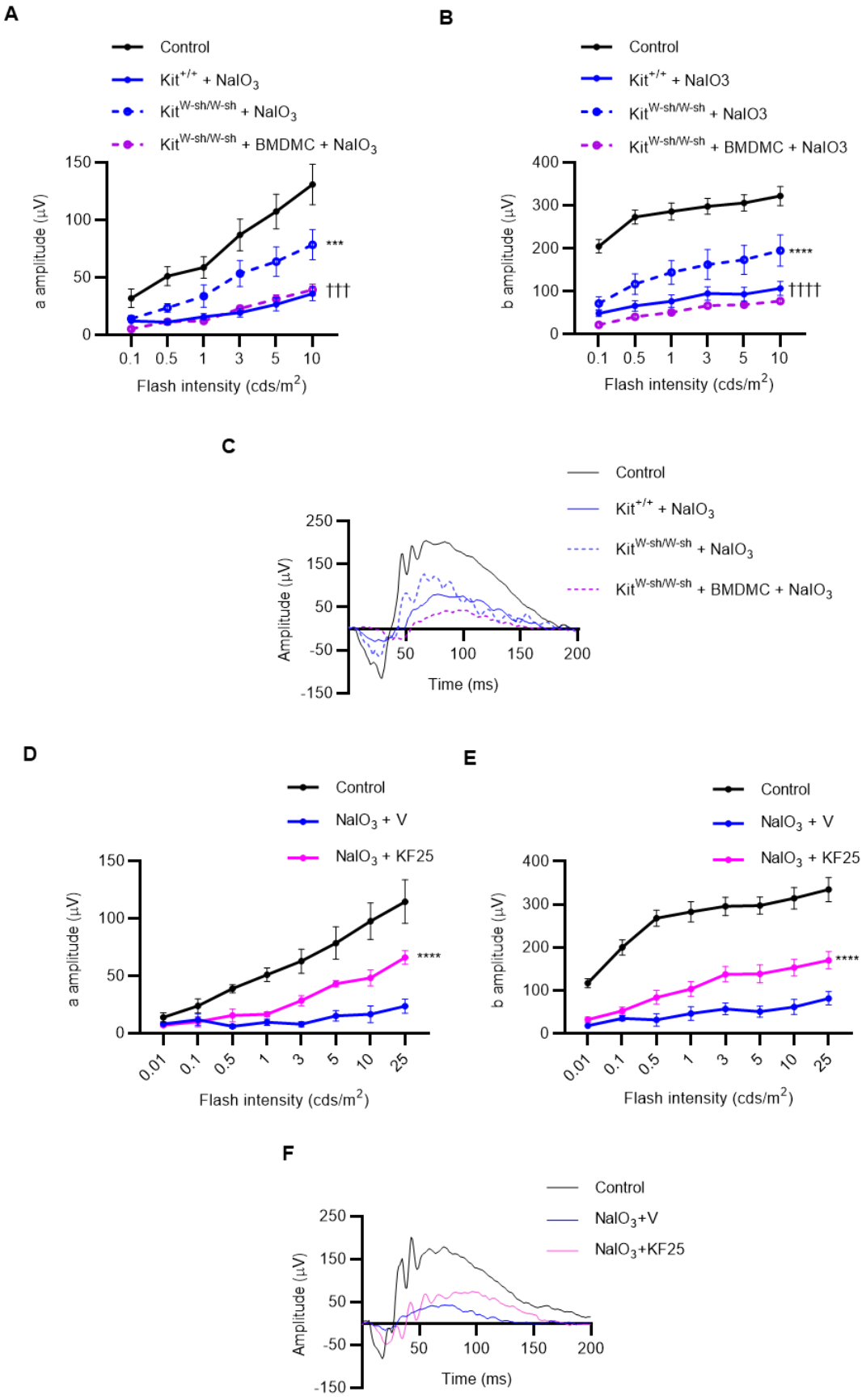
A
Control
Kit+/+ + NaIO3
KitW-sh/W-sh + NaIO3
KitW-sh/W-sh + BMDMC + NaIO3
a amplitude (μV)
Flash intensity (cds/m2)
***
†††
B
Control
Kit+/+ + NaIO3
KitW-sh/W-sh + NaIO3
KitW-sh/W-sh + BMDMC + NaIO3
b amplitude (μV)
Flash intensity (cds/m2)
****
††††
C
Control
Kit+/+ + NaIO3
KitW-sh/W-sh + NaIO3
KitW-sh/W-sh + BMDMC + NaIO3
Amplitude (μV)
Time (ms)
D
Control
NaIO3 + V
NaIO3 + KF25
a amplitude (μV)
Flash intensity (cds/m2)
****
E
Control
NaIO3 + V
NaIO3 + KF25
b amplitude (μV)
Flash intensity (cds/m2)
****
F
Control
NaIO3+V
NaIO3+KF25
Amplitude (μV)
Time (ms)

Figure 5. Effect of mast cell inhibition on retinal function

ERG analysis was performed using flash intensities of 0.01, 0.1, 0.5, 1, 3, 5, 10, and 25 cds/m^2. (A) a-wave amplitude and (B) b-wave amplitude of WT control, sodium iodate-treaded WT, $Kit^{W\text{-}sh/W\text{-}sh}$, $Kit^{W\text{-}sh/W\text{-}sh}$ + BMDMCs mice 3 days following sodium iodate injection. Data are expressed as mean ± SEM and analyzed using two-way repeated measures ANOVA with Holm-Sidak corrections for multiple comparisons; n = 6-16 per group. ****p < 0.0001, ***p < 0.001 compared to WT + $NaIO_3$ group. ††††p < 0.0001, †††p < 0.001 compared to $Kit^{W\text{-}sh/W\text{-}sh}$ + $NaIO_3$ group. (C) Graph depicting the electroretinogram recordings at a flash intensity of 5 cds/m^2 from control and sodium iodate-treated WT, $Kit^{W\text{-}sh/W\text{-}sh}$, $Kit^{W\text{-}sh/W\text{-}sh}$ + BMDMCs animals. Quantification of (D) a-wave amplitude and (E) b-wave amplitude of control, and sodium iodate-treated mice treated with ketotifen fumarate or vehicle. Data are expressed as mean ± SEM and analyzed using two-way repeated measures ANOVA with Holm-Sidak corrections for multiple comparisons; n = 5-7 per group. ****p < 0.0001 compared to WT + $NaIO_3$ group. (F) Representative electroretinogram waveforms recorded at a flash intensity of 5 cds/m^2, comparing control with sodium iodate-injected mice treated with vehicle or ketotifen fumarate.

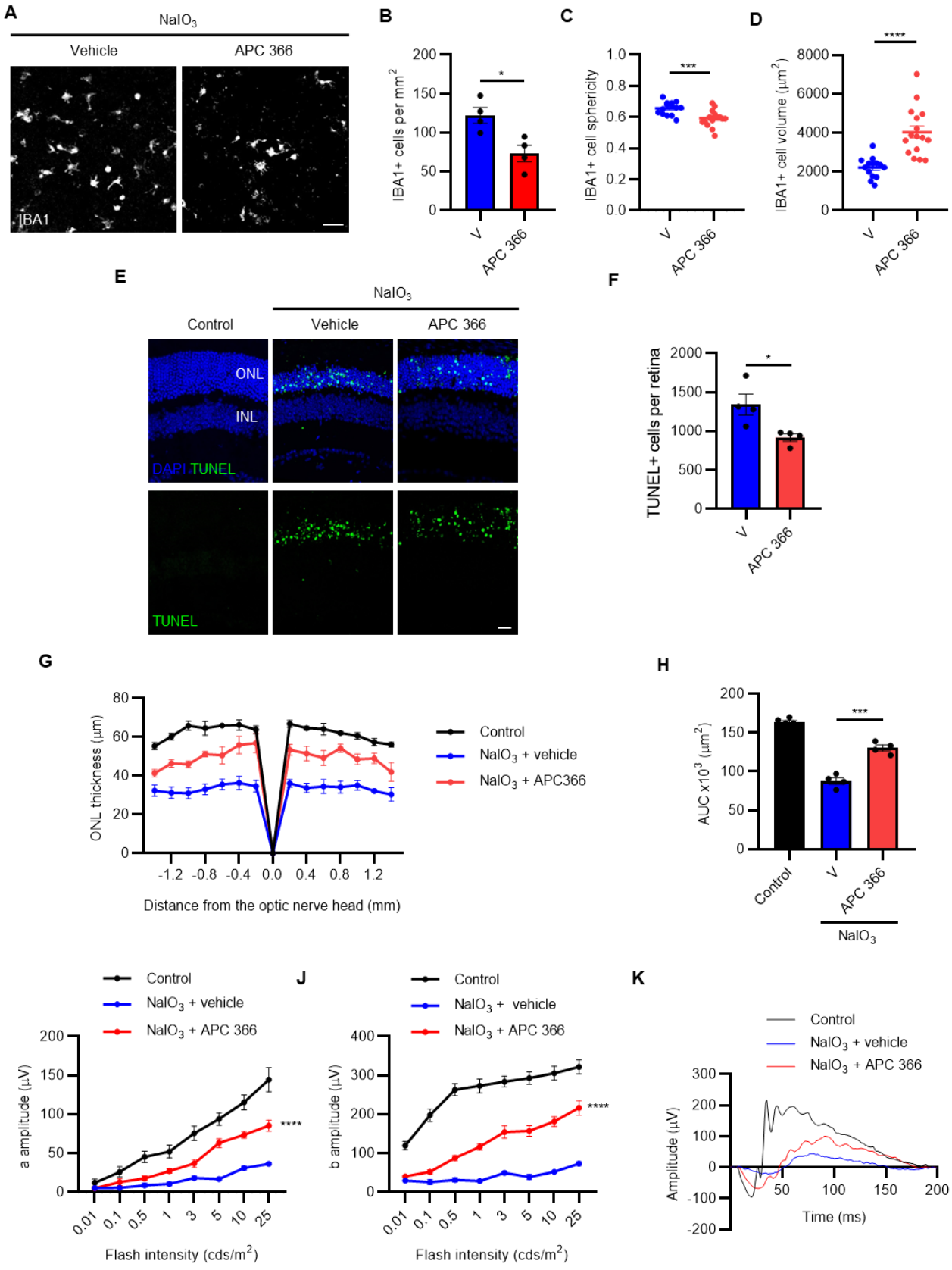
A
NaIO3
Vehicle
APC 366
IBA1
B
IBA1+ cells per mm2
V
APC 366
C
IBA1+ cell sphericity
D
IBA1+ cell volume (µm2)
E
NaIO3
Control
Vehicle
APC 366
ONL
INL
DAPI TUNEL
TUNEL
F
TUNEL+ cells per retina
G
ONL thickness (µm)
Distance from the optic nerve head (mm)
Control
NaIO3 + vehicle
NaIO3 + APC366
H
AUC x10-3 (µm2)
Control
V
APC 366
NaIO3
I
Control
NaIO3 + vehicle
NaIO3 + APC 366
a amplitude (µV)
Flash intensity (cds/m2)
J
Control
NaIO3 + vehicle
NaIO3 + APC 366
b amplitude (µV)
Flash intensity (cds/m2)
K
Control
NaIO3 + vehicle
NaIO3 + APC 366
Amplitude (µV)
Time (ms)

Figure 6. Effects of mast cell tryptase on subretinal inflammation and photoreceptor survival

(A) Representative images of RPE flat-mount illustrating IBA1-positive MPs of sodium-iodate-injected mice treated with APC 366 or vehicle. Scale bar: 50 µm. (B) The graph represents the quantification of subretinal MPs. Unpaired t-test; n = 4 per group. *p < 0.05. (C) Analysis of sphericity and volume of IBA-1 cells. Unpaired t-test n = 14-16. ****p < 0.0001, ***p < 0.001. (D) Representative images of TUNEL-stained retinal sections control and sodium iodate-injected mice treated with vehicle or APC 366. ONL: outer nuclear layer. (E) Quantitative analysis of TUNEL-positive cells in photoreceptors. Unpaired t-test; n = 4 per group. *p < 0.05. (F) Spider graph depicting the ONL thickness of the ONL measured at specified intervals of the optic nerve. (G) Graph showing ONL AUC. n = 4-5 per group. *p < 0.05. AUC: area under the curve Quantification of a (H) and b (I) wave amplitudes ERG from control and sodium iodate-injected mice treated or not with APC 366. ****p < 0.0001, ***p < 0.001, **p < 0.01, *p < 0.05. (J) Representative scotopic ERG responses recorded at a flash intensity of 5 cds/m^2.

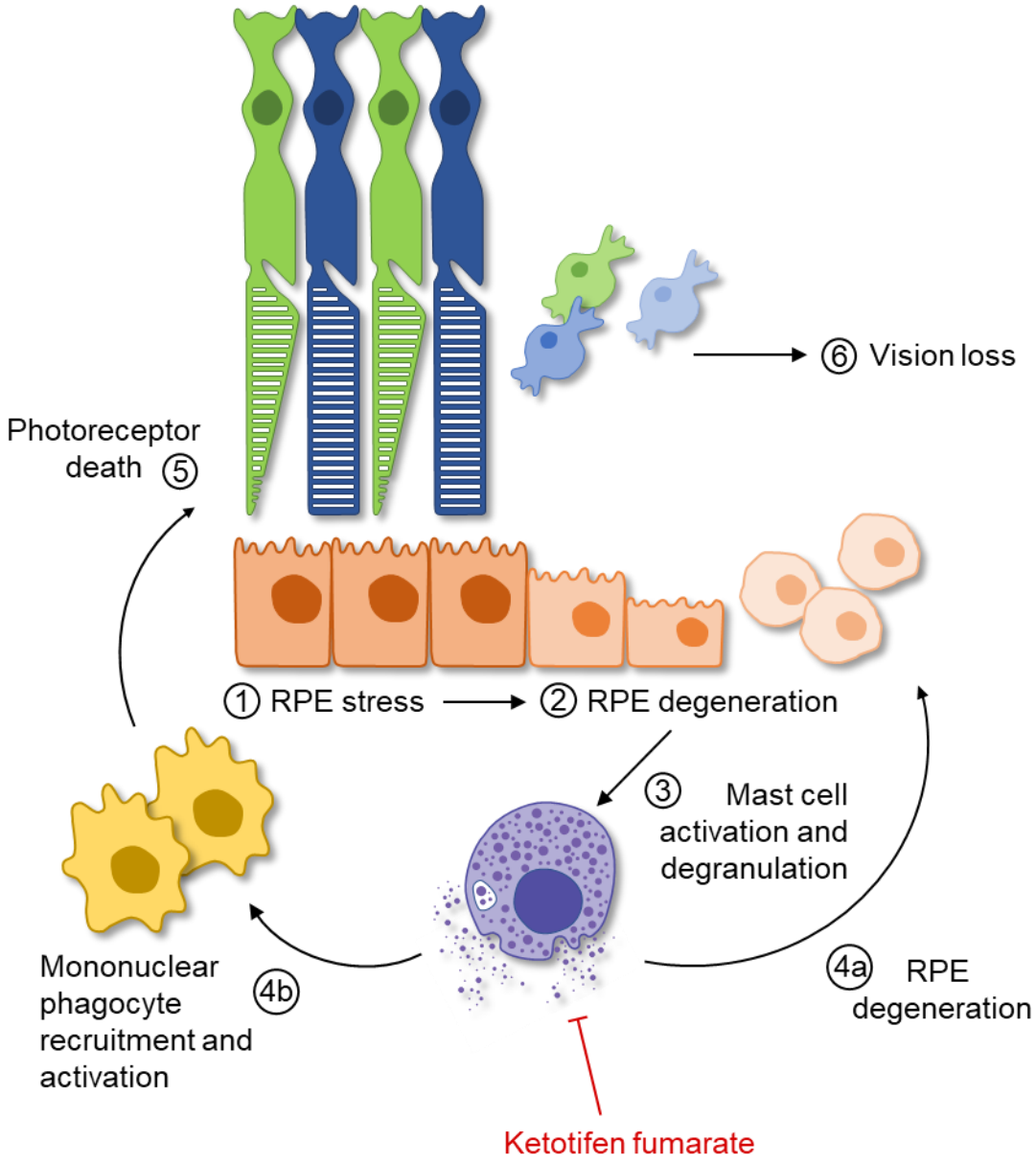

Figure 7. Schematic overview of the proposed mechanisms: Illustration of how mast cells contribute to sodium iodate-induced retinal degeneration.

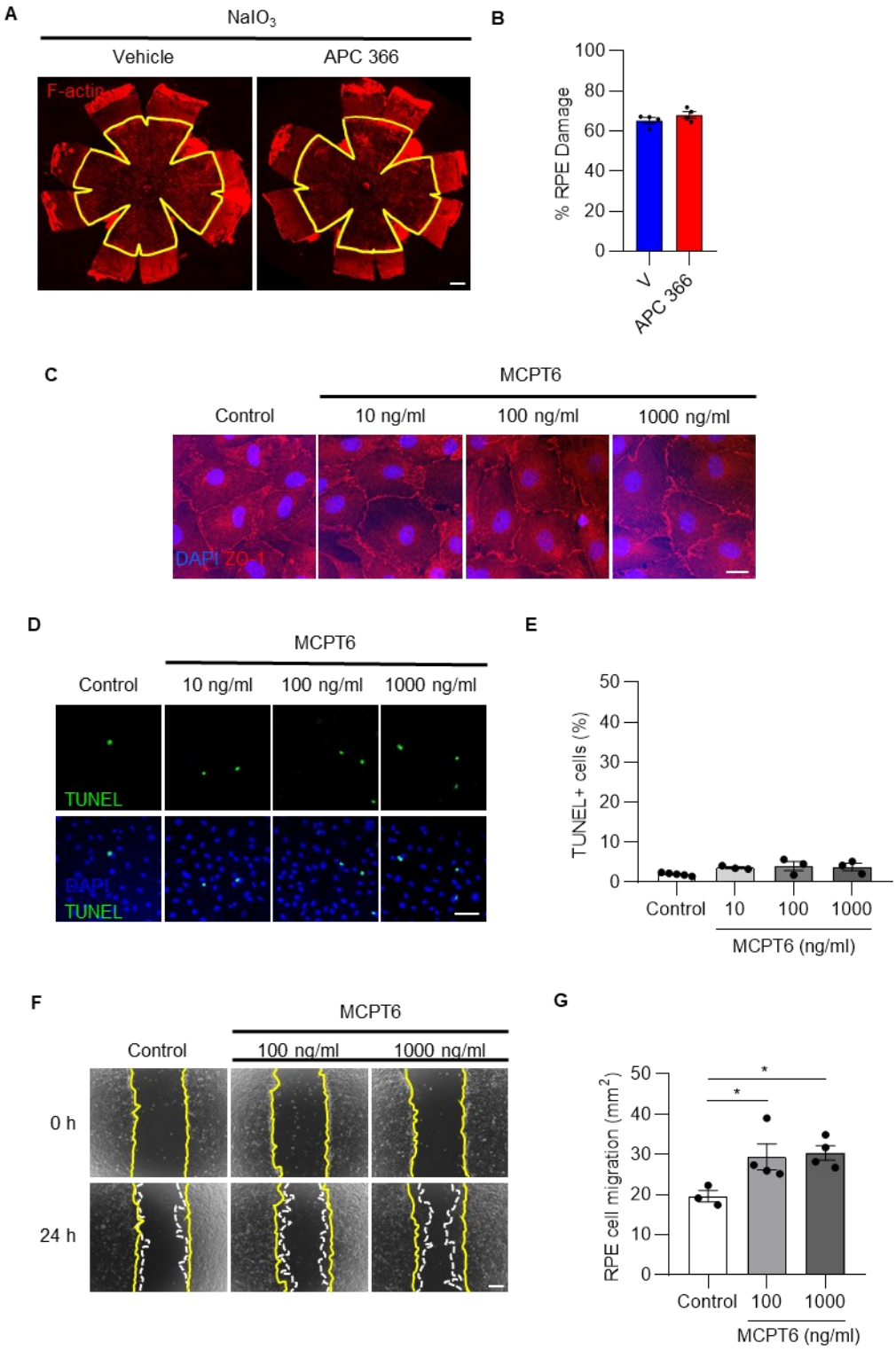
A
NaIO3
Vehicle
APC 366
F-actin
B
% RPE Damage
100
80
60
40
20
0
V
APC 366
C
MCPT6
Control
10 ng/ml
100 ng/ml
1000 ng/ml
DAPI ZO-1
D
MCPT6
Control
10 ng/ml
100 ng/ml
1000 ng/ml
TUNEL
DAPI
TUNEL
E
TUNEL+ cells (%)
50
40
30
20
10
0
Control
10
100
1000
MCPT6 (ng/ml)
F
MCPT6
Control
100 ng/ml
1000 ng/ml
0 h
24 h
G
RPE cell migration (mm2)
50
40
30
20
10
0
*
*
Control
100
1000
MCPT6 (ng/ml)

Supplementary Figure 1. Effect of tryptase on RPE cells

(A) F-actin in RPE cells was stained with rhodamine phalloidin in flat-mounted eyecups to observe RPE damage in sodium iodate-injected mice, with or without APC 366 treatment. Scale bar: 200 μm. (B) Quantification of RPE damage percentage. (C) Effects of mouse tryptase (MCPT6) on primary RPE cells stained with ZO-1. Scale bar: 10 μm. (D) Effects of mouse tryptase (MCPT6) on primary RPE stained with TUNEL. Scale bar: 50 μm. (E) The graph shows the percentage of TUNEL+ cells. (F) Effects of MCPT6 on the migration of primary RPE cells. Scale bar: 500 μm. (G) Effects of MCPT6 on primary RPE cell migration. Data are expressed as mean ± SEM and analyzed using one-way ANOVA with Holm-Sidak corrections for multiple comparisons; n = 3-4. *$p < 0.05$.

CHAPTER 5 - Mast cells promote experimental choroidal neovascularization in AMD

Authors: Rabah Dabouz[1,2], Pénélope Abram[2,3], Jose Carlos Rivera[4,5], Sylvain Chemtob[1,2,5]

[1]Department of Pharmacology and Therapeutics, McGill University, Montréal, QC, Canada.

[2]Department of Ophthalmology, Hôpital Maisonneuve-Rosemont, Montréal, QC, Canada.

[3]Department of Pharmacology, University of Montreal, Montréal, QC, Canada.

[4]CHU-Sainte Justine Research Center, Montreal, QC, Canada.

[5]Department of Ophthalmology, University of Montreal, Montréal, QC, Canada.

Preface

In the preceding chapter, we examined the role of mast cells in retinal inflammation, demonstrating their early activation in a sodium iodate model, which simulates the advanced form of AMD known as geographic atrophy. This model revealed that choroidal inflammation elicited by activated mast cells leads to subsequent inflammation in the subretinal space. However, AMD presents in two distinct, though not mutually exclusive, forms: the dry form, characterized by geographic atrophy, and the wet, neovascular form. It is not uncommon for these forms to transition from one to the other or even coexist within the same patient, adding layers of complexity to the disease's progression and treatment. Furthermore, histological examinations have not only confirmed mast cell activation in cases of geographic atrophy but have also identified their presence in patients with the wet form of AMD. This finding suggests a potential role for mast cells across the spectrum of AMD pathology, extending beyond the confines of geographic atrophy to the mechanisms underlying macular neovascularization. Thus, in the following chapter, we examine the specific contribution of choroidal mast cells to the process of CNV. To this end, we employ a laser-induced model of CNV, aiming to elucidate how mast cells might influence the neovascular processes that characterize the wet form of AMD. This exploration is essential for understanding the full scope of mast cell involvement in AMD and opens new avenues for targeted therapies in both the prevention and management of this complex disease.

Abstract

'Wet' age-related macular degeneration (AMD) is characterized by pathologic choroidal neovascularization (CNV) that destroys central vision. Abundant evidence points to inflammation and immune cell dysfunction in the progression of CNV in AMD. Mast cells are resident immune cells that control the inflammatory response. Mast cells accumulate and degranulate in the choroid of patients with AMD, suggesting they play a role in CNV. Activated mast cells secrete various biologically active mediators, including inflammatory cytokines and proteolytic enzymes such as tryptase. We investigated the role of mast cells in AMD using a model of CNV. Conditioned media from activated mast cells exerts proangiogenic effects on choroidal endothelial cells and choroidal explants. Mast cell-derived tryptase contributed substantially to choroidal endothelial cell migration and vascular sprouting. Laser-induced CNV *in vivo* was markedly attenuated in mice genetically depleted of mast cells ($Kit^{W\text{-}sh/W\text{-}sh}$) and in wild-type mice treated with mast cell stabilizer, ketotifen fumarate. Tryptase was found to elicit pronounced choroidal endothelial cell sprouting, migration and tubulogenesis; while tryptase inhibition diminished CNV. Transcriptomic analysis of laser-treated RPE/choroid complex revealed collagen catabolism and extra-cellular matrix (ECM) reorganization as significant events correlated in clusters of mast cell activation. Consistent with these analyses, compared to wildtype mice choroids of laser-treated mast cell-deficient mice displayed less ECM remodelling evaluated using collagen hybridizing peptide tissue binding. Findings herein provide strong support for mast cells as key players in the progression of pathologic choroidal angiogenesis and as potential therapeutic targets to prevent pathological neovascularization in 'wet' AMD.

Keywords: Retinal degeneration, choroidal neovascularization, mast cells, angiogenesis, laser CNV.

Introduction

Choroidal neovascularization (CNV) is a pathological manifestation that involves the abnormal growth of blood vessels from the choroid through the Bruch's membrane extending into the subretinal and outer retinal space [1]. CNV is a leading cause of severe

vision loss and is frequently linked with ocular disorders, notably age-related macular degeneration (AMD) [2]. While anti- vascular endothelial growth factor (VEGF) therapy has shown success in improving vision [3], it carries risks and drawbacks. A notable concern is that some patients might develop geographic atrophy as a response to the anti-VEGF treatment [4, 5], and there is still potential progression to fibrotic scars [6]. Hence, the search for new therapeutic modalities remains significant.

The role of inflammation and particularly mononuclear phagocytes in the pathogenesis of CNV has been a topic of great interest for several decades. Mast cells are tissue-resident immune cells that play a significant role in defense against pathogens and diseases [7]. Mast cells are prevalent in vascularized tissues and in locations directly exposed to external environments [8]. Upon activation, mast cells release a spectrum of pre-stored or *de novo* generated mediators. These include biogenic amines, an array of serine and other proteases, lysosomal enzymes, cytokines, chemokines, growth factors, and lipid mediators [9, 10, 11]. Mast cells are commonly linked to conditions like asthma, allergies, and anaphylaxis [12]. But their role goes beyond these illnesses. These cells play a fundamental role in the immune system, with their evolutionarily preserved ability to act as first responders in recognizing pathogens and signs of infection contributing to both innate and adaptive immune responses [13]. There is increasing evidence that mast cells influence a wide spectrum of diseases, such as mastocytosis, chronic pain, cancer, cardiovascular, and neurodegenerative diseases [14, 15, 16, 17]. In the eye, mast cells have been observed in varying amounts in the uvea, displaying a specific distribution pattern in the choroid, ciliary body, and iris [18, 19, 20]. Importantly, there is a marked increase in mast cell numbers and degranulation in the choroid in vasoproliferative AMD [21], but the mechanisms implicated in the development of CNV remain poorly characterized. In the present study, we investigated the contribution of mast cells to CNV.

Materials and Methods

Animals

All animal experiments were approved by the Maisonneuve Rosemont Hospital Animal Care Committee and were performed in accordance with the Association for Research in Vision and Ophthalmology Statement for the Use of Animals in Ophthalmic

and Visual Research. Adult C57BL/6J and $Kit^{W\text{-}sh/W\text{-}sh}$ (Stock #030764) mice of age 10 to 12 weeks were purchased from Jackson Laboratory (strain 30764); these mice do not harbor rd1 or rd8 mutations. The animals were housed and maintained at local animal facilities under a 12-h light/dark cycle (100–200 lux) with water and normal diet food available ad libitum.

Laser-Induced CNV

Mice were anesthetized with an intraperitoneal injection of a mix of ketamine (100 mg/kg) and xylazine (20 mg/kg). Corneas were anesthetized with proxymetacaine hydrochloride (0.5% Alcaine; Alcon, Fort Worth, TX, USA) and pupils dilated with 0.5% atropine (Alcon, Fort Worth, TX, USA). Argon laser photocoagulation (50 μm, 400 mW, 0.05 seconds) was utilized to rupture the Bruch's membrane. Burns were induced at four locations per eye around the optic nerve. Mice were randomly grouped to receive intraperitoneal injections of ketotifen fumarate (25 mg/kg), tryptase inhibitor APC 366 (5 mg/kg), or vehicle. Ketotifen was administered starting 48 hours before the laser burn and continued daily until the day before sacrifice. APC 366 was administered starting on the day of the laser burn and continued daily until the day before sacrifice. Mice were euthanized and eyes enucleated at different time points after laser photocoagulation.

Fundus fluorescein angiography

Fluorescein angiography was performed using a scanning laser ophthalmoscope (Micron IV; Phoenix Laboratories, Pleasanton, CA, USA). Pupils were dilated with 0.5% atropine (Alcon, Fort Worth, TX, USA) and mice were euthanized. Fluorescein (Alcon) was administered intraperitoneally at a dose of 1 unit/gram of body weight using a 5% fluorescein dilution in 0.9% sodium chloride solution. Images were taken 5 min after fluorescein administration. A computer-assisted method was used to quantify fluorescence intensity using ImageJ software. The intensity of basal level of fluorescence in nonleakage areas was used as background fluorescence. After deduction of background signals, the total intensity of fluorescence contributed by the leaked fluorescein was used to represent the leakage. Mice injected with fluorescein were not further processed for imaging using the green channel.

Immunohistochemistry

Eyes were fixed in 4% paraformaldehyde (PFA) for 1 h and then rinsed twice with phosphate-buffered saline (PBS). The neuroretina was carefully separated from the retinal pigmented epithelium (RPE)/choroid/sclera complex which was processed for immunostaining. The RPE/choroid complex was incubated at room temperature for 1 h with a blocking solution consisting of 1% bovine serum albumin (BSA), 1% normal goat serum, 0.1% Triton X-100, and 0.05% Tween-20 in PBS. The RPE/choroid complex was then stained with 1:100 FITC-labeled isolectin (Vector Lab; FL-1201), rhodamine-labeled isolectin (Vector Lab; #RL-1102), 1:200 rhodamine phalloidin (Cedarlane Laboratories), 1:100 tryptase (ThermoFisher: #PA5-119480), or 1:400 fluorescein-conjugated Avidin D (Vector Lab; #A-2001-5) overnight. Subsequently, they were washed thrice the next day before being stained with the secondary antibody. Cell nuclei were stained with 4′,6-diamidino-2-phenylindole (DAPI) (1:5000; Sigma-Aldrich). Labeled flat mounts were examined using the same settings with a laser scanning confocal microscope (Leica Stellaris 8), across all experiments.

Isolation of peritoneal mast cells

Peritoneal mast cells (PMCs) were isolated from 8-week-old C57 mice. 3 mL of cold PBS and 2 mL of air were injected into the peritoneal cavity using a 27-gauge needle. After 2 minutes of gently massage of the peritoneum, a 25-gauge needle was inserted into the peritoneal cavity to collect the fluid while carefully avoiding contamination with blood. Cells were isolated by centrifugation (500 g for 5 min) and resuspended in Roswell Park Memorial Institute (RPMI) 1640 medium (A1049101, Thermo Fisher) supplemented with glutamine, interleukin (IL)-3 (10 ng/mL), stem cell factor (30 ng/mL), 10% fetal bovine serum (FBS) and 1% penicillin/streptomycin. The culture medium was renewed every 2 days for 1 week. Immunophenotyping of PMCs was performed by flow cytometry analysis using antibodies against mast cell surface markers CD117 (Biolegend; #105827) and FcεR-1α (Biolegend; #134306). Flow cytometry was conducted on a BD LSRFortessa X-20, and data were analyzed using FlowJo software (Supp Fig. 1A). PMCs were treated

or not with compound 48/80 (Sigma) at 20 µM for 30 min. The culture medium was then centrifuged, and the supernatant served as conditioned media.

Isolation of bone marrow-derived mast cells

Bone marrow-derived mast cells (BMDMC) were harvested from C57BL/6 mice aged 8 weeks, euthanized via cervical dislocation. In brief, bone marrow cells were obtained from the femurs and tibias of mice and flushed using RPMI 1640. Following collection, the medium was centrifuged at 1200 rpm for five minutes at ambient temperature. After discarding the supernatant, the cell pellet was resuspended in new medium and subjected to another centrifugation at the same conditions. The resultant pellet was then resuspended in RPMI 1640 supplemented with 2 mM L-glutamine, 0.07% β-mercaptoethanol, 10 mM HEPES, 10% fetal calf serum (Wisent Bioproducts #085-150), 1% antibiotics (penicillin and streptomycin), and 30 ng/mL of recombinant mouse interleukin-3 (R&D Systems #403-ML). This cell suspension was strained through 40 µm sterile filters (Corning #352340) and placed in petri dishes. Cultured at 37°C with 5% CO2 in a humidified incubator, the medium was refreshed biweekly through gentle centrifugation. Six weeks later, BMDMCs were fully differentiated. The purity of the population was determined by flow cytometric analysis. Cells were stained with antibodies against CD117 (Biolegend; #105827) and FcεR-1α (Biolegend; #134306). Flow cytometry was performed on a BD LSRFortessa X-20, and data were analyzed using FlowJo software (Supp Fig. 1B). Cells were collected, and then suspended in baseline RPMI 1640 medium to a density of $1x10^7$ cells per 200 µl. These cells were administered intravenously at a dose of 200 µl into four-week-old $Kit^{W\text{-}sh/W\text{-}sh}$ mice.

Treatment of choroidal explants

Choroidal explants were obtained from 6-week-old mice. The choroidal explants were prepared according to a previously described procedure [22]. Briefly, mice eyes were dissected in a Petri dish containing Hank's balanced salt solution (HBSS; 02-0121-0500; VWR, QC, Canada). The eyes were dissected below the ora serrata to remove the lens and cornea and the neuroretina was carefully removed. The complexes formed by RPE-choroid-sclera were then collected, cut in 16 explant fragments, and plated on

Matrigel (BD biosciences) in 24-well plates. Choroidal explants were cultured at 37°C in 5% CO_2 for 4 days in endothelial cell growth basal medium (EBM-2) supplemented with Microvascular Endothelial SingleQuots kit (EGM-2MV; respectively, CC-3156 and CC-4147; Lonza Bioscience, Basel, Switzerland). Explants were stimulated (at day 1 and day 3) with conditioned media of peritoneal mast cells activated with compound 48/80 or tryptase and imaged at day 4. Quantification of sprouting area was performed using ImageJ software analysis.

Preparation of anti-CD31 antibody coated magnetic beads

Sheep anti-rat Dynabeads (Dynal Biotech) were washed three times with serum-free DMEM (Dulbecco's Modified Eagle's Medium; Invitrogen) and then incubated with rat anti-mouse CD31 monoclonal antibody MEC13.3 (BD Pharmingen) overnight at 4°C. Following incubation, beads were washed three times with DMEM containing 10% fetal bovine serum (FBS) and resuspended in the same medium, and stored at 4°C.

Isolation and culture of choroidal endothelial cells

Twelve eyes of 4-week-old pups (C57BL/6) were enucleated, and the RPE/Choroid/sclera complex was dissected under a stereoscopic microscope in cold DMEM. Each isolation used a litter of 6 pups, resulting in 12 RPE/Choroid/sclera complexes pooled together. These complexes were rinsed with DMEM and minced into small pieces in a tissue culture dish using sterile stainless steel surgical blades. Small pieces of tissue were digested in 5 mL of collagenase type I (1 mg/mL in serum-free DMEM for 45 min at 37°C. After digestion, DMEM supplemented with 10% FBS was added to stop collagenase activity and the cells were then filtered through a double layer of sterile 40 mm nylon mesh (Fisher Scientific) and centrifuged at 500 x g for 10 min to settle the cells. Then, cells were washed twice with DMEM containing 10% FBS. The cells were resuspended in 1 mL medium (DMEM with 10% FBS) and incubated with sheep anti-rat magnetic beads precoated with anti-CD31 as described above. After affinity binding, magnetic beads were washed 6 times with DMEM with 10% FBS and bound cells in endothelial cell growth medium were plated into a single well of a 24-well plate pre-coated with 2 mg/mL of attachment factor (Life Technologies). Endothelial cells were

grown in DMEM containing 10% FBS, 2 mM L-glutamine, 2 mM sodium pyruvate, 20 mM HEPES, 1% non-essential amino acids, 1% streptomycin/ penicillin, 55 U/mL freshly added heparin (Sigma), and 100 mg/mL endothelial growth supplement (Sigma). Cells were maintained in an incubator at 37°C and with 5% CO_2. Cells were progressively propagated in attachment factor-coated 60 mm dishes and used in early passages (3-5) for our experiments.

Scratch-wound assay

Confluent choroidal endothelial cells were grown in 6-well plates. Cells were starved 18 h in EBM-2 medium with 1% FBS. A horizontal wound was created using a sterile 200 µl pipette tip. The cells were washed with EBM2 at 37°C and incubated in PMC conditioned media or EBM-2 supplemented recombinant tryptase. Pictures of scratch wounds were taken just before stimulation (time 0) and after 24 h. Migration % was calculated using ImageJ software.

Tubule formation assay

Choroidal endothelial cells were plated at a density of 30,000 cells/well in 96-well plates precoated with 50 µL of growth factor-reduced Matrigel Matrix (Fisher Scientific, New Hampshire, USA) and cultured at 37°C for 6 h in complete endothelial growth medium. Capillary-like tubes were observed under a light microscope. Images were obtained at 10X magnification. In each well, images were taken from four random fields. Tubes and branching point were counted.

RNA-seq sample preparation, sequencing, and analysis

Total RNA was extracted from the RPE/choroid complex of C57BL6 mice, including both CNV eyes at day 3 post laser burn, and age-matched control eyes (not subjected to laser burn). RNA extraction was performed using RNeasy Mini Kit (QIAGEN) according to the manufacturer's protocol. RNA was quantified using Qubit (Thermo Scientific) and quality was assessed with the 2100 Bioanalyzer (Agilent Technologies). Transcriptome libraries were generated using the KAPA RNA HyperPrep (Roche) using a poly-A selection (Thermo Scientific). Sequencing was performed on the Illumina NextSeq500,

obtaining around 25M single-end 75bp reads per sample. Sequences were trimmed for sequencing adapters and low-quality 3' bases using Trimmomatic (version 0.35) and aligned to the reference mouse genome version GRCm38 (gene annotation from Gencode version M23, based on Ensembl 98) using STAR version 2.7.1a. Gene expressions were obtained as read counts directly from the STAR output and also computed transcript-level expressions via RSEM, generating normalized values in transcripts per million (TPM) for these stranded RNA libraries. DESeq2 (version 1.22.2) was used to normalize gene read counts which allowed the hierarchical clustering of samples based on normalized log-transformed read counts. Additionally, principal component analysis was used to elucidate the two most significant components. Genes were sorted by adjusted p-values. Significant differentially expressed genes (DEGs) were defined as those with padj lower than 0.05.

Gene set enrichment analysis

The gene set enrichment analysis (GSEA) was carried out using GSEA software version 4.3.3, developed by the Broad Institute affiliated with both MIT and Harvard University. Selected gene sets were retrieved from the catalog of the Molecular Signature Database, which provides functionally annotated gene sets. For the analysis, the phenotype was subjected to 1,000 permutations, and the distinction between CNV versus control was used to define the phenotype label. Gene sets containing fewer than 15 or more than 500 genes were not included in the study. The analysis employed a weighted p2 statistic to identify significant genes, and a t-test was used as the metric to differentiate the classes.

GO pathway enrichment analysis

Gene ontology (GO) pathway enrichment analysis was performed using EnrichR Classification System. The top 100 up-regulated genes of CNV compared with control were used.

Collagen hybridizing peptide (CHP) binding

CHP binding was performed according to manufacturer's instructions. A solution containing 15 μM of 5-FAP-CHP (3Helix) in PBS was heated at 80 °C for 5 min, and immediately cooled down to room temperature in an ice/water bath. The quenched CHP solution was quickly added onto the RPE/choroid complex. The RPE/choroid complex was incubated with the quenched CHP solution overnight at 4°C and then washed. It was subsequently incubated with the TrueView Autofluorescence Quenching Kit (Vector; SP-8400-15) for 5 minutes at room temperature to reduce autofluorescence. The RPE/choroid complex was washed and flat-mounted onto glass slides with coverslips and Fluoro-Gel mounting medium (Electron Microscopy Sciences, Hatfield, PA).

Statistical analysis

Data are presented as mean ± standard error of the mean (SEM). Student's t-test was used to compare two different groups. Additionally, a one-way analysis of variance (ANOVA) was conducted, followed by post hoc Holm-Sidak tests for comparison of means. A p-value < 0.05 was considered statistically significant.

Results

Mast cells promote choroidal endothelial cell sprouting angiogenesis and migration

To assess the proangiogenic role of mast cells, we used different models of angiogenesis *ex-vivo* and *in vitro*. First, we used a reproducible *ex-vivo* choroidal sprouting assay as a model of choroidal microvascular proliferation [22]. Mouse choroidal explants were treated with conditioned medium from compound 48/80-stimulated peritoneal mast cells for 24 hours; peritoneal mast cells display properties akin to connective tissue mast cells as found in choroid [23]. C48/80 had negligible effect on choroidal sprouting likely because of the heterogeneous distribution of tissue-resident mast cells [24]. In contrast, treatment with conditioned medium from compound 48/80-stimulated peritoneal mast cells resulted in a marked increase in choroidal sprouting (Fig. 1A, B). Compound 48/80-stimulated peritoneal mast cells also

accelerated choroidal endothelial cell migration using a scratch assay (Fig. 1C, D) and enhanced tubulogenesis (Fig. 1E-G).

Mast cell deficiency (and stabilization) precludes choroidal neovascularization

Given the observed proangiogenic effects of mast cells on choroidal endothelial cells, both *in vitro* and *ex vivo*, we sought to determine their potential influence on CNV *in vivo*. Mast cells and their products are known to be present in sufficient quantities to exert substantial effects on physiological, immunological, and inflammatory responses in the choroid [25]. Following laser burn (as depicted in Fig. 2A), an increase in the number of mast cells undergoing degranulation (Avidin D) was observed in choroidal flat mounts co-stained with lectins (vessel marker red; Fig. 2B). Mast cells were predominantly located at the CNV site (confirmed by z-stack analysis) on day 1 and furthermore on day 3 post-burn (Fig 2. B), and subsided by day 7.

The role of mast cells was ascertained in choroidal neovascularization, using mast cell deficient-$Kit^{W\text{-}sh/W\text{-}sh}$ mice. Following laser burn, we assessed the formation of new vessels using lectin (green) staining on RPE/choroidal flat mounts. $Kit^{W\text{-}sh/W\text{-}sh}$ mice showed a marked decrease in CNV size on day 7 after laser injury (Fig 2C, D); this decrease in CNV was prevented by mast cell replenishment upon systemic injection of BMDMCs.

We further determined the role of mast cells by pharmacologically stabilizing them. Pre-treatment of mice subjected to laser burn with mast cell stabilizer ketotifen fumarate revealed a marked decrease in CNV size 7 days after laser impact (Fig. 2E-G). We also evaluated vascular permeability using fundus fluorescein angiography at the same interval. Ketotifen lessened the extent of vascular leakage at day 7 post-laser burn (Fig. 2H, I). Collectively, our findings using genetic and pharmacologic approaches reveal that mast cells contribute to the extent of CNV.

Mast cell tryptase promote pathological angiogenesis in the choroid

Next, we evaluated mast cell-derived tryptase as a critical pro-angiogenic agent in promoting CNV. Tryptase, a prominent protease present in mast cell granules, is a classic indicator of mast cell activation [26], and a potent angiogenic factor [27] upregulated in

the choroid of AMD patients [28]. To explore the potential contribution of tryptase in choroidal angiogenesis, we treated choroidal endothelial cells with two different doses of mouse tryptase, mMCPT6 (100 and 1000 ng/mL), and subsequently performed migration and tube formation assays. Both doses of mMCPT6 promoted endothelial cell migration (Fig. 3A, B) and tubulogenesis (Fig. 3C-E). Coherently, mMCPT6 increased choroidal sprouting *ex vivo* compared to control (Fig. 3F, G). As expected, we detected a substantial increase in tryptase-positive cells on day 3 post-laser burn (Fig. 3H), corroborating with clinical observations in AMD [29]. To validate *in vivo* the proangiogenic role of tryptase, we found that the tryptase inhibitor, APC 366, significantly reduced CNV lesion size by day 7 post-laser burn (Fig. 3I-K).

Mast cells promote ECM remodelling

Finally, to elucidate the cellular processes that are associated with mast cell activation, we conducted a comprehensive and unbiased transcriptomic analysis on the RPE/choroid complex 3 days after laser burn. GSEA revealed a significant correlation in clusters of mast cell activation (normalized enrichment score [NES], 1.59; false discovery rate [FDRq], 0.005), collagen catabolism (NES, 1.57; FDRq, 0.007), and ECM organization (NES, 1.56; FDRq, 0.032) (Fig. 4A). Gene ontology (GO) enrichment analysis of the top upregulated genes in laser burns (relative to control) uncovered ECM remodeling and innate immune response pathways (Fig. 4B, C). Consistent with these observations, increased CHP binding was observed in the choroidal tissue of submacular sections of individuals at high genetic risk for developing AMD and in those with AMD [29]. To assess if mast cells promote pathological collagen deposition and dysfunctional ECM synthesis in choroidal neovascularization, we used CHP to assess collagen turnover - an indicator of ECM remodelling; CHP is a short amino acid sequence that has a high affinity for denatured collagen, typically found in damaged or remodeling tissues, by triple helix hybridization [30]. Compared to wild-type animals CHP binding on day 7 post-laser burn to eyes was decreased in $Kit^{W\text{-}sh/W\text{-}sh}$ mice and restored by mast cell reconstitution (Fig. 4D, E), indicative of a pivotal role for mast cells in collagen remodeling.

Discussion

Chronic inflammation is recognized as a key contributor in the development and progression of CNV. In this context, the choroid in AMD patients emerges as an inflammatory milieu where macrophages and mast cells become more abundant [21, 31]. Prior findings have provided evidence that activated mast cells can influence choroidal function, particularly by increasing vasodilation and vascular permeability [32]. Mast cells also induce angiogenesis and have been shown to be present around the Bruch's membrane in both the early and late stage of CNV [21]. In this regard, we reveal that following laser burn induction, there is a rapid activation and migration of tissue resident mast cells to the site of injury highlighting the potential of mast cells as early initiators in CNV pathogenesis. Furthermore, mast cells clearly promoted choroidal endothelial cell migration and vessel sprouting *ex vivo* in choroidal explants. The proangiogenic role of mast cells was revealed in experiments with mast cell-deficient $Kit^{W\text{-}sh/W\text{-}sh}$ mice as well as using a pharmacologic stabilizer of mast cells, ketotifen fumarate. Importantly, when mast cells were reconstituted, the extent of CNV was readily exacerbated. Interestingly, in the context of resistance against VEGF-based therapy, often seen in some AMD patients, mast cells have been identified to confer this resistance in tumorigenesis [33]. A high level of granzyme B immunoreactivity was observed in the choroid of AMD donor eyes [34], correlating with its role in enhancing choroidal angiogenesis [35]. Thus, mast cells should be considered an important therapeutic target in AMD subjects.

A key feature of our work applies to secreted factors from mast cells. A myriad of mediators such as histamines, lipid mediators, cytokines, and chemokines are released by mast cells upon activation. We clearly found that cell media from activated mast cells induced endothelial cell migration, tubulogenesis, and neovascularization, consistent with evidence of bioactive secreted factors. Relevantly, in individuals with a high genetic predisposition for AMD, mast cell protease levels were found to be augmented [29]. Among them, tryptase stood out with the most pronounced expression. As high-risk patients progressed to AMD, there was a steady increase in tryptase levels [29]. Interestingly, tryptase has also been shown to be associated with pathological retinal neovascularization in other vasoproliferative retinopathies [36]. In support of these findings, we demonstrated that tryptase was able to promote choroidal endothelial cell

migration and choroidal sprouting *ex vivo*; conversely, the selective mast cell tryptase inhibitor, APC 366 was able to reduce CNV lesion size in the laser impact model of AMD by reversing these endothelial proliferative effects *in vivo*. Collectively, these results suggest that suppression of mast cell activity should be considered as a possible therapeutic option to prevent pathological neovascularization in ocular disorders.

As part of the proliferative influence of mast cells on the endothelium, the CHP binding assay revealed that mast cells influence ECM composition. During angiogenesis, endothelial cells need to migrate across the ECM and the basement membrane, which pose as physical barriers. Matrix metalloproteases and other enzymes facilitate this process by degrading the ECM components, thereby allowing the migrating endothelial cells to invade the surrounding tissue and establish new vascular structures [37]. Moreover, the significance of ECM extends to the modulation of angiogenesis. Components of ECM can sequester a reservoir of growth factors such as VEGF and fibroblast growth factor (FGF) that can be released upon degradation of the ECM [38, 39]. Our findings showed that ECM remodeling is an important event during CNV and that mast cells promote pathological collagen deposition and dysfunctional ECM synthesis. Interestingly, genetic variants of the ECM have been associated with AMD [40]. Mast cells, known for their impact on tissue remodeling, can influence ECM directly through their proteolytic enzymes or by activating ECM-degrading enzymes such as matrix metalloproteinases (MMPs) [41]. Bruch's membrane, a complex network located between the RPE and the choriocapillaris, is mainly composed of various types of collagens, fibronectin, laminin, and proteoglycans [42]. Therefore, choroidal mast cells can rupture Bruch's membrane and basement membrane, allowing the advancement of choroidal blood vessels toward the RPE and subretina; ultimately resulting in edema, hemorrhage, and fibrosis.

Limitations of this study applies to models of age-related macular degeneration. In this study we conducted our work on 10-12 week old mice to uncover the role of mast cells in CNV; the approach of using 10-12 week old mice was mostly based on practicality. Exploring the role of mast cells in older animals would provide a complementary dimension to this work, as more severe CNV is expected in older subjects [43]. Moreover, although the laser-burn induced CNV does not reflect the human condition of

vasoproliferative age-related macular degeneration, it is the model most used in this context and thus contributes to the broader understanding of CNV pathogenesis and the development of novel treatment strategies for wet AMD.

In summary this study illustrates the profound impact of mast cells in promoting CNV and ECM remodeling; a model depicting mast cell role in CNV is shown in Fig. 5. Laser burn induces damage to the RPE leading to its degeneration, resulting in massive mast cell recruitment and activation. Local mast cell degranulation induces ocular inflammation and tryptases activation that cause damage to neighboring cells or an angiogenic response resulting in choroidal pathological neovascularization. Pharmacological inhibition of mast cell degranulation or their secreted factors could pave the way for beneficial therapeutic interventions for AMD patients that complement current anti-VEGF treatments.

References

1. Mitchell P, Liew G, Gopinath B, Wong TY. Age-related macular degeneration. Lancet. 2018;392(10153):1147-59.
2. Wong WL, Su X, Li X, Cheung CM, Klein R, Cheng CY, et al. Global prevalence of age-related macular degeneration and disease burden projection for 2020 and 2040: a systematic review and meta-analysis. Lancet Glob Health. 2014;2(2):e106-16.
3. Maberley D. Pegaptanib for neovascular age-related macular degeneration. Issues Emerg Health Technol. 2005(76):1-4.
4. Grunwald JE, Daniel E, Huang J, Ying GS, Maguire MG, Toth CA, et al. Risk of geographic atrophy in the comparison of age-related macular degeneration treatments trials. Ophthalmology. 2014;121(1):150-61.
5. Grunwald JE, Pistilli M, Daniel E, Ying GS, Pan W, Jaffe GJ, et al. Incidence and Growth of Geographic Atrophy during 5 Years of Comparison of Age-Related Macular Degeneration Treatments Trials. Ophthalmology. 2017;124(1):97-104.
6. Daniel E, Toth CA, Grunwald JE, Jaffe GJ, Martin DF, Fine SL, et al. Risk of scar in the comparison of age-related macular degeneration treatments trials. Ophthalmology. 2014;121(3):656-66.

7. Galli SJ, Gaudenzio N, Tsai M. Mast Cells in Inflammation and Disease: Recent Progress and Ongoing Concerns. Annu Rev Immunol. 2020;38:49-77.
8. Grimbaldeston MA, Metz M, Yu M, Tsai M, Galli SJ. Effector and potential immunoregulatory roles of mast cells in IgE-associated acquired immune responses. Curr Opin Immunol. 2006;18(6):751-60.
9. Moon TC, Befus AD, Kulka M. Mast cell mediators: their differential release and the secretory pathways involved. Front Immunol. 2014;5:569.
10. Mukai K, Tsai M, Saito H, Galli SJ. Mast cells as sources of cytokines, chemokines, and growth factors. Immunol Rev. 2018;282(1):121-50.
11. Theoharides TC, Alysandratos KD, Angelidou A, Delivanis DA, Sismanopoulos N, Zhang B, et al. Mast cells and inflammation. Biochim Biophys Acta. 2012;1822(1):21-33.
12. Galli SJ, Tsai M. IgE and mast cells in allergic disease. Nat Med. 2012;18(5):693-704.
13. Abraham SN, St John AL. Mast cell-orchestrated immunity to pathogens. Nat Rev Immunol. 2010;10(6):440-52.
14. Varricchi G, de Paulis A, Marone G, Galli SJ. Future Needs in Mast Cell Biology. Int J Mol Sci. 2019;20(18).
15. Jones MK, Nair A, Gupta M. Mast Cells in Neurodegenerative Disease. Front Cell Neurosci. 2019;13:171.
16. Valent P, Akin C, Sperr WR, Horny HP, Arock M, Metcalfe DD, et al. New Insights into the Pathogenesis of Mastocytosis: Emerging Concepts in Diagnosis and Therapy. Annu Rev Pathol. 2023;18:361-86.
17. Gupta K, Harvima IT. Mast cell-neural interactions contribute to pain and itch. Immunol Rev. 2018;282(1):168-87.
18. Lanzieri M, Cricchi M. Mast Cells and Vessels of the Choroid of Albino Guinea Pigs during the Uveal Anaphylactic Reaction. Arch Ophthalmol. 1965;74:367-70.
19. Larsen G. The mast cells in the uveal tract of the eye and changes induced by hormones and avitaminosis-C. Am J Ophthalmol. 1959;47(1 Pt 2):509-19.
20. McMenamin PG. The distribution of immune cells in the uveal tract of the normal eye. Eye (Lond). 1997;11 (Pt 2):183-93.

21. Bhutto IA, McLeod DS, Jing T, Sunness JS, Seddon JM, Lutty GA. Increased choroidal mast cells and their degranulation in age-related macular degeneration. Br J Ophthalmol. 2016;100(5):720-6.
22. Shao Z, Friedlander M, Hurst CG, Cui Z, Pei DT, Evans LP, et al. Choroid sprouting assay: an ex vivo model of microvascular angiogenesis. PLoS One. 2013;8(7):e69552.
23. Akula S, Paivandy A, Fu Z, Thorpe M, Pejler G, Hellman L. How Relevant Are Bone Marrow-Derived Mast Cells (BMMCs) as Models for Tissue Mast Cells? A Comparative Transcriptome Analysis of BMMCs and Peritoneal Mast Cells. Cells. 2020;9(9).
24. Zaitoun IS, Song YS, Zaitoun HB, Sorenson CM, Sheibani N. Assessment of Choroidal Vasculature and Innate Immune Cells in the Eyes of Albino and Pigmented Mice. Cells. 2022;11(20).
25. Godfrey WA. Characterization of the choroidal mast cell. Trans Am Ophthalmol Soc. 1987;85:557-99.
26. Schwartz LB, Metcalfe DD, Miller JS, Earl H, Sullivan T. Tryptase levels as an indicator of mast-cell activation in systemic anaphylaxis and mastocytosis. N Engl J Med. 1987;316(26):1622-6.
27. Blair RJ, Meng H, Marchese MJ, Ren S, Schwartz LB, Tonnesen MG, et al. Human mast cells stimulate vascular tube formation. Tryptase is a novel, potent angiogenic factor. J Clin Invest. 1997;99(11):2691-700.
28. McLeod DS, Bhutto I, Edwards MM, Gedam M, Baldeosingh R, Lutty GA. Mast Cell-Derived Tryptase in Geographic Atrophy. Invest Ophthalmol Vis Sci. 2017;58(13):5887-96.
29. McHarg S, Booth L, Perveen R, Riba Garcia I, Brace N, Bayatti N, et al. Mast cell infiltration of the choroid and protease release are early events in age-related macular degeneration associated with genetic risk at both chromosomes 1q32 and 10q26. Proc Natl Acad Sci U S A. 2022;119(20):e2118510119.
30. Li Y, Yu SM. Targeting and mimicking collagens via triple helical peptide assembly. Curr Opin Chem Biol. 2013;17(6):968-75.
31. McLeod DS, Bhutto I, Edwards MM, Silver RE, Seddon JM, Lutty GA. Distribution and Quantification of Choroidal Macrophages in Human Eyes With Age-Related Macular Degeneration. Invest Ophthalmol Vis Sci. 2016;57(14):5843-55.

32. Bousquet E, Zhao M, Thillaye-Goldenberg B, Lorena V, Castaneda B, Naud MC, et al. Choroidal mast cells in retinal pathology: a potential target for intervention. Am J Pathol. 2015;185(8):2083-95.
33. Wroblewski M, Bauer R, Cubas Cordova M, Udonta F, Ben-Batalla I, Legler K, et al. Mast cells decrease efficacy of anti-angiogenic therapy by secreting matrix-degrading granzyme B. Nat Commun. 2017;8(1):269.
34. Matsubara JA, Tian Y, Cui JZ, Zeglinski MR, Hiroyasu S, Turner CT, et al. Retinal Distribution and Extracellular Activity of Granzyme B: A Serine Protease That Degrades Retinal Pigment Epithelial Tight Junctions and Extracellular Matrix Proteins. Front Immunol. 2020;11:574.
35. Obasanmi G, Uppal M, Cui JZ, Xi J, Ju MJ, Song J, et al. Granzyme B degrades extracellular matrix and promotes inflammation and choroidal neovascularization. Angiogenesis. 2024.
36. Matsuda K, Okamoto N, Kondo M, Arkwright PD, Karasawa K, Ishizaka S, et al. Mast cell hyperactivity underpins the development of oxygen-induced retinopathy. J Clin Invest. 2017;127(11):3987-4000.
37. Kalluri R. Basement membranes: structure, assembly and role in tumour angiogenesis. Nat Rev Cancer. 2003;3(6):422-33.
38. Hynes RO. The extracellular matrix: not just pretty fibrils. Science. 2009;326(5957):1216-9.
39. Kessenbrock K, Plaks V, Werb Z. Matrix metalloproteinases: regulators of the tumor microenvironment. Cell. 2010;141(1):52-67.
40. Fritsche LG, Igl W, Bailey JN, Grassmann F, Sengupta S, Bragg-Gresham JL, et al. A large genome-wide association study of age-related macular degeneration highlights contributions of rare and common variants. Nat Genet. 2016;48(2):134-43.
41. Kovanen PT. Mast cells and degradation of pericellular and extracellular matrices: potential contributions to erosion, rupture and intraplaque haemorrhage of atherosclerotic plaques. Biochem Soc Trans. 2007;35(Pt 5):857-61.
42. Bhutto I, Lutty G. Understanding age-related macular degeneration (AMD): relationships between the photoreceptor/retinal pigment epithelium/Bruch's membrane/choriocapillaris complex. Mol Aspects Med. 2012;33(4):295-317.

43. Espinosa-Heidmann DG, Suner I, Hernandez EP, Frazier WD, Csaky KG, Cousins SW. Age as an independent risk factor for severity of experimental choroidal neovascularization. Invest Ophthalmol Vis Sci. 2002;43(5):1567-73.

Ethics declarations

Ethics approval

Animal studies were approved by the Maisonneuve Rosemont Hospital Animal Care Committee in accordance with the guidelines of the Canadian Council on Animal Care. Experiments were conducted in accordance with the Association for Research in Vision and Ophthalmology (ARVO) Statement for the Use of Animals in Ophthalmic and Visual Research.

Availability of data and materials

The data sets generated during the current study are available from the corresponding author on reasonable request.

Competing interests

The authors declare no competing interests.

Acknowledgement

This study was funded by the Canadian Institutes of Health Research (CIHR) 950-231837 (SC). RD is supported by Fonds de Recherche du Québec-Santé (FRQS). PA is supported by CIHR, FRQS, The Vision Health Research Network, and FROUM. SC holds a Canada Research Chair (Vision Science) and the Leopoldine Wolfe Chair in translational research in age-related macular degeneration.

Author contributions

R.D. conceptualized and designed the study. R.D. and P.A. planned and carried out experiments and analyzed the data. J.C.R. provided technical assistance. R.D. and P.A. wrote the manuscript. S.C. and J.C.R. edited the manuscript.

Funding

This study was funded by the Canadian Institutes of Health Research (CIHR). RD is supported by Fonds de Recherche du Québec-Santé (FRQS). PA is supported by CIHR, FRQS, The Vision Health Research Network, and FROUM.

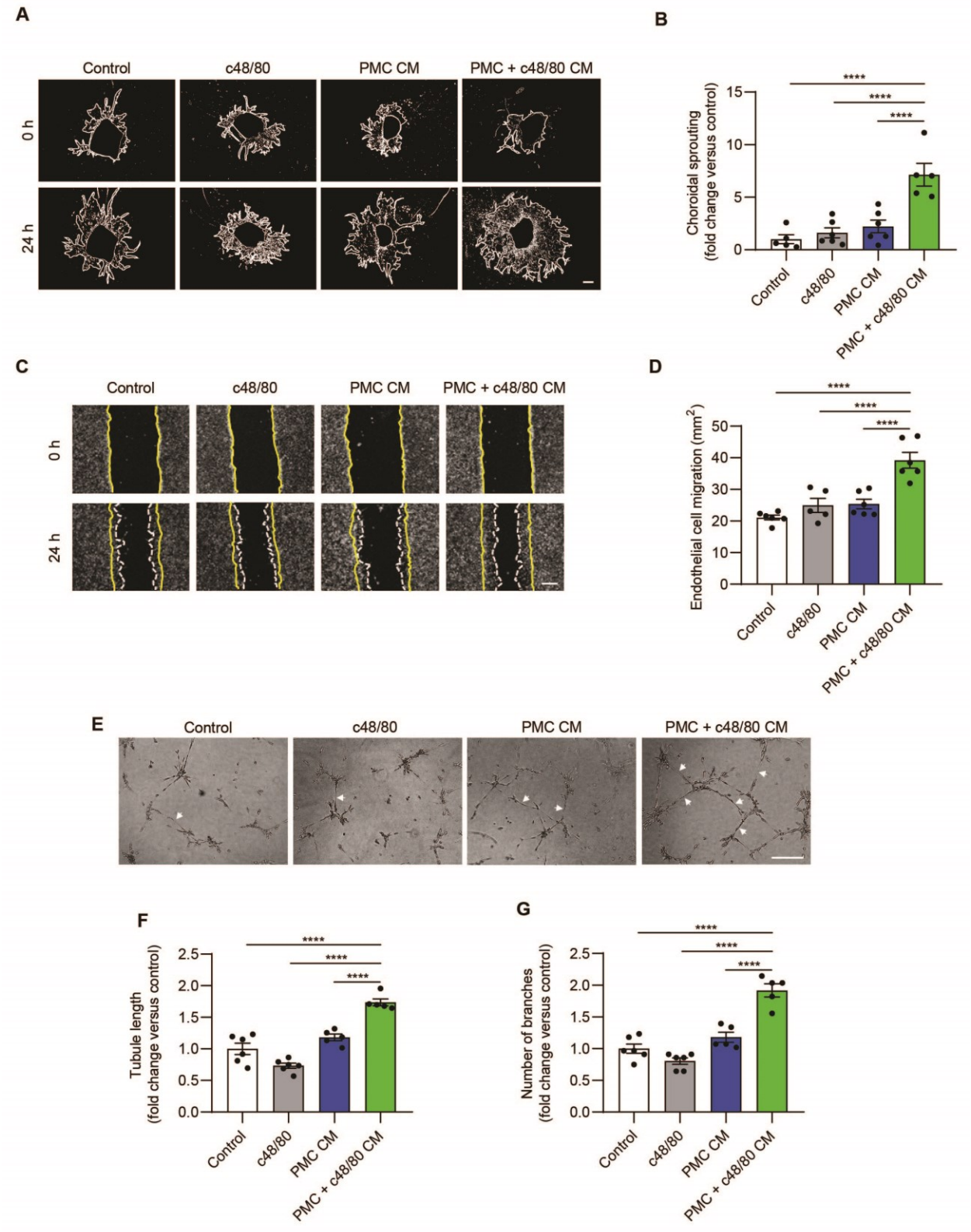

Figure 1. Effects of mast cells on choroidal angiogenesis. A Representative image of choroidal explants cultured in the presence or absence of peritoneal mast cells (PMCs)

treated or not with mast cell degranulator compound 48/80 (c48/80). Scale bar: 500 µm. B Graph representing the quantification of sprouting surface area (n = 5-6). Statistical analyses were performed using one-way ANOVA. ***p < 0.001, ****p < 0.0001. C Effects of mast cells on scratch wound migration after 24 h. Scale bar: 500 µm. D Quantification of wound closure (n = 5-6). Statistical analyses were performed using one-way ANOVA. ****p < 0.0001. E Effects of mast cells on tubulogenesis as assessed in choroidal endothelial cells cultured in Matrigel. The arrows point to the tube-like structures. Scale bar: 500 µm. Quantification of the length of tubules (F) and the number of branches (G) (n = 5-6). Statistical analyses were performed using one-way ANOVA. ****p < 0.0001. The control group contains control media without any additives. C48/80 Treatment: media containing C48/80. PMC CM: Conditioned media derived from untreated PMCs. PMC + C48/80 CM: Conditioned media derived from C48/80-stimulated PMCs.

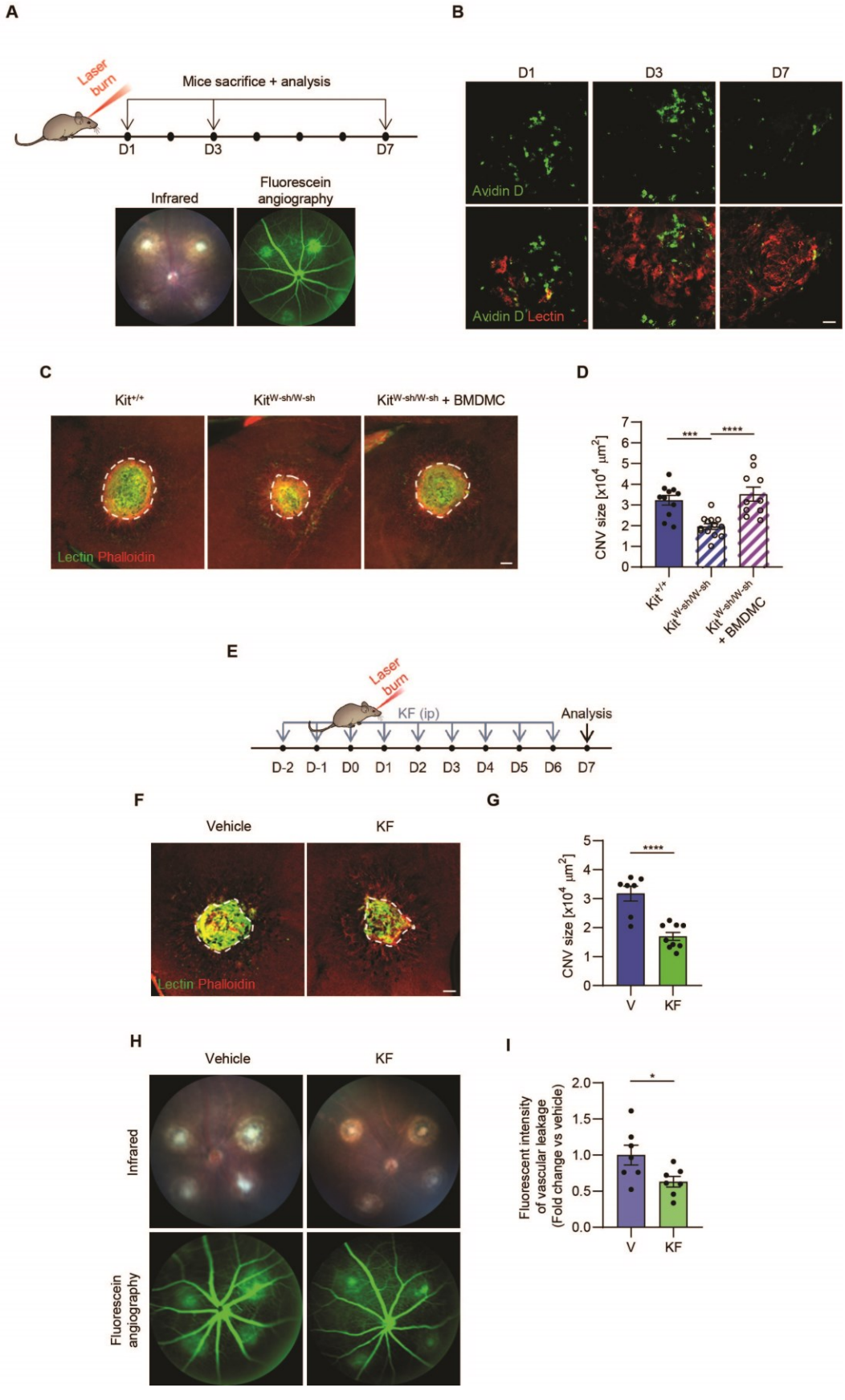
A
Laser burn
Mice sacrifice + analysis
D1
D3
D7
Infrared
Fluorescein angiography
B
D1
D3
D7
Avidin D
Avidin D Lectin
C
Kit+/+
KitW-sh/W-sh
KitW-sh/W-sh + BMDMC
Lectin Phalloidin
D
CNV size [x10⁴ µm²]
***
****
Kit+/+
KitW-sh/W-sh
KitW-sh/W-sh + BMDMC
E
Laser burn
KF (ip)
Analysis
D-2 D-1 D0 D1 D2 D3 D4 D5 D6 D7
F
Vehicle
KF
Lectin Phalloidin
G
CNV size [x10⁴ µm²]
****
V
KF
H
Vehicle
KF
Infrared
Fluorescein angiography
I
Fluorescent intensity of vascular leakage (Fold change vs vehicle)
*
V
KF

Figure 2. Effects of mast cell deficiency on choroidal neovascularization. A Illustration of the laser-induced CNV model in mice, with fundus fluorescein angiography images from mice following laser burn. B RPE/choroid complex flat mounts illustrating the accumulation of mast cells (green) in the CNV lesion (red). Scale bar: 50 μm. C Representative image of RPE/choroid complex flat mount staining with FITC lectin (green) and rhodamine phalloidin (red) in WT mice, $Kit^{W\text{-}sh/W\text{-}sh}$ mice, and $Kit^{W\text{-}sh/W\text{-}sh}$ mice reconstituted with BMDMCs at day 7 following laser burn. Scale bar: 50 μm. D Quantification of the CNV lesion size in RPE/choroid complex flat mounts (n = 10-13). Statistical analyses were performed using one-way ANOVA. ***p < 0.001, ****p < 0.0001. E Experimental timeline for ketotifen fumarate treatment in laser-induced CNV. F Representative image of RPE/choroid complex flat mounts after staining with FITC lectin (green) and rhodamine phalloidin (red) from mice at day 7 after receiving laser burn (LB) and treatment with vehicle or ketotifen fumarate (KF) at 25 mg/kg. Scale bar: 50 μm. G Quantification of the CNV lesion size in RPE/choroid complex flat mounts. Statistical analyses were performed using unpaired t-tests. ****p < 0.0001. n = 7-9. H Representative fundus fluorescein angiography images of mice receiving vehicle or KF 7 days after laser burn. I Quantification of vascular leakage. Statistical analyses were performed using Welch's t-test. *p < 0.05. n = 7.

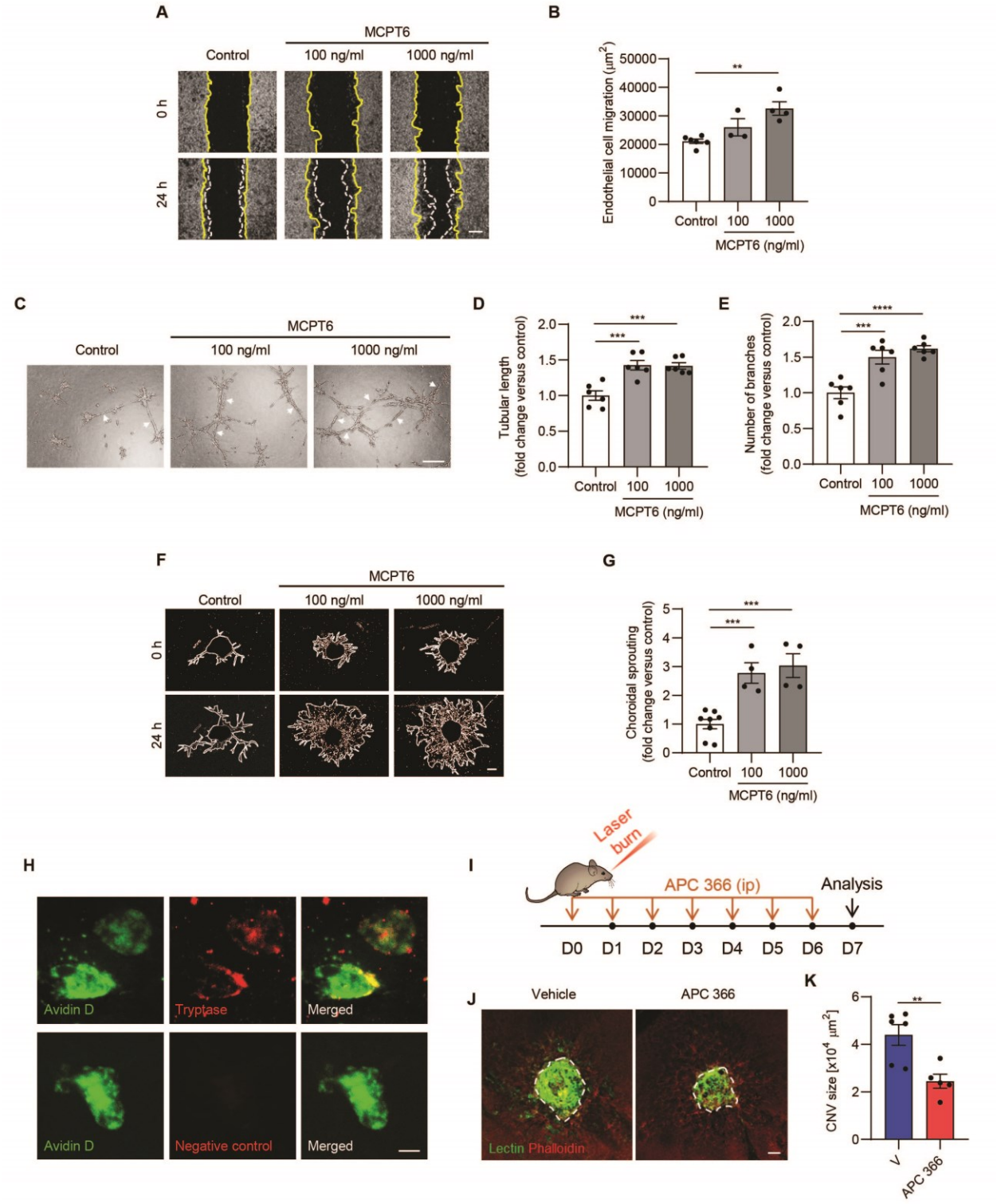

Figure 3. Effects of tryptase on choroidal angiogenesis. **A** Effects of mouse tryptase (mcpt6) at the indicated dose on scratch wound migration after 24 h. Scale bar: 500 μm. **B** Quantification of wound closure (n = 4-6). Statistical analyses were performed using

one-way ANOVA. **p < 0.01. **C** Effects of mcpt6 on tubulogenesis using choroidal endothelial cells. The arrows indicate tube-like structures. Scale bar: 500 µm. Quantification of (**D**) the length of tubules and (**E**) the number of branches (n = 6). Statistical analyses were performed using one-way ANOVA. **F** Representative image of choroidal explants treated or not with mcpt6. Scale bar: 500 µm. **G** Graph representing the quantification of sprouting surface area (n = 4-7). Statistical analyses were performed using one-way ANOVA. **H** Representative images of mast cells expressing tryptase (red) 3 days following laser burn. Scale bar: 5 µm. **I** Schematic illustration of the APC 366 treatment in laser-induced CNV mouse model. **J** Representative images of lectin-stained RPE/choroidal flat mounts of mice treated with APC 366 or vehicle 7 days after laser burn. Scale bar: 50 µm. **K** Quantification of the CNV lesion size in RPE/choroid complex flat mounts of mice treated with APC 366 or vehicle (n = 5, 6). Statistical analyses were performed using unpaired t-test. *p < 0.05.

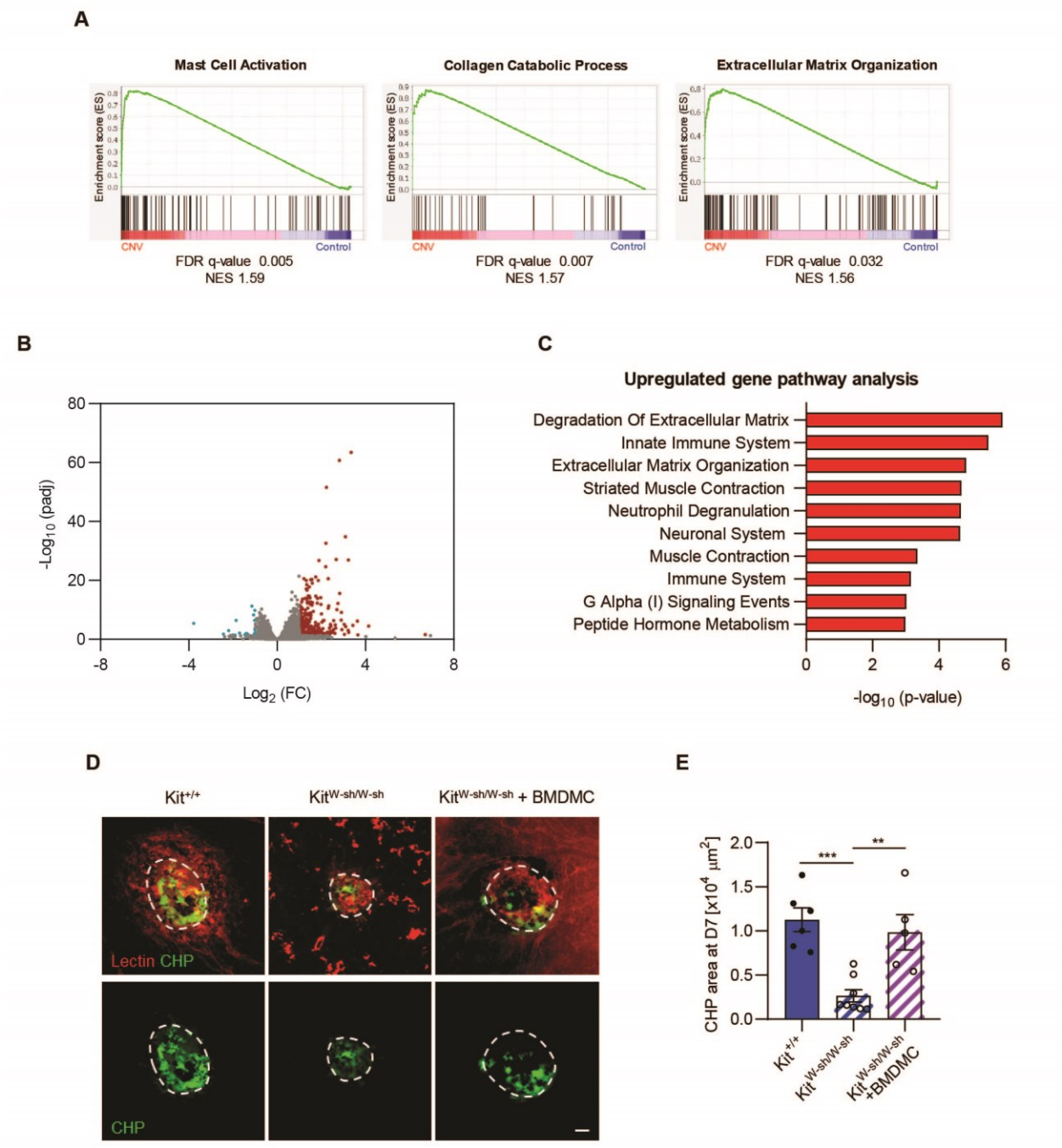

Figure 4. Mast cells regulate collagen deposition in CNV. **A** GSEA pathway analysis of laser burn at day 3 versus control in RPE/choroid complex. **B** Volcano plot illustrating RNA-seq data from the choroid/RPE complex. Genes marked with red dots signify those with an adjusted p-value below 0.05 and a $\log_2$ fold change > 1, while blue dots indicate genes with the same adjusted p-value and a $\log_2$ fold change < −1. All remaining genes

are depicted in gray. **C** Bar graph ranking the top 10 pathways based on their significance, as determined by gene ontology-term pathway enrichment analysis. **D** Representative images of RPE/choroid complex flat mounts stained with lectin (red) and collagen hybridizing peptide (CHP; green). Scale bar: 500 μm. **E** Quantification of CHP area. Statistical analyses were performed using one way ANOVA; n = 5-8. ****$p < 0.0001$, ***$p < 0.001$, **$p < 0.01$.

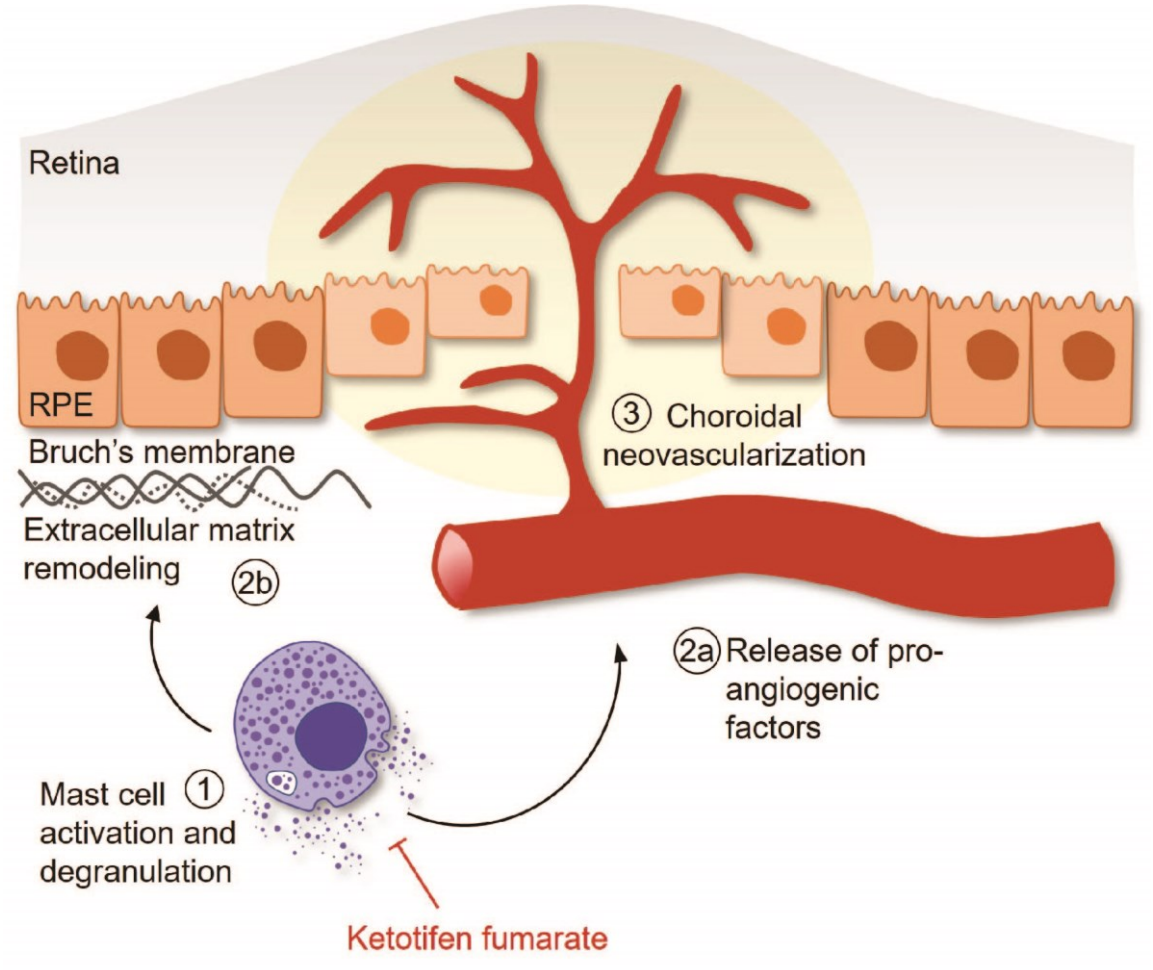

Figure 5. A brief overview of how mast cells are implicated in choroidal neovascularization. Mast cell activation and degranulation results in ECM modelling and release of pro-angiogenic factors, and this can be alleviated using ketotifen fumarate.

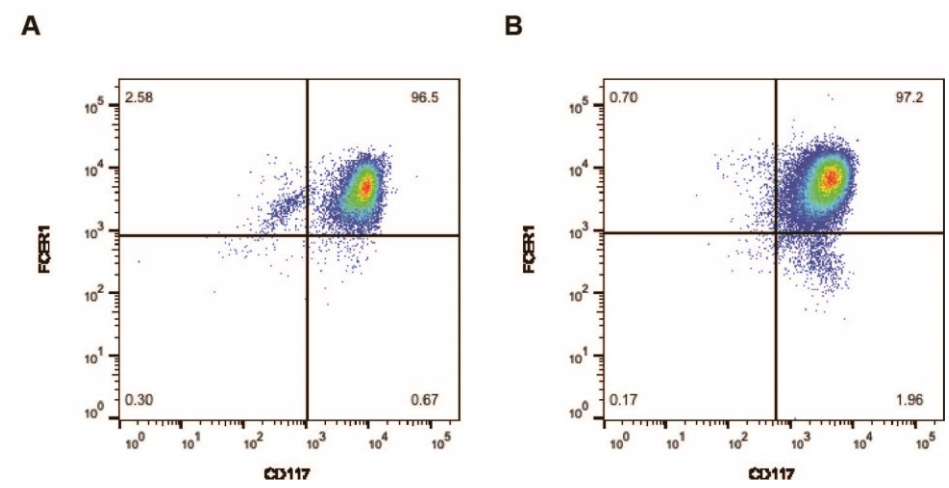

Supplementary Figure 1. Characterization of mast cells. Flow cytometry analysis of (A) peritoneal mast cells and (B) bone marrow-derive mast cells demonstrated expression of the positive markers CD117 and FcεR-1α.

CHAPTER 6 - Necroptosis blockade mitigates retinal toxicity in oxidative stress-induced retinal degeneration

Authors: Rabah Dabouz[1,2], Pénélope Abram[2,3], Avishekh Gautam[4], Samy Omri[5], Nancy Braverman[5], Siddharth Balachandran[4], Sylvain Chemtob[1,2,3]

[1]Department of Pharmacology and Therapeutics, McGill University, Montréal, QC, Canada.

[2]Department of Ophthalmology, Hôpital Maisonneuve-Rosemont, Montréal, QC, Canada.

[3]Department of Pharmacology, Université de Montréal, Montréal, QC, Canada.

[4]Fox Chase Cancer Center, Philadelphia, PA, USA

[5]McGill University Health Center, Montréal, QC, Canada.

Preface

In the preceding chapters we investigated inflammation and its contribution to CNV and photoreceptor cell death in animal models of AMD. Notably, photoreceptor cell death represents a critical juncture, marking the terminal phase across all forms of AMD and culminating in irreversible vision loss. Chapter 6 explores the cellular mechanisms underpinning photoreceptor demise, with a particular emphasis on necroptosis. This form of programmed cell death, distinct from apoptosis, has emerged as a key player in the pathophysiology of degenerative diseases. The objective of the next study is to examine the role of necroptosis in photoreceptor cell death, and importantly, whether pharmacological targeting of this pathway using a novel RIKP3 inhibitor results in the preservation of photoreceptors. Given that necroptosis can release cellular components that act as pro-inflammatory signals, we investigate whether the death of photoreceptors perpetuates and amplifies the inflammatory response, thereby fueling the cycle of degeneration. By elucidating these connections, we deepen our understanding of the complex pathology of AMD and open the door to novel therapeutic strategies. Targeting necroptosis could represent a transformative approach in halting the cycle of degeneration and inflammation in AMD.

Abstract

Age-related macular degeneration (AMD), a leading cause of vision loss, is characterized by the degeneration of retinal pigment epithelium (RPE), subretinal inflammation, and subsequent photoreceptor cell death. Understanding the mechanisms underlying photoreceptor loss is crucial for developing effective treatments. In this study, we explored the roles of necroptosis and apoptosis in photoreceptor cell death using a sodium iodate-induced model of retinal degeneration. We discovered that photoreceptor death, a critical event in AMD, coincides with an upregulation of mixed lineage kinase domain-like protein (MLKL) and the presence of active phospho-MLKL and cleaved caspase-3 in photoreceptor cells. We further explored the therapeutic potential of pharmacologically targeting necroptosis. The administration of UH15-38, an allosteric RIPK3 inhibitor, significantly preserved photoreceptor density and function. Interestingly, the combination of UH15-38 with emricasan, a pancaspase inhibitor, demonstrated a synergistic effect, offering superior protection against photoreceptor loss. Additionally, RIPK3 kinase inhibition effectively reduced subretinal inflammation, a hallmark of AMD. This was observed as a decrease in the number of inflammatory mononuclear phagocytes and their altered morphology towards a less inflammatory state. Similarly, MLKL deficiency in mice resulted in preserved photoreceptor density and reduced subretinal inflammation, highlighting the crucial role of MLKL-driven necroptosis in retinal degeneration. In conclusion, our findings provide compelling evidence that both necroptosis and apoptosis are critical contributors to photoreceptor cell death in retinal degeneration. The inhibition of key components in the necroptotic pathway, particularly RIPK3 and MLKL, emerges as a promising therapeutic strategy for retinal degenerative diseases, offering a novel approach to preserving vision and mitigating inflammation.

Keywords: Age-related Macular Degeneration, Retina, Photoreceptors, Cell Death, Necroptosis, RIPK3, MLKL.

Introduction

Photoreceptor loss is at the core of numerous ocular pathologies, including age-related macular degeneration (AMD), retinitis pigmentosa, and a range of inheritable ocular diseases (1). AMD, in particular, stands out as a leading cause of vision impairment and blindness across the globe. Its prevalence continues to rise annually, signaling a growing public health concern (2). Clinically, AMD manifests in two end-stage forms: neovascular (wet) AMD, characterized by abnormal blood vessel growth beneath the retinal pigment epithelium (RPE) or within the retina, and atrophic (dry) AMD, identified by significant loss of both the RPE and photoreceptors (3). Neuroinflammation is critical to the progressive pathogenesis of AMD, leading ultimately to the death of photoreceptors and substantial central vision impairment (4, 5). Postmortem examination of AMD eyes revealed the presence of photoreceptors showing signs of cell death, which is a characteristic feature observed in AMD patients (6). The mechanisms by which photoreceptors degenerate and die in the context of AMD are still not fully elucidated.

The regulation of cell death, particularly in photoreceptors, can significantly impact the progression of these diseases. Apoptosis and necroptosis are two forms of regulated cell death mechanisms, arising from disturbances in either intra- or extracellular homeostasis (7). Apoptosis revolves around two pathways: extrinsic and intrinsic. Both pathways culminate in the activation of caspases, whose role is critical in driving the process of apoptosis (8). While apoptosis has been researched extensively, there is increasing interest in necroptosis, another form of regulated cell death. Necroptosis is a caspase-independent form of cell death that is primarily driven by receptor-interacting serine/threonine-protein kinase 3 (RIPK3) and its substrate mixed lineage kinase domain like pseudokinase (MLKL) (9). RIPK3, upon phosphorylation, recruits and phosphorylates the pseudokinase MLKL at specific serine and threonine residues (9, 10). Once phosphorylated, MLKL undergoes a structural rearrangement that exposes the 4-helical bundle domain (4HB) (11, 12, 13). The 4HB domain is essential for oligomerization MLKL, enabling the formation of multi-molecule MLKL complexes (14). These activated MLKL oligomers then move to the plasma membrane, forming pores that increase membrane permeability and lead to cell death (13, 15, 16). Unlike apoptosis, necroptosis is a pro-inflammatory process (17), which is particularly significant in the context of AMD, where

chronic inflammation is a known catalyst for disease progression. The purpose of this study is to identify the underlying mechanisms of photoreceptor cell degeneration in a model of AMD. In this study we employed a sodium iodate-induced AMD model, which reproduces key features of the disease, notably primary RPE damage followed by death of the photoreceptors. Our data indicates that necroptotic machinery is activated in photoreceptor cells during retinal degeneration. Necroptosis represents an additional target for therapeutic intervention in retinal degenerative diseases.

Materials and Methods

Animals

All animal experiments were approved by the Maisonneuve Rosemont Hospital Animal Care Committee and were performed in accordance with the Association for Research in Vision and Ophthalmology Statement for the Use of Animals in Ophthalmic and Visual Research. Male C57BL/6 mice were purchased from Jackson Laboratory. MLKL KO mice were generated by Dr. J. Han and donated by Dr. J. Rauch. Ten- to twelve-week-old mice were used in this study. Mice were genotyped to rule out confounding rd8 mutations. Mice were housed with a 12-h light/dark cycle (100-200 lux) with water and normal diet food available *ad libitum.*

Sodium iodate and drug treatment

Sodium iodate was diluted in PBS and injected intraperitoneally (ip) at a dose of 30 mg/kg. Emricasan and UH15-30 were supplied as lyophilized powders, dissolved in dimethyl sulfoxide (DMSO) and solutol, and diluted to the concentrations required for the experiments described below.

Retinal section preparation

Eyes were enucleated and fixed in a 4% paraformaldehyde (PFA) solution at room temperature for 1 h, with subsequent rinsing in phosphate-buffered saline (PBS). The cornea and lens were delicately extracted from the eye, and the posterior eyecups were immersed in 30% sucrose overnight before being frozen in optimal cutting temperature (OCT) medium. Sections of the entire retina along the optic nerve were cut into 12 µm

sagittal sections. These retinal sections were incubated at room temperature for 1 h with a blocking solution consisting of 10% fetal bovine serum, 0.1% Triton X-100, and 0.05% Tween-20 in PBS. Following the blocking step, retinal sections were then incubated overnight with primary antibodies, including phospho MLKL (Abcam, ab196436), cleaved caspase-3 (Asp175) (New England Biolabs, 9661), and IBA1 (Wako, 019-19741). Subsequently, the retinal sections underwent three washes with PBS and were then incubated with a secondary antibody solution, consisting of 1% bovine serum albumin (BSA), 0.1% Triton X-100, 0.05% Tween-20, 1:500 Alexa Fluor donkey 594 anti-rat (A21209, Invitrogen), and 1:500 Alexa Fluor 647 goat anti-rabbit (A11072, Invitrogen) for 2 h at room temperature. After three additional PBS washes, the retinal sections were flat-mounted onto glass slides, covered with coverslips, and sealed with Fluoro-Gel mounting medium (Electron Microscopy Sciences, Hatfield, PA). These sections were then imaged at 60X magnification using a laser scanning confocal microscope (Olympus IX81 with Fluoview FV1000 Scanhead).

Measurement of photoreceptor layer thickness

To measure the thickness of the photoreceptor layer, fourteen measurements per central retinal section (including the optic nerve) were taken at defined distances from the optic nerve. Outer nuclear layer thickness was quantified using ImageJ software, and the area under the curve was calculated and integrated using Prism software version 8 (GraphPad software).

RPE flat mount preparation

Eyes were enucleated and then fixed in a 4% PFA solution for one hour and subsequently rinsed twice with PBS. Careful separation of the neuroretina from the RPE/choroid/sclera complex was carried out to prepare for immunostaining. The RPE/choroid complex underwent a one-hour incubation at room temperature with a blocking solution consisting of 1% BSA, 1% normal goat serum, 0.1% Triton X-100, and 0.05% Tween-20 in PBS. Following this step, the retinas were labeled overnight at 4°C using F-actin or the primary antibody 1:400 anti-IBA1 (Dako, 019-19741). Subsequently, the RPE/choroid complexes underwent three PBS washes and were then incubated with

a secondary antibody solution, comprising 1% BSA, 0.1% Triton X-100, 0.05% Tween-20, 1:500 Alexa Fluor donkey 594 anti-rat (A21209, Invitrogen), and 1:500 Alexa Fluor 647 goat anti-rabbit (A11072, Invitrogen) for 2 hours at room temperature. Retinas were washed thrice with PBS and then flat-mounted onto glass slides with coverslips using Fluoro-Gel mounting medium (Electron Microscopy Sciences, Hatfield, PA).

Quantification of mononuclear phagocytes (MPs) in the subretinal space

IBA1-positive cells were quantified on flat mounts with the RPE facing the objective, and cell numbers were expressed as the average number of IBA1-positive cells per mm^2.

Analysis of volume and shape of MPs

The assessment of MP volume and shape was conducted by examining four random fields for each mouse on RPE/choroid complex flat mounts with the RPE facing the objective. Z-stack images were acquired using a laser scanning confocal microscope (Olympus IX81 with a Fluoview FV1000 scanner) at 40x magnification. These images were processed using Imaris 8.1 Surpass View software (Bitplane USA, Concord, MA, USA), where surface creation was carried out after background noise reduction (0.5 µm). To remove irrelevant particles, voxel filtering was employed on these surfaces. Any cells that were in contact with the image edge or that were incompletely imaged were excluded from analysis. The final step involved quantifying the volume and sphericity of each IBA1-positive cell using the Imaris software**.**

Terminal deoxynucleotidyl transferase dUTP nick end labeling (TUNEL) assay

The TUNEL staining procedure was executed in accordance with the manufacturer's protocol (In Situ Cell Death Detection Kit; Roche Diagnostics). Briefly, retinal sections were fixed in 4% PFA for 30 minutes and subsequently washed with PBS. Sections were then incubated for 90 minutes at 37°C with the reaction mixture, and the reaction was halted by washing with PBS. Nuclei were stained using 4',6-diamidino-2-phenylindole (DAPI, Sigma, St. Louis, MO, USA). Imaging was carried out with a laser

scanning confocal microscope (Olympus IX81 with Fluoview FV1000 Scanhead) using the Fluoview Software at a magnification of 30X.

Western Blotting

Proteins were extracted from mice retinas and RPE/choroid complexes by sonication in lysis buffer RIPA buffer with a pH of 8. This buffer composition included 50 mM Tris–HCl, 150 mM NaCl, 5 mM EDTA, 1% Triton 100×, 0.5% sodium deoxycholate, 0.1% SDS, and a mixture of protease and phosphatase inhibitors (MiniComplete, PhosphoStop and PMSF, Roche, Bâle, Switzerland). The concentration of proteins was determined using the Bicinchoninic Acid Protein Assay Kit (Pierce, Rockford, IL, USA). Each well was loaded with 30 µg of protein and electrophoresed on a 12% sodium dodecyl sulfate–polyacrylamide gel (Mini-Protean Tetra System, Bio-Rad, Hercules, CA, USA). Subsequently, the proteins were transferred onto polyvinylidene difluoride membranes (Millipore, Billerica, MA, USA). The membranes were then blocked with 5% skim milk in Tris-buffered saline containing 0.1% Tween-20 for 1 h at room temperature. They were then incubated with the primary antibodies as follows: 1:200 MLKL (EMD Millipore, MABC604), 1:500 RIPK3 (Novus Biological, 77299), and 1:1000 β-actin (Santa Cruz, sc47778). Subsequently, the membranes were incubated with horseradish peroxidase-conjugated secondary antibodies at a dilution of 1:6000 (Millipore, AP307P and Millipore, AP308P).

Gene set enrichment analysis

The gene set enrichment analysis (GSEA) was applied to a dataset originating from the research conducted by Enzbrenner et al (18). The analysis utilized version 4.3.3 of the GSEA software, developed by the Broad Institute affiliated with both MIT and Harvard University. Relevant gene sets were accessed from the Molecular Signature Database, known for its comprehensive annotations of gene groups. The phenotype was designated through 1,000 permutations, focusing on the comparison of sodium iodate and Control to categorize the phenotype. Gene sets with less than 15 or more than 500 genes were excluded from the analysis. To detect significant gene changes, the weighted p2 statistic, alongside a t0test for class differentiation were employed.

Electroretinogram (ERG)

ERGs were recorded using an Espion ERG Diagnosys apparatus that was equipped with a ColorDome Ganzfeld stimulator (Diagnosys LLC, Lowell, MA). Prior to the ERG recording, mice underwent overnight dark adaptation and were subsequently anesthetized intraperitoneally using a combination of ketamine (100 mg/kg) and xylazine (20 mg/kg). To ensure corneal anesthesia, proxymetacaine hydrochloride (0.5% Alcaine; Alcon, Fort Worth, TX, USA) was applied, and pupil dilation was achieved using 0.5% atropine (Alcon, Fort Worth, TX, USA). The body temperature was maintained at 37.5°C using a heating pad during the procedure. For ERG measurements, corneal DTL Plus electrodes (Diagnosys LLC) were used in conjunction with a forehead reference electrode, while a ground electrode was placed subcutaneously in the tail. To assess rod photoreceptor function under scotopic conditions, a series of five-strobe flash stimuli were presented, with flash intensities ranging from 0.01 cds/m^2, 0.1 cds/m^2, 0.5 cds/m^2,1.0 cds/m^2, 3.0 cds/m^2, 5.0 cds/m^2, 10 cds/m^2, and 25 cds/m^2. All ERG procedures were conducted in a dark room under dim red-light illumination. The amplitude of the a-wave was measured by determining the difference from baseline to the primary negative peak, while the b-wave was measured as the difference from the trough of the a-wave to the maximum of the fourth positive peak.

Statistics

Data are presented as mean ± standard error of the mean (SEM). Student's t-test was used to compare two different groups or, when indicated, a one-way analysis of variance (ANOVA) followed by post hoc Holm-Sidak tests for comparison of means. A $p < 0.05$ was considered statistically significant.

Results

Necroptosis and apoptosis are engaged in retinal degeneration

Pathological features of AMD include RPE degeneration, subretinal inflammation, and photoreceptor loss. To examine mechanisms of photoreceptor cell death, we used the sodium iodate model of retinal degeneration characterized by RPE loss followed by

the death of photoreceptors (19). To determine whether necroptosis is triggered during photoreceptor death, we measured the expression of RIPK3 and MLKL. Three days following sodium iodate injection, which corresponds to the peak of photoreceptor death, we observed an upregulation of MLKL levels in sodium iodate-treated mice whereas RIPK3 levels remained unchanged (Fig. 1A). The findings are consistent with transcriptomic analysis where genes related to necroptotic machinery were enriched in the sodium iodate phenotype (Fig. 1B). Immunofluorescence experiments confirmed the presence of the active phospho-MLKL in the photoreceptor segments (Fig. 1C). Of note, cleaved caspase-3, a marker of apoptosis, was also detected in the photoreceptor nuclear layer and photoreceptor segments (Fig. 1D). These findings suggest that concurrent activation of apoptosis and necroptosis contribute to photoreceptor loss in retinal degeneration.

MLKL deficiency alleviated photoreceptor loss and subretinal inflammation

The role of MLKL in necroptosis involves its oligomerization and translocation to the plasma membrane, leading to increased membrane permeability (20). We investigated the contribution of MLKL-driven necroptosis to photoreceptor loss by treating MLKL-deficient mice with sodium iodate. This treatment induced significant photoreceptor cell death in wild-type mice. However, MLKL deficiency was associated with a notable preservation of photoreceptor density and a reduction in TUNEL-positive photoreceptor cells compared to wild-type mice (Fig. 2A-D). These findings highlight the vital role of MLKL-driven necroptosis in the degeneration of photoreceptor cells. Given the proposed involvement of necroptosis in the death of RPE cells due to sodium iodate, we investigated its role in RPE cell death (21). Contrary to our observations in photoreceptor cells, we did not observe a protective effect against RPE cell loss in mice lacking MLKL (Supp Fig. 1). This was also the case when we used a pharmacological inhibitor of RIPK3 kinase, alone or in combination with emricasan (Supp Fig. 1). This suggests that the mechanisms of RPE cell death in sodium iodate-induced degeneration might differ from those in photoreceptor cells.

Further, we assessed the impact of MLKL deficiency on the inflammatory response in the subretina. Post-treatment, there was a migration of IBA1+ MPs into the subretinal

space of WT mice. The MLKL KO mice exhibited fewer MPs in this area compared to their WT counterparts (Fig. 2E, F). Additionally, the MPs in MLKL KO mice displayed a more ramified morphology, an indicator of a reduced inflammatory phenotype. These findings indicate that necroptotic photoreceptors contribute to inflammation by promoting the infiltration and activation of MPs in the subretinal space.

Pharmacological targeting of necroptosis alleviated photoreceptor loss

Active phosphorylated RIPK3 phosphorylates MLKL, targeting specific serine and the threonine residues MLKL (9, 10). This phosphorylation triggers MLKL oligomerization and then translocation to the plasma membrane, forming pores that enhance membrane permeability (13, 15, 16). We next determined whether pharmacologically targeting the kinase activity of RIPK3 influenced photoreceptor death. We utilized an allosteric RIPK3 inhibitor known as UH15-38 in sodium iodate-induced photoreceptor death. Mice were administered daily doses of UH15-38 until the day of sacrifice. Sodium iodate treatment caused a marked loss of photoreceptors shown by the thinning of photoreceptor layer and a huge number of TUNEL+ photoreceptors (Fig. 3A-D). Remarkably, UH15-38 administration resulted in a notable preservation of photoreceptor density (Fig. 3). This protective effect was demonstrated by the diminished count of TUNEL-positive cells (Fig. 3 A, B), indicating reduced cell death. To ascertain the contribution of apoptosis in the death of photoreceptors, we employed emricasan, a pancaspase inhibitor. In our study, emricasan on its own provided only mild protection to the photoreceptors. However, a synergistic effect was observed when UH15-38 and emricasan were co-administered, resulting in superior photoreceptor protection compared to the use of UH15-38 alone (Fig. 3 A-D).

To gauge the impact of these treatments on retinal function, we employed multifocal scotopic ERG. The sodium iodate challenge led to a substantial drop in both the a-wave ERG amplitude (Fig. 4A), which originates from the photoreceptors, and the b-wave amplitude, which is associated with bipolar and Müller cells, in the vehicle-treated group (Fig. 4B). Interestingly, while emricasan treatment alone did not yield significant preservation of these amplitudes, UH15-38 did provide notable protection (Figure 4A-C). Notably, the combined regimen of UH15-38 and emricasan amplified this protective effect

(Fig. 4A-C). Collectively, these findings indicate a parallel contribution of necroptosis and apoptosis in the death of photoreceptors, both of which can be pharmacologically targeted.

RIPK3 kinase inhibition dampens subretinal inflammation

Necroptosis is a highly immunogenic programmed form of necrosis that leads to a strong inflammatory response (17). This is particularly relevant in the context of AMD, where dysregulated parainflammation culminates in persistent chronic inflammation within the subretinal space (22). We explored the potential of modulating the catalytic activity of RIPK3 to alleviate this inflammation in retinal degeneration. Three days following administration of sodium iodate, a notable infiltration of IBA1+ immune cells was observed in the subretinal space, indicative of strong inflammation. Treatment with the RIPK3 kinase inhibitor, UH15-38, led to a marked reduction in the number of MPs in this area. Notably, the combination of UH15-38 and emricasan resulted in a more pronounced decrease in MPs than UH15-38 alone (Fig. 5A, B). Additionally, MPs in the UH15-38 and combined treatment groups exhibited changes in morphology - reduced sphericity and increased size - indicative of a less inflammatory state compared to the vehicle-treated group (Fig. 5C, D). These results suggest that RIPK3 inhibition, notably when combined with emricasan, offers a promising approach to mitigating inflammation associated with AMD.

Discussion

Necroptosis, a form of programmed cell death distinct from apoptosis, is increasingly implicated in various neurodegenerative diseases such as Alzheimer’s disease (23, 24, 25), Parkinson’s disease (26), multiple sclerosis (27), and amyotrophic lateral sclerosis (28). Particularly in the retina, a RIPK3-dependent mechanism was shown to mediate photoreceptor cell death under conditions of retinal detachment and ultraviolet light exposure (29, 30). Herein, we provide compelling evidence that necroptosis is a key mechanism in retinal degeneration, leading to photoreceptor cell loss and correlating with an inflammatory response Our findings indicate that pharmacological inhibition of RIPK3 kinase activity or ablation of MLKL rescues photoreceptor neurons

from death. This suggests that in cases of retinal degeneration, photoreceptor death is primarily driven by necroptosis, linking cell loss to an inflammatory response.

Multiple biological processes, such as apoptosis, necrosis, and autophagy have been suggested as potential contributors of photoreceptor cell loss (31). For instance, the apoptosis of photoreceptor cells following light exposure was suggested as a causative factor (32). However, there is a lack of compelling evidence to support the idea that this directly leads to photoreceptor cell loss. The pan-caspase inhibitor Z-VAD, while protective under specific conditions, does not consistently prevent photoreceptor loss after light exposure (33, 34). We report that both apoptosis and necroptosis are activated simultaneously in response to oxidative stress, leading to retinal degeneration. An agglomeration of pMLKL was observed in the photoreceptor segments. MLKL directly induces the exposure of phosphatidylserine on the cell membrane, leading to the formation of plasma membrane bubbles during necroptotic cell death (35). Notably, a key observation of the study was that the deletion of MLKL significantly protected against photoreceptor death and mitigated subretinal inflammation.

Necroptosis is a druggable pathway in a number of diseases. Our experiments with a novel allosteric RIPK3 modulator that inhibits its kinase activity revealed its potency in mitigating photoreceptor death. This protective effect was amplified when combined with a pancaspase inhibitor, emricasan. Conversely, while emricasan marginally preserved photoreceptor density, it did not effectively preserve retinal function. Notably, beyond its ocular effects, emricasan has also been shown to reduce liver injury and inflammation, indicating its therapeutic benefits (36, 37). The enhanced protective effect observed when combining the RIPK3 modulator with emricasan is attributed to the unique action of the RIPK3 modulator. This modulator alone can shift the balance of cell death mechanisms towards apoptosis rather than necroptosis. In fact, inhibiting RIPK3 kinase activity stabilizes the FADD-caspase-8 complex, effectively tipping the cellular response in favor of apoptosis (38). This is contrasted by the non-viability of $RIPK3^{D161N/D161N}$ mice, which lack catalytic activity and exhibit increased apoptosis driven by caspase-8 in contrast to viable RIPK3 KO mice (39). Thus, the dual approach of combining a novel allosteric RIPK3 modulator, which inhibits its kinase activity, with the pancaspase inhibitor emricasan, showed enhanced protective effects on photoreceptor density. In agreement

with these findings, a RIPK3-dependent mechanism was shown to mediate cell death in retinal detachment and ultraviolet exposure. While Z-VAD reduced apoptosis, it inadvertently increased necrotic photoreceptor death. Conversely, when combined with necrostatin-1, a RIPK1 inhibitor, this co-treatment effectively curbed necrotic photoreceptor death (29, 30).

Classically, necroptosis can be triggered by a variety of receptors, including death receptors (TNFR1, TRAILR, FAS), along with interferon-alpha/beta receptor subunit 1 (IFNARI) (17). Yet, the main trigger of necroptosis in photoreceptors remains elusive. In retinal detachment, TNF was found to control autophagy in photoreceptors (40) and its inhibition has shown protective effects (40, 41). Additionally, glutamate excitotoxicity, a common mechanism in various neurodegenerative diseases, including photoreceptor death, may also trigger the necroptotic cascade. There is emerging evidence suggesting that the necroptotic cascade can be initiated by glutamate-driven excitotoxicity (42). This connection is particularly relevant, considering the high levels of glutamate found in retinal diseases.

In conclusion, our study identifies necroptosis as a major driver of photoreceptor cell death in retinal degeneration. We demonstrate that a targeted approach, inhibiting key components of the necroptotic pathway, can significantly protect photoreceptors from death. This opens up potential therapeutic avenues for retinal degenerative conditions and highlights the complexity of cell death mechanisms in neurodegeneration.

References

1. Murakami Y, Notomi S, Hisatomi T, Nakazawa T, Ishibashi T, Miller JW, et al. Photoreceptor cell death and rescue in retinal detachment and degenerations. Prog Retin Eye Res. 2013;37:114-40.

2. Blindness GBD, Vision Impairment C, Vision Loss Expert Group of the Global Burden of Disease S. Causes of blindness and vision impairment in 2020 and trends over 30 years, and prevalence of avoidable blindness in relation to VISION 2020: the Right to Sight: an analysis for the Global Burden of Disease Study. Lancet Glob Health. 2021;9(2):e144-e60.

3. Mitchell P, Liew G, Gopinath B, Wong TY. Age-related macular degeneration. Lancet. 2018;392(10153):1147-59.
4. Dabouz R, Cheng CWH, Abram P, Omri S, Cagnone G, Sawmy KV, et al. An allosteric interleukin-1 receptor modulator mitigates inflammation and photoreceptor toxicity in a model of retinal degeneration. J Neuroinflammation. 2020;17(1):359.
5. Guillonneau X, Eandi CM, Paques M, Sahel JA, Sapieha P, Sennlaub F. On phagocytes and macular degeneration. Prog Retin Eye Res. 2017;61:98-128.
6. Dunaief JL, Dentchev T, Ying GS, Milam AH. The role of apoptosis in age-related macular degeneration. Arch Ophthalmol. 2002;120(11):1435-42.
7. Galluzzi L, Vitale I, Aaronson SA, Abrams JM, Adam D, Agostinis P, et al. Molecular mechanisms of cell death: recommendations of the Nomenclature Committee on Cell Death 2018. Cell Death Differ. 2018;25(3):486-541.
8. Kesavardhana S, Malireddi RKS, Kanneganti TD. Caspases in Cell Death, Inflammation, and Pyroptosis. Annu Rev Immunol. 2020;38:567-95.
9. Sun L, Wang H, Wang Z, He S, Chen S, Liao D, et al. Mixed lineage kinase domain-like protein mediates necrosis signaling downstream of RIP3 kinase. Cell. 2012;148(1-2):213-27.
10. Rodriguez DA, Weinlich R, Brown S, Guy C, Fitzgerald P, Dillon CP, et al. Characterization of RIPK3-mediated phosphorylation of the activation loop of MLKL during necroptosis. Cell Death Differ. 2016;23(1):76-88.
11. Petrie EJ, Sandow JJ, Jacobsen AV, Smith BJ, Griffin MDW, Lucet IS, et al. Conformational switching of the pseudokinase domain promotes human MLKL tetramerization and cell death by necroptosis. Nat Commun. 2018;9(1):2422.
12. Davies KA, Tanzer MC, Griffin MDW, Mok YF, Young SN, Qin R, et al. The brace helices of MLKL mediate interdomain communication and oligomerisation to regulate cell death by necroptosis. Cell Death Differ. 2018;25(9):1567-80.
13. Hildebrand JM, Tanzer MC, Lucet IS, Young SN, Spall SK, Sharma P, et al. Activation of the pseudokinase MLKL unleashes the four-helix bundle domain to induce membrane localization and necroptotic cell death. Proc Natl Acad Sci U S A. 2014;111(42):15072-7.

14. Dondelinger Y, Declercq W, Montessuit S, Roelandt R, Goncalves A, Bruggeman I, et al. MLKL compromises plasma membrane integrity by binding to phosphatidylinositol phosphates. Cell Rep. 2014;7(4):971-81.
15. Murphy JM, Czabotar PE, Hildebrand JM, Lucet IS, Zhang JG, Alvarez-Diaz S, et al. The pseudokinase MLKL mediates necroptosis via a molecular switch mechanism. Immunity. 2013;39(3):443-53.
16. Chen X, Li W, Ren J, Huang D, He WT, Song Y, et al. Translocation of mixed lineage kinase domain-like protein to plasma membrane leads to necrotic cell death. Cell Res. 2014;24(1):105-21.
17. Pasparakis M, Vandenabeele P. Necroptosis and its role in inflammation. Nature. 2015;517(7534):311-20.
18. Enzbrenner A, Zulliger R, Biber J, Pousa AMQ, Schafer N, Stucki C, et al. Sodium Iodate-Induced Degeneration Results in Local Complement Changes and Inflammatory Processes in Murine Retina. Int J Mol Sci. 2021;22(17).
19. Sorsby A. Experimental Pigmentary Degeneration of the Retina by Sodium Iodate. Br J Ophthalmol. 1941;25(2):58-62.
20. Samson AL, Zhang Y, Geoghegan ND, Gavin XJ, Davies KA, Mlodzianoski MJ, et al. MLKL trafficking and accumulation at the plasma membrane control the kinetics and threshold for necroptosis. Nat Commun. 2020;11(1):3151.
21. Hanus J, Anderson C, Sarraf D, Ma J, Wang S. Retinal pigment epithelial cell necroptosis in response to sodium iodate. Cell Death Discov. 2016;2:16054.
22. Chen M, Xu H. Parainflammation, chronic inflammation, and age-related macular degeneration. J Leukoc Biol. 2015;98(5):713-25.
23. Caccamo A, Branca C, Piras IS, Ferreira E, Huentelman MJ, Liang WS, et al. Necroptosis activation in Alzheimer's disease. Nat Neurosci. 2017;20(9):1236-46.
24. Balusu S, Horre K, Thrupp N, Craessaerts K, Snellinx A, Serneels L, et al. MEG3 activates necroptosis in human neuron xenografts modeling Alzheimer's disease. Science. 2023;381(6663):1176-82.
25. Salvadores N, Moreno-Gonzalez I, Gamez N, Quiroz G, Vegas-Gomez L, Escandon M, et al. Abeta oligomers trigger necroptosis-mediated neurodegeneration via microglia activation in Alzheimer's disease. Acta Neuropathol Commun. 2022;10(1):31.

26. Iannielli A, Bido S, Folladori L, Segnali A, Cancellieri C, Maresca A, et al. Pharmacological Inhibition of Necroptosis Protects from Dopaminergic Neuronal Cell Death in Parkinson's Disease Models. Cell Rep. 2018;22(8):2066-79.
27. Ofengeim D, Ito Y, Najafov A, Zhang Y, Shan B, DeWitt JP, et al. Activation of necroptosis in multiple sclerosis. Cell Rep. 2015;10(11):1836-49.
28. Ito Y, Ofengeim D, Najafov A, Das S, Saberi S, Li Y, et al. RIPK1 mediates axonal degeneration by promoting inflammation and necroptosis in ALS. Science. 2016;353(6299):603-8.
29. Trichonas G, Murakami Y, Thanos A, Morizane Y, Kayama M, Debouck CM, et al. Receptor interacting protein kinases mediate retinal detachment-induced photoreceptor necrosis and compensate for inhibition of apoptosis. Proc Natl Acad Sci U S A. 2010;107(50):21695-700.
30. Yu Z, Correa V, Efstathiou NE, Albertos-Arranz H, Chen X, Ishihara K, et al. UVA induces retinal photoreceptor cell death via receptor interacting protein 3 kinase mediated necroptosis. Cell Death Discov. 2022;8(1):489.
31. Lohr HR, Kuntchithapautham K, Sharma AK, Rohrer B. Multiple, parallel cellular suicide mechanisms participate in photoreceptor cell death. Exp Eye Res. 2006;83(2):380-9.
32. Wenzel A, Grimm C, Samardzija M, Reme CE. Molecular mechanisms of light-induced photoreceptor apoptosis and neuroprotection for retinal degeneration. Prog Retin Eye Res. 2005;24(2):275-306.
33. Donovan M, Cotter TG. Caspase-independent photoreceptor apoptosis in vivo and differential expression of apoptotic protease activating factor-1 and caspase-3 during retinal development. Cell Death Differ. 2002;9(11):1220-31.
34. Perche O, Doly M, Ranchon-Cole I. Caspase-dependent apoptosis in light-induced retinal degeneration. Invest Ophthalmol Vis Sci. 2007;48(6):2753-9.
35. Gong YN, Guy C, Olauson H, Becker JU, Yang M, Fitzgerald P, et al. ESCRT-III Acts Downstream of MLKL to Regulate Necroptotic Cell Death and Its Consequences. Cell. 2017;169(2):286-300 e16.

36. Barreyro FJ, Holod S, Finocchietto PV, Camino AM, Aquino JB, Avagnina A, et al. The pan-caspase inhibitor Emricasan (IDN-6556) decreases liver injury and fibrosis in a murine model of non-alcoholic steatohepatitis. Liver Int. 2015;35(3):953-66.
37. Witek RP, Stone WC, Karaca FG, Syn WK, Pereira TA, Agboola KM, et al. Pan-caspase inhibitor VX-166 reduces fibrosis in an animal model of nonalcoholic steatohepatitis. Hepatology. 2009;50(5):1421-30.
38. Mandal P, Berger SB, Pillay S, Moriwaki K, Huang C, Guo H, et al. RIP3 induces apoptosis independent of pronecrotic kinase activity. Mol Cell. 2014;56(4):481-95.
39. Newton K, Dugger DL, Wickliffe KE, Kapoor N, de Almagro MC, Vucic D, et al. Activity of protein kinase RIPK3 determines whether cells die by necroptosis or apoptosis. Science. 2014;343(6177):1357-60.
40. Xie J, Zhu R, Peng Y, Gao W, Du J, Zhao L, et al. Tumor necrosis factor-alpha regulates photoreceptor cell autophagy after retinal detachment. Sci Rep. 2017;7(1):17108.
41. Nakazawa T, Kayama M, Ryu M, Kunikata H, Watanabe R, Yasuda M, et al. Tumor necrosis factor-alpha mediates photoreceptor death in a rodent model of retinal detachment. Invest Ophthalmol Vis Sci. 2011;52(3):1384-91.
42. Hernandez DE, Salvadores NA, Moya-Alvarado G, Catalan RJ, Bronfman FC, Court FA. Axonal degeneration induced by glutamate excitotoxicity is mediated by necroptosis. J Cell Sci. 2018;131(22).

Funding

This study was funded by the Canadian Institutes of Health Research (CIHR) RD is supported by Fonds de Recherche du Québec-Santé (FRQS). PA is supported by CIHR, FRQS, The Vision Health Research Network, and FROUM.

Contributions

RD conceptualized and designed the study. RD and PA planned and carried out experiments and analyzed the data. AG, SO, NB, JR provided technical assistance. SB provided scientific expertise. RD wrote the manuscript. SC was involved in grant acquisition.

Conflict of interest statement

The authors have no conflict with the subject matter or materials discussed in the manuscript. Siddharth Balachandran is a co-inventor on the patent application related to the UH15-38.

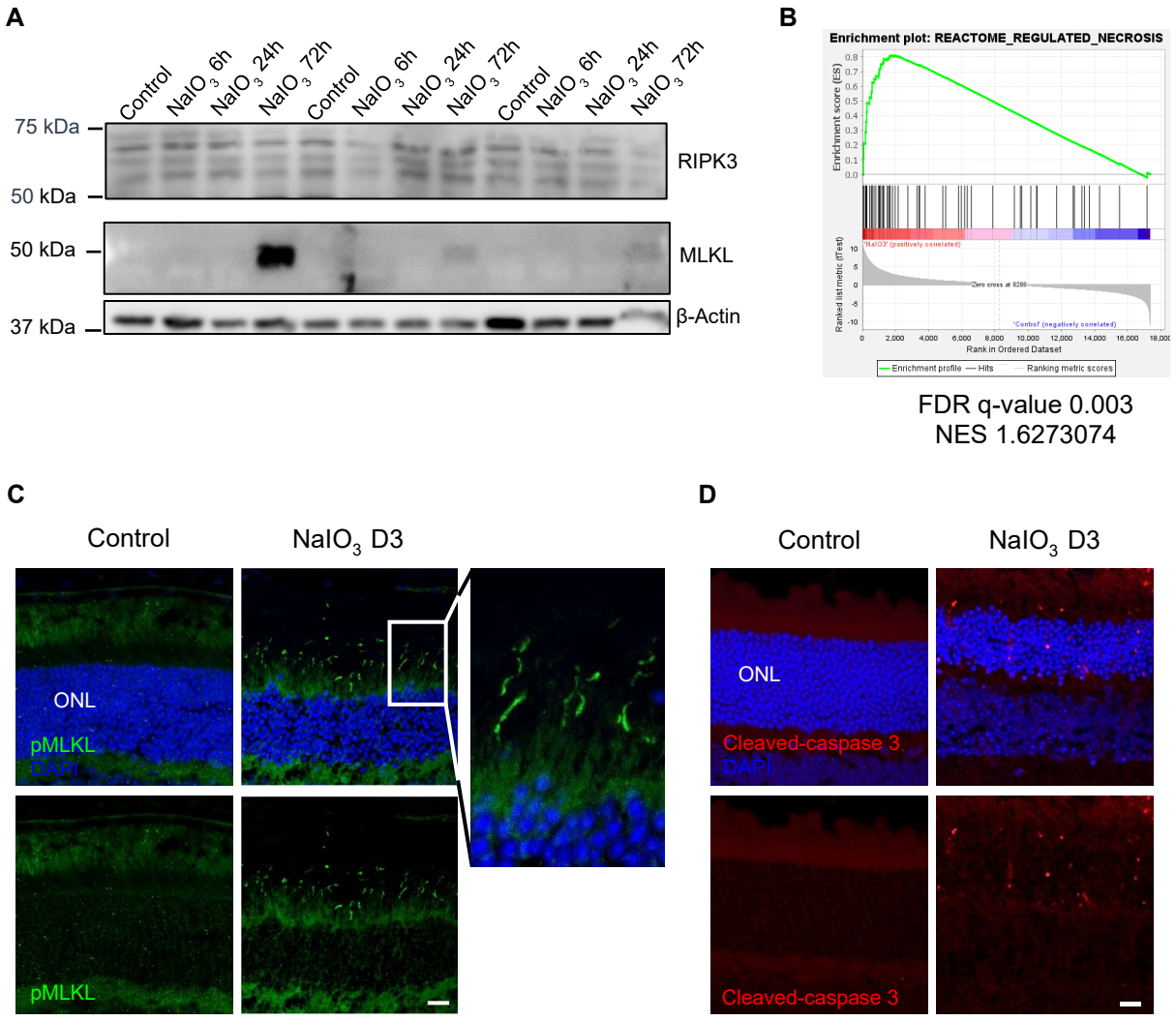

Figure 1. Necroptosis and apoptosis activation in response to sodium iodate. (**A**) Western blots showing the expression of RIPK3 and MLKL in retinal samples from sodium iodate-treated animals. (**B**) Enrichment plots from gene set enrichment analysis showing signaling pathways related to necroptosis enriched in sodium iodate-treated retina. (**C**) Representative images of pMLKL immunoreactivity (green) showing necroptosis activation in sodium iodate-treated animals. Scale bar: 20 µm. (**D**) Representative images of cleaved caspase-3 immunoreactivity (red) showing activation of apoptosis in sodium iodate-treated animals. Scale bar: 20 µm.

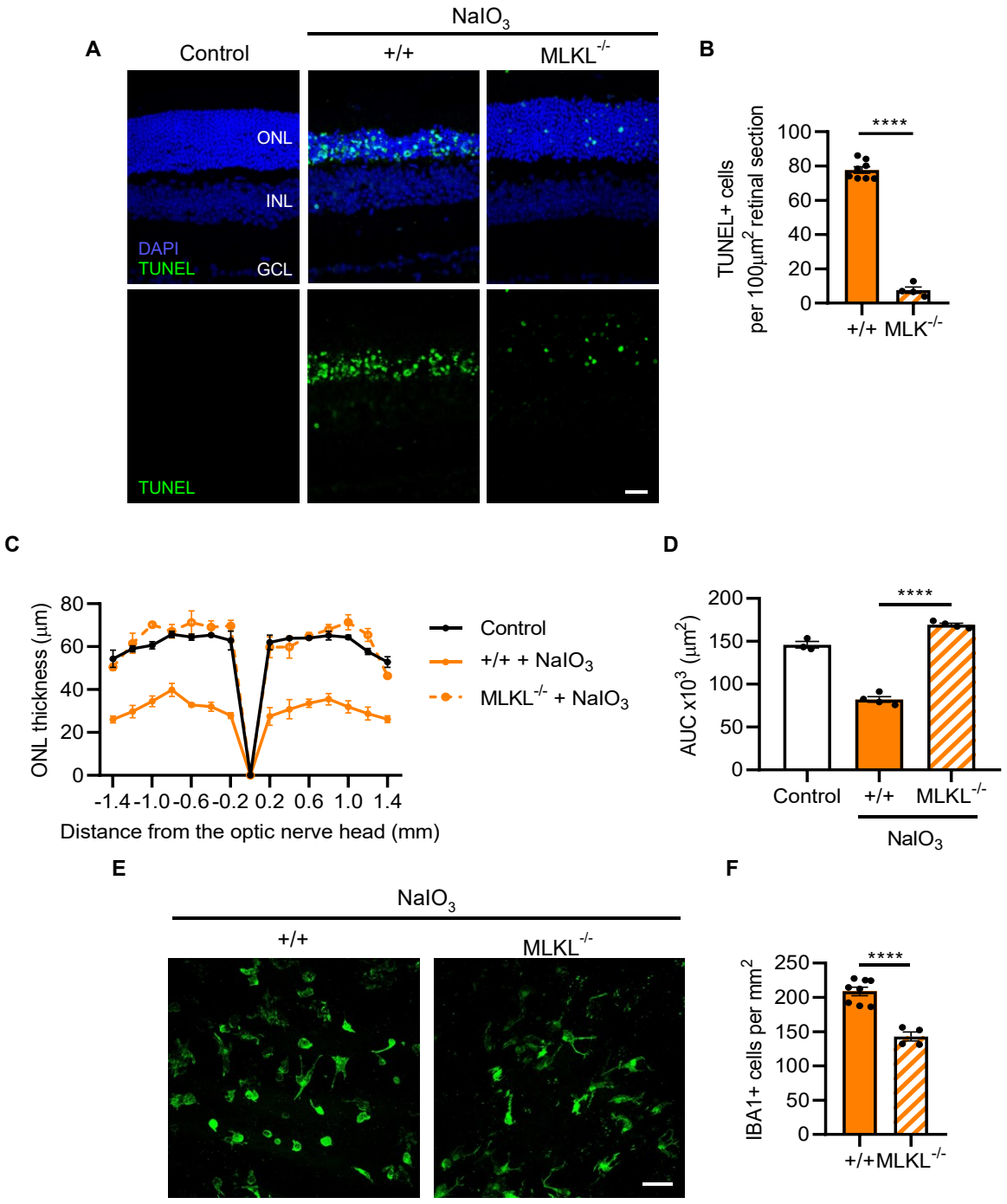
A
Control
NaIO3
+/+
MLKL-/-
ONL
INL
GCL
DAPI
TUNEL
TUNEL
B
TUNEL+ cells per 100µm2 retinal section
****
+/+
MLK-/-
C
ONL thickness (µm)
Distance from the optic nerve head (mm)
Control
+/+ + NaIO3
MLKL-/- + NaIO3
D
AUC x10^3 (µm2)
****
Control
+/+
MLKL-/-
NaIO3
E
NaIO3
+/+
MLKL-/-
F
IBA1+ cells per mm2
****
+/+
MLKL-/-

Figure 2. Effects of MLKL deficiency in sodium iodate-induced retinal degeneration. (**A**) Representative images of TUNEL (green)-stained retinas in control and sodium iodate-treated WT and MLKL KO mice. Scale bar: 20 μm. ONL: outer nuclear layer, INL: inner nuclear layer, GCL: ganglion cell layer. (**B**) The graph illustrates the quantitative analysis of TUNEL-positive cells in the ONL. Data are expressed as mean ± SEM and analyzed using one-way ANOVA with Holm-Sidak correction for multiple comparisons; n = 4-8. ****p < 0.0001. (**C**) Spider-graph quantification of ONL thickness on DAPI-stained retinal sections from control mice and sodium iodate-treated WT and MLKL KO mice. (**D**) Statistical analysis was performed using the area under the curve values (to assess photoreceptor density). Data are expressed as mean ± SEM and analyzed using one-way ANOVA with Holm-Sidak correction for multiple comparisons; n = 3-4. ****p < 0.0001. AUC: area under the curve. (**E**) Representative images of RPE flat mounts showing infiltration of IBA1-labeled mononuclear phagocytes of mice treated with sodium. Scale bar: 50 μm. (**F**) The graph represents compiled data on IBA1+ cell density in the subretina presented as a histogram. Data are expressed as mean ± SEM and analyzed by one-way ANOVA with Holm-Sidak correction for multiple comparisons; n = 4–8 per group. ****p < 0.0001.

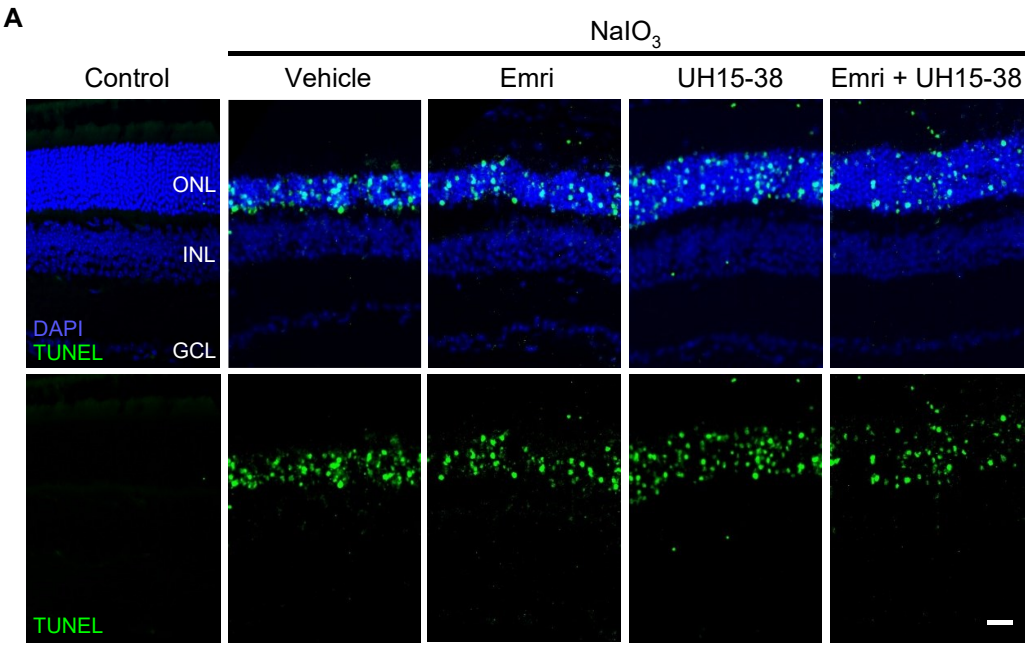
A
NaIO3
Control
Vehicle
Emri
UH15-38
Emri + UH15-38
ONL
INL
GCL
DAPI
TUNEL
TUNEL

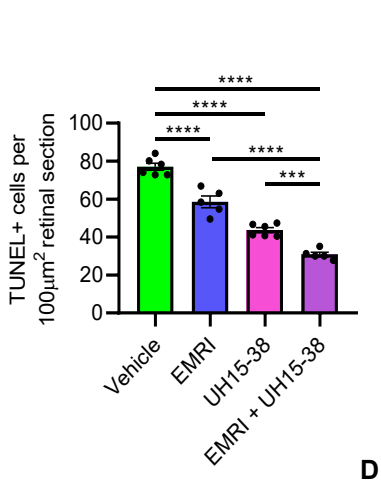
B
TUNEL+ cells per 100μm2 retinal section
Vehicle
EMRI
UH15-38
EMRI + UH15-38

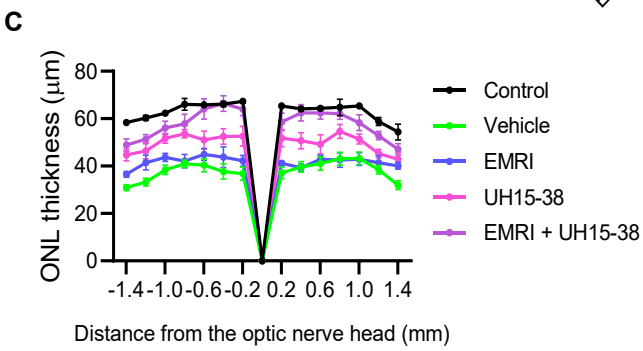
C
ONL thickness (μm)
Distance from the optic nerve head (mm)
Control
Vehicle
EMRI
UH15-38
EMRI + UH15-38

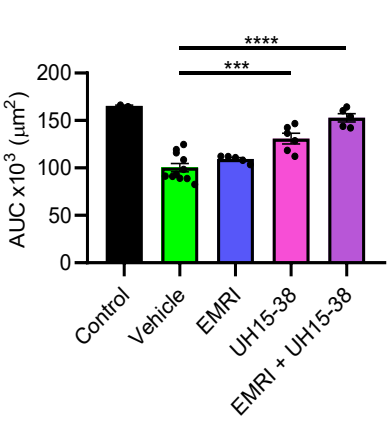
D
AUC x10^3 (μm^2)
Control
Vehicle
EMRI
UH15-38
EMRI + UH15-38

Figure 3. Preservation of photoreceptors by the RIPK3 modulator UH15-38. (**A**) Representative images of TUNEL (green)-stained retinas in control and sodium iodate-treated mice administrated with vehicle, emricasan, UH15-38, and a combination of both drugs. Scale bar: 20 µm. ONL: outer nuclear layer, INL: inner nuclear layer, GCL: ganglion cell layer. (**B**) Graph illustrating the quantitative analysis of TUNEL-positive cells in the ONL. Data are expressed as mean ± SEM and analyzed using one-way ANOVA with Holm-Sidak correction for multiple comparisons; n = 5-6 per group. ****$p < 0.0001$. (**C**) Spider-graph quantification of ONL thickness on DAPI-stained retinal sections from control and sodium iodate-treated animals treated with vehicle, emricasan, UH15-38, or a combination of both drugs. (**D**) Statistical analysis was performed using the area under the curve values. Data are expressed as mean ± SEM and analyzed using one-way ANOVA with Holm-Sidak correction for multiple comparisons; n = 5-11. ****$p < 0.0001$, ***$p < 0.001$.

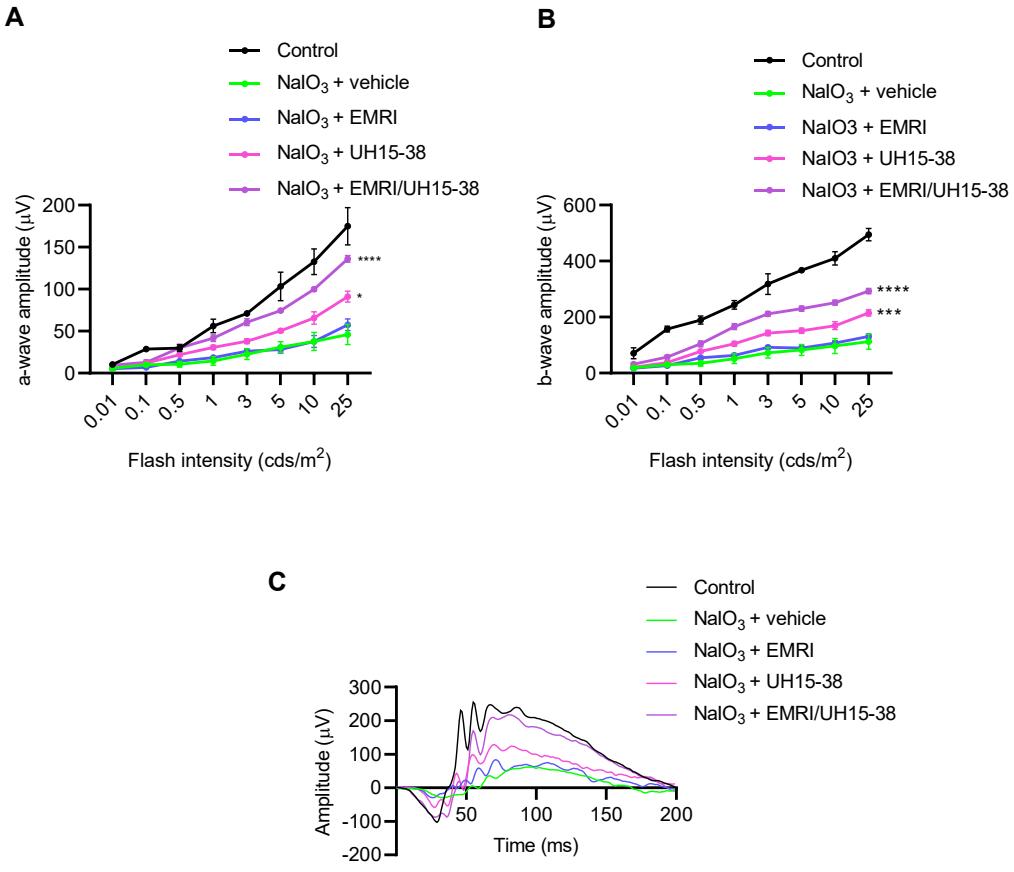

Figure 4. Preservation of retinal function by the RIPK3 modulator UH15-38. Quantification of (**A**) a-wave amplitude and (**B**) b-wave amplitude of control, and sodium iodate-treated mice treated or not with vehicle, emricasan, UH15-38, or emricasan + UH15-38. Data are expressed as mean ± SEM and analyzed using two-way ANOVA with Holm-Sidak corrections for multiple comparisons; n = 5–10 per group. ****p < 0.0001, ***p < 0.001, *p < 0.05 compared to the vehicle group. (**C**) Representative waveforms of the electroretinogram recording at the flash intensity 5 cds/m^2 from control mice and from sodium iodate–injected mice treated with vehicle, emricasan, UH15-38, or UH15-38 + emricasan.

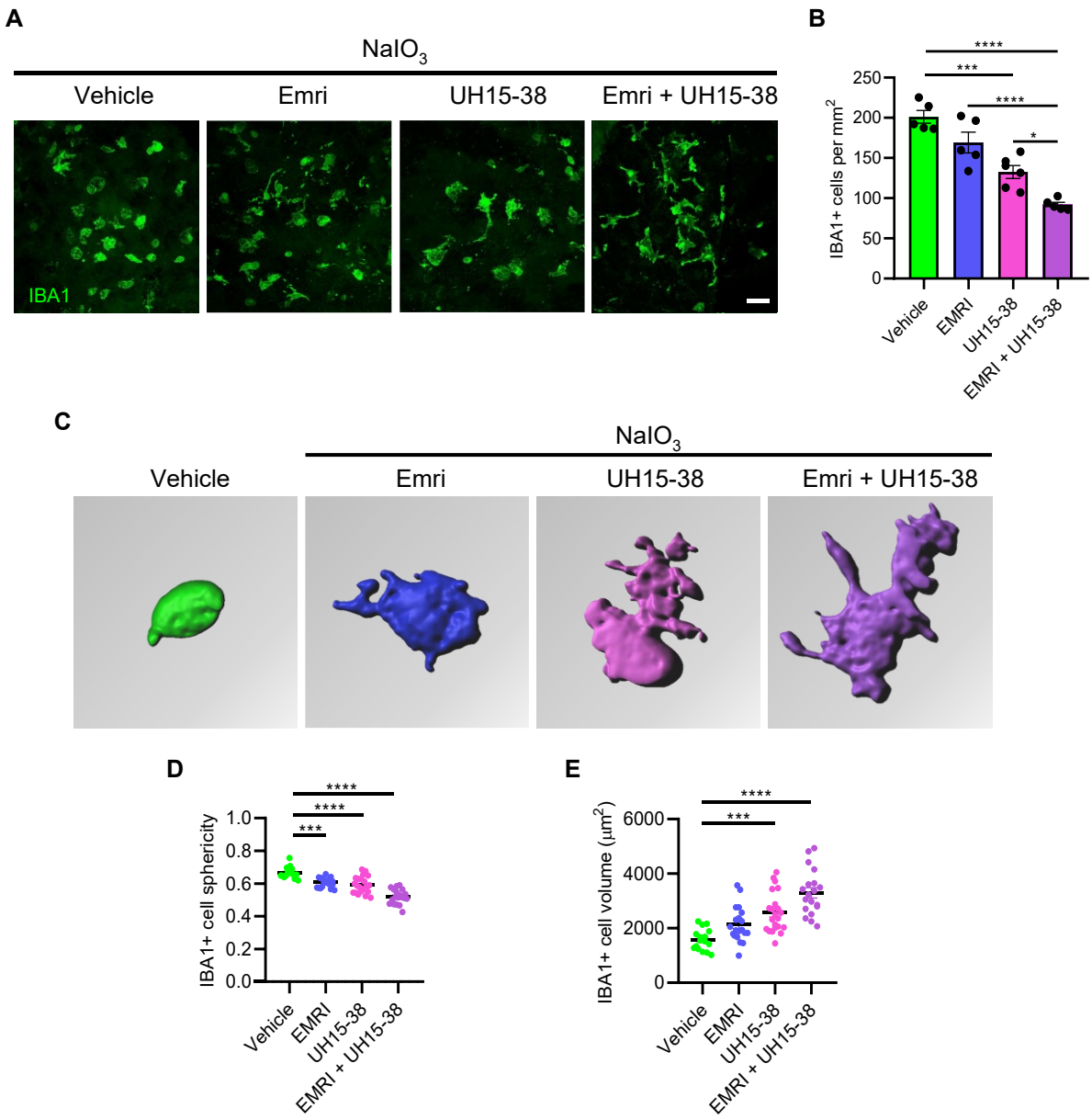

Figure 5. Subretinal mononuclear phagocyte infiltration in response to sodium iodate. (**A**) Representative images of RPE flat mounts showing infiltration of IBA1-labeled mononuclear phagocytes of sodium iodate-treated mice administered with vehicle, emricasan, UH15-38, or emricasan + UH15-38. Scale bar: 20 µm. (**B**) Graph representing compiled data on IBA1+ cell density in the subretina presented as a histogram. Data are expressed as mean ± SEM and analyzed by one-way ANOVA with Holm-Sidak corrections for multiple comparisons; n = 4–8 per group. ****p < 0.0001, ***p < 0.001, *p < 0.05. (**C**) Reconstructed images of a representative IBA1-positive cell. Imaris analysis of sphericity (**D**) and volume (**E**) of IBA1-positive cells. Data are expressed as mean ±

SEM and analyzed by one-way ANOVA with Holm-Sidak corrections for multiple comparisons; n = 16-22. ****p < 0.0001, ***p < 0.001.

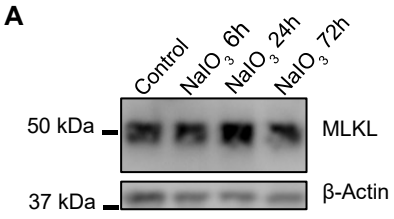
A
Control
NaIO3 6h
NaIO3 24h
NaIO3 72h
50 kDa
MLKL
37 kDa
β-Actin

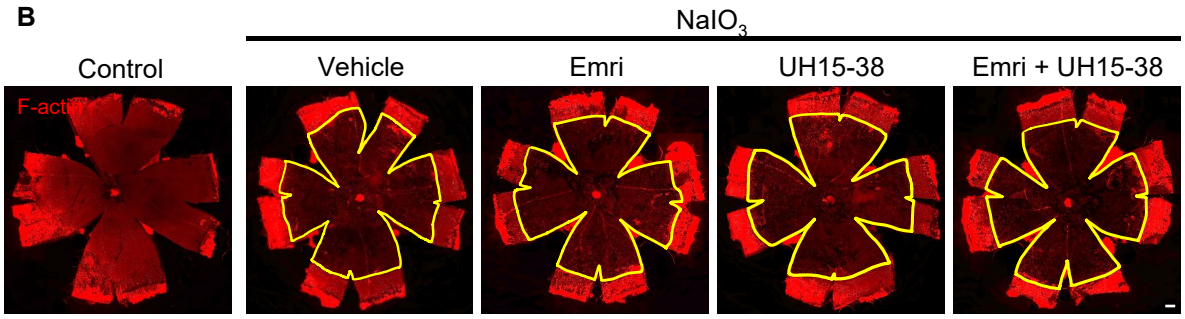
B
NaIO3
Control
Vehicle
Emri
UH15-38
Emri + UH15-38
F-actin

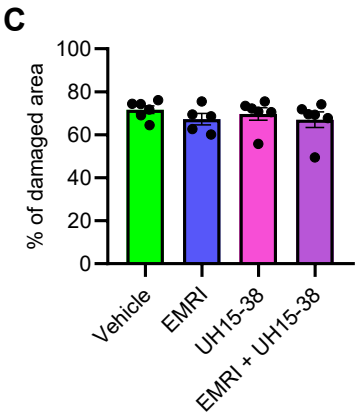
C
% of damaged area
100
80
60
40
20
0
Vehicle
EMRI
UH15-38
EMRI + UH15-38

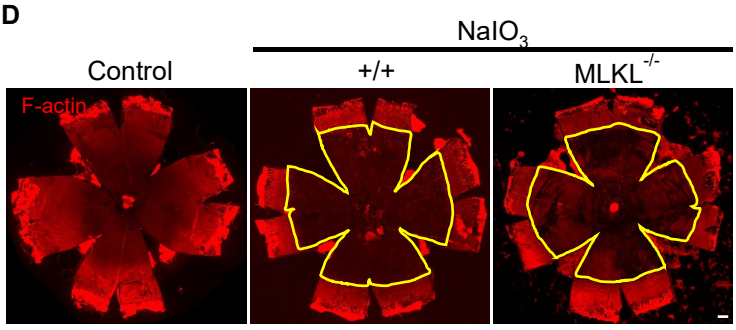
D
NaIO3
Control
+/+
MLKL-/-
F-actin

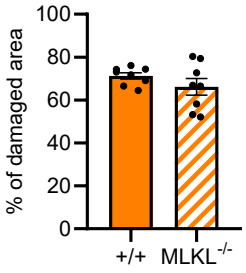
E
% of damaged area
100
80
60
40
20
0
+/+
MLKL-/-

Supplementary Figure 1. (**A**) Western blots showing the expression of MLKL, in RPE/choroid samples from sodium iodate-treated animals. (**B**) F-actin staining of flat-mounted eyecups to observe RPE damage from control and sodium iodate-treated mice administered with vehicle, emricasan, UH15-38, or emricasan + UH15-38. Scale bar: 200 μm. (**C**) Graph illustrating the damaged areas measured in eyecups; data were plotted as a percentage of the total area of RPE that was damaged. Data are expressed as mean ± SEM. n = 5-6. (**D**) F-actin staining of flat-mounted eyecups to observe RPE damage from control and sodium iodate-treated WT and MLKL KO mice. Scale bar: 200 μm. (**E**) Graph illustrating the damaged areas measured in eyecups from WT and MLKL KO mice. Data were plotted as a percentage of total damaged RPE morphology. Data are expressed as mean ± SEM. n = 8.

CHAPTER 7 – GENERAL DISCUSSION

7.1 Interplay between inflammation and cell death in neurodegeneration

Inflammation within the CNS, particularly in the retina, significantly threatens neuronal integrity due to the limited regenerative capacity of these cells. The CNS was once considered immune-privileged, suggesting isolation from immune activities. However, this notion is challenged by evidence that demonstrates complex communications between the CNS and the immune system. This interaction, mediated by cytokines, neurotransmitters, and trophic factors, is crucial for maintaining homeostasis and plays a key role in the pathogenesis of neurodegenerative diseases (439, 440). The relationship between cell death and inflammation is particularly noteworthy; they are interdependent processes that form core components of the innate immune response, working together to manage infection and repair tissue. Proper detection and response to pathological signals are vital for cellular equilibrium. Yet, when inflammatory reactions or cell death become uncontrolled, they can induce damage and contribute to neuronal loss (441). Additionally, the signaling functions of dying cells are significant and extend beyond marking the end of cellular life as they engage in essential communication with immune cells, influencing the recruitment and activity of these cells and thus modulating the scale and progression of the inflammatory response (442). In the aging or diseased retina, the interplay between these processes becomes even more critical, as the survival of photoreceptors is vulnerable to environmental and immune-related disturbances. Understanding the cell-cell interactions in the retina is essential for addressing various retinopathies.

7.2 Inflammation, IL-1, and AMD

The interplay between inflammation, IL-1, and AMD further exemplifies the critical roles of neuro-immune interactions and their impacts on photoreceptor health. MPs play a pivotal role in maintaining retinal integrity (443). In their quiescent state, they contribute to synaptic balance and debris clearance; however, when activated in response to cellular stress or damage, they can adopt a pro-inflammatory phenotype, characterized by the secretion of cytokines and chemokines. A number of studies revealed involvement of

components of innate-immune inflammation involving activation of the inflammasome and generation of IL-1 in AMD-associated neurodegeneration (292, 296, 444). In this thesis, we have elucidated the function of MP-derived IL-1β, demonstrating its capacity to influence astroglial cells, subsequently leading to photoreceptor toxicity. Activated MP-derived IL-1β can induce the death of photoreceptors directly by phagoptosis (260) or indirectly via excitotoxicity such as by glutamate release or iNOS overexpression (445, 446).

Furthermore, our findings indicate a remarkable heterogeneity among MP populations within the retina. Macrophages are highly adaptable, and depending on the signals they receive, they can adopt different activation states. Traditionally, they were classified as M1 (pro-inflammatory) or M2 (anti-inflammatory) (447). In inflammation, M1 macrophages produce pro-inflammatory cytokines and contribute to the elimination of pathogens, while M2 macrophages are involved in resolution of inflammation and tissue repair (448). However, it became evident that macrophage responses are more complex than this binary classification suggests. In fact, the emergence of single-cell technologies has revealed co-expression of M1 and M2 markers, contradicting the rigid categorization (449). Accordingly, this heterogeneity is highlighted in our study by the ability of MPs to produce IL-1, where it is specifically the perivascular macrophages that possess this ability, while it is essential to highlight that microglia appear to exert a protective function in the context of retinal degeneration (251, 450).

An important distinction arises between perivascular macrophages and microglia, the two primary types of resident macrophages within the retina. While extensive research has elucidated the diverse roles of microglia in retinal health, the specific contributions of perivascular macrophages have not been examined as much. Perivascular macrophages occupy a critical interface between the retinal parenchyma and blood circulation, suggesting a unique role and acting as initial responders in various neuroimmune interactions. In the brain, they have been implicated in regulating cerebrospinal fluid dynamics and maintaining brain homeostasis (451). Furthermore, they were shown to possess deleterious function in conditions like chronic hypertension (452), Alzheimer's disease (453), stroke, and experimental autoimmune encephalomyelitis (454), highlighting their impact on neuroinflammation and neurodegeneration. Yet, their

contribution to retinal health and pathology remains an interesting area of future investigations. Previously, the scarcity of specific tools has historically hampered the investigation into their specific role. However, advancements, including the development of specific markers and genetic models such as Mrc1^{CreERT2} and Lyve1^{CreERT2}-based reporter mice (233), offer new opportunities to probe the roles of perivascular macrophages in the retina. These tools can help delineate their interactions with endothelial cells, pericytes, and glial cells, which may illuminate their contributions to neurovascular integrity, inflammatory responses, and AMD pathogenesis.

Considering its central role, targeting IL-1 signaling presents a strategic approach to ameliorate AMD progression. Several pharmacological interventions have been developed to counteract IL-1β, including monoclonal antibodies and IL-1 receptor antagonists. Specifically, the allosteric modulation of the IL-1 receptor through rytvela has shown promising results, providing selective pathway modulation and preserving retinal integrity in ischemic/degenerative retinopathies (291, 455). To enhance the therapeutic potential of rytvela, optimizing its formulation for intravitreal injection can offer benefits. This entails improving the drug's stability, slowing its release, and ensuring its biocompatibility and biodegradability. Such improvements are expected to facilitate administration, paving the way for clinical trials. Additionally, structure-activity studies on rytvela derivatives have identified several candidates with heightened efficacy in ischemic retinopathies (456). These high-efficacy derivatives present themselves as promising leads for future therapeutic interventions, further strengthening the strategy to target IL-1 signaling in tackling AMD.

7.3 Glia at the crossroads of neuroimmune interactions

Glial cells are integral to the CNS, where they maintain homeostasis, support neurons, and participate in repair processes following injury (457). However, under certain circumstances when responding to injury or disease, these cells can undergo a transformation into reactive states, marked by significant morphological and molecular changes. This shift often changes their role from supportive entities to ones that can potentially harm, influencing their ability to protect or damage neurons (458). In the context of retinal degeneration, there is a notable activation of glial cells, namely

astrocytes and Muller cells. coinciding with the loss of photoreceptors (459, 460). We found that IL-1 signaling is central to this process, and its inhibition using rytvela effectively suppressed retinal gliosis in response to light exposure. Relevantly, a more recent study supported the significance of IL-1 signaling in the pathogenesis of late-stage neovascular AMD, primarily through stimulating the production of astrocyte-derived VEGF (461). IL-1 is a key player in inducing neurotoxic reactive astrocytes, which contribute to neuronal and oligodendrocyte death, potentially exacerbating CNS injuries and neurodegenerative diseases (462, 463).

Strikingly, interactions between microglia and astrocytes, mediated by IL-1 and IL-1R1, have been shown to offer protection against NMDA-induced neuronal death in the retina (464). This duality underscores the complex roles astrocytes can adopt in response to CNS injury, including secreting toxic mediators or, conversely, defending against and repairing damage through neurotrophic factors (465). This reactive versatility, especially in the face of chronic inflammation or neurodegenerative conditions, exemplifies the need for further investigation into the mechanisms governing astrocyte responses and their secretion of toxic substances. To deepen understanding of neuroinflammatory processes in AMD and the role of glia therein, exploring how IL-1 influences astrocyte activation states, secretion profiles, and interactions with other cell types is paramount. Leveraging advanced research tools, such as single-cell RNA sequencing and spatial transcriptomics, can shed light on the heterogeneity and functions of astrocytes within the diseased retina. These insights are crucial for developing strategies to modulate the pathogenesis of AMD. Recently, innovative screening techniques integrating CRISPR-Cas9 mutations, dual-cell culture within tiny droplets, and a microfluidic device for sorting based on fluorescence have emerged. One such technique, SPEAC-seq (systematic perturbation of encapsulated associated cells followed by sequencing), has facilitated new understanding of astrocyte–microglia interactions (466). This breakthrough tool paves the way for a better understanding of immuno-glial interactions within the retina and unraveling the complexities of the retinal diseases.

7.4 Mast cells and choroidal inflammation

Within the ocular environment, the choroid serves as an important immune niche, enriched with immune cells that foster an inflammatory setting, profoundly influencing retinal health. This region is instrumental in mediating immune responses, with mast cells playing a central role as initiators and sustainers of inflammation, directly affecting the neuroretina's integrity. The presence of these immune cells in the choroid underscores its significance in ocular immunology, with the inflammatory milieu they create being detrimental to retinal health. Disruptions in the RPE can compromise the outer blood-retinal barrier, signaling the immune system to potential hazards like infections or traumas, which could adversely affect the neuroretina. Mast cells, strategically positioned at key interfaces between the host and external environment, act as primary responders and initiators of inflammation. Their extensive distribution across the choroid points to a role in ocular immune defense (358). The involvement of mast cells in the immune response is particularly pronounced when the integrity of epithelial barriers is breached (467, 468, 469), a condition posited to elicit a type 2 inflammatory response. Historically perceived as a defense against parasites and venoms (470, 471), this response involves a variety of immune cells, including T helper 2 cells, innate lymphoid type 2 cells (ILC2), eosinophils, basophils, alternatively activated macrophages, and mast cells themselves, which may exert either protective or harmful effects contingent upon the specific context. Originally, type 2 immunity was thought to counterbalance the inflammation driven by type 1 responses. However, current understanding acknowledges that type 2 inflammation can arise from both structural and functional damage that compromise epithelial barriers (472). The dynamics between type 2 choroidal immune cells and disruptions in the RPE, and their subsequent impact on retinal inflammation, are an important area for further investigation.

7.5 Deciphering the role of choroidal mast cells in AMD pathogenesis

Evidence supporting the role of mast cells in the pathogenesis of AMD is illustrated by observations of their activation within the choroid of AMD patients (217). Upon activation, mast cells undergo degranulation, initiating a cascade of events characterized by the release of a variety of mediators, both pre-stored and synthesized de novo. This

includes histamine, proteases, cytokines, and lipid-derived substances such as prostaglandins and leukotrienes, contributing to inflammatory processes (473). In an attempt to delineate the influence of mast cell activation on the retina, experimental induction of degranulation in choroidal mast cells, using compound c48/80, has been shown to mimic features of geographic atrophy, including RPE degeneration, enhanced phagocyte recruitment, and photoreceptor loss (361). Building on these findings, we further investigated the implications of mast cells in the pathogenesis of AMD using a sodium iodate-induced model, which promotes RPE destruction through mechanisms involving oxidative stress. This model revealed mast cell activation as a pivotal event in disease progression, with depletion or stabilization of mast cells, as well as tryptase inhibition, leading to a reduction in infiltrating MPs and preservation of photoreceptor structure and function. This points to a critical crosstalk between choroidal mast cells and the subretina, allowing mast cell-derived mediators to diffuse to the subretina and impact subretinal immune cells. The broader significance of neuro-immune reactions at the CNS interfaces is increasingly recognized for its relevance to CNS diseases (474). Barrier dysfunction is closely associated with various neurological pathologies (475, 476). Notably, a compromised blood-brain barrier allows peripheral mediators, including those from mast cells, to influence brain-resident microglia and astrocytes (477). This insight highlights the potential for choroidal mast cell-derived soluble mediators to diffuse and act on subretinal MPs following the breakdown of the RPE.

Beyond contributing to non-resolving inflammation and geographic atrophy-like lesions, we report that mast cells are implicated in promoting choroidal angiogenesis. This is evident in the wound healing model of neovascularization, where mast cells were found to be a significant source of proangiogenic factors, including tryptase. Tryptase directly affects choroidal endothelial cells, fostering proangiogenic effects. Additionally, mast cells can exert indirect proangiogenic effects via granzyme B which degrades the antiangiogenic factor thrombospondin 1, thus promoting choroidal angiogenesis (478). Another noteworthy aspect of our study is the implication of mast cells in ECM remodeling, a critical process for the formation of choroidal neovessels. Mast cell proteases, by cleaving and activating matrix metalloproteases, disrupt ECM composition, facilitating endothelial cell migration and neovessel formation (140). Mast cell-derived granzyme B

has been demonstrated to cleave ECM proteins collagen IV, laminin-5, and fibronectin, implicating its role in ECM remodeling and its proangiogenic properties through such remodeling (479).

The interaction between mast cells and the RPE is complex and involves multiple biochemical signals. Oxidative stress can elevate the levels of certain mediators derived from the RPE such as IL-33 (480), an alarmin that signals tissue damage, as well as complement fragments C3a and C5a (481, 482), all of which are powerful triggers for mast cell activation. Mast cells, in response to these signals, can exacerbate damage to the RPE. Interestingly though, while mast cell tryptase has been observed to promote inflammation beneath the retina, it did not lead to degeneration of the RPE, which agrees with (483) but not (362). Nevertheless, mast cells release other factors that can affect the RPE. They store large amounts of preformed TNF, which they can rapidly release (484). This release of TNF can disrupt the structural integrity of the RPE and compromise its barrier function (485). Moreover, granzyme B has also been shown to disrupt the junctions between RPE cells (479). Thus, the bidirectional communication between mast cells and the RPE can be central events in the pathogenesis of AMD.

Collectively, we propose that mast cell activation, depending on the initial stimulus, leads to distinct outcomes in the context of AMD. While our findings confirm that tryptase plays a dual role in these processes, it is crucial to recognize that a variety of mast cell-derived factors contribute to the progression of the disease. More importantly, it is necessary to highlight that mast cells are not simply bipolar "on-off" cells, but they can tailor their responses based on the nature of the stimuli (486, 487), adding a layer of complexity to the understanding of their function and role in immune response and inflammation.

Our study leveraged $Kit^{W\text{-}sh/W\text{-}sh}$ mice to investigate mast cell functions, while acknowledging that these animals exhibit altered myelopoiesis, which results in an increased number of neutrophils (488, 489) and basophils (490) in addition to behaviour changes. Additionally, while mast cell stabilizers are targeted therapies, their broad-spectrum action may inadvertently affect other cell types, including neutrophils (491) and eosinophils (492). Nevertheless, combining genetic and pharmacological approaches

along with knock-in strategies provide robust frameworks to ascertain the roles of mast cells in this context.

Investigating the mechanisms underlying mast cell activation, particularly in the context of AMD, will help understand their regulatory dynamics in the choroid. Future research could leverage mast cell-deficient mice reconstituted with mast cells lacking specific receptors like IL-33R, C3aR, and MRGPRX2. Such an approach aims to clarify these cells' activation processes and functionalities. In fact, identifying how distinct activation pathways influence AMD pathophysiology may unveil novel intervention targets. Additionally, integrating single-cell RNA sequencing of sorted retinal MPs can provide an in-depth perspective on how mast cell activity affects the transcriptional landscape and functionalities of these immune cells.

7.6 Targeting mast cells in AMD

The involvement of mast cells in the pathogenesis of AMD presents a valuable therapeutic avenue. Anti-VEGF therapies, while transformative for neovascular AMD, carry the risk of promoting the development of geographic atrophy, and a subset of patients exhibit resistance to this line of treatment. A recent FDA-approved anti-complement 3 therapy for geographic atrophy has not shown substantial improvement and carries risks such as the development of neovascular lesions and vasculitis (493). Furthermore, the concurrent existence of dry and wet AMD forms within the same patient (494) complicates therapeutic interventions, necessitating precision in targeting specific lesion types. Mast cell activation in both clinical forms of AMD, highlights their centrality in the pathophysiology of the disease. Here, we show that mast cell stabilization confers retinal protection across both dry and wet AMD models, encouraging a paradigm shift toward targeting mast cells in an effort to halt AMD progression. Mast cell stabilizers inhibit cell degranulation by stabilizing the cell membrane, thereby preventing the release of various mediators, with yet unclear mechanisms of action (495). The mast cell stabilizers cromolyn and ketotifen are already approved and in use for asthma and rhinitis, allergic conjunctivitis (496, 497). Furthermore, the phase 3 clinical trial evaluating the efficacy of masitinib, a tyrosine kinase inhibitor that targets mast cells, in treating patients with mild-to-moderate Alzheimer's disease, has shown promising enhancements in cognitive

function (498), Given these observed benefits and the potential efficacy of such drugs in various neurodegenerative disorders, repurposing them holds significant promise. By repurposing such drugs, there is potential to mitigate the inflammatory responses, limit neovascular lesions, preserve photoreceptor integrity, and ultimately enhance visual function preservation in AMD patients.

7.7 Complex pathways of photoreceptor cell death in: from apoptosis to necroptosis and beyond

Vision loss in numerous retinal degenerative diseases is principally due to photoreceptor cell death. Gaining an understanding of the mechanisms that underlie this cell death is essential for the development of new therapeutic strategies targeting these diseases. While apoptosis was once deemed the predominant mechanism in retinal degeneration (499), this view has been questioned by various studies that investigated the role of caspase inhibitors. These studies have reported inconsistent neuroprotective effects (433, 434, 500), prompting a re-evaluation towards alternative death pathways. Our study identifies MLKL-driven necroptosis, facilitated by RIPK3 kinase activity, as a critical pathway contributing to photoreceptor demise, suggesting that RIPK3 inhibition could be a novel strategy for preserving retinal function and mitigating inflammation. We have employed a novel potent RIPK3 kinase inhibitor, UH15-38, which effectively and selectively blocks activation of necroptosis (unpublished). We demonstrated the potential of UH15-38 in preserving photoreceptor integrity. Notably, combining UH15-38 with caspase inhibitor emricasan yielded synergistic benefits, underscoring the complex interplay between different cell death processes. This finding aligns with evidence showing that inhibition of RIPK3 kinase using GSK' compounds can actually promote apoptosis (501). Of note, inhibiting caspases with emricasan alone did not effectively preserve retinal function. Given that RIPK3 is crucial for all established pathways of necroptosis, it is imperative to approach AMD treatment with a focus on leveraging RIPK3 kinase inhibitors like UH15-38. These inhibitors hold significant promise in mitigating the progression of the condition.

The necroptotic process leads to the release of DAMPs and other pro-inflammatory mediators, which in turn initiate an immune response and amplify tissue damage.

Specifically, molecules such as ATP (502), HMGB1 (503), and nucleic acids (504) can activate the inflammasome, leading to the secretion of IL-1β, a cytokine we discussed in Chapter 3 for its significant role in this context. By employing UH15-38, we observed a marked reduction in death, thereby mitigating the influx of MPs into the subretina. These observations are crucial as they establish a direct link between cell death and the inflammatory environment characteristic of AMD. They underscore the potential of controlling cell death to ameliorate inflammation. UH15-38 appears to interrupt this cycle by inhibiting necroptosis in compromised retinal cells. By curtailing necroptosis, UH15-38 consequently diminishes the release of DAMPs and other inflammatory agents from photoreceptors, which in turn lessens the recruitment of MPs to the retina. This reduction in necroinflammatory activity is likely to protect retinal tissue integrity and avert additional photoreceptor loss.

Interestingly, photoreceptors, akin to other cell types, are also susceptible to other forms of cell death, such as pyroptosis (505) and ferroptosis (506). Understanding why photoreceptors are particularly susceptible to certain cell death mechanisms remains a compelling area of interest. We anticipated that the assembly of each signalling complex for each form of cell death is tailored to the cell type, context, and specific trigger. Intriguingly, from an evolutionary standpoint, necroptosis is thought to be a defense mechanism against viral infections (507). This raises an interesting question: why do photoreceptors employ this specific cell death pathway? Susceptibility to various cell death pathways poses a significant challenge and should be taken into consideration in developing strategies to prevent cell death, since inhibiting one pathway may inadvertently activate another. For instance, this complexity is mirrored in the challenges faced when attempting to target apoptotic pathways through caspase inhibition. Despite the potential of caspase inhibitors demonstrated in preclinical studies, their translation into clinical use has been limited, mainly because impeding caspases could trigger other pathways of cell death or inflammation (508).

The simultaneous presence of several types of cell death, such as apoptosis, necroptosis, pyroptosis, and ferroptosis, each with distinct mechanisms, is understood to result in divergent outcomes. These different types of cell death are thought to influence one another in terms of how they affect adjacent cells and the inflammatory response,

thereby controlling the kinetics and degree of the inflammatory response (509). Thus, one can consider that the balance among these cell death processes can be linked to the control of inflammation and, by extension, the progression of retinal degenerative disorders. Nonetheless, it is crucial to recognize that even if, hypothetically, all known forms of cell death could be inhibited, this would not completely prevent cell death but would only delay the inevitable, as cells would eventually succumb to necrosis. This reality highlights the complexity inherent in developing treatments aimed at effectively preventing photoreceptor cell death in retinal degenerative disorders. Nevertheless, it is significant to note that while merely delaying cell death may not entirely prevent the loss of photoreceptor cells, such a postponement could be of clinical significance. Slowing down the progression of cell death could potentially extend the duration of functional vision for individuals with retinal degenerative conditions. This could prove especially advantageous for older adults, as preserving photoreceptor cells and sustaining good vision for a few extra years remains a valuable pursuit, with the potential to significantly impact their independence and quality of life.

While the study provides critical insights into the mechanisms underlying AMD and potential therapeutic targets, the translational relevance of findings from animal models to human disease remains a significant challenge. More specifically, it is unknown whether human photoreceptors are equipped with necroptotic machinery which may limit the direct applicability of RIPK3 inhibition to clinical settings. Furthermore, the therapeutic interventions explored, although promising in preclinical models, require rigorous validation in human trials to ascertain their efficacy and safety in AMD patients.

7.8 Concluding remarks

The landscape of retinal degenerative diseases, exemplified by AMD, is a complex interplay of neuroimmune interactions, inflammatory responses, and an array of cell death mechanisms. Understanding of the pathophysiology of AMD has significantly advanced, guiding the development of targeted therapeutic strategies. Among these, VEGF and complement inhibitors have shown promise and are advancing through various stages of clinical evaluation to mitigate AMD progression. Emerging therapies of complement inhibitors that are currently in various stages of development and clinical trials,

This thesis has dissected several aspects of AMD pathogenesis while identifying specific therapeutic targets. Firstly, the interplay between neurodegeneration and inflammation, notably via IL-1 signaling, underscores a viable therapeutic avenue, given its pivotal role in AMD. Secondly, our examination of mast cells elucidates their significant, yet dualistic, functions in retinal health and disease, suggesting that modulating their activity could offer benefits in AMD management. Thirdly, our findings on the concurrent engagement of apoptosis and necroptosis pathways illuminate the possibility of pharmacological intervention to prevent photoreceptor cell loss. Crucially, therapeutic strategies need not be singular in focus. A combined approach, targeting various AMD-associated pathways, could yield synergistic effects, providing comprehensive protection against retinal deterioration. The effectiveness of such therapies is intrinsically linked to the timing of intervention; early and precise identification of high-risk AMD patients is essential for optimizing treatment outcomes. Emerging technologies, particularly advanced imaging and artificial intelligence, are transforming our diagnostic capabilities, offering the promise of earlier detection and refined predictions of AMD progression. These innovations can greatly enhance patient monitoring and guide clinical decision-making. Furthermore, it is pertinent to consider the regeneration of postmitotic entities like photoreceptors as a critical goal. In this context, cell-based therapies, including induced pluripotent stem cell (iPSC) approaches, represent a frontier in regenerative medicine, holding the potential to replace lost or damaged retinal cells and restore visual function. In summary, the complexity of AMD requires a well-rounded therapeutic approach. Targeting key factors like inflammation and cell death at the right moments could enhance the effectiveness of new treatments, helping to slow retinal degeneration and preserve vision in AMD patients.

References

1. Campello L, Singh N, Advani J, Mondal AK, Corso-Diaz X, Swaroop A. Aging of the Retina: Molecular and Metabolic Turbulences and Potential Interventions. Annu Rev Vis Sci. 2021;7:633-64.
2. Brody BL, Gamst AC, Williams RA, Smith AR, Lau PW, Dolnak D, et al. Depression, visual acuity, comorbidity, and disability associated with age-related macular degeneration. Ophthalmology. 2001;108(10):1893-900; discussion 900-1.
3. Mitchell J, Bradley C. Quality of life in age-related macular degeneration: a review of the literature. Health Qual Life Outcomes. 2006;4:97.
4. Blindness GBD, Vision Impairment C, Vision Loss Expert Group of the Global Burden of Disease S. Causes of blindness and vision impairment in 2020 and trends over 30 years, and prevalence of avoidable blindness in relation to VISION 2020: the Right to Sight: an analysis for the Global Burden of Disease Study. Lancet Glob Health. 2021;9(2):e144-e60.
5. Russell SR, Mullins RF, Schneider BL, Hageman GS. Location, substructure, and composition of basal laminar drusen compared with drusen associated with aging and age-related macular degeneration. Am J Ophthalmol. 2000;129(2):205-14.
6. Guymer RH, Campbell TG. Age-related macular degeneration. Lancet. 2023;401(10386):1459-72.
7. Fleckenstein M, Keenan TDL, Guymer RH, Chakravarthy U, Schmitz-Valckenberg S, Klaver CC, et al. Age-related macular degeneration. Nat Rev Dis Primers. 2021;7(1):31.
8. Rivera JC, Dabouz R, Noueihed B, Omri S, Tahiri H, Chemtob S. Ischemic Retinopathies: Oxidative Stress and Inflammation. Oxid Med Cell Longev. 2017;2017:3940241.
9. Kauppinen A, Paterno JJ, Blasiak J, Salminen A, Kaarniranta K. Inflammation and its role in age-related macular degeneration. Cell Mol Life Sci. 2016;73(9):1765-86.
10. Khan H, Aziz AA, Sulahria H, Khan H, Ahmed A, Choudhry N, et al. Emerging Treatment Options for Geographic Atrophy (GA) Secondary to Age-Related Macular Degeneration. Clin Ophthalmol. 2023;17:321-7.

11. Liao DS, Grossi FV, El Mehdi D, Gerber MR, Brown DM, Heier JS, et al. Complement C3 Inhibitor Pegcetacoplan for Geographic Atrophy Secondary to Age-Related Macular Degeneration: A Randomized Phase 2 Trial. Ophthalmology. 2020;127(2):186-95.
12. Andersen SR. The eye and its diseases in Ancient Egypt. Acta Ophthalmol Scand. 1997;75(3):338-44.
13. Martin-Araguz A, Bustamante-Martinez C, Fernandez-Armayor Ajo V, Moreno-Martinez JM. [Neuroscience in Al Andalus and its influence on medieval scholastic medicine]. Rev Neurol. 2002;34(9):877-92.
14. Wedl C. Grundzüge der pathologischen Histologie. Wien: Gerold; 1854.
15. De Jong P. Elusive drusen and changing terminology of AMD. Eye (Lond). 2018;32(5):904-14.
16. de Jong PT. A Historical Analysis of the Quest for the Origins of Aging Macula Disorder, the Tissues Involved, and Its Terminology. Ophthalmol Eye Dis. 2016;8(Suppl 1):5-14.
17. Donders FC. Beiträge zur pathologischen Anatomie des Auges. Albrecht von Graefes Archiv für Ophthalmologie. 1855;2(1):106-18.
18. Müller H. Anatomische Beitrage zur Ophthalmologie - Untersuchungen uber die Glashaute des Auges, insbesondere die Glaslamelle der Choroidea und ihre senilen Veranderungen. Graefe's Arch Clin Exp Ophthalmol [Albrecht von Graefes Archiv Klin Exp Ophthalmol]. 1856;2:1-69.
19. Hutchinson J. Symmetrical central choroido-retinal disease occurring in senile persons. Royal London Ophthalmic Hospital Reports. 1875;8:231-44.
20. Pagenstecher HG, C. Atlas der Pathologischen Anatomie des Augapfels. Wiesbaden: CW Kreidel; 1875.
21. Sattler H. Ueber den feineren Bau der Choroidea des Menschen nebst Beiträgen zur pathologischen und vergleichenden Anatomie der Aderhaut. Albrecht von Graefes Archiv für Ophthalmologie. 1876;22(Pt 2):1-100.
22. Nettleship E. Central senile areolar choroidal atrophy. Transactions of the Ophthalmological Society of the United Kingdom. 1884;4:165-7.

23. Haab O. Erkrankungen der Macula lutea. Centralblat fur practische Augenheilkunde. 1885;9:383-4.
24. Haab O, De Schweinitz GE. Atlas and epitome of ophthalmoscopy and ophthalmoscopic diagnosis, ... Authorized tr. from the 3d rev. and enl. German ed. Philadelphia, London,: W.B. Saunders & company; 1901. 85 p. p.
25. Gass JD. Drusen and disciform macular detachment and degeneration. Arch Ophthalmol. 1973;90(3):206-17.
26. Wong WL, Su X, Li X, Cheung CM, Klein R, Cheng CY, et al. Global prevalence of age-related macular degeneration and disease burden projection for 2020 and 2040: a systematic review and meta-analysis. Lancet Glob Health. 2014;2(2):e106-16.
27. Bressler SB, Munoz B, Solomon SD, West SK, Salisbury Eye Evaluation Study T. Racial differences in the prevalence of age-related macular degeneration: the Salisbury Eye Evaluation (SEE) Project. Arch Ophthalmol. 2008;126(2):241-5.
28. Lambert NG, ElShelmani H, Singh MK, Mansergh FC, Wride MA, Padilla M, et al. Risk factors and biomarkers of age-related macular degeneration. Prog Retin Eye Res. 2016;54:64-102.
29. Rudnicka AR, Jarrar Z, Wormald R, Cook DG, Fletcher A, Owen CG. Age and gender variations in age-related macular degeneration prevalence in populations of European ancestry: a meta-analysis. Ophthalmology. 2012;119(3):571-80.
30. Smith W, Mitchell P, Leeder SR. Smoking and age-related maculopathy. The Blue Mountains Eye Study. Arch Ophthalmol. 1996;114(12):1518-23.
31. Smith W, Assink J, Klein R, Mitchell P, Klaver CC, Klein BE, et al. Risk factors for age-related macular degeneration: Pooled findings from three continents. Ophthalmology. 2001;108(4):697-704.
32. Keenan TD, Agron E, Mares J, Clemons TE, van Asten F, Swaroop A, et al. Adherence to the Mediterranean Diet and Progression to Late Age-Related Macular Degeneration in the Age-Related Eye Disease Studies 1 and 2. Ophthalmology. 2020;127(11):1515-28.
33. Merle BMJ, Colijn JM, Cougnard-Gregoire A, de Koning-Backus APM, Delyfer MN, Kiefte-de Jong JC, et al. Mediterranean Diet and Incidence of Advanced Age-Related Macular Degeneration: The EYE-RISK Consortium. Ophthalmology. 2019;126(3):381-90.

34. Mauschitz MM, Schmitz MT, Verzijden T, Schmid M, Thee EF, Colijn JM, et al. Physical Activity, Incidence, and Progression of Age-Related Macular Degeneration: A Multicohort Study. Am J Ophthalmol. 2022;236:99-106.
35. Seddon JM, Ajani UA, Mitchell BD. Familial aggregation of age-related maculopathy. Am J Ophthalmol. 1997;123(2):199-206.
36. Seddon JM, Cote J, Page WF, Aggen SH, Neale MC. The US twin study of age-related macular degeneration: relative roles of genetic and environmental influences. Arch Ophthalmol. 2005;123(3):321-7.
37. Klein RJ, Zeiss C, Chew EY, Tsai JY, Sackler RS, Haynes C, et al. Complement factor H polymorphism in age-related macular degeneration. Science. 2005;308(5720):385-9.
38. Edwards AO, Ritter R, 3rd, Abel KJ, Manning A, Panhuysen C, Farrer LA. Complement factor H polymorphism and age-related macular degeneration. Science. 2005;308(5720):421-4.
39. Haines JL, Hauser MA, Schmidt S, Scott WK, Olson LM, Gallins P, et al. Complement factor H variant increases the risk of age-related macular degeneration. Science. 2005;308(5720):419-21.
40. Dewan A, Liu M, Hartman S, Zhang SS, Liu DT, Zhao C, et al. HTRA1 promoter polymorphism in wet age-related macular degeneration. Science. 2006;314(5801):989-92.
41. Jakobsdottir J, Conley YP, Weeks DE, Mah TS, Ferrell RE, Gorin MB. Susceptibility genes for age-related maculopathy on chromosome 10q26. Am J Hum Genet. 2005;77(3):389-407.
42. Yang Z, Camp NJ, Sun H, Tong Z, Gibbs D, Cameron DJ, et al. A variant of the HTRA1 gene increases susceptibility to age-related macular degeneration. Science. 2006;314(5801):992-3.
43. Fritsche LG, Igl W, Bailey JN, Grassmann F, Sengupta S, Bragg-Gresham JL, et al. A large genome-wide association study of age-related macular degeneration highlights contributions of rare and common variants. Nat Genet. 2016;48(2):134-43.

44. Han X, Gharahkhani P, Mitchell P, Liew G, Hewitt AW, MacGregor S. Genome-wide meta-analysis identifies novel loci associated with age-related macular degeneration. J Hum Genet. 2020;65(8):657-65.
45. Liew G, Joachim N, Mitchell P, Burlutsky G, Wang JJ. Validating the AREDS Simplified Severity Scale of Age-Related Macular Degeneration with 5- and 10-Year Incident Data in a Population-Based Sample. Ophthalmology. 2016;123(9):1874-8.
46. Ferris FL, 3rd, Wilkinson CP, Bird A, Chakravarthy U, Chew E, Csaky K, et al. Clinical classification of age-related macular degeneration. Ophthalmology. 2013;120(4):844-51.
47. Mitchell P, Liew G, Gopinath B, Wong TY. Age-related macular degeneration. Lancet. 2018;392(10153):1147-59.
48. Wu Z, Luu CD, Ayton LN, Goh JK, Lucci LM, Hubbard WC, et al. Optical coherence tomography-defined changes preceding the development of drusen-associated atrophy in age-related macular degeneration. Ophthalmology. 2014;121(12):2415-22.
49. Blasiak J, Sobczuk P, Pawlowska E, Kaarniranta K. Interplay between aging and other factors of the pathogenesis of age-related macular degeneration. Ageing Res Rev. 2022;81:101735.
50. Feeney-Burns L, Hilderbrand ES, Eldridge S. Aging human RPE: morphometric analysis of macular, equatorial, and peripheral cells. Invest Ophthalmol Vis Sci. 1984;25(2):195-200.
51. Kaarniranta K, Uusitalo H, Blasiak J, Felszeghy S, Kannan R, Kauppinen A, et al. Mechanisms of mitochondrial dysfunction and their impact on age-related macular degeneration. Prog Retin Eye Res. 2020;79:100858.
52. Moore DJ, Clover GM. The effect of age on the macromolecular permeability of human Bruch's membrane. Invest Ophthalmol Vis Sci. 2001;42(12):2970-5.
53. Guymer R, Luthert P, Bird A. Changes in Bruch's membrane and related structures with age. Prog Retin Eye Res. 1999;18(1):59-90.
54. Booij JC, Baas DC, Beisekeeva J, Gorgels TG, Bergen AA. The dynamic nature of Bruch's membrane. Prog Retin Eye Res. 2010;29(1):1-18.
55. Curcio CA, Johnson M, Rudolf M, Huang JD. The oil spill in ageing Bruch membrane. Br J Ophthalmol. 2011;95(12):1638-45.

56. Curcio CA, Millican CL, Bailey T, Kruth HS. Accumulation of cholesterol with age in human Bruch's membrane. Invest Ophthalmol Vis Sci. 2001;42(1):265-74.
57. Moreira EF, Larrayoz IM, Lee JW, Rodriguez IR. 7-Ketocholesterol is present in lipid deposits in the primate retina: potential implication in the induction of VEGF and CNV formation. Invest Ophthalmol Vis Sci. 2009;50(2):523-32.
58. Handa JT, Verzijl N, Matsunaga H, Aotaki-Keen A, Lutty GA, te Koppele JM, et al. Increase in the advanced glycation end product pentosidine in Bruch's membrane with age. Invest Ophthalmol Vis Sci. 1999;40(3):775-9.
59. van der Schaft TL, Mooy CM, de Bruijn WC, Oron FG, Mulder PG, de Jong PT. Histologic features of the early stages of age-related macular degeneration. A statistical analysis. Ophthalmology. 1992;99(2):278-86.
60. Nivison-Smith L, Khandelwal N, Tong J, Mahajan S, Kalloniatis M, Agrawal R. Normal aging changes in the choroidal angioarchitecture of the macula. Sci Rep. 2020;10(1):10810.
61. Wakatsuki Y, Shinojima A, Kawamura A, Yuzawa M. Correlation of Aging and Segmental Choroidal Thickness Measurement using Swept Source Optical Coherence Tomography in Healthy Eyes. PLoS One. 2015;10(12):e0144156.
62. Mullins RF, Schoo DP, Sohn EH, Flamme-Wiese MJ, Workamelahu G, Johnston RM, et al. The membrane attack complex in aging human choriocapillaris: relationship to macular degeneration and choroidal thinning. Am J Pathol. 2014;184(11):3142-53.
63. Gao H, Hollyfield JG. Aging of the human retina. Differential loss of neurons and retinal pigment epithelial cells. Invest Ophthalmol Vis Sci. 1992;33(1):1-17.
64. Curcio CA, Millican CL, Allen KA, Kalina RE. Aging of the human photoreceptor mosaic: evidence for selective vulnerability of rods in central retina. Invest Ophthalmol Vis Sci. 1993;34(12):3278-96.
65. Jorge L, Canario N, Quental H, Bernardes R, Castelo-Branco M. Is the Retina a Mirror of the Aging Brain? Aging of Neural Retina Layers and Primary Visual Cortex Across the Lifespan. Front Aging Neurosci. 2019;11:360.
66. Ait-Ali N, Fridlich R, Millet-Puel G, Clerin E, Delalande F, Jaillard C, et al. Rod-derived cone viability factor promotes cone survival by stimulating aerobic glycolysis. Cell. 2015;161(4):817-32.

67. Joyal JS, Gantner ML, Smith LEH. Retinal energy demands control vascular supply of the retina in development and disease: The role of neuronal lipid and glucose metabolism. Prog Retin Eye Res. 2018;64:131-56.
68. Sies H. JD. Oxidative stress. In: G. F, editor. Encyclopedia of Stress. 3. 2nd ed. ed. Amsterdam: Elsevier; 2007. p. 45–8.
69. Schieber M, Chandel NS. ROS function in redox signaling and oxidative stress. Curr Biol. 2014;24(10):R453-62.
70. Beatty S, Koh H, Phil M, Henson D, Boulton M. The role of oxidative stress in the pathogenesis of age-related macular degeneration. Surv Ophthalmol. 2000;45(2):115-34.
71. Toma C, De Cilla S, Palumbo A, Garhwal DP, Grossini E. Oxidative and Nitrosative Stress in Age-Related Macular Degeneration: A Review of Their Role in Different Stages of Disease. Antioxidants (Basel). 2021;10(5).
72. Datta S, Cano M, Ebrahimi K, Wang L, Handa JT. The impact of oxidative stress and inflammation on RPE degeneration in non-neovascular AMD. Prog Retin Eye Res. 2017;60:201-18.
73. Holmstrom KM, Finkel T. Cellular mechanisms and physiological consequences of redox-dependent signalling. Nat Rev Mol Cell Biol. 2014;15(6):411-21.
74. Nita M, Grzybowski A. The Role of the Reactive Oxygen Species and Oxidative Stress in the Pathomechanism of the Age-Related Ocular Diseases and Other Pathologies of the Anterior and Posterior Eye Segments in Adults. Oxid Med Cell Longev. 2016;2016:3164734.
75. Winkler BS, Boulton ME, Gottsch JD, Sternberg P. Oxidative damage and age-related macular degeneration. Mol Vis. 1999;5:32.
76. Zhou J, Jang YP, Kim SR, Sparrow JR. Complement activation by photooxidation products of A2E, a lipofuscin constituent of the retinal pigment epithelium. Proc Natl Acad Sci U S A. 2006;103(44):16182-7.
77. Jabbehdari S, Handa JT. Oxidative stress as a therapeutic target for the prevention and treatment of early age-related macular degeneration. Surv Ophthalmol. 2021;66(3):423-40.
78. Handa JT. How does the macula protect itself from oxidative stress? Mol Aspects Med. 2012;33(4):418-35.

79. Yadav UC, Ramana KV. Regulation of NF-kappaB-induced inflammatory signaling by lipid peroxidation-derived aldehydes. Oxid Med Cell Longev. 2013;2013:690545.
80. Ambati J, Ambati BK, Yoo SH, Ianchulev S, Adamis AP. Age-related macular degeneration: etiology, pathogenesis, and therapeutic strategies. Surv Ophthalmol. 2003;48(3):257-93.
81. Feher J, Kovacs I, Artico M, Cavallotti C, Papale A, Balacco Gabrieli C. Mitochondrial alterations of retinal pigment epithelium in age-related macular degeneration. Neurobiol Aging. 2006;27(7):983-93.
82. Terluk MR, Kapphahn RJ, Soukup LM, Gong H, Gallardo C, Montezuma SR, et al. Investigating mitochondria as a target for treating age-related macular degeneration. J Neurosci. 2015;35(18):7304-11.
83. Nordgaard CL, Berg KM, Kapphahn RJ, Reilly C, Feng X, Olsen TW, et al. Proteomics of the retinal pigment epithelium reveals altered protein expression at progressive stages of age-related macular degeneration. Invest Ophthalmol Vis Sci. 2006;47(3):815-22.
84. Nordgaard CL, Karunadharma PP, Feng X, Olsen TW, Ferrington DA. Mitochondrial proteomics of the retinal pigment epithelium at progressive stages of age-related macular degeneration. Invest Ophthalmol Vis Sci. 2008;49(7):2848-55.
85. Galber C, Carissimi S, Baracca A, Giorgio V. The ATP Synthase Deficiency in Human Diseases. Life (Basel). 2021;11(4).
86. Voos W. Chaperone-protease networks in mitochondrial protein homeostasis. Biochim Biophys Acta. 2013;1833(2):388-99.
87. Bottinger L, Guiard B, Oeljeklaus S, Kulawiak B, Zufall N, Wiedemann N, et al. A complex of Cox4 and mitochondrial Hsp70 plays an important role in the assembly of the cytochrome c oxidase. Mol Biol Cell. 2013;24(17):2609-19.
88. Song J, Steidle L, Steymans I, Singh J, Sanner A, Bottinger L, et al. The mitochondrial Hsp70 controls the assembly of the F(1)F(O)-ATP synthase. Nat Commun. 2023;14(1):39.
89. Jin GF, Hurst JS, Godley BF. Rod outer segments mediate mitochondrial DNA damage and apoptosis in human retinal pigment epithelium. Curr Eye Res. 2001;23(1):11-9.

90. Godley BF, Shamsi FA, Liang FQ, Jarrett SG, Davies S, Boulton M. Blue light induces mitochondrial DNA damage and free radical production in epithelial cells. J Biol Chem. 2005;280(22):21061-6.
91. Kerur N, Fukuda S, Banerjee D, Kim Y, Fu D, Apicella I, et al. cGAS drives noncanonical-inflammasome activation in age-related macular degeneration. Nat Med. 2018;24(1):50-61.
92. Saada J, McAuley RJ, Marcatti M, Tang TZ, Motamedi M, Szczesny B. Oxidative stress induces Z-DNA-binding protein 1-dependent activation of microglia via mtDNA released from retinal pigment epithelial cells. J Biol Chem. 2022;298(1):101523.
93. Mitter SK, Song C, Qi X, Mao H, Rao H, Akin D, et al. Dysregulated autophagy in the RPE is associated with increased susceptibility to oxidative stress and AMD. Autophagy. 2014;10(11):1989-2005.
94. Golestaneh N, Chu Y, Xiao YY, Stoleru GL, Theos AC. Dysfunctional autophagy in RPE, a contributing factor in age-related macular degeneration. Cell Death Dis. 2017;8(1):e2537.
95. Wang AL, Lukas TJ, Yuan M, Du N, Tso MO, Neufeld AH. Autophagy and exosomes in the aged retinal pigment epithelium: possible relevance to drusen formation and age-related macular degeneration. PLoS One. 2009;4(1):e4160.
96. Zhu Y, Zhao KK, Tong Y, Zhou YL, Wang YX, Zhao PQ, et al. Exogenous NAD(+) decreases oxidative stress and protects H2O2-treated RPE cells against necrotic death through the up-regulation of autophagy. Sci Rep. 2016;6:26322.
97. Liu J, Copland DA, Theodoropoulou S, Chiu HA, Barba MD, Mak KW, et al. Impairing autophagy in retinal pigment epithelium leads to inflammasome activation and enhanced macrophage-mediated angiogenesis. Sci Rep. 2016;6:20639.
98. van Deursen JM. The role of senescent cells in ageing. Nature. 2014;509(7501):439-46.
99. Kozlowski MR. RPE cell senescence: a key contributor to age-related macular degeneration. Med Hypotheses. 2012;78(4):505-10.
100. Matsunaga H, Handa JT, Aotaki-Keen A, Sherwood SW, West MD, Hjelmeland LM. Beta-galactosidase histochemistry and telomere loss in senescent retinal pigment epithelial cells. Invest Ophthalmol Vis Sci. 1999;40(1):197-202.

101. Crespo-Garcia S, Tsuruda PR, Dejda A, Ryan RD, Fournier F, Chaney SY, et al. Pathological angiogenesis in retinopathy engages cellular senescence and is amenable to therapeutic elimination via BCL-xL inhibition. Cell Metab. 2021;33(4):818-32 e7.
102. Marazita MC, Dugour A, Marquioni-Ramella MD, Figueroa JM, Suburo AM. Oxidative stress-induced premature senescence dysregulates VEGF and CFH expression in retinal pigment epithelial cells: Implications for Age-related Macular Degeneration. Redox Biol. 2016;7:78-87.
103. Jadeja RN, Powell FL, Jones MA, Fuller J, Joseph E, Thounaojam MC, et al. Loss of NAMPT in aging retinal pigment epithelium reduces NAD(+) availability and promotes cellular senescence. Aging (Albany NY). 2018;10(6):1306-23.
104. Chae JB, Jang H, Son C, Park CW, Choi H, Jin S, et al. Targeting senescent retinal pigment epithelial cells facilitates retinal regeneration in mouse models of age-related macular degeneration. Geroscience. 2021;43(6):2809-33.
105. Campisi J, Andersen JK, Kapahi P, Melov S. Cellular senescence: a link between cancer and age-related degenerative disease? Semin Cancer Biol. 2011;21(6):354-9.
106. Al-Hussaini H, Kam JH, Vugler A, Semo M, Jeffery G. Mature retinal pigment epithelium cells are retained in the cell cycle and proliferate in vivo. Mol Vis. 2008;14:1784-91.
107. Zacks DN, Kocab AJ, Choi JJ, Gregory-Ksander MS, Cano M, Handa JT. Cell Death in AMD: The Rationale for Targeting Fas. J Clin Med. 2022;11(3).
108. Dunaief JL, Dentchev T, Ying GS, Milam AH. The role of apoptosis in age-related macular degeneration. Arch Ophthalmol. 2002;120(11):1435-42.
109. Kaneko H, Dridi S, Tarallo V, Gelfand BD, Fowler BJ, Cho WG, et al. DICER1 deficit induces Alu RNA toxicity in age-related macular degeneration. Nature. 2011;471(7338):325-30.
110. Bertheloot D, Latz E, Franklin BS. Necroptosis, pyroptosis and apoptosis: an intricate game of cell death. Cell Mol Immunol. 2021;18(5):1106-21.
111. Kim Y, Tarallo V, Kerur N, Yasuma T, Gelfand BD, Bastos-Carvalho A, et al. DICER1/Alu RNA dysmetabolism induces Caspase-8-mediated cell death in age-related macular degeneration. Proc Natl Acad Sci U S A. 2014;111(45):16082-7.

112. Gao J, Cui JZ, To E, Cao S, Matsubara JA. Evidence for the activation of pyroptotic and apoptotic pathways in RPE cells associated with NLRP3 inflammasome in the rodent eye. J Neuroinflammation. 2018;15(1):15.
113. Brandstetter C, Patt J, Holz FG, Krohne TU. Inflammasome priming increases retinal pigment epithelial cell susceptibility to lipofuscin phototoxicity by changing the cell death mechanism from apoptosis to pyroptosis. J Photochem Photobiol B. 2016;161:177-83.
114. Pasparakis M, Vandenabeele P. Necroptosis and its role in inflammation. Nature. 2015;517(7534):311-20.
115. Kim MH, Chung J, Yang JW, Chung SM, Kwag NH, Yoo JS. Hydrogen peroxide-induced cell death in a human retinal pigment epithelial cell line, ARPE-19. Korean J Ophthalmol. 2003;17(1):19-28.
116. Li GY, Fan B, Zheng YC. Calcium overload is a critical step in programmed necrosis of ARPE-19 cells induced by high-concentration H(2)O(2). Biomed Environ Sci. 2010;23(5):371-7.
117. Hanus J, Zhang H, Wang Z, Liu Q, Zhou Q, Wang S. Induction of necrotic cell death by oxidative stress in retinal pigment epithelial cells. Cell Death Dis. 2013;4(12):e965.
118. Hanus J, Anderson C, Sarraf D, Ma J, Wang S. Retinal pigment epithelial cell necroptosis in response to sodium iodate. Cell Death Discov. 2016;2:16054.
119. Murakami Y, Matsumoto H, Roh M, Giani A, Kataoka K, Morizane Y, et al. Programmed necrosis, not apoptosis, is a key mediator of cell loss and DAMP-mediated inflammation in dsRNA-induced retinal degeneration. Cell Death Differ. 2014;21(2):270-7.
120. Murphy JM, Czabotar PE, Hildebrand JM, Lucet IS, Zhang JG, Alvarez-Diaz S, et al. The pseudokinase MLKL mediates necroptosis via a molecular switch mechanism. Immunity. 2013;39(3):443-53.
121. Conrad M, Lorenz SM, Proneth B. Targeting Ferroptosis: New Hope for As-Yet-Incurable Diseases. Trends Mol Med. 2021;27(2):113-22.

122. Totsuka K, Ueta T, Uchida T, Roggia MF, Nakagawa S, Vavvas DG, et al. Oxidative stress induces ferroptotic cell death in retinal pigment epithelial cells. Exp Eye Res. 2019;181:316-24.
123. Liu B, Wang W, Shah A, Yu M, Liu Y, He L, et al. Sodium iodate induces ferroptosis in human retinal pigment epithelium ARPE-19 cells. Cell Death Dis. 2021;12(3):230.
124. Yang M, Tsui MG, Tsang JKW, Goit RK, Yao KM, So KF, et al. Involvement of FSP1-CoQ(10)-NADH and GSH-GPx-4 pathways in retinal pigment epithelium ferroptosis. Cell Death Dis. 2022;13(5):468.
125. McLeod DS, Grebe R, Bhutto I, Merges C, Baba T, Lutty GA. Relationship between RPE and choriocapillaris in age-related macular degeneration. Invest Ophthalmol Vis Sci. 2009;50(10):4982-91.
126. Mullins RF, Johnson MN, Faidley EA, Skeie JM, Huang J. Choriocapillaris vascular dropout related to density of drusen in human eyes with early age-related macular degeneration. Invest Ophthalmol Vis Sci. 2011;52(3):1606-12.
127. Bhutto IA, Baba T, Merges C, McLeod DS, Lutty GA. Low nitric oxide synthases (NOSs) in eyes with age-related macular degeneration (AMD). Exp Eye Res. 2010;90(1):155-67.
128. Grebe R, Mughal I, Bryden W, McLeod S, Edwards M, Hageman GS, et al. Ultrastructural analysis of submacular choriocapillaris and its transport systems in AMD and aged control eyes. Exp Eye Res. 2019;181:252-62.
129. Saint-Geniez M, Kurihara T, Sekiyama E, Maldonado AE, D'Amore PA. An essential role for RPE-derived soluble VEGF in the maintenance of the choriocapillaris. Proc Natl Acad Sci U S A. 2009;106(44):18751-6.
130. Yamazaki T, Koizumi H, Yamagishi T, Kinoshita S. Subfoveal choroidal thickness after ranibizumab therapy for neovascular age-related macular degeneration: 12-month results. Ophthalmology. 2012;119(8):1621-7.
131. Koizumi H, Kano M, Yamamoto A, Saito M, Maruko I, Kawasaki R, et al. Short-term changes in choroidal thickness after aflibercept therapy for neovascular age-related macular degeneration. Am J Ophthalmol. 2015;159(4):627-33.

132. Metelitsina TI, Grunwald JE, DuPont JC, Ying GS, Brucker AJ, Dunaief JL. Foveolar choroidal circulation and choroidal neovascularization in age-related macular degeneration. Invest Ophthalmol Vis Sci. 2008;49(1):358-63.
133. Grunwald JE, Metelitsina TI, Dupont JC, Ying GS, Maguire MG. Reduced foveolar choroidal blood flow in eyes with increasing AMD severity. Invest Ophthalmol Vis Sci. 2005;46(3):1033-8.
134. Carmeliet P, Jain RK. Molecular mechanisms and clinical applications of angiogenesis. Nature. 2011;473(7347):298-307.
135. Lee HW, Shin JH, Simons M. Flow goes forward and cells step backward: endothelial migration. Exp Mol Med. 2022;54(6):711-9.
136. Mongiat M, Andreuzzi E, Tarticchio G, Paulitti A. Extracellular Matrix, a Hard Player in Angiogenesis. Int J Mol Sci. 2016;17(11).
137. Page-McCaw A, Ewald AJ, Werb Z. Matrix metalloproteinases and the regulation of tissue remodelling. Nat Rev Mol Cell Biol. 2007;8(3):221-33.
138. Chung AS, Ferrara N. Developmental and pathological angiogenesis. Annu Rev Cell Dev Biol. 2011;27:563-84.
139. Eelen G, Treps L, Li X, Carmeliet P. Basic and Therapeutic Aspects of Angiogenesis Updated. Circ Res. 2020;127(2):310-29.
140. Edwards M, Lutty GA. Bruch's Membrane and the Choroid in Age-Related Macular Degeneration. Adv Exp Med Biol. 2021;1256:89-119.
141. Ferrara N. Vascular endothelial growth factor and age-related macular degeneration: from basic science to therapy. Nat Med. 2010;16(10):1107-11.
142. Ferrara N. Vascular endothelial growth factor: basic science and clinical progress. Endocr Rev. 2004;25(4):581-611.
143. Sengupta N, Caballero S, Mames RN, Butler JM, Scott EW, Grant MB. The role of adult bone marrow-derived stem cells in choroidal neovascularization. Invest Ophthalmol Vis Sci. 2003;44(11):4908-13.
144. Tomita M, Yamada H, Adachi Y, Cui Y, Yamada E, Higuchi A, et al. Choroidal neovascularization is provided by bone marrow cells. Stem Cells. 2004;22(1):21-6.

145. Sheridan CM, Rice D, Hiscott PS, Wong D, Kent DL. The presence of AC133-positive cells suggests a possible role of endothelial progenitor cells in the formation of choroidal neovascularization. Invest Ophthalmol Vis Sci. 2006;47(4):1642-5.
146. Okuno Y, Nakamura-Ishizu A, Kishi K, Suda T, Kubota Y. Bone marrow-derived cells serve as proangiogenic macrophages but not endothelial cells in wound healing. Blood. 2011;117(19):5264-72.
147. Grunewald M, Avraham I, Dor Y, Bachar-Lustig E, Itin A, Jung S, et al. VEGF-induced adult neovascularization: recruitment, retention, and role of accessory cells. Cell. 2006;124(1):175-89.
148. Purhonen S, Palm J, Rossi D, Kaskenpaa N, Rajantie I, Yla-Herttuala S, et al. Bone marrow-derived circulating endothelial precursors do not contribute to vascular endothelium and are not needed for tumor growth. Proc Natl Acad Sci U S A. 2008;105(18):6620-5.
149. Wakabayashi T, Naito H, Takara K, Kidoya H, Sakimoto S, Oshima Y, et al. Identification of vascular endothelial side population cells in the choroidal vessels and their potential role in age-related macular degeneration. Invest Ophthalmol Vis Sci. 2013;54(10):6686-93.
150. Seddon JM, George S, Rosner B, Rifai N. Progression of age-related macular degeneration: prospective assessment of C-reactive protein, interleukin 6, and other cardiovascular biomarkers. Arch Ophthalmol. 2005;123(6):774-82.
151. Guillonneau X, Eandi CM, Paques M, Sahel JA, Sapieha P, Sennlaub F. On phagocytes and macular degeneration. Prog Retin Eye Res. 2017;61:98-128.
152. Johnson LV, Leitner WP, Staples MK, Anderson DH. Complement activation and inflammatory processes in Drusen formation and age related macular degeneration. Exp Eye Res. 2001;73(6):887-96.
153. Coleman HR, Chan CC, Ferris FL, 3rd, Chew EY. Age-related macular degeneration. Lancet. 2008;372(9652):1835-45.
154. Maberley D. Pegaptanib for neovascular age-related macular degeneration. Issues Emerg Health Technol. 2005(76):1-4.

155. Behar-Cohen F, Dernigoghossian M, Andrieu-Soler C, Levy R, Cohen R, Zhao M. Potential antiedematous effects of intravitreous anti-VEGF, unrelated to VEGF neutralization. Drug Discov Today. 2019;24(8):1436-9.
156. Iqbal S, Lenz HJ. Integration of novel agents in the treatment of colorectal cancer. Cancer Chemother Pharmacol. 2004;54 Suppl 1:S32-9.
157. Avery RL, Pieramici DJ, Rabena MD, Castellarin AA, Nasir MA, Giust MJ. Intravitreal bevacizumab (Avastin) for neovascular age-related macular degeneration. Ophthalmology. 2006;113(3):363-72 e5.
158. Ferrara N, Damico L, Shams N, Lowman H, Kim R. Development of ranibizumab, an anti-vascular endothelial growth factor antigen binding fragment, as therapy for neovascular age-related macular degeneration. Retina. 2006;26(8):859-70.
159. Rosenfeld PJ, Brown DM, Heier JS, Boyer DS, Kaiser PK, Chung CY, et al. Ranibizumab for neovascular age-related macular degeneration. N Engl J Med. 2006;355(14):1419-31.
160. Papadopoulos N, Martin J, Ruan Q, Rafique A, Rosconi MP, Shi E, et al. Binding and neutralization of vascular endothelial growth factor (VEGF) and related ligands by VEGF Trap, ranibizumab and bevacizumab. Angiogenesis. 2012;15(2):171-85.
161. Heier JS, Brown DM, Chong V, Korobelnik JF, Kaiser PK, Nguyen QD, et al. Intravitreal aflibercept (VEGF trap-eye) in wet age-related macular degeneration. Ophthalmology. 2012;119(12):2537-48.
162. Heier JS, Khanani AM, Quezada Ruiz C, Basu K, Ferrone PJ, Brittain C, et al. Efficacy, durability, and safety of intravitreal faricimab up to every 16 weeks for neovascular age-related macular degeneration (TENAYA and LUCERNE): two randomised, double-masked, phase 3, non-inferiority trials. Lancet. 2022;399(10326):729-40.
163. Khanani AM, Thomas MJ, Aziz AA, Weng CY, Danzig CJ, Yiu G, et al. Review of gene therapies for age-related macular degeneration. Eye (Lond). 2022;36(2):303-11.
164. Grunwald JE, Daniel E, Huang J, Ying GS, Maguire MG, Toth CA, et al. Risk of geographic atrophy in the comparison of age-related macular degeneration treatments trials. Ophthalmology. 2014;121(1):150-61.

165. Grunwald JE, Pistilli M, Daniel E, Ying GS, Pan W, Jaffe GJ, et al. Incidence and Growth of Geographic Atrophy during 5 Years of Comparison of Age-Related Macular Degeneration Treatments Trials. Ophthalmology. 2017;124(1):97-104.
166. Daniel E, Toth CA, Grunwald JE, Jaffe GJ, Martin DF, Fine SL, et al. Risk of scar in the comparison of age-related macular degeneration treatments trials. Ophthalmology. 2014;121(3):656-66.
167. Rubner R, Li KV, Canto-Soler MV. Progress of clinical therapies for dry age-related macular degeneration. Int J Ophthalmol. 2022;15(1):157-66.
168. Jaffe GJ, Westby K, Csaky KG, Mones J, Pearlman JA, Patel SS, et al. C5 Inhibitor Avacincaptad Pegol for Geographic Atrophy Due to Age-Related Macular Degeneration: A Randomized Pivotal Phase 2/3 Trial. Ophthalmology. 2021;128(4):576-86.
169. Patel SS, Lally DR, Hsu J, Wykoff CC, Eichenbaum D, Heier JS, et al. Avacincaptad pegol for geographic atrophy secondary to age-related macular degeneration: 18-month findings from the GATHER1 trial. Eye (Lond). 2023.
170. Yeong JL, Loveman E, Colquitt JL, Royle P, Waugh N, Lois N. Visual cycle modulators versus placebo or observation for the prevention and treatment of geographic atrophy due to age-related macular degeneration. Cochrane Database Syst Rev. 2020;12:CD013154.
171. Sharma A, Jaganathan BG. Stem Cell Therapy for Retinal Degeneration: The Evidence to Date. Biologics. 2021;15:299-306.
172. Fernandez-Robredo P, Sancho A, Johnen S, Recalde S, Gama N, Thumann G, et al. Current treatment limitations in age-related macular degeneration and future approaches based on cell therapy and tissue engineering. J Ophthalmol. 2014;2014:510285.
173. Soundara Pandi SP, Ratnayaka JA, Lotery AJ, Teeling JL. Progress in developing rodent models of age-related macular degeneration (AMD). Exp Eye Res. 2021;203:108404.
174. Pennesi ME, Neuringer M, Courtney RJ. Animal models of age related macular degeneration. Mol Aspects Med. 2012;33(4):487-509.
175. Grimm C, Reme CE. Light Damage Models of Retinal Degeneration. Methods Mol Biol. 2019;1834:167-78.

176. Enzmann V, Row BW, Yamauchi Y, Kheirandish L, Gozal D, Kaplan HJ, et al. Behavioral and anatomical abnormalities in a sodium iodate-induced model of retinal pigment epithelium degeneration. Exp Eye Res. 2006;82(3):441-8.
177. Lambert V, Lecomte J, Hansen S, Blacher S, Gonzalez ML, Struman I, et al. Laser-induced choroidal neovascularization model to study age-related macular degeneration in mice. Nat Protoc. 2013;8(11):2197-211.
178. Chovatiya R, Medzhitov R. Stress, inflammation, and defense of homeostasis. Mol Cell. 2014;54(2):281-8.
179. Medzhitov R. Origin and physiological roles of inflammation. Nature. 2008;454(7203):428-35.
180. Chen GY, Nunez G. Sterile inflammation: sensing and reacting to damage. Nat Rev Immunol. 2010;10(12):826-37.
181. Takeuchi O, Akira S. Pattern recognition receptors and inflammation. Cell. 2010;140(6):805-20.
182. Meizlish ML, Franklin RA, Zhou X, Medzhitov R. Tissue Homeostasis and Inflammation. Annu Rev Immunol. 2021;39:557-81.
183. Nathan C, Ding A. Nonresolving inflammation. Cell. 2010;140(6):871-82.
184. Chen M, Luo C, Zhao J, Devarajan G, Xu H. Immune regulation in the aging retina. Prog Retin Eye Res. 2019;69:159-72.
185. Streilein JW. Ocular immune privilege: therapeutic opportunities from an experiment of nature. Nat Rev Immunol. 2003;3(11):879-89.
186. Niederkorn JY. See no evil, hear no evil, do no evil: the lessons of immune privilege. Nat Immunol. 2006;7(4):354-9.
187. Taylor AW. Ocular immune privilege. Eye (Lond). 2009;23(10):1885-9.
188. Streilein JW, Ma N, Wenkel H, Ng TF, Zamiri P. Immunobiology and privilege of neuronal retina and pigment epithelium transplants. Vision Res. 2002;42(4):487-95.
189. Griffith TS, Brunner T, Fletcher SM, Green DR, Ferguson TA. Fas ligand-induced apoptosis as a mechanism of immune privilege. Science. 1995;270(5239):1189-92.
190. Zamiri P, Sugita S, Streilein JW. Immunosuppressive properties of the pigmented epithelial cells and the subretinal space. Chem Immunol Allergy. 2007;92:86-93.

191. Levy O, Calippe B, Lavalette S, Hu SJ, Raoul W, Dominguez E, et al. Apolipoprotein E promotes subretinal mononuclear phagocyte survival and chronic inflammation in age-related macular degeneration. EMBO Mol Med. 2015;7(2):211-26.
192. Limatola C, Ransohoff RM. Modulating neurotoxicity through CX3CL1/CX3CR1 signaling. Front Cell Neurosci. 2014;8:229.
193. Combadiere C, Feumi C, Raoul W, Keller N, Rodero M, Pezard A, et al. CX3CR1-dependent subretinal microglia cell accumulation is associated with cardinal features of age-related macular degeneration. J Clin Invest. 2007;117(10):2920-8.
194. Franceschi C, Garagnani P, Parini P, Giuliani C, Santoro A. Inflammaging: a new immune-metabolic viewpoint for age-related diseases. Nat Rev Endocrinol. 2018;14(10):576-90.
195. Sennlaub F, Auvynet C, Calippe B, Lavalette S, Poupel L, Hu SJ, et al. CCR2(+) monocytes infiltrate atrophic lesions in age-related macular disease and mediate photoreceptor degeneration in experimental subretinal inflammation in Cx3cr1 deficient mice. EMBO Mol Med. 2013;5(11):1775-93.
196. Ambati J, Atkinson JP, Gelfand BD. Immunology of age-related macular degeneration. Nat Rev Immunol. 2013;13(6):438-51.
197. Penfold PL, Killingsworth MC, Sarks SH. Senile macular degeneration: the involvement of immunocompetent cells. Graefes Arch Clin Exp Ophthalmol. 1985;223(2):69-76.
198. Chen M, Xu H. Parainflammation, chronic inflammation, and age-related macular degeneration. J Leukoc Biol. 2015;98(5):713-25.
199. Tuo J, Grob S, Zhang K, Chan CC. Genetics of immunological and inflammatory components in age-related macular degeneration. Ocul Immunol Inflamm. 2012;20(1):27-36.
200. McKay GJ, Patterson CC, Chakravarthy U, Dasari S, Klaver CC, Vingerling JR, et al. Evidence of association of APOE with age-related macular degeneration: a pooled analysis of 15 studies. Hum Mutat. 2011;32(12):1407-16.
201. Beguier F, Housset M, Roubeix C, Augustin S, Zagar Y, Nous C, et al. The 10q26 Risk Haplotype of Age-Related Macular Degeneration Aggravates Subretinal Inflammation by Impairing Monocyte Elimination. Immunity. 2020;53(2):429-41 e8.

202. Ricklin D, Hajishengallis G, Yang K, Lambris JD. Complement: a key system for immune surveillance and homeostasis. Nat Immunol. 2010;11(9):785-97.
203. Anderson DH, Radeke MJ, Gallo NB, Chapin EA, Johnson PT, Curletti CR, et al. The pivotal role of the complement system in aging and age-related macular degeneration: hypothesis re-visited. Prog Retin Eye Res. 2010;29(2):95-112.
204. Calippe B, Augustin S, Beguier F, Charles-Messance H, Poupel L, Conart JB, et al. Complement Factor H Inhibits CD47-Mediated Resolution of Inflammation. Immunity. 2017;46(2):261-72.
205. Bora PS, Sohn JH, Cruz JM, Jha P, Nishihori H, Wang Y, et al. Role of complement and complement membrane attack complex in laser-induced choroidal neovascularization. J Immunol. 2005;174(1):491-7.
206. Nozaki M, Raisler BJ, Sakurai E, Sarma JV, Barnum SR, Lambris JD, et al. Drusen complement components C3a and C5a promote choroidal neovascularization. Proc Natl Acad Sci U S A. 2006;103(7):2328-33.
207. Enzbrenner A, Zulliger R, Biber J, Pousa AMQ, Schafer N, Stucki C, et al. Sodium Iodate-Induced Degeneration Results in Local Complement Changes and Inflammatory Processes in Murine Retina. Int J Mol Sci. 2021;22(17).
208. Katschke KJ, Jr., Xi H, Cox C, Truong T, Malato Y, Lee WP, et al. Classical and alternative complement activation on photoreceptor outer segments drives monocyte-dependent retinal atrophy. Sci Rep. 2018;8(1):7348.
209. Wang S, Du L, Yuan S, Peng GH. Complement C3a receptor inactivation attenuates retinal degeneration induced by oxidative damage. Front Neurosci. 2022;16:951491.
210. Gupta N, Brown KE, Milam AH. Activated microglia in human retinitis pigmentosa, late-onset retinal degeneration, and age-related macular degeneration. Exp Eye Res. 2003;76(4):463-71.
211. Lad EM, Cousins SW, Van Arnam JS, Proia AD. Abundance of infiltrating CD163+ cells in the retina of postmortem eyes with dry and neovascular age-related macular degeneration. Graefes Arch Clin Exp Ophthalmol. 2015;253(11):1941-5.

212. Ghosh S, Shang P, Yazdankhah M, Bhutto I, Hose S, Montezuma SR, et al. Activating the AKT2-nuclear factor-kappaB-lipocalin-2 axis elicits an inflammatory response in age-related macular degeneration. J Pathol. 2017;241(5):583-8.
213. Chen J, Zhao L, Ding X, Wen Y, Wang L, Shu Q, et al. Abeta1-40 Oligomers Trigger Neutrophil Extracellular Trap Formation through TLR4- and NADPH Oxidase-Dependent Pathways in Age-Related Macular Degeneration. Oxid Med Cell Longev. 2022;2022:6489923.
214. Lavalette S, Raoul W, Houssier M, Camelo S, Levy O, Calippe B, et al. Interleukin-1beta inhibition prevents choroidal neovascularization and does not exacerbate photoreceptor degeneration. Am J Pathol. 2011;178(5):2416-23.
215. Zhou J, Pham L, Zhang N, He S, Gamulescu MA, Spee C, et al. Neutrophils promote experimental choroidal neovascularization. Mol Vis. 2005;11:414-24.
216. Zhou J, He S, Zhang N, Spee C, Zhou P, Ryan SJ, et al. Neutrophils compromise retinal pigment epithelial barrier integrity. J Biomed Biotechnol. 2010;2010:289360.
217. Bhutto IA, McLeod DS, Jing T, Sunness JS, Seddon JM, Lutty GA. Increased choroidal mast cells and their degranulation in age-related macular degeneration. Br J Ophthalmol. 2016;100(5):720-6.
218. Coughlin B, Schnabolk G, Joseph K, Raikwar H, Kunchithapautham K, Johnson K, et al. Connecting the innate and adaptive immune responses in mouse choroidal neovascularization via the anaphylatoxin C5a and gammadeltaT-cells. Sci Rep. 2016;6:23794.
219. Zhao Z, Liang Y, Liu Y, Xu P, Flamme-Wiese MJ, Sun D, et al. Choroidal gammadelta T cells in protection against retinal pigment epithelium and retinal injury. FASEB J. 2017;31(11):4903-16.
220. Ezzat MK, Hann CR, Vuk-Pavlovic S, Pulido JS. Immune cells in the human choroid. Br J Ophthalmol. 2008;92(7):976-80.
221. Patel N, Ohbayashi M, Nugent AK, Ramchand K, Toda M, Chau KY, et al. Circulating anti-retinal antibodies as immune markers in age-related macular degeneration. Immunology. 2005;115(3):422-30.

222. Morohoshi K, Ohbayashi M, Patel N, Chong V, Bird AC, Ono SJ. Identification of anti-retinal antibodies in patients with age-related macular degeneration. Exp Mol Pathol. 2012;93(2):193-9.
223. Morohoshi K, Patel N, Ohbayashi M, Chong V, Grossniklaus HE, Bird AC, et al. Serum autoantibody biomarkers for age-related macular degeneration and possible regulators of neovascularization. Exp Mol Pathol. 2012;92(1):64-73.
224. Ginhoux F, Jung S. Monocytes and macrophages: developmental pathways and tissue homeostasis. Nat Rev Immunol. 2014;14(6):392-404.
225. Shi C, Pamer EG. Monocyte recruitment during infection and inflammation. Nat Rev Immunol. 2011;11(11):762-74.
226. Banchereau J, Steinman RM. Dendritic cells and the control of immunity. Nature. 1998;392(6673):245-52.
227. Merad M, Sathe P, Helft J, Miller J, Mortha A. The dendritic cell lineage: ontogeny and function of dendritic cells and their subsets in the steady state and the inflamed setting. Annu Rev Immunol. 2013;31:563-604.
228. Wynn TA, Chawla A, Pollard JW. Macrophage biology in development, homeostasis and disease. Nature. 2013;496(7446):445-55.
229. Ginhoux F, Greter M, Leboeuf M, Nandi S, See P, Gokhan S, et al. Fate mapping analysis reveals that adult microglia derive from primitive macrophages. Science. 2010;330(6005):841-5.
230. Paolicelli RC, Ferretti MT. Function and Dysfunction of Microglia during Brain Development: Consequences for Synapses and Neural Circuits. Front Synaptic Neurosci. 2017;9:9.
231. Prinz M, Priller J. Microglia and brain macrophages in the molecular age: from origin to neuropsychiatric disease. Nat Rev Neurosci. 2014;15(5):300-12.
232. Goldmann T, Wieghofer P, Jordao MJ, Prutek F, Hagemeyer N, Frenzel K, et al. Origin, fate and dynamics of macrophages at central nervous system interfaces. Nat Immunol. 2016;17(7):797-805.
233. Masuda T, Amann L, Monaco G, Sankowski R, Staszewski O, Krueger M, et al. Specification of CNS macrophage subsets occurs postnatally in defined niches. Nature. 2022;604(7907):740-8.

234. Lapenna A, De Palma M, Lewis CE. Perivascular macrophages in health and disease. Nat Rev Immunol. 2018;18(11):689-702.
235. Zheng L, Guo Y, Zhai X, Zhang Y, Chen W, Zhu Z, et al. Perivascular macrophages in the CNS: From health to neurovascular diseases. CNS Neurosci Ther. 2022;28(12):1908-20.
236. Hume DA, Perry VH, Gordon S. Immunohistochemical localization of a macrophage-specific antigen in developing mouse retina: phagocytosis of dying neurons and differentiation of microglial cells to form a regular array in the plexiform layers. J Cell Biol. 1983;97(1):253-7.
237. Rathnasamy G, Foulds WS, Ling EA, Kaur C. Retinal microglia - A key player in healthy and diseased retina. Prog Neurobiol. 2019;173:18-40.
238. Karlstetter M, Scholz R, Rutar M, Wong WT, Provis JM, Langmann T. Retinal microglia: just bystander or target for therapy? Prog Retin Eye Res. 2015;45:30-57.
239. Wang X, Zhao L, Zhang J, Fariss RN, Ma W, Kretschmer F, et al. Requirement for Microglia for the Maintenance of Synaptic Function and Integrity in the Mature Retina. J Neurosci. 2016;36(9):2827-42.
240. Rashid K, Akhtar-Schaefer I, Langmann T. Microglia in Retinal Degeneration. Front Immunol. 2019;10:1975.
241. McMenamin PG, Saban DR, Dando SJ. Immune cells in the retina and choroid: Two different tissue environments that require different defenses and surveillance. Prog Retin Eye Res. 2019;70:85-98.
242. Mendes-Jorge L, Ramos D, Luppo M, Llombart C, Alexandre-Pires G, Nacher V, et al. Scavenger function of resident autofluorescent perivascular macrophages and their contribution to the maintenance of the blood-retinal barrier. Invest Ophthalmol Vis Sci. 2009;50(12):5997-6005.
243. Kumar A, Zhao L, Fariss RN, McMenamin PG, Wong WT. Vascular associations and dynamic process motility in perivascular myeloid cells of the mouse choroid: implications for function and senescent change. Invest Ophthalmol Vis Sci. 2014;55(3):1787-96.
244. Chinnery HR, McMenamin PG, Dando SJ. Macrophage physiology in the eye. Pflugers Arch. 2017;469(3-4):501-15.

245. McMenamin PG. Dendritic cells and macrophages in the uveal tract of the normal mouse eye. Br J Ophthalmol. 1999;83(5):598-604.
246. Droho S, Perlman H, Lavine JA. Dendritic cells play no significant role in the laser-induced choroidal neovascularization model. Sci Rep. 2021;11(1):17254.
247. Forrester JV, Xu H, Kuffova L, Dick AD, McMenamin PG. Dendritic cell physiology and function in the eye. Immunol Rev. 2010;234(1):282-304.
248. Yu C, Roubeix C, Sennlaub F, Saban DR. Microglia versus Monocytes: Distinct Roles in Degenerative Diseases of the Retina. Trends Neurosci. 2020;43(6):433-49.
249. McLeod DS, Bhutto I, Edwards MM, Silver RE, Seddon JM, Lutty GA. Distribution and Quantification of Choroidal Macrophages in Human Eyes With Age-Related Macular Degeneration. Invest Ophthalmol Vis Sci. 2016;57(14):5843-55.
250. Damani MR, Zhao L, Fontainhas AM, Amaral J, Fariss RN, Wong WT. Age-related alterations in the dynamic behavior of microglia. Aging Cell. 2011;10(2):263-76.
251. O'Koren EG, Yu C, Klingeborn M, Wong AYW, Prigge CL, Mathew R, et al. Microglial Function Is Distinct in Different Anatomical Locations during Retinal Homeostasis and Degeneration. Immunity. 2019;50(3):723-37 e7.
252. Ma W, Zhang Y, Gao C, Fariss RN, Tam J, Wong WT. Monocyte infiltration and proliferation reestablish myeloid cell homeostasis in the mouse retina following retinal pigment epithelial cell injury. Sci Rep. 2017;7(1):8433.
253. Kohno H, Koso H, Okano K, Sundermeier TR, Saito S, Watanabe S, et al. Expression pattern of Ccr2 and Cx3cr1 in inherited retinal degeneration. J Neuroinflammation. 2015;12:188.
254. Bruban J, Maoui A, Chalour N, An N, Jonet L, Feumi C, et al. CCR2/CCL2-mediated inflammation protects photoreceptor cells from amyloid-beta-induced apoptosis. Neurobiol Dis. 2011;42(1):55-72.
255. Okunuki Y, Mukai R, Pearsall EA, Klokman G, Husain D, Park DH, et al. Microglia inhibit photoreceptor cell death and regulate immune cell infiltration in response to retinal detachment. Proc Natl Acad Sci U S A. 2018;115(27):E6264-E73.
256. Hu Z, Zhang Y, Wang J, Mao P, Lv X, Yuan S, et al. Knockout of Ccr2 alleviates photoreceptor cell death in rodent retina exposed to chronic blue light. Cell Death Dis. 2016;7(11):e2468.

257. Luhmann UF, Robbie S, Munro PM, Barker SE, Duran Y, Luong V, et al. The drusenlike phenotype in aging Ccl2-knockout mice is caused by an accelerated accumulation of swollen autofluorescent subretinal macrophages. Invest Ophthalmol Vis Sci. 2009;50(12):5934-43.
258. Tsutsumi C, Sonoda KH, Egashira K, Qiao H, Hisatomi T, Nakao S, et al. The critical role of ocular-infiltrating macrophages in the development of choroidal neovascularization. J Leukoc Biol. 2003;74(1):25-32.
259. Sakurai E, Anand A, Ambati BK, van Rooijen N, Ambati J. Macrophage depletion inhibits experimental choroidal neovascularization. Invest Ophthalmol Vis Sci. 2003;44(8):3578-85.
260. Zhao L, Zabel MK, Wang X, Ma W, Shah P, Fariss RN, et al. Microglial phagocytosis of living photoreceptors contributes to inherited retinal degeneration. EMBO Mol Med. 2015;7(9):1179-97.
261. Brown GC, Neher JJ. Microglial phagocytosis of live neurons. Nat Rev Neurosci. 2014;15(4):209-16.
262. Akdis M, Aab A, Altunbulakli C, Azkur K, Costa RA, Crameri R, et al. Interleukins (from IL-1 to IL-38), interferons, transforming growth factor beta, and TNF-alpha: Receptors, functions, and roles in diseases. J Allergy Clin Immunol. 2016;138(4):984-1010.
263. Dinarello CA, Renfer L, Wolff SM. Human leukocytic pyrogen: purification and development of a radioimmunoassay. Proc Natl Acad Sci U S A. 1977;74(10):4624-7.
264. Mantovani A, Dinarello CA, Molgora M, Garlanda C. Interleukin-1 and Related Cytokines in the Regulation of Inflammation and Immunity. Immunity. 2019;50(4):778-95.
265. Garlanda C, Dinarello CA, Mantovani A. The interleukin-1 family: back to the future. Immunity. 2013;39(6):1003-18.
266. Arend WP. The balance between IL-1 and IL-1Ra in disease. Cytokine Growth Factor Rev. 2002;13(4-5):323-40.
267. Dinarello CA. Biologic basis for interleukin-1 in disease. Blood. 1996;87(6):2095-147.
268. Schroder K, Tschopp J. The inflammasomes. Cell. 2010;140(6):821-32.

269. Lamkanfi M, Dixit VM. Mechanisms and functions of inflammasomes. Cell. 2014;157(5):1013-22.
270. Netea MG, van de Veerdonk FL, van der Meer JW, Dinarello CA, Joosten LA. Inflammasome-independent regulation of IL-1-family cytokines. Annu Rev Immunol. 2015;33:49-77.
271. Lopez-Castejon G, Brough D. Understanding the mechanism of IL-1beta secretion. Cytokine Growth Factor Rev. 2011;22(4):189-95.
272. Evavold CL, Ruan J, Tan Y, Xia S, Wu H, Kagan JC. The Pore-Forming Protein Gasdermin D Regulates Interleukin-1 Secretion from Living Macrophages. Immunity. 2018;48(1):35-44 e6.
273. Monteleone M, Stanley AC, Chen KW, Brown DL, Bezbradica JS, von Pein JB, et al. Interleukin-1beta Maturation Triggers Its Relocation to the Plasma Membrane for Gasdermin-D-Dependent and -Independent Secretion. Cell Rep. 2018;24(6):1425-33.
274. Zhou B, Abbott DW. Gasdermin E permits interleukin-1 beta release in distinct sublytic and pyroptotic phases. Cell Rep. 2021;35(2):108998.
275. Gutierrez KD, Davis MA, Daniels BP, Olsen TM, Ralli-Jain P, Tait SW, et al. MLKL Activation Triggers NLRP3-Mediated Processing and Release of IL-1beta Independently of Gasdermin-D. J Immunol. 2017;198(5):2156-64.
276. Tschopp J, Schroder K. NLRP3 inflammasome activation: The convergence of multiple signalling pathways on ROS production? Nat Rev Immunol. 2010;10(3):210-5.
277. Swanson KV, Deng M, Ting JP. The NLRP3 inflammasome: molecular activation and regulation to therapeutics. Nat Rev Immunol. 2019;19(8):477-89.
278. Lamkanfi M, Dixit VM. Inflammasomes and their roles in health and disease. Annu Rev Cell Dev Biol. 2012;28:137-61.
279. Boraschi D, Tagliabue A. The interleukin-1 receptor family. Semin Immunol. 2013;25(6):394-407.
280. Weber A, Wasiliew P, Kracht M. Interleukin-1 (IL-1) pathway. Sci Signal. 2010;3(105):cm1.
281. Gabay C, Lamacchia C, Palmer G. IL-1 pathways in inflammation and human diseases. Nat Rev Rheumatol. 2010;6(4):232-41.

282. Dinarello CA, Simon A, van der Meer JW. Treating inflammation by blocking interleukin-1 in a broad spectrum of diseases. Nat Rev Drug Discov. 2012;11(8):633-52.
283. Kenakin T. Emergent Concepts of Receptor Pharmacology. Handb Exp Pharmacol. 2019;260:17-41.
284. Christopoulos A. Allosteric binding sites on cell-surface receptors: novel targets for drug discovery. Nat Rev Drug Discov. 2002;1(3):198-210.
285. Saito A, Alvi S, Valant C, Christopoulos A, Carbone SE, Poole DP. Therapeutic potential of allosteric modulators for the treatment of gastrointestinal motility disorders. Br J Pharmacol. 2024;181(14):2232-46.
286. Christopoulos A. Advances in G protein-coupled receptor allostery: from function to structure. Mol Pharmacol. 2014;86(5):463-78.
287. Issafras H, Corbin JA, Goldfine ID, Roell MK. Detailed mechanistic analysis of gevokizumab, an allosteric anti-IL-1beta antibody with differential receptor-modulating properties. J Pharmacol Exp Ther. 2014;348(1):202-15.
288. Quiniou C, Sapieha P, Lahaie I, Hou X, Brault S, Beauchamp M, et al. Development of a novel noncompetitive antagonist of IL-1 receptor. J Immunol. 2008;180(10):6977-87.
289. Nadeau-Vallee M, Quiniou C, Palacios J, Hou X, Erfani A, Madaan A, et al. Novel Noncompetitive IL-1 Receptor-Biased Ligand Prevents Infection- and Inflammation-Induced Preterm Birth. J Immunol. 2015;195(7):3402-15.
290. Ranjbar M, Schneider T, Brand C, Grisanti S, Luke J, Luke M. The effect of anakinra on retinal function in isolated perfused vertebrate retina. J Curr Ophthalmol. 2017;29(1):69-71.
291. Beaudry-Richard A, Nadeau-Vallee M, Prairie E, Maurice N, Heckel E, Nezhady M, et al. Antenatal IL-1-dependent inflammation persists postnatally and causes retinal and sub-retinal vasculopathy in progeny. Sci Rep. 2018;8(1):11875.
292. Wooff Y, Man SM, Aggio-Bruce R, Natoli R, Fernando N. IL-1 Family Members Mediate Cell Death, Inflammation and Angiogenesis in Retinal Degenerative Diseases. Front Immunol. 2019;10:1618.
293. Ildefonso CJ, Biswal MR, Ahmed CM, Lewin AS. The NLRP3 Inflammasome and its Role in Age-Related Macular Degeneration. Adv Exp Med Biol. 2016;854:59-65.

294. Celkova L, Doyle SL, Campbell M. NLRP3 Inflammasome and Pathobiology in AMD. J Clin Med. 2015;4(1):172-92.
295. Hu SJ, Calippe B, Lavalette S, Roubeix C, Montassar F, Housset M, et al. Upregulation of P2RX7 in Cx3cr1-Deficient Mononuclear Phagocytes Leads to Increased Interleukin-1beta Secretion and Photoreceptor Neurodegeneration. J Neurosci. 2015;35(18):6987-96.
296. Tarallo V, Hirano Y, Gelfand BD, Dridi S, Kerur N, Kim Y, et al. DICER1 loss and Alu RNA induce age-related macular degeneration via the NLRP3 inflammasome and MyD88. Cell. 2012;149(4):847-59.
297. Liu RT, Gao J, Cao S, Sandhu N, Cui JZ, Chou CL, et al. Inflammatory mediators induced by amyloid-beta in the retina and RPE in vivo: implications for inflammasome activation in age-related macular degeneration. Invest Ophthalmol Vis Sci. 2013;54(3):2225-37.
298. Natoli R, Fernando N, Madigan M, Chu-Tan JA, Valter K, Provis J, et al. Microglia-derived IL-1beta promotes chemokine expression by Muller cells and RPE in focal retinal degeneration. Mol Neurodegener. 2017;12(1):31.
299. Eandi CM, Charles Messance H, Augustin S, Dominguez E, Lavalette S, Forster V, et al. Subretinal mononuclear phagocytes induce cone segment loss via IL-1beta. Elife. 2016;5.
300. Mellal K, Omri S, Mulumba M, Tahiri H, Fortin C, Dorion MF, et al. Immunometabolic modulation of retinal inflammation by CD36 ligand. Sci Rep. 2019;9(1):12903.
301. Crivellato E, Beltrami C, Mallardi F, Ribatti D. Paul Ehrlich's doctoral thesis: a milestone in the study of mast cells. Br J Haematol. 2003;123(1):19-21.
302. Galli SJ, Nakae S, Tsai M. Mast cells in the development of adaptive immune responses. Nat Immunol. 2005;6(2):135-42.
303. Galli SJ, Tsai M. IgE and mast cells in allergic disease. Nat Med. 2012;18(5):693-704.
304. Abraham SN, St John AL. Mast cell-orchestrated immunity to pathogens. Nat Rev Immunol. 2010;10(6):440-52.

305. Varricchi G, de Paulis A, Marone G, Galli SJ. Future Needs in Mast Cell Biology. Int J Mol Sci. 2019;20(18).
306. Jones MK, Nair A, Gupta M. Mast Cells in Neurodegenerative Disease. Front Cell Neurosci. 2019;13:171.
307. Valent P, Akin C, Sperr WR, Horny HP, Arock M, Metcalfe DD, et al. New Insights into the Pathogenesis of Mastocytosis: Emerging Concepts in Diagnosis and Therapy. Annu Rev Pathol. 2023;18:361-86.
308. Gupta K, Harvima IT. Mast cell-neural interactions contribute to pain and itch. Immunol Rev. 2018;282(1):168-87.
309. Florsheim EB, Bachtel ND, Cullen J, Lima BGC, Godazgar M, Carvalho F, et al. Immune sensing of food allergens promotes avoidance behaviour. Nature. 2023.
310. Plum T, Binzberger R, Thiele R, Shang F, Postrach D, Fung C, et al. Mast cells link immune sensing to antigen-avoidance behaviour. Nature. 2023.
311. Chia SL, Kapoor S, Carvalho C, Bajenoff M, Gentek R. Mast cell ontogeny: From fetal development to life-long health and disease. Immunol Rev. 2023;315(1):31-53.
312. Galli SJ, Gaudenzio N, Tsai M. Mast Cells in Inflammation and Disease: Recent Progress and Ongoing Concerns. Annu Rev Immunol. 2020;38:49-77.
313. St John AL, Rathore APS, Ginhoux F. New perspectives on the origins and heterogeneity of mast cells. Nat Rev Immunol. 2023;23(1):55-68.
314. Cildir G, Yip KH, Pant H, Tergaonkar V, Lopez AF, Tumes DJ. Understanding mast cell heterogeneity at single cell resolution. Trends Immunol. 2021;42(6):523-35.
315. Frossi B, Mion F, Sibilano R, Danelli L, Pucillo CEM. Is it time for a new classification of mast cells? What do we know about mast cell heterogeneity? Immunol Rev. 2018;282(1):35-46.
316. Wernersson S, Pejler G. Mast cell secretory granules: armed for battle. Nat Rev Immunol. 2014;14(7):478-94.
317. Iskarpatyoti JA, Shi J, Abraham MA, Rathore APS, Miao Y, Abraham SN. Mast cell regranulation requires a metabolic switch involving mTORC1 and a glucose-6-phosphate transporter. Cell Rep. 2022;40(13):111346.
318. Forsythe P. Mast Cells in Neuroimmune Interactions. Trends Neurosci. 2019;42(1):43-55.

319. Schafer B, Piliponsky AM, Oka T, Song CH, Gerard NP, Gerard C, et al. Mast cell anaphylatoxin receptor expression can enhance IgE-dependent skin inflammation in mice. J Allergy Clin Immunol. 2013;131(2):541-8 e1-9.
320. de Vries MR, Wezel A, Schepers A, van Santbrink PJ, Woodruff TM, Niessen HW, et al. Complement factor C5a as mast cell activator mediates vascular remodelling in vein graft disease. Cardiovasc Res. 2013;97(2):311-20.
321. Redegeld FA, Yu Y, Kumari S, Charles N, Blank U. Non-IgE mediated mast cell activation. Immunol Rev. 2018;282(1):87-113.
322. McNeil BD, Pundir P, Meeker S, Han L, Undem BJ, Kulka M, et al. Identification of a mast-cell-specific receptor crucial for pseudo-allergic drug reactions. Nature. 2015;519(7542):237-41.
323. Lansu K, Karpiak J, Liu J, Huang XP, McCorvy JD, Kroeze WK, et al. In silico design of novel probes for the atypical opioid receptor MRGPRX2. Nat Chem Biol. 2017;13(5):529-36.
324. Green DP, Limjunyawong N, Gour N, Pundir P, Dong X. A Mast-Cell-Specific Receptor Mediates Neurogenic Inflammation and Pain. Neuron. 2019;101(3):412-20 e3.
325. Olivera A, Beaven MA, Metcalfe DD. Mast cells signal their importance in health and disease. J Allergy Clin Immunol. 2018;142(2):381-93.
326. Church MK, Kolkhir P, Metz M, Maurer M. The role and relevance of mast cells in urticaria. Immunol Rev. 2018;282(1):232-47.
327. Moon TC, Befus AD, Kulka M. Mast cell mediators: their differential release and the secretory pathways involved. Front Immunol. 2014;5:569.
328. Mukai K, Tsai M, Saito H, Galli SJ. Mast cells as sources of cytokines, chemokines, and growth factors. Immunol Rev. 2018;282(1):121-50.
329. Theoharides TC, Alysandratos KD, Angelidou A, Delivanis DA, Sismanopoulos N, Zhang B, et al. Mast cells and inflammation. Biochim Biophys Acta. 2012;1822(1):21-33.
330. Weng Z, Zhang B, Tsilioni I, Theoharides TC. Nanotube Formation: A Rapid Form of "Alarm Signaling"? Clin Ther. 2016;38(5):1066-72.
331. Ahani E, Fereydouni M, Motaghed M, Kepley CL. Identification and Characterization of Tunneling Nanotubes Involved in Human Mast Cell FcepsilonRI-Mediated Apoptosis of Cancer Cells. Cancers (Basel). 2022;14(12).

332. von Kockritz-Blickwede M, Goldmann O, Thulin P, Heinemann K, Norrby-Teglund A, Rohde M, et al. Phagocytosis-independent antimicrobial activity of mast cells by means of extracellular trap formation. Blood. 2008;111(6):3070-80.
333. Groot Kormelink T, Arkesteijn GJ, van de Lest CH, Geerts WJ, Goerdayal SS, Altelaar MA, et al. Mast Cell Degranulation Is Accompanied by the Release of a Selective Subset of Extracellular Vesicles That Contain Mast Cell-Specific Proteases. J Immunol. 2016;197(8):3382-92.
334. McNeil HP, Adachi R, Stevens RL. Mast cell-restricted tryptases: structure and function in inflammation and pathogen defense. J Biol Chem. 2007;282(29):20785-9.
335. Sakai K, Ren S, Schwartz LB. A novel heparin-dependent processing pathway for human tryptase. Autocatalysis followed by activation with dipeptidyl peptidase I. J Clin Invest. 1996;97(4):988-95.
336. Ren S, Sakai K, Schwartz LB. Regulation of human mast cell beta-tryptase: conversion of inactive monomer to active tetramer at acid pH. J Immunol. 1998;160(9):4561-9.
337. Schwartz LB, Sakai K, Bradford TR, Ren S, Zweiman B, Worobec AS, et al. The alpha form of human tryptase is the predominant type present in blood at baseline in normal subjects and is elevated in those with systemic mastocytosis. J Clin Invest. 1995;96(6):2702-10.
338. Le QT, Gomez G, Zhao W, Hu J, Xia HZ, Fukuoka Y, et al. Processing of human protryptase in mast cells involves cathepsins L, B, and C. J Immunol. 2011;187(4):1912-8.
339. Schwartz LB, Bradford TR. Regulation of tryptase from human lung mast cells by heparin. Stabilization of the active tetramer. J Biol Chem. 1986;261(16):7372-9.
340. Pereira PJ, Bergner A, Macedo-Ribeiro S, Huber R, Matschiner G, Fritz H, et al. Human beta-tryptase is a ring-like tetramer with active sites facing a central pore. Nature. 1998;392(6673):306-11.
341. Sommerhoff CP, Bode W, Pereira PJ, Stubbs MT, Sturzebecher J, Piechottka GP, et al. The structure of the human betaII-tryptase tetramer: fo(u)r better or worse. Proc Natl Acad Sci U S A. 1999;96(20):10984-91.

342. Alter SC, Kramps JA, Janoff A, Schwartz LB. Interactions of human mast cell tryptase with biological protease inhibitors. Arch Biochem Biophys. 1990;276(1):26-31.
343. Marquardt U, Zettl F, Huber R, Bode W, Sommerhoff C. The crystal structure of human alpha1-tryptase reveals a blocked substrate-binding region. J Mol Biol. 2002;321(3):491-502.
344. Le QT, Lyons JJ, Naranjo AN, Olivera A, Lazarus RA, Metcalfe DD, et al. Impact of naturally forming human alpha/beta-tryptase heterotetramers in the pathogenesis of hereditary alpha-tryptasemia. J Exp Med. 2019;216(10):2348-61.
345. Hallgren J, Spillmann D, Pejler G. Structural requirements and mechanism for heparin-induced activation of a recombinant mouse mast cell tryptase, mouse mast cell protease-6: formation of active tryptase monomers in the presence of low molecular weight heparin. J Biol Chem. 2001;276(46):42774-81.
346. Hallgren J, Lindahl S, Pejler G. Structural requirements and mechanism for heparin-dependent activation and tetramerization of human betaI- and betaII-tryptase. J Mol Biol. 2005;345(1):129-39.
347. Fajardo I, Pejler G. Formation of active monomers from tetrameric human beta-tryptase. Biochem J. 2003;369(Pt 3):603-10.
348. Hallgren J, Pejler G. Biology of mast cell tryptase. An inflammatory mediator. FEBS J. 2006;273(9):1871-95.
349. Pejler G, Abrink M, Ringvall M, Wernersson S. Mast cell proteases. Adv Immunol. 2007;95:167-255.
350. Ossovskaya VS, Bunnett NW. Protease-activated receptors: contribution to physiology and disease. Physiol Rev. 2004;84(2):579-621.
351. Lefrancais E, Duval A, Mirey E, Roga S, Espinosa E, Cayrol C, et al. Central domain of IL-33 is cleaved by mast cell proteases for potent activation of group-2 innate lymphoid cells. Proc Natl Acad Sci U S A. 2014;111(43):15502-7.
352. Melo FR, Vita F, Berent-Maoz B, Levi-Schaffer F, Zabucchi G, Pejler G. Proteolytic histone modification by mast cell tryptase, a serglycin proteoglycan-dependent secretory granule protease. J Biol Chem. 2014;289(11):7682-90.

353. Melo FR, Wallerman O, Paivandy A, Calounova G, Gustafson AM, Sabari BR, et al. Tryptase-catalyzed core histone truncation: A novel epigenetic regulatory mechanism in mast cells. J Allergy Clin Immunol. 2017;140(2):474-85.
354. Pejler G, Ronnberg E, Waern I, Wernersson S. Mast cell proteases: multifaceted regulators of inflammatory disease. Blood. 2010;115(24):4981-90.
355. Lyons JJ, Yi T. Mast cell tryptases in allergic inflammation and immediate hypersensitivity. Curr Opin Immunol. 2021;72:94-106.
356. Lanzieri M, Cricchi M. Mast Cells and Vessels of the Choroid of Albino Guinea Pigs during the Uveal Anaphylactic Reaction. Arch Ophthalmol. 1965;74:367-70.
357. Larsen G. The mast cells in the uveal tract of the eye and changes induced by hormones and avitaminosis-C. Am J Ophthalmol. 1959;47(1 Pt 2):509-19.
358. McMenamin PG. The distribution of immune cells in the uveal tract of the normal eye. Eye (Lond). 1997;11 (Pt 2):183-93.
359. McLeod DS, Bhutto I, Edwards MM, Gedam M, Baldeosingh R, Lutty GA. Mast Cell-Derived Tryptase in Geographic Atrophy. Invest Ophthalmol Vis Sci. 2017;58(13):5887-96.
360. McHarg S, Booth L, Perveen R, Riba Garcia I, Brace N, Bayatti N, et al. Mast cell infiltration of the choroid and protease release are early events in age-related macular degeneration associated with genetic risk at both chromosomes 1q32 and 10q26. Proc Natl Acad Sci U S A. 2022;119(20):e2118510119.
361. Bousquet E, Zhao M, Thillaye-Goldenberg B, Lorena V, Castaneda B, Naud MC, et al. Choroidal mast cells in retinal pathology: a potential target for intervention. Am J Pathol. 2015;185(8):2083-95.
362. Ogura S, Baldeosingh R, Bhutto IA, Kambhampati SP, Scott McLeod D, Edwards MM, et al. A role for mast cells in geographic atrophy. FASEB J. 2020;34(8):10117-31.
363. Galluzzi L, Bravo-San Pedro JM, Vitale I, Aaronson SA, Abrams JM, Adam D, et al. Essential versus accessory aspects of cell death: recommendations of the NCCD 2015. Cell Death Differ. 2015;22(1):58-73.
364. Galluzzi L, Bravo-San Pedro JM, Kepp O, Kroemer G. Regulated cell death and adaptive stress responses. Cell Mol Life Sci. 2016;73(11-12):2405-10.

365. Vitale I, Pietrocola F, Guilbaud E, Aaronson SA, Abrams JM, Adam D, et al. Apoptotic cell death in disease-Current understanding of the NCCD 2023. Cell Death Differ. 2023;30(5):1097-154.
366. Galluzzi L, Vitale I, Aaronson SA, Abrams JM, Adam D, Agostinis P, et al. Molecular mechanisms of cell death: recommendations of the Nomenclature Committee on Cell Death 2018. Cell Death Differ. 2018;25(3):486-541.
367. Kerr JF, Wyllie AH, Currie AR. Apoptosis: a basic biological phenomenon with wide-ranging implications in tissue kinetics. Br J Cancer. 1972;26(4):239-57.
368. Elmore S. Apoptosis: a review of programmed cell death. Toxicol Pathol. 2007;35(4):495-516.
369. Boada-Romero E, Martinez J, Heckmann BL, Green DR. The clearance of dead cells by efferocytosis. Nat Rev Mol Cell Biol. 2020;21(7):398-414.
370. Chen KW, Demarco B, Heilig R, Shkarina K, Boettcher A, Farady CJ, et al. Extrinsic and intrinsic apoptosis activate pannexin-1 to drive NLRP3 inflammasome assembly. EMBO J. 2019;38(10).
371. Kesavardhana S, Malireddi RKS, Kanneganti TD. Caspases in Cell Death, Inflammation, and Pyroptosis. Annu Rev Immunol. 2020;38:567-95.
372. Alnemri ES, Livingston DJ, Nicholson DW, Salvesen G, Thornberry NA, Wong WW, et al. Human ICE/CED-3 protease nomenclature. Cell. 1996;87(2):171.
373. Ashkenazi A, Dixit VM. Death receptors: signaling and modulation. Science. 1998;281(5381):1305-8.
374. Ashkenazi A. Targeting death and decoy receptors of the tumour-necrosis factor superfamily. Nat Rev Cancer. 2002;2(6):420-30.
375. von Karstedt S, Montinaro A, Walczak H. Exploring the TRAILs less travelled: TRAIL in cancer biology and therapy. Nat Rev Cancer. 2017;17(6):352-66.
376. Gibert B, Mehlen P. Dependence Receptors and Cancer: Addiction to Trophic Ligands. Cancer Res. 2015;75(24):5171-5.
377. Brisset M, Grandin M, Bernet A, Mehlen P, Hollande F. Dependence receptors: new targets for cancer therapy. EMBO Mol Med. 2021;13(11):e14495.
378. Johnstone RW, Frew AJ, Smyth MJ. The TRAIL apoptotic pathway in cancer onset, progression and therapy. Nat Rev Cancer. 2008;8(10):782-98.

379. Wajant H. The Fas signaling pathway: more than a paradigm. Science. 2002;296(5573):1635-6.
380. Riley JS, Malik A, Holohan C, Longley DB. DED or alive: assembly and regulation of the death effector domain complexes. Cell Death Dis. 2015;6(8):e1866.
381. Aggarwal BB. Signalling pathways of the TNF superfamily: a double-edged sword. Nat Rev Immunol. 2003;3(9):745-56.
382. Ting AT, Bertrand MJM. More to Life than NF-kappaB in TNFR1 Signaling. Trends Immunol. 2016;37(8):535-45.
383. Peltzer N, Darding M, Walczak H. Holding RIPK1 on the Ubiquitin Leash in TNFR1 Signaling. Trends Cell Biol. 2016;26(6):445-61.
384. Micheau O, Tschopp J. Induction of TNF receptor I-mediated apoptosis via two sequential signaling complexes. Cell. 2003;114(2):181-90.
385. Brenner D, Blaser H, Mak TW. Regulation of tumour necrosis factor signalling: live or let die. Nat Rev Immunol. 2015;15(6):362-74.
386. Tsuchiya Y, Nakabayashi O, Nakano H. FLIP the Switch: Regulation of Apoptosis and Necroptosis by cFLIP. Int J Mol Sci. 2015;16(12):30321-41.
387. Hughes MA, Powley IR, Jukes-Jones R, Horn S, Feoktistova M, Fairall L, et al. Co-operative and Hierarchical Binding of c-FLIP and Caspase-8: A Unified Model Defines How c-FLIP Isoforms Differentially Control Cell Fate. Mol Cell. 2016;61(6):834-49.
388. Cullen SP, Martin SJ. Caspase activation pathways: some recent progress. Cell Death Differ. 2009;16(7):935-8.
389. Enari M, Sakahira H, Yokoyama H, Okawa K, Iwamatsu A, Nagata S. A caspase-activated DNase that degrades DNA during apoptosis, and its inhibitor ICAD. Nature. 1998;391(6662):43-50.
390. Segawa K, Kurata S, Yanagihashi Y, Brummelkamp TR, Matsuda F, Nagata S. Caspase-mediated cleavage of phospholipid flippase for apoptotic phosphatidylserine exposure. Science. 2014;344(6188):1164-8.
391. Segawa K, Kurata S, Nagata S. Human Type IV P-type ATPases That Work as Plasma Membrane Phospholipid Flippases and Their Regulation by Caspase and Calcium. J Biol Chem. 2016;291(2):762-72.

392. Suzuki J, Denning DP, Imanishi E, Horvitz HR, Nagata S. Xk-related protein 8 and CED-8 promote phosphatidylserine exposure in apoptotic cells. Science. 2013;341(6144):403-6.
393. Suzuki J, Imanishi E, Nagata S. Xkr8 phospholipid scrambling complex in apoptotic phosphatidylserine exposure. Proc Natl Acad Sci U S A. 2016;113(34):9509-14.
394. Sebbagh M, Renvoize C, Hamelin J, Riche N, Bertoglio J, Breard J. Caspase-3-mediated cleavage of ROCK I induces MLC phosphorylation and apoptotic membrane blebbing. Nat Cell Biol. 2001;3(4):346-52.
395. Singh R, Letai A, Sarosiek K. Regulation of apoptosis in health and disease: the balancing act of BCL-2 family proteins. Nat Rev Mol Cell Biol. 2019;20(3):175-93.
396. Youle RJ, Strasser A. The BCL-2 protein family: opposing activities that mediate cell death. Nat Rev Mol Cell Biol. 2008;9(1):47-59.
397. Bock FJ, Tait SWG. Mitochondria as multifaceted regulators of cell death. Nat Rev Mol Cell Biol. 2020;21(2):85-100.
398. Czabotar PE, Lessene G, Strasser A, Adams JM. Control of apoptosis by the BCL-2 protein family: implications for physiology and therapy. Nat Rev Mol Cell Biol. 2014;15(1):49-63.
399. Llambi F, Wang YM, Victor B, Yang M, Schneider DM, Gingras S, et al. BOK Is a Non-canonical BCL-2 Family Effector of Apoptosis Regulated by ER-Associated Degradation. Cell. 2016;165(2):421-33.
400. Tait SW, Green DR. Mitochondria and cell death: outer membrane permeabilization and beyond. Nat Rev Mol Cell Biol. 2010;11(9):621-32.
401. Degterev A, Huang Z, Boyce M, Li Y, Jagtap P, Mizushima N, et al. Chemical inhibitor of nonapoptotic cell death with therapeutic potential for ischemic brain injury. Nat Chem Biol. 2005;1(2):112-9.
402. Zhang W, Fan W, Guo J, Wang X. Osmotic stress activates RIPK3/MLKL-mediated necroptosis by increasing cytosolic pH through a plasma membrane Na(+)/H(+) exchanger. Sci Signal. 2022;15(734):eabn5881.
403. Yuan F, Cai J, Wu J, Tang Y, Zhao K, Liang F, et al. Z-DNA binding protein 1 promotes heatstroke-induced cell death. Science. 2022;376(6593):609-15.

404. Sun L, Wang H, Wang Z, He S, Chen S, Liao D, et al. Mixed lineage kinase domain-like protein mediates necrosis signaling downstream of RIP3 kinase. Cell. 2012;148(1-2):213-27.
405. Newton K, Wickliffe KE, Dugger DL, Maltzman A, Roose-Girma M, Dohse M, et al. Cleavage of RIPK1 by caspase-8 is crucial for limiting apoptosis and necroptosis. Nature. 2019;574(7778):428-31.
406. Fritsch M, Gunther SD, Schwarzer R, Albert MC, Schorn F, Werthenbach JP, et al. Caspase-8 is the molecular switch for apoptosis, necroptosis and pyroptosis. Nature. 2019;575(7784):683-7.
407. Grootjans S, Vanden Berghe T, Vandenabeele P. Initiation and execution mechanisms of necroptosis: an overview. Cell Death Differ. 2017;24(7):1184-95.
408. Vandenabeele P, Declercq W, Van Herreweghe F, Vanden Berghe T. The role of the kinases RIP1 and RIP3 in TNF-induced necrosis. Sci Signal. 2010;3(115):re4.
409. Cho YS, Challa S, Moquin D, Genga R, Ray TD, Guildford M, et al. Phosphorylation-driven assembly of the RIP1-RIP3 complex regulates programmed necrosis and virus-induced inflammation. Cell. 2009;137(6):1112-23.
410. Li J, McQuade T, Siemer AB, Napetschnig J, Moriwaki K, Hsiao YS, et al. The RIP1/RIP3 necrosome forms a functional amyloid signaling complex required for programmed necrosis. Cell. 2012;150(2):339-50.
411. Mompean M, Li W, Li J, Laage S, Siemer AB, Bozkurt G, et al. The Structure of the Necrosome RIPK1-RIPK3 Core, a Human Hetero-Amyloid Signaling Complex. Cell. 2018;173(5):1244-53 e10.
412. Chen X, Zhu R, Zhong J, Ying Y, Wang W, Cao Y, et al. Mosaic composition of RIP1-RIP3 signalling hub and its role in regulating cell death. Nat Cell Biol. 2022;24(4):471-82.
413. Laurien L, Nagata M, Schunke H, Delanghe T, Wiederstein JL, Kumari S, et al. Autophosphorylation at serine 166 regulates RIP kinase 1-mediated cell death and inflammation. Nat Commun. 2020;11(1):1747.
414. Raju S, Whalen DM, Mengistu M, Swanson C, Quinn JG, Taylor SS, et al. Kinase domain dimerization drives RIPK3-dependent necroptosis. Sci Signal. 2018;11(544).

415. Kaiser WJ, Sridharan H, Huang C, Mandal P, Upton JW, Gough PJ, et al. Toll-like receptor 3-mediated necrosis via TRIF, RIP3, and MLKL. J Biol Chem. 2013;288(43):31268-79.
416. Upton JW, Kaiser WJ, Mocarski ES. DAI/ZBP1/DLM-1 complexes with RIP3 to mediate virus-induced programmed necrosis that is targeted by murine cytomegalovirus vIRA. Cell Host Microbe. 2012;11(3):290-7.
417. Yang D, Liang Y, Zhao S, Ding Y, Zhuang Q, Shi Q, et al. ZBP1 mediates interferon-induced necroptosis. Cell Mol Immunol. 2020;17(4):356-68.
418. Maelfait J, Liverpool L, Bridgeman A, Ragan KB, Upton JW, Rehwinkel J. Sensing of viral and endogenous RNA by ZBP1/DAI induces necroptosis. EMBO J. 2017;36(17):2529-43.
419. Newton K, Wickliffe KE, Maltzman A, Dugger DL, Strasser A, Pham VC, et al. RIPK1 inhibits ZBP1-driven necroptosis during development. Nature. 2016;540(7631):129-33.
420. Lin J, Kumari S, Kim C, Van TM, Wachsmuth L, Polykratis A, et al. RIPK1 counteracts ZBP1-mediated necroptosis to inhibit inflammation. Nature. 2016;540(7631):124-8.
421. Rodriguez DA, Weinlich R, Brown S, Guy C, Fitzgerald P, Dillon CP, et al. Characterization of RIPK3-mediated phosphorylation of the activation loop of MLKL during necroptosis. Cell Death Differ. 2016;23(1):76-88.
422. Petrie EJ, Sandow JJ, Jacobsen AV, Smith BJ, Griffin MDW, Lucet IS, et al. Conformational switching of the pseudokinase domain promotes human MLKL tetramerization and cell death by necroptosis. Nat Commun. 2018;9(1):2422.
423. Davies KA, Tanzer MC, Griffin MDW, Mok YF, Young SN, Qin R, et al. The brace helices of MLKL mediate interdomain communication and oligomerisation to regulate cell death by necroptosis. Cell Death Differ. 2018;25(9):1567-80.
424. Hildebrand JM, Tanzer MC, Lucet IS, Young SN, Spall SK, Sharma P, et al. Activation of the pseudokinase MLKL unleashes the four-helix bundle domain to induce membrane localization and necroptotic cell death. Proc Natl Acad Sci U S A. 2014;111(42):15072-7.

425. Dondelinger Y, Declercq W, Montessuit S, Roelandt R, Goncalves A, Bruggeman I, et al. MLKL compromises plasma membrane integrity by binding to phosphatidylinositol phosphates. Cell Rep. 2014;7(4):971-81.
426. Chen X, Li W, Ren J, Huang D, He WT, Song Y, et al. Translocation of mixed lineage kinase domain-like protein to plasma membrane leads to necrotic cell death. Cell Res. 2014;24(1):105-21.
427. Cai Z, Jitkaew S, Zhao J, Chiang HC, Choksi S, Liu J, et al. Plasma membrane translocation of trimerized MLKL protein is required for TNF-induced necroptosis. Nat Cell Biol. 2014;16(1):55-65.
428. Gong YN, Guy C, Olauson H, Becker JU, Yang M, Fitzgerald P, et al. ESCRT-III Acts Downstream of MLKL to Regulate Necroptotic Cell Death and Its Consequences. Cell. 2017;169(2):286-300 e16.
429. Samson AL, Zhang Y, Geoghegan ND, Gavin XJ, Davies KA, Mlodzianoski MJ, et al. MLKL trafficking and accumulation at the plasma membrane control the kinetics and threshold for necroptosis. Nat Commun. 2020;11(1):3151.
430. Kayagaki N, Kornfeld OS, Lee BL, Stowe IB, O'Rourke K, Li Q, et al. NINJ1 mediates plasma membrane rupture during lytic cell death. Nature. 2021;591(7848):131-6.
431. Lohr HR, Kuntchithapautham K, Sharma AK, Rohrer B. Multiple, parallel cellular suicide mechanisms participate in photoreceptor cell death. Exp Eye Res. 2006;83(2):380-9.
432. Wenzel A, Grimm C, Samardzija M, Reme CE. Molecular mechanisms of light-induced photoreceptor apoptosis and neuroprotection for retinal degeneration. Prog Retin Eye Res. 2005;24(2):275-306.
433. Donovan M, Cotter TG. Caspase-independent photoreceptor apoptosis in vivo and differential expression of apoptotic protease activating factor-1 and caspase-3 during retinal development. Cell Death Differ. 2002;9(11):1220-31.
434. Perche O, Doly M, Ranchon-Cole I. Caspase-dependent apoptosis in light-induced retinal degeneration. Invest Ophthalmol Vis Sci. 2007;48(6):2753-9.

435. Doonan F, Donovan M, Cotter TG. Activation of multiple pathways during photoreceptor apoptosis in the rd mouse. Invest Ophthalmol Vis Sci. 2005;46(10):3530-8.
436. Trichonas G, Murakami Y, Thanos A, Morizane Y, Kayama M, Debouck CM, et al. Receptor interacting protein kinases mediate retinal detachment-induced photoreceptor necrosis and compensate for inhibition of apoptosis. Proc Natl Acad Sci U S A. 2010;107(50):21695-700.
437. Sanges D, Comitato A, Tammaro R, Marigo V. Apoptosis in retinal degeneration involves cross-talk between apoptosis-inducing factor (AIF) and caspase-12 and is blocked by calpain inhibitors. Proc Natl Acad Sci U S A. 2006;103(46):17366-71.
438. Pan C, Banerjee K, Lehmann GL, Almeida D, Hajjar KA, Benedicto I, et al. Lipofuscin causes atypical necroptosis through lysosomal membrane permeabilization. Proc Natl Acad Sci U S A. 2021;118(47).
439. Schiller M, Ben-Shaanan TL, Rolls A. Neuronal regulation of immunity: why, how and where? Nat Rev Immunol. 2021;21(1):20-36.
440. Dantzer R. Neuroimmune Interactions: From the Brain to the Immune System and Vice Versa. Physiol Rev. 2018;98(1):477-504.
441. Scheiblich H, Trombly M, Ramirez A, Heneka MT. Neuroimmune Connections in Aging and Neurodegenerative Diseases. Trends Immunol. 2020;41(4):300-12.
442. Zitvogel L, Kepp O, Kroemer G. Decoding cell death signals in inflammation and immunity. Cell. 2010;140(6):798-804.
443. Karg MM, Moorefield M, Hoffmann E, Philipose H, Krasniqi D, Hoppe C, et al. Microglia preserve visual function loss in the aging retina by supporting retinal pigment epithelial health. Immun Ageing. 2023;20(1):53.
444. Li B, Yang Z, Zhao X, Chen Y, Li D, Zhang L, et al. Early onset drusen and RPE dysfunction in a patient with NLRP3-AID. Ocul Immunol Inflamm. 2023;31(9):1877-80.
445. Brown GC, Vilalta A. How microglia kill neurons. Brain Res. 2015;1628(Pt B):288-97.
446. Charles-Messance H, Blot G, Couturier A, Vignaud L, Touhami S, Beguier F, et al. IL-1beta induces rod degeneration through the disruption of retinal glutamate homeostasis. J Neuroinflammation. 2020;17(1):1.

447. Murray PJ, Wynn TA. Protective and pathogenic functions of macrophage subsets. Nat Rev Immunol. 2011;11(11):723-37.
448. Murray PJ. Macrophage Polarization. Annu Rev Physiol. 2017;79:541-66.
449. Paolicelli RC, Sierra A, Stevens B, Tremblay ME, Aguzzi A, Ajami B, et al. Microglia states and nomenclature: A field at its crossroads. Neuron. 2022;110(21):3458-83.
450. Yu C, Lad EM, Mathew R, Shiraki N, Littleton S, Chen Y, et al. Microglia at sites of atrophy restrict the progression of retinal degeneration via galectin-3 and Trem2. J Exp Med. 2024;221(3).
451. Drieu A, Du S, Storck SE, Rustenhoven J, Papadopoulos Z, Dykstra T, et al. Parenchymal border macrophages regulate the flow dynamics of the cerebrospinal fluid. Nature. 2022;611(7936):585-93.
452. Faraco G, Sugiyama Y, Lane D, Garcia-Bonilla L, Chang H, Santisteban MM, et al. Perivascular macrophages mediate the neurovascular and cognitive dysfunction associated with hypertension. J Clin Invest. 2016;126(12):4674-89.
453. Park L, Uekawa K, Garcia-Bonilla L, Koizumi K, Murphy M, Pistik R, et al. Brain Perivascular Macrophages Initiate the Neurovascular Dysfunction of Alzheimer Abeta Peptides. Circ Res. 2017;121(3):258-69.
454. Jordao MJC, Sankowski R, Brendecke SM, Sagar, Locatelli G, Tai YH, et al. Single-cell profiling identifies myeloid cell subsets with distinct fates during neuroinflammation. Science. 2019;363(6425).
455. Rivera JC, Sitaras N, Noueihed B, Hamel D, Madaan A, Zhou T, et al. Microglia and interleukin-1beta in ischemic retinopathy elicit microvascular degeneration through neuronal semaphorin-3A. Arterioscler Thromb Vasc Biol. 2013;33(8):1881-91.
456. Geranurimi A, Cheng CWH, Quiniou C, Zhu T, Hou X, Rivera JC, et al. Probing Anti-inflammatory Properties Independent of NF-kappaB Through Conformational Constraint of Peptide-Based Interleukin-1 Receptor Biased Ligands. Front Chem. 2019;7:23.
457. Sofroniew MV, Vinters HV. Astrocytes: biology and pathology. Acta Neuropathol. 2010;119(1):7-35.
458. Patani R, Hardingham GE, Liddelow SA. Functional roles of reactive astrocytes in neuroinflammation and neurodegeneration. Nat Rev Neurol. 2023;19(7):395-409.

459. Fernandez-Sanchez L, Lax P, Campello L, Pinilla I, Cuenca N. Astrocytes and Muller Cell Alterations During Retinal Degeneration in a Transgenic Rat Model of Retinitis Pigmentosa. Front Cell Neurosci. 2015;9:484.
460. Bringmann A, Iandiev I, Pannicke T, Wurm A, Hollborn M, Wiedemann P, et al. Cellular signaling and factors involved in Muller cell gliosis: neuroprotective and detrimental effects. Prog Retin Eye Res. 2009;28(6):423-51.
461. Kuchroo M, DiStasio M, Song E, Calapkulu E, Zhang L, Ige M, et al. Single-cell analysis reveals inflammatory interactions driving macular degeneration. Nat Commun. 2023;14(1):2589.
462. Liddelow SA, Guttenplan KA, Clarke LE, Bennett FC, Bohlen CJ, Schirmer L, et al. Neurotoxic reactive astrocytes are induced by activated microglia. Nature. 2017;541(7638):481-7.
463. Rothhammer V, Borucki DM, Tjon EC, Takenaka MC, Chao CC, Ardura-Fabregat A, et al. Microglial control of astrocytes in response to microbial metabolites. Nature. 2018;557(7707):724-8.
464. Todd L, Palazzo I, Suarez L, Liu X, Volkov L, Hoang TV, et al. Reactive microglia and IL1beta/IL-1R1-signaling mediate neuroprotection in excitotoxin-damaged mouse retina. J Neuroinflammation. 2019;16(1):118.
465. Brandebura AN, Paumier A, Onur TS, Allen NJ. Astrocyte contribution to dysfunction, risk and progression in neurodegenerative disorders. Nat Rev Neurosci. 2023;24(1):23-39.
466. Wheeler MA, Clark IC, Lee HG, Li Z, Linnerbauer M, Rone JM, et al. Droplet-based forward genetic screening of astrocyte-microglia cross-talk. Science. 2023;379(6636):1023-30.
467. Altman MC, Lai Y, Nolin JD, Long S, Chen CC, Piliponsky AM, et al. Airway epithelium-shifted mast cell infiltration regulates asthmatic inflammation via IL-33 signaling. J Clin Invest. 2019;129(11):4979-91.
468. Kleuskens MTA, Bek MK, Al Halabi Y, Blokhuis BRJ, Diks MAP, Haasnoot ML, et al. Mast cells disrupt the function of the esophageal epithelial barrier. Mucosal Immunol. 2023;16(5):567-77.

469. McDermott JR, Bartram RE, Knight PA, Miller HR, Garrod DR, Grencis RK. Mast cells disrupt epithelial barrier function during enteric nematode infection. Proc Natl Acad Sci U S A. 2003;100(13):7761-6.
470. Akdis CA. Does the epithelial barrier hypothesis explain the increase in allergy, autoimmunity and other chronic conditions? Nat Rev Immunol. 2021;21(11):739-51.
471. Pothoven KL, Schleimer RP. The barrier hypothesis and Oncostatin M: Restoration of epithelial barrier function as a novel therapeutic strategy for the treatment of type 2 inflammatory disease. Tissue Barriers. 2017;5(3):e1341367.
472. Mamuladze T, Kipnis J. Type 2 immunity in the brain and brain borders. Cell Mol Immunol. 2023;20(11):1290-9.
473. Galli SJ, Kalesnikoff J, Grimbaldeston MA, Piliponsky AM, Williams CM, Tsai M. Mast cells as "tunable" effector and immunoregulatory cells: recent advances. Annu Rev Immunol. 2005;23:749-86.
474. Rustenhoven J, Kipnis J. Brain borders at the central stage of neuroimmunology. Nature. 2022;612(7940):417-29.
475. Sweeney MD, Zhao Z, Montagne A, Nelson AR, Zlokovic BV. Blood-Brain Barrier: From Physiology to Disease and Back. Physiol Rev. 2019;99(1):21-78.
476. Sweeney MD, Sagare AP, Zlokovic BV. Blood-brain barrier breakdown in Alzheimer disease and other neurodegenerative disorders. Nat Rev Neurol. 2018;14(3):133-50.
477. Lin CJ, Herisson F, Le H, Jaafar N, Chetal K, Oram MK, et al. Mast cell deficiency improves cognition and enhances disease-associated microglia in 5XFAD mice. Cell Rep. 2023;42(9):113141.
478. Obasanmi G, Zeglinski MR, Hardie E, Wilhelm AC, Turner CT, Hiroyasu S, et al. Granzyme B Contributes to Choroidal Neovascularization and Age-Related Macular Degeneration Through Proteolysis of Thrombospondin-1. Lab Invest. 2023;103(6):100123.
479. Matsubara JA, Tian Y, Cui JZ, Zeglinski MR, Hiroyasu S, Turner CT, et al. Retinal Distribution and Extracellular Activity of Granzyme B: A Serine Protease That Degrades Retinal Pigment Epithelial Tight Junctions and Extracellular Matrix Proteins. Front Immunol. 2020;11:574.

480. Xi H, Katschke KJ, Jr., Li Y, Truong T, Lee WP, Diehl L, et al. IL-33 amplifies an innate immune response in the degenerating retina. J Exp Med. 2016;213(2):189-207.
481. Wang Y, Shen H, Pang L, Qiu B, Yuan Y, Guan X, et al. Qihuang Granule protects the retinal pigment epithelium from oxidative stress via regulation of the alternative complement pathway. BMC Complement Med Ther. 2023;23(1):55.
482. Trakkides TO, Schafer N, Reichenthaler M, Kuhn K, Brandwijk R, Toonen EJM, et al. Oxidative Stress Increases Endogenous Complement-Dependent Inflammatory and Angiogenic Responses in Retinal Pigment Epithelial Cells Independently of Exogenous Complement Sources. Antioxidants (Basel). 2019;8(11).
483. Arai R, Usui-Ouchi A, Ito Y, Mashimo K, Murakami A, Ebihara N. Effects of Secreted Mast Cell Mediators on Retinal Pigment Epithelial Cells: Focus on Mast Cell Tryptase. Mediators Inflamm. 2017;2017:3124753.
484. Zhang B, Weng Z, Sismanopoulos N, Asadi S, Therianou A, Alysandratos KD, et al. Mitochondria distinguish granule-stored from de novo synthesized tumor necrosis factor secretion in human mast cells. Int Arch Allergy Immunol. 2012;159(1):23-32.
485. Touhami S, Beguier F, Augustin S, Charles-Messance H, Vignaud L, Nandrot EF, et al. Chronic exposure to tumor necrosis factor alpha induces retinal pigment epithelium cell dedifferentiation. J Neuroinflammation. 2018;15(1):85.
486. Gaudenzio N, Sibilano R, Marichal T, Starkl P, Reber LL, Cenac N, et al. Different activation signals induce distinct mast cell degranulation strategies. J Clin Invest. 2016;126(10):3981-98.
487. Meixiong J, Anderson M, Limjunyawong N, Sabbagh MF, Hu E, Mack MR, et al. Activation of Mast-Cell-Expressed Mas-Related G-Protein-Coupled Receptors Drives Non-histaminergic Itch. Immunity. 2019;50(5):1163-71 e5.
488. Nigrovic PA, Gray DH, Jones T, Hallgren J, Kuo FC, Chaletzky B, et al. Genetic inversion in mast cell-deficient (Wsh) mice interrupts corin and manifests as hematopoietic and cardiac aberrancy. Am J Pathol. 2008;173(6):1693-701.
489. Zhou JS, Xing W, Friend DS, Austen KF, Katz HR. Mast cell deficiency in Kit(W-sh) mice does not impair antibody-mediated arthritis. J Exp Med. 2007;204(12):2797-802.

490. Piliponsky AM, Chen CC, Grimbaldeston MA, Burns-Guydish SM, Hardy J, Kalesnikoff J, et al. Mast cell-derived TNF can exacerbate mortality during severe bacterial infections in C57BL/6-KitW-sh/W-sh mice. Am J Pathol. 2010;176(2):926-38.
491. Gonzalez JA, Lorente F, Romo A, Muriel M, Palomero B, Salazar V. Action of ketotifen on different functions of neutrophil polymorphonuclear cells. Allergol Immunopathol (Madr). 1986;14(3):215-20.
492. Podleski WK, Panaszek BA, Schmidt JL, Burns RB. Inhibition of eosinophils degranulation by Ketotifen in a patient with milk allergy, manifested as bronchial asthma--an electron microscopic study. Agents Actions. 1984;15(3-4):177-81.
493. Apellis Provides Updates on Injection Kits and Rare Safety Events with SYFOVRE® (pegcetacoplan injection) [press release]. 2023.
494. Kaszubski P, Ben Ami T, Saade C, Smith RT. Geographic Atrophy and Choroidal Neovascularization in the Same Eye: A Review. Ophthalmic Res. 2016;55(4):185-93.
495. Zhang T, Finn DF, Barlow JW, Walsh JJ. Mast cell stabilisers. Eur J Pharmacol. 2016;778:158-68.
496. Grant SM, Goa KL, Fitton A, Sorkin EM. Ketotifen. A review of its pharmacodynamic and pharmacokinetic properties, and therapeutic use in asthma and allergic disorders. Drugs. 1990;40(3):412-48.
497. Sinniah A, Yazid S, Flower RJ. The Anti-allergic Cromones: Past, Present, and Future. Front Pharmacol. 2017;8:827.
498. Dubois B, Lopez-Arrieta J, Lipschitz S, Doskas T, Spiru L, Moroz S, et al. Masitinib for mild-to-moderate Alzheimer's disease: results from a randomized, placebo-controlled, phase 3, clinical trial. Alzheimers Res Ther. 2023;15(1):39.
499. Reme CE, Grimm C, Hafezi F, Marti A, Wenzel A. Apoptotic cell death in retinal degenerations. Prog Retin Eye Res. 1998;17(4):443-64.
500. Hisatomi T, Sakamoto T, Murata T, Yamanaka I, Oshima Y, Hata Y, et al. Relocalization of apoptosis-inducing factor in photoreceptor apoptosis induced by retinal detachment in vivo. Am J Pathol. 2001;158(4):1271-8.
501. Mandal P, Berger SB, Pillay S, Moriwaki K, Huang C, Guo H, et al. RIP3 induces apoptosis independent of pronecrotic kinase activity. Mol Cell. 2014;56(4):481-95.

502. Ghiringhelli F, Apetoh L, Tesniere A, Aymeric L, Ma Y, Ortiz C, et al. Activation of the NLRP3 inflammasome in dendritic cells induces IL-1beta-dependent adaptive immunity against tumors. Nat Med. 2009;15(10):1170-8.
503. Chi W, Chen H, Li F, Zhu Y, Yin W, Zhuo Y. HMGB1 promotes the activation of NLRP3 and caspase-8 inflammasomes via NF-kappaB pathway in acute glaucoma. J Neuroinflammation. 2015;12:137.
504. Hornung V, Ablasser A, Charrel-Dennis M, Bauernfeind F, Horvath G, Caffrey DR, et al. AIM2 recognizes cytosolic dsDNA and forms a caspase-1-activating inflammasome with ASC. Nature. 2009;458(7237):514-8.
505. Cai B, Liao C, He D, Chen J, Han J, Lu J, et al. Gasdermin E mediates photoreceptor damage by all-trans-retinal in the mouse retina. J Biol Chem. 2022;298(2):101553.
506. Chen C, Chen J, Wang Y, Liu Z, Wu Y. Ferroptosis drives photoreceptor degeneration in mice with defects in all-trans-retinal clearance. J Biol Chem. 2021;296:100187.
507. Mocarski ES, Upton JW, Kaiser WJ. Viral infection and the evolution of caspase 8-regulated apoptotic and necrotic death pathways. Nat Rev Immunol. 2011;12(2):79-88.
508. Dhani S, Zhao Y, Zhivotovsky B. A long way to go: caspase inhibitors in clinical use. Cell Death Dis. 2021;12(10):949.
509. Green DR, Victor B. The pantheon of the fallen: why are there so many forms of cell death? Trends Cell Biol. 2012;22(11):555-6.